AN ABSTRACT OF THE DISSERTATION OF

Alan J. Tepley for the degree of Doctor of Philosophy in Forest Science and Geography presented on July 12, 2010

Title: Age Structure, Developmental Pathways, and Fire Regime Characterization of Douglas-fir/Western Hemlock Forests in the Central Western Cascades of Oregon

Abstract approved:

_____

Frederick J. Swanson Julia A. Jones

Descriptions of the fire regime in the Douglas-fir/western hemlock region of the Pacific Northwest traditionally have emphasized infrequent, predominantly stand-replacement fires and an associated linear pathway of stand development, where all stands proceed along a common pathway until reset by the next fire. Although such a description may apply in wetter parts of the region, recent fire-history research suggests drier parts of the region support a mixed-severity regime, where most fires have substantial representation of all severity classes and most stands experience at least one non-stand-replacing fire between stand-replacement events. This study combines field and modeling approaches to better understand the complex fire regime in the central western Cascades of Oregon. Stand-structure data and ages of more than 3,000 trees were collected at 124 stands throughout two study areas with physiography representative of western and eastern portions of the western Cascade Range. Major objectives were to (1) develop a conceptual model of fire-mediated pathways of stand development, (2) determine the strengths of influences of topography on spatial variation in the fire regime, (3) provide a stronger understanding of modeling approaches commonly used to gain

insight into historical landscape structure, and (4) develop methods to predict trajectories of change in landscape age structure under a non-stationary fire regime.

In the study area, non-stand-replacing fire interspersed with infrequent, stand-replacement events led to a variety of even-aged and multi-cohort stands. The majority of stands (75%) had two or more age cohorts, where post-fire cohorts were dominated either by shade-intolerant species or shade-tolerant species, depending largely on fire severity. Age structure, used as a proxy for the cumulative effects of fire on stand development, showed a moderately strong relationship to topography overall, but relationships were strongest at both extremes of a continuum of the influences of fire frequency and severity on stand development and relatively weak in the middle. High topographic relief in the eastern part of the western Cascades may amplify variation in microclimate and fuel moisture, leading to a finer-scale spatial variation in fire spread and behavior, and thus a broader range of stand age structures and stronger fidelity of age structure to slope position and terrain shape in the deeply dissected terrain of the eastern part of the western Cascades than in the gentler terrain of the western part.

In the modeling component of my research, I was able to use analytical procedures to reproduce much of the output provided by a stochastic, spatial simulation model previously applied to evaluate historical landscape structure of the Oregon Coast Range. The analytical approximation provides an explicit representation of the effects of input parameters and interactions among them. The increased transparency of model function given by such an analysis may facilitate communication of model output and uncertainty among ecologists and forest managers.

Analytical modeling approaches were expanded to characterize trajectories of change in forest age structure in response to changes in the fire regime. Following a change in fire frequency, the proportion of the landscape covered by stands of a given age class is expected to change along a non-monotonic trajectory rather than transition directly to its equilibrium abundance under the new regime. Under some scenarios of change in fire frequency, the time for the expected age distribution of a landscape to

converge to the equilibrium distribution of the new regime can be determined based only on the magnitude of change in fire frequency, regardless of the initial value or the direction of change.

The theoretical modeling exercises provide insight into historical trends in the study area. Compiled across all sample sites, the age distribution of Douglas-fir trees was strongly bimodal. Peaks of establishment dates in the 16th and 19th centuries were synchronous between the two study areas, and each peak of Douglas-fir establishment coincides with one of the two periods of region-wide extensive fire identified in a previous synthesis of fire-history studies. The modeling exercises support the development of such a bimodal age distribution in response to centennial-scale changes in fire frequency, and they illustrate how the relative abundance of different stand-structure types may have varied over the last several centuries.

Age Structure, Developmental Pathways, and Fire Regime Characterization of Douglas-fir/Western Hemlock Forests in the Central Western Cascades of Oregon

by
Alan J. Tepley

A DISSERTATION

submitted to

Oregon State University

in partial fulfillment of
the requirements for the
degree of

Doctor of Philosophy

Presented July 12, 2010
Commencement June 2011

Doctor of Philosophy dissertation of Alan J. Tepley presented on July 12, 2010.

APPROVED:

_____

Major Professor, representing Forest Science

_____

Head of the Department of Forest Ecosystems and Society

_____

Major Professor, representing Geography

_____

Chair of the Department of Geosciences

_____

Dean of the Graduate School

I understand that my dissertation will become part of the permanent collection of Oregon State University libraries. My signature below authorizes release of my dissertation to any reader upon request.

_____

Alan J. Tepley, Author

ACKNOWLEDGEMENTS

I would like to thank Fred Swanson, who has contributed greatly to the conceptual formulation of my research. Numerous conversations with Fred have improved my understanding of the ecological and social context for my work. He also has facilitated interactions with Forest Service researchers and managers that strengthened my understanding of management implications of my research. Julia Jones has provided valuable feedback throughout the development of my research, and she facilitated interactions with students and faculty across several departments under the Integrative Graduate Education and Research Traineeship (IGERT) program on Ecosystem Informatics, which greatly contributed to ability to work across disciplines. The modeling components of my dissertation would not have been possible without collaboration with Enrique Thomann. As a mathematician, he was quick to catch on to concepts and terminology related to fire and forest ecology, and he was patient with my limited background in math. Tom Spies provided substantial assistance in developing my study design, on data analyses, and his feedback greatly improved my understanding of how my research fits in with the broader body of research in the region. Conversations with Chris Daly on climate in complex terrain greatly contributed to my understanding of potential influences of topography on spatial variation in the fire regime. Bryan Black provided my initial training in dendrochronological methods, and he always was available to answer questions and provide feedback on my work.

This research was supported primarily by funding provided by the IGERT program on Ecosystem Informatics. Involvement in this program improved my ability to work as part of an interdisciplinary team, which was essential to the modeling component of my research. The IGERT program also funded an internship, which included participation in the Dendroecology course at the Laboratory of Tree-Ring Research (LTRR) of the University of Arizona. This course and the interactions with people at the LTRR, including Tom Swetnam, Don Falk, Chris Baisan, and Rex Adams, greatly improved my tree-ring analyses.

I am grateful for additional funding provided by the Long-Term Ecological Research Network (LTER) and the James H. Duke, Jr. Graduate Fellowship, the Alfred W. Moltke Memorial Scholarship, and the College of Forestry Graduate Fellowship. Valuable administrative and computer support was provided by staff of the Departments of Geosciences and Forest Ecosystems and Society, including Cheryll Alex, Melinda Peterson, Stacey Schulte, and Mark Meyers. Katherine Hoffmann was very helpful in all administrative aspects of the IGERT program.

My summer field work was based at the H. J. Andrews Experimental Forest, where I gained substantial ecological insight through interactions with other students and researchers. Kari O'Connell and Kathy Keeble aided in my housing arrangements, and Terry Cryer provided several repairs of field equipment on short notice. I received assistance in the field from Aidan Padilla and Keala Hagmann. Dan Irvine and Biniam Iyob helped with processing tree cores.

I received substantial feedback on my research and gained a stronger understanding of the management implications of my research through participation in field tours and numerous conversations with Forest Service researchers and managers involved in the Blue River Landscape Strategy, including Cheryl Friesen, Jane Kertis, and Norm Michaels.

Support and encouragement from friends, family, and fellow graduate students were very helpful throughout my dissertation research.

CONTRIBUTION OF AUTHORS

Fred Swanson, Julia Jones, and Tom Spies assisted in developing the study design for the field component of this dissertation, and they provided feedback that contributed to the analysis and writing of all chapters. Enrique Thomann contributed to the conceptual development of the modeling component of this dissertation, and he assisted in formulating the equations used in chapters 4 and 5 and Appendices B and C. Chris Daly provided feedback that improved the analysis and writing of chapter 3.

TABLE OF CONTENTS

Page

TABLE OF CONTENTS (continued)

Page

TABLE OF CONTENTS (continued)

Page

TABLE OF CONTENTS (continued)

Page

LIST OF FIGURES

LIST OF FIGURES (continued)

LIST OF FIGURES (continued)

LIST OF FIGURES (continued)

Figure Page

LIST OF TABLES

LIST OF APPENDIX FIGURES

CHAPTER 1: INTRODUCTION

BACKGROUND

Mixed-Severity Fire Regimes

Fire regimes can be characterized along a continuum from dominance by frequent, low-severity fires, to relatively infrequent, predominantly stand-replacement fires. Both extremes of such a continuum are fairly well understood in terms of their geographic distribution, forest stand and landscape structures associated with them, methods for fire-history analysis, and the relative influences of weather and fuel on fire behavior (Covington and Moore 1994, Bessie and Johnson 1995).

The mixed-severity fire regime accounts for a broad range of conditions in the middle of the fire-regime continuum. Mixed-severity systems are widespread in diverse forest types ranging from relatively dry mixed-conifer forests of northern California (Taylor and Skinner 1998, Beaty and Taylor 2001) and mid elevations of the Colorado Front Range (Sherriff and Veblen 2006), to more mesic forests in portions of the highly productive Douglas-fir (*Pseudotsuga menziesii* (Mirb.) Franco)/western hemlock (*Tsuga heterophylla* (Raf.) Sarg.) region of the Pacific Northwest (Morrison and Swanson 1990). Mixed-severity regimes may account for as much as 50% of the forested area in some regions of the western United States (Schoennagel et al. 2004), yet a conceptual framework for this complex regime type is lacking. Instead, mixed-severity regime has become a catch-all category that provides little guidance in (1) understanding the historical dynamics of these systems, (2) determining the degree that 20th century management and climatic change have altered these dynamics, or (3) developing forest management strategies in the context of climate variability and change. More detailed understanding of the regional and local variation in this complex regime type and the factors driving this variation is needed to identify meaningful subdivisions and avoid over-generalization about fire regimes at the level of forest cover types.

In mixed-severity systems, burn severity in individual fires and over successive events is mixed at stand and landscape scales (Agee 2005). Mixed-severity systems are

not necessarily characterized by a dominance of moderate-severity fire (e.g., fire that leads to 30–70% mortality of overstory trees), but rather, by representation of substantial areas of all severity classes in most fires (Agee 1998, 2005). In most fires, patch-size distributions may be similar among the severity classes such that no severity class consistently forms a matrix within which smaller patches of the other classes are embedded.

Despite the broad range of fire frequencies and forest types included within the mixed-severity regime, several attributes may be common to most mixed-severity systems. These include (1) fine-scale mosaics of even-aged and multi-cohort stands, with variable stand densities and structures (Hessburg et al. 2007), (2) multiple pathways of stand development (Zenner 2005), and (3) potential for individual species to play multiple successional roles (i.e., traditional distinctions between early- and late-seral species do not necessarily apply). The primary drivers or facilitators of these attributes are differences in resistance to fire-caused mortality by species and by tree age or position in the stand, complex topography, and spatial and temporal variation in the relative importance of weather and fuel in limiting fire extent and behavior.

Unlike stand-replacement regimes that commonly lack fire-resistant species (Agee 1997), or surface-fire regimes, where fire-sensitive, shade-tolerant species were a minor component of stand structure under historical conditions (Allen et al. 2002), the dominant species in most mixed-severity systems represent a broad range of fire resistance and shade tolerance. Differences in fire resistance among species and by tree age and position within a stand contribute to a range of fire severity and post-fire developmental pathways. Fire-free intervals may be long enough, at least in portions of the landscape, that fire-sensitive, shade-tolerant species are an important component of stand structure (Taylor and Skinner 1998). Also, abrupt pulses of establishment leading to dense stands following fires that open the canopy are likely to be found within these systems (Sherriff and Veblen 2006, Hessburg et al. 2007).

Almost all mixed-severity systems are associated with topographically-complex terrain (Noss et al. 2006). Steep terrain with high topographic relief contributes to stronger differentiation in microclimate and fuel moisture than gentler terrain (Daly et al. 2007), thereby contributing to greater variation in burn severity than typically found in gentler terrain (Duffy et al. 2007). To the extent that topography consistently influences fire behavior, a local mixed-severity landscape may be composed of several spatially distinct regions, each with a different fire frequency and with differences in the representation of each severity class. For example, in the Klamath Mountains of northern California, fire frequency generally was higher on south than north aspects, and fire severity tended to increase from lower to upper slopes, contributing to an abundance of old stands with multi-layered canopies on lower slopes and cool aspects, whereas upper slopes and warm aspects were likely to support younger, even-aged stands, sometimes with a low density of remnant older trees (Taylor and Skinner 1998).

The predictable landscape patterns driven by topographic influences on fire behavior sometimes may be overridden by weather or fuel (Thompson and Spies 2009). Because mixed-severity systems are situated in the middle of a gradient from weather-driven to fuel-driven systems, the relative influences of weather, fuel, and topography on fire behavior may change over time, especially in the context of long-term climatic fluctuation, leading to temporal variation in the patterns and relative abundances of different stand conditions. Thus, landscape structure found at any point in time may be a mosaic of legacies of previous changes in the fire regime.

Fire Regimes in the Douglas-fir Region of the Pacific Northwest

Although descriptions of the fire regime in the Douglas-fir/western hemlock region of the Pacific Northwest traditionally have emphasized infrequent, predominantly stand-replacement fires, recent fire history research has demonstrated substantial variation in the fire regime along regional climatic gradients, with a prominent role for non-stand-replacing fire in drier parts of the region. Infrequent, predominantly stand-replacement fire is dominant in northern parts of the Cascade Range (Hemstrom and

Franklin 1982, Agee and Krusemark 2001) and coastal areas (Huff 1995, Impara 1997). Drier areas, including much of the western Cascades of Oregon (Garza 1995, Van Norman 1998, Weisberg 1998) and rainshadows of coastal mountain ranges (Impara 1997, Wetzel and Fonda 2000) support more of a mixed-severity regime.

The emphasis on large, stand-replacement fires in early descriptions of forest dynamics in this region may have been influenced, in part, by several large fires of the late 19th and early 20th century that left a substantial imprint on the landscape at the time of some of the earliest studies. These fires include the Siletz Fire of 1849 (3,240 km^2), the Yaquina Fire of 1853 (1,940 km^2), the Yacolt Fire of 1902 (1,940 km^2), the Tillamook Fire of 1933 (970 km^2), and several others (Hofman 1924, Ballou 2002). Effects of such fires are evident in the following description of fire and stand initiation:

> "Fires in this region are apt to be very destructive and therefore have a cataclysmic effect on the life cycle of the forest. Imagine a severe fire hitting an old mixed forest, killing most of the trees over a considerable area and leaving the ground bare and exposed to summer drought. On such an area hemlocks, cedars, etc., can not establish themselves, but Douglas fir can. Result—the burn springs up to Douglas fir almost to the exclusion of everything else" (Munger 1930).

Munger (1930, 1940) continued to describe a scenario where Douglas-fir could no longer establish in the shaded understory, but the shade-tolerant species gradually would establish and eventually replace the Douglas-fir trees of the upper canopy over a fire-free interval lasting several centuries.

In contrast to the above description, contributions of non-stand-replacing fire to multiple developmental pathways were noted even in some of the earliest descriptions of stand development in the region. For example, Isaac (1940) suggested a role for non-stand-replacing fire in generating stands with multiple cohorts of Douglas-fir trees:

> "If younger Douglas firs do occur in the stand they will be found to belong to one or more distinct younger age classes that developed because part of the original forest was removed by fire, wind, insects, or disease. Thus there may be forests of one, two, or even three distinct age classes of Douglas fir occurring more or less groupwise, but there will not be an all-age forest unless the intermediate ages are made up of the more tolerant species that come in as an understory."

Isaac (1940) also noted that following fire stands may arise either as pure stands of Douglas-fir, or as mixed-stands of Douglas-fir with shade-tolerant trees. In addition, Hofmann (1924) described how fire of low intensity may lead to a post-fire cohort of shade-tolerant species:

> "The mature Douglas fir trees generally are not killed by this type of fire on account of the thick root bark at the crown of the roots, but the thin bark at the root crown of western red cedar, western hemlock, noble fir, and silver fir leaves these species easy victims. The remaining green Douglas-fir trees may continue to produce seed, but the shade of the dead and living trees is too dense for success of the Douglas fir seedlings. Consequently the shade-enduring species, such as western red cedar and western hemlock, have the advantage; an understory of these species develops."

Because all fires exhibit heterogeneous patterns of burn severity (Romme 2005), effects of non-stand-replacing fire are likely to be found even in a regime dominated by large, stand-replacement fires. Thus, understanding the shifts in the relative abundance of different fire severities across the region and associated changes in the representation of different stand-structure types and landscape patterns is important for identifying the range of processes and structures likely to be sustainable in a particular setting. Geographic differences in the relative abundance of different fire severity classes across the region are illustrated by a comparison of aerial-photo-based interpretation of the severity of 19th-century fires in the northern and central parts of the western Cascades of Oregon, where annual precipitation differs by about 50 cm. High-severity fire accounted for 69% of the area burned by three late 19th-century fires in the wetter, northern study area (Agee and Krusemark 2001). However, only 26% of the area burned by 19th-century fires experienced high-severity fire in the drier study area in the central western Cascades (Morrison and Swanson 1990). In the northern study area, low- and moderate-severity patches were small in size and limited to areas near the fire perimeter, riparian areas, and sparsely-vegetated, rocky areas (Agee and Krusemark 2001). In the central western Cascades, low- and moderate-severity patches together accounted for 74% of the burned area, and each of these classes formed a patch-size distribution resembling that of high-severity fire (Morrison and Swanson 1990).

Similarly high representation of low- and moderate-severity fire was found in other fire-history studies in the central western Cascades of Oregon (Stewart 1986, 1989; Teensma 1987; Weisberg 1998, 2004) and in recent fires (Kushla and Ripple 1997). However, the factors guiding the spatial patterns of the mosaics of different burn severity and the effects of variable fire severity on stand development remain poorly understood.

In addition to variable fire severity in drier parts of the region, there is evidence suggesting variable fire frequency. A synthesis of ten fire-history studies west of the crest of the Cascades in Oregon and Washington suggests the occurrence of two periods of region-wide, extensive fire, primarily in the 16th and 19th centuries, separated by a long period of reduced burning (Weisberg and Swanson 2003). The earlier period of widespread burning (from the late 1400s to the early 1600s) also may have had greater representation of high-severity fire based on the low abundance of trees that predate this period (though the lack of older trees also may reflect mortality by more recent fires). The factors contributing to the spatial variability of burn severity within individual fires, temporal variability in fire frequency (and possibly fire size and the representation of different fire-severity classes), and the effects of this spatial and temporal variability on contemporary forest structures in this region are largely unknown.

OVERVIEW

I combined field and modeling approaches to better understand the factors influencing spatial and temporal variation in the fire regime of the central western Cascades of Oregon and the effects of this variable fire regime on stand development and forest dynamics. Field work was conducted in two study areas, each centered on a large (240–300 km^2) watershed with physiography representative of the eastern or western part of the western Cascade Range. Forest stand and age-structure data, including diameter distributions of live and standing dead trees, direct evidence of fire (charred bark and healed-over fire scars within increment cores), and ages of more than 3,000 trees, were collected at 124 stands located in groups of 3, at upper, mid, and lower slope positions, along randomly selected slope facets.

The primary objective of chapter 2 is to develop a conceptual model of fire-mediated pathways of stand development. Data collected in the field are used identify groups of stands with similar age distributions of shade-intolerant and shade-tolerant species. These age distributions along with the densities of trees in different age classes and evidence of fire, such as charred tree bark, are used to infer the contribution of fire to the developmental history of each group of stands. The goal is to develop a model of the various pathways of forest development mediated by fire of different frequency and severity, with an overall model structure that applies broadly across much of the variation in the fire regime along regional climate gradients, but the representation of each developmental stage is likely to shift with changes in the relative frequency of stand-replacing and non-stand-replacing fire.

In chapter 3, the objective is to gain a stronger understanding of the contribution of topography to spatial variation in the fire regime at the local level. To determine the contribution of topography to local patterns of fire spread and fire behavior, relationships between age structure and topography are evaluated, where age structure is used as a proxy for the cumulative effects of one or more fires (or the absence of fire) on stand development. A continuous gradient developed by ordination of stands by age-structure variables and the discrete age-structure types identified in chapter 2 are related to their topographic context in order to better understand the degree that certain types of fire frequencies and behaviors and associated stand conditions are likely to be associated with specific portions of the landscape and are unlikely to be found in other areas.

In chapter 4, I develop an analytical approximation of a stochastic, spatial simulation model of fire and forest dynamics (LADS; Wimberly 2002) in order to demonstrate that relatively complex simulation models sometimes can be broken down into the fundamental equations that guide model behavior, and thereby provide greater transparency into the functioning of such models. Stochastic, spatial simulation models commonly are used to expand upon the insight gained from field studies to better understand landscape dynamics at broader spatial scales and over longer time periods. However, most of these models lack transparency for understanding the effects of input

parameters and modeling algorithms. The analytical approximation is not suggested as a replacement for simulation models, but rather as a complementary approach to clarify model function and provide a better understanding of the uncertainty in model output for forest ecologists and managers interested in applying the insight gained from modeling studies.

The overall objective of chapter 5 is to develop analytical methods to predict trajectories of change in the age structure of a forest landscape in response to changes in the fire regime. In this chapter, I expand upon the analytical modeling approaches of the previous chapter in order to develop a method to calculate the expected age distribution of a landscape in any year following an abrupt change in fire frequency from any known initial age distribution. Then an approach is presented to determine the time required for the expected age distribution of a landscape to converge to the equilibrium age distribution of the new fire regime following a change in in fire frequency. Finally, the above methods are applied in a numerical example using a stand-level model of forest development that I designed based on the analyses of chapter 2. The model is evaluated under a non-stationary scenario similar to the changes in the fire regime of the last 500 years inferred from a synthesis of 10 fire-history studies in the region (Weisberg and Swanson 2003).

Appendices are provided to elaborate on the GIS methods used to generate variables describing the physiographic context of sample sites as used in chapter 3, to provide a proof for the calculation of the equilibrium age distribution as used in chapters 4 and 5, to describe the stand-level successional pathways model used in chapter 5, and to evaluate temporal variation in the fire regime of the study area with an emphasis on potential influences of climatic fluctuation.

CHAPTER 2: AGE STRUCTURE, POST-FIRE ESTABLISHMENT, AND FIRE-MEDIATED DEVELOPMENTAL PATHWAYS IN DOUGLAS-FIR/WESTERN HEMLOCK FORESTS IN THE CENTRAL WESTERN CASCADES OF OREGON

ABSTRACT

Fire-history research in the Douglas-fir/western hemlock region of the Pacific Northwest reveals substantial variation in the fire regime along regional climatic gradients. Non-stand-replacing (NSR) fire is common in drier parts of the region, but its effects on stand development are poorly understood. The objective of this study was to generate a conceptual model of fire-mediated forest developmental pathways in Douglas-fir/western hemlock forests subject to a mixed-severity fire regime. Forest stand and age-structure data were collected at 124 stands in two watersheds in the central western Cascades of Oregon. Hierarchical clustering of variables describing the age distributions of shade-intolerant and shade-tolerant species produced six distinct groups, each representing a different range of fire influences on stand development. NSR fire was primarily an episodic occurrence. Most old-growth stands had evidence of NSR fire, but many of these stands probably experienced a fire-free interval at least 100–200 years long. Fifteen percent of stands lacked evidence of fire for > 400 years, whereas 10% probably have not gone much longer than 100 years without fire. The differences in NSR fire frequency contribute to substantial differences in stand structure and successional roles of shade-intolerant and shade-tolerant species. Shade-intolerant species formed even-aged stands following stand-replacing fire, or they formed up to four cohorts per stand in response to non-stand-replacing fire. Almost all establishment dates for shade-intolerant species were in pulses < 40 years long, with little indication that the duration of cohort establishment varied over time or across the study area. Shade-intolerant trees were common in post-fire cohorts beneath older trees at densities up to 2/3 the density of shade-intolerant trees in unburned old-growth stands. Where greater numbers of trees predate the fire, shade-tolerant species formed a distinct post-fire cohort. Management guided by historical fire regimes in this region should incorporate effects of NSR fire but also acknowledge its episodic occurrence and the importance of relatively long, fire-free intervals.

INTRODUCTION

Understanding disturbance regimes and the effects of disturbance on forest development is essential for interpreting historical landscape patterns and predicting trajectories of stand and landscape change in response to future disturbance or management scenarios (Cissel et al. 1999, Swetnam et al. 1999). A generalized linear sequence of stand development that is reset by each disturbance has been shown to apply broadly (provided seed sources and suitable seedbeds are available) in forests subject to predominantly stand-replacement (SR) disturbances (Oliver 1981, Peet and Christensen 1987, Franklin et al. 2002). However, development along a single pathway may account only for a small portion of stand conditions found where forests are subject to both SR and non-stand-replacing (NSR) disturbances. Mixed-severity fire regimes, for instance, may be viewed as regimes where burn severity in individual fires and over successive events is mixed at forest stand and landscape scales, producing fine-scale mosaics of even-aged and multi-cohort stands. Such variation in burn severity may bring about multiple developmental pathways with several successional roles for shade-intolerant (fire-resistant) and shade-tolerant (fire-sensitive) species.

Recent fire-history research in the Douglas-fir (*Pseudotsuga menziesii* (Mirb.) Franco)/western hemlock (*Tsuga heterophylla* (Raf.) Sarg.) region of the Pacific Northwest (PNW) reveals substantial variation in the fire regime along regional climatic gradients. Infrequent, predominantly SR fire is dominant in northern parts of the Cascade Range (Hemstrom and Franklin 1982, Agee and Krusemark 2001, Winter et al. 2002a) and coastal areas (Huff 1995, Impara 1997). However, evidence of NSR fire was common in drier parts of the region, including much of the western Cascade Range of Oregon (Morrison and Swanson 1990, Garza 1995, Van Norman 1998, Weisberg 1998) and rainshadows of coastal mountain ranges (Impara 1997, Wetzel and Fonda 2000). For example, evidence of up to 7 NSR fires per stand was found in 49, 400–550-year-old stands in the central western Cascades of Oregon, with the largest portion of stands showing evidence of 3 NSR fires since stand initiation (Weisberg 1998, 2004). The increasing knowledge of geographic variation in the fire regime and the prevalence of

NSR fire in drier parts of the region call for further evaluation of the effects of NSR fire on forest development.

Most previous fire-history research in this region was conducted by counting tree rings in the field in recently harvested stands to date fire scars and age Douglas-fir trees (Teensma 1987, Morrison and Swanson 1990, Weisberg 1998). Recently-harvested stands, which were widespread by the 1980s, provided a rare opportunity to view the fire-scar record, which otherwise was unavailable for sampling in intact stands. Unlike drier regions, where external evidence of multiple fire scars is available on live trees and slowly decaying snags and logs (Swetnam and Baisan 1996), trees with large fire-caused wounds (> ca. 20% of bole circumference) in relatively mesic forests west of the crest of the Cascades are susceptible to rot and are unlikely to retain a long fire record. Small scars form in bark fissures of mature Douglas-fir trees. However, the wounds tend to heal within about 15 years, which provides protection from rot, but also conceals the scar (Morrison and Swanson 1990, Skinner and Taylor 2006). The lack of timber harvest in older stands in the last two decades and relatively rapid decay of stumps from earlier harvests severely limit most additional fire-scar sampling in the region.

The ages of Douglas-fir trees determined in previous studies were useful in approximating the timing of the earliest fire in a stand, for which there was no scar evidence. The age data also challenged previous interpretations that the prompt establishment observed following fires in the early 20th century (Munger 1930, Isaac 1943) was similar to the initiation of many old-growth stands. Several retrospective studies unexpectedly found that old-growth trees had nearly continuous establishment over intervals > 100 years, with no evidence of multiple pulses of establishment (Franklin and Hemstrom 1981, Tappeiner et al. 1997, Poage and Tappeiner 2002). The long establishment periods along with rapid early growth in many trees led to the hypothesis that many existing old-growth stands originated gradually with a period of low tree density persisting for several decades to more than a century (Tappeiner et al. 1997, Poage and Tappeiner 2002). However, other studies found that all of the old-growth trees

present in some stands established in a single, abrupt pulse following fire (Yamaguchi 1993, Winter et al. 2002a).

Although previous fire-history research demonstrates the prominence of NSR fire in drier parts of the Douglas-fir/western hemlock region of the PNW, the poor accuracy of field-counted data (Weisberg and Swanson 2001), and the emphasis on ages primarily, if not exclusively of Douglas-fir trees (Poage et al. 2009), provides limited insight into patterns of stand development in this highly variable fire regime. The few studies that characterized age distributions of all species are valuable case studies, but only for a small number of stands (Means 1982; Stewart 1986, 1989; Goslin 1997), and some of them were in wetter parts of the region and lacked evidence of NSR fire (Huff 1995, Winter et al. 2002a and b). More extensive sampling of age distributions of all species in parts of the region subject to a mixed-severity fire regime may provide a broader picture of stand development and enable synthesis of common trends repeated at multiple stands.

The primary objective of this study is to use age-structure from numerous stands in the central western Cascades of Oregon to develop a conceptual model of fire-mediated pathways of stand development. Specific objectives are to (1) evaluate successional roles of shade-intolerant and shade-tolerant species in terms of their establishment and recruitment patterns in response to fire of varying severity, (2) identify differences in stand structure associated with stand development under different frequencies of NSR fire, and (3) evaluate the duration of post-fire establishment periods in Douglas-fir stands, and determine if they differ depending on the timing of cohort initiation.

STUDY AREA

Sampling was conducted in two study areas, each centered on a large watershed in the central western Cascades of Oregon (Figure 2.1). The Blue River study area has deeply dissected terrain characteristic of the eastern part of the western Cascade Range. It includes the 240-km^2 Blue River watershed and 3 smaller watersheds (totaling 33 km^2) to

the north. Elevation ranges from 316 to 1,753 m, and most major ridges reach elevations above 1,200 m. The Fall Creek study area has somewhat gentler terrain and lower topographic relief, representative of the western part of the western Cascades. It is the eastern 300 km^2 of the Fall Creek watershed, including the majority of the watershed within the Willamette National Forest (Figure 2.1). Elevation ranges from 254 to 1,519 m, but only the highest ridges along the southern perimeter of the study area are higher than 1,200 m.

The climate of the central western Cascade Range in Oregon is transitional from Mediterranean to maritime temperate. Winters are mild and wet, and summers are warm and dry. Mean annual precipitation (1971–2000) averages 233 cm in the Blue River study area and 182 cm at Fall Creek (Daly et al. 2008). Most precipitation falls in the winter, and a persistent snowpack accumulates above about 900 m. Only about 10% of annual precipitation falls between June 1 and September 30, and the fire season typically occupies the latter part of this dry season. In the second half of the 20th century, large fire years on the west side of the Cascade Range were associated with multi-season drought initiating the previous fall, followed by summertime circulation anomalies that favor warm, dry, east (foehn) winds (Gedalof et al. 2005).

Two vegetation zones comprise the majority of both study areas. The Western Hemlock zone (Franklin and Dyrness 1973) accounts for almost the entire Fall Creek study area and most of the Blue River study area, excluding ridgetops above about 1,200 m. Essentially all forests of this zone are dominated by Douglas-fir. Major shade-tolerant associates are western hemlock and western redcedar (*Thuja plicata* Donn ex D. Don). The Pacific Silver Fir zone is represented on ridges higher than about 1,200 m, including most major ridges in the Blue River study area and a few ridges in the southern part of Fall Creek. Abundant species of this zone are Douglas-fir, Pacific silver fir (*Abies amabilis* (Dougl. ex Loud.) Dougl. ex Forbes), noble fir (*Abies procera* Rehd.), western hemlock, and mountain hemlock (*Tsuga mertensiana* (Bong.) Carr.). The Mountain Hemlock zone is found in small patches on the highest ridgetops in the Blue River study area, and the Douglas-fir climax type occurs locally on the driest sites in both study areas.

METHODS

Field Methods

Sampling was conducted in 124 stands: 71 in the Blue River study area and 53 at Fall Creek. Stands were located using a stratified random method that distributes sampling intensity throughout each study area while capturing most of the physiographic variation. To select sample sites, a 5x5-km grid was overlaid on each study area, and 3 transects were sampled at upper, mid, and lower slope positions along a randomly selected slope facet in each 25-km^2 cell. Slope facets (contiguous areas with similar aspect extending from ridgetop to valley bottom) were delineated by first applying a Gaussian filter to a 30-m Digital Elevation Model (DEM) to smooth features up to 240 m in extent. Aspect of the smoothed DEM was classified as northeast (0–90º), southeast (91–180º), southwest (181–270º), or northwest (271–360º). Then, areas of each aspect class smaller than 40 ha were combined with the more inclusive class. Slope facets were chosen for sampling by using a random number generator to identify one, 1-km^2 cell within each 25-km^2 cell, and selecting the slope facet that accounted for the majority of that cell.

Sample sites were determined by generating a random point at the upper, mid, and lower slope position of the selected slope facet. Slope positions were defined by dividing the elevation range of the slope facet into three equal portions. Aerial photos were used to draw polygons encompassing the forested area lacking 20^{th}-century anthropogenic disturbance at each slope position, excluding areas within 100 m of roads, perennial streams, harvested stands, and non-forest vegetation. Then, Universal Trans Mercator (UTM) coordinates were generated for a random point within the polygon at each slope position, and a GPS receiver was used to locate the point in the field. In addition to sampling along one slope facet in each 25-km^2 grid cell, topographic settings that were poorly represented in the dataset were selected for sampling. Sample locations within these settings were identified as described above.

The random point within each polygon served as the midpoint of a 120-m long transect for sampling forest stand and age structure. Each transect consisted of 5, 0.02-ha circular plots located at 30-m intervals between plot centers. Transects were oriented parallel to slope contours, and the entire transect was treated as one sample unit. Sampling was conducted in 5 plots along a 120-m long transect rather than a single plot of equivalent area to ensure that age classes found in the sample set were spread over broad areas, and thus were likely to represent establishment in response to widespread disturbance rather than local treefall gaps.

Stand structure variables recorded at each plot include the diameter at breast height (dbh) of all live and standing dead trees > 15 cm dbh, the number of trees and shrubs 1.5–15.0 cm dbh by species in a 0.01-ha subplot. Evidence of fire including charred bark and open catfaces, was recorded for each tree. Also, a list of all vascular plant species present in the ground cover of each plot was recorded to enable classification of stands by plant association.

Forest age-structure data were collected by coring a subset of 3,279 trees > 15 cm dbh (or > 10 cm dbh for Pacific yew (*Taxus brevifolia* Nutt.)), representing an average of 27 trees per transect, or 76% of the live trees. The subset was determined by dividing each 0.02-ha plot into 4 quadrants and coring the largest tree of each species in each quadrant. These criteria ensured that each species was sampled nearly proportional to its frequency in the transect. Selecting the largest tree increased the likelihood of sampling the oldest tree of each species, but sampling one tree per species per quadrant ensured that smaller trees also were sampled. Trees were cored as close to the ground as possible to reduce uncertainty in the time to reach coring height. The height of core extraction above the mineral soil surface was recorded for each tree. If trees had heartrot or were too large to reach the pith with an 81-cm increment borer, the area in close proximity to the transect was searched for trees of the same species and similar size to substitute for the tree in the plot. If no suitable trees were available, an incomplete core from the tree in the plot was collected as a minimum estimate of tree age, but establishment dates were not estimated for these trees.

Age-Structure Dataset

Tree cores were mounted and sanded until cell structure was visible under a binocular microscope, and the majority (85%) of cores was cross-dated. Cross-dating was conducted using skeleton plotting and the list-year method (Yamaguchi 1991, Stokes and Smiley 1996). Then, master ring-width chronologies were developed by measuring ring width in more than 200 Douglas-fir and 50 western hemlock cores to the nearest 0.001 mm using a Velmex sliding-stage micrometer. The remaining cores were cross-dated by visual comparison to the master chronologies. Fifteen percent of the cores that could not be cross-dated were deciduous species, which were excluded from the analyses due to representation in a small portion (23%) of stands. The remaining non-cross-dated cores were primarily from Pacific yew (16%), or from other shade-tolerant species that had suppressed growth within their first 100 years, which precluded cross-dating of the innermost rings. These cores were retained in the analyses because potential dating errors were assumed to be minor relative to the timescale of stand development, and such errors were likely to have little influence on the age-structure variables used in the analysis.

Establishment dates were estimated for 3,046 trees (89% of the cores), limited to those that either intersected the pith, or where the innermost ring formed a complete arc and the number of years to the pith could be estimated without extrapolating beyond the end of the core. For these off-center cores, the geometric method of Duncan (1989) was applied to estimate an average of seven years to the pith. An additional four years, on average, was added to account for the time to reach coring height above the mineral soil surface by applying the equation of Morrison and Swanson (1990) to all species.

The age-structure dataset was developed to characterize the overall shape of age distributions of shade-intolerant and shade-tolerant species, where stands with similar overall age distributions are assumed to have followed similar development trajectories. Variables were not defined to emphasize establishment in specific time periods (e.g., the proportion of establishment dates in each decade), because such an approach would likely

group stands affected by the same events (Taylor and Skinner 2003), but not necessarily those that followed similar trajectories of development after burning in different fires.

The dataset consists of four variables characterizing the age distribution of shade-intolerant species and four for shade-tolerant species. For shade-intolerant species, the variables include the proportion of trees that established before 1780, the overall age range, the age range of trees that established after 1780, and the proportion of trees with charred bark. Variables characterizing the age distribution of shade-tolerant species include the proportion of trees that established before 1780 and the range, mean, and standard deviation (SD) of shade-tolerant tree age. The year 1780 was used as a threshold distinguishing trees that predate the more recent of two region-wide periods of extensive burning identified in a synthesis of fire-history studies in western Oregon and Washington (Weisberg and Swanson 2003).

The range of shade-intolerant tree age was calculated after excluding the oldest and youngest tree at each stand to minimize the influence of a single tree that predates a younger cohort or an individual young tree that may have established after a disturbance of small-scale or low-intensity that otherwise did not generate canopy openings of sufficient size for widespread regeneration of shade-intolerant species. The oldest shade-tolerant tree at each stand was excluded from calculation of the range, mean, and SD of shade-tolerant age to minimize the influence of individual outlier trees that may have survived a fire and predate a post-fire cohort.

Analyses

Prior to statistical analyses, values of the age-structure variables were standardized by subtracting the mean and dividing by the SD of each variable in order to equalize variance among variables measured on different scales and in different units. Then the data set was evaluated for outliers by calculating Euclidean distance (in the multivariate space of the eight age-structure variables) among all pairs of transects and comparing the average distance of each transect from all other transects to the overall average distance among pairs of transects. Using two SDs from the overall mean as a

threshold, seven transects were identified as potential outliers. Each of these transects had values at or near the extreme value for one or more variables, but there was no ecological reason to exclude them from the analyses.

Transects were grouped by age-structure variables using hierarchical agglomerative cluster analysis with Euclidean distance and Ward's linkage method (Ward 1963). Dendrograms were scaled by Wishard's objective function (the sum of the error sum of squares from each group centroid to the group members), which was scaled to the percent of information remaining (McCune and Grace 2002). Dendrograms were cut by examining stem length and branching distribution to identify a pruning point that compromises between maximizing within-group homogeneity and between-group differences and minimizing the number of groups.

For the groups of transects identified by clustering of age-structure variables, differences in stand structure were evaluated using one-way Analysis of Variance (ANOVA), followed by multiple comparisons using Tukey's HSD test (Venables and Ripley 1992). Assumptions of normality and homogeneity of variance were evaluated with normal probability plots and Levene's test (Fox 1997). If these assumptions were not met, the Kruskal-Wallis test was used, followed by multiple comparisons using the Behrens-Fisher test (Munzel and Hothorn 2001) conducted in R (R Development Core Team 2006).

The duration of post-fire establishment by shade-intolerant species was evaluated by converting the calendar year of establishment for each tree to the number of years after cohort initiation, where the year of cohort initiation was estimated by the earliest establishment date within a cohort. Then, cohorts were superimposed to generate a frequency distribution representing the proportion of all establishment dates that fall within a given interval following cohort initiation. Multiple cohorts per stand were identified using thresholds of 40, 60, and 80 years with no recorded establishment of any species to separate two cohorts. The gap in the age distribution was assumed to represent the period after canopy closure, when further establishment of shade-intolerant species is

likely to be minimal until the next fire that opens the canopy (Spies and Franklin 1989). Also, trees that established in this interval would have been young at the time of the fire and unlikely to have survived. Because fire scars usually were not available to facilitate identification of post-fire establishment pulses, thresholds of 40, 60, and 80 years with no recorded establishment dates of any species were used to distinguish multiple cohorts per stand in order to test the sensitivity of the interpretation of the duration of post-fire establishment periods to the rules for distinguishing multiple cohorts per stand.

Pulses of establishment separated by intervals shorter than the threshold also were identified as separate cohorts if there was a fire scar within an increment core. To avoid circular reasoning, fire scars were used only if they could confidently be identified as scars independent from the age distribution. Fire scars had to have a break in the core (usually with a pitch deposit preceding the break and one or more locally absent rings after the break), followed by wider, slanted or curled rings (Barrett and Arno 1988). Because fire scars usually are recorded over a small portion of the circumference of Douglas-fir trees (Morrison and Swanson 1990, Skinner and Taylor 2006), the scars found within increment cores probably represent a small portion of scars present on the sampled trees. Thus, it is possible that the period of establishment for a single cohort identified in the present study may include pulses of establishment following two or more fires.

RESULTS

Age Structure and Stand Development

Almost all (96%) shade-intolerant trees in the age-structure dataset are Douglas-fir. The remaining shade-intolerant species are noble fir, incense-cedar (*Calocedrus decurrens* (Torr.) Florin), western white pine (*Pinus monticola* Dougl. ex D. Don), and sugar pine. Although these species may be characterized as midtolerant relative to a broader suite of western conifers, they are hereafter referred to as shade-intolerant to emphasize differences in tolerance from the shade-tolerant species of the study area. The most abundant shade-tolerant species in the dataset are western hemlock (69%), western

redcedar (14%), and Pacific silver fir (11%). Pacific yew, mountain hemlock, grand fir (*Abies grandis* (Dougl. ex D. Don) Lindl.), and Alaska yellow-cedar (*Chamaecyparis nootkatensis* (D. Don) Spach) comprise the remaining 6%.

Six age-structure types were identified by hierarchical clustering of eight age-structure variables (Figure 2.2). Branching was concentrated at short distances, which allowed the dendrogram to be pruned to produce a small number of relatively homogenous groups with substantial variability between them. The primary division of the dendrogram reflects differences in the age distribution of shade-intolerant species. Almost all shade-intolerant trees in age-structure types 1–3 established before 1780, whereas all stands of types 4–6 have at least one cohort initiated after 1780, usually in addition to older cohorts (Figure 2.3).

Stands of age-structure type 1 each have a single cohort of shade-intolerant trees, usually dating to the late 15^{th} or 16^{th} century. These stands lack charred bark or age cohort evidence of fire since stand initiation, and live shade-tolerant trees exhibit nearly continuous establishment from stand initiation to the present (Figure 2.4a). The basal area of shade-tolerant trees (56.9 m^2/ha) and the density of large shade-tolerant trees (39 trees/ha) are significantly greater than that of all other age-structure types (Table 2.1). Horizontal patchiness in stand structure, consistent with response to local canopy gaps rather than extensive disturbance, is most evident in the small-tree layer, which is dense overall (1,947 stems/ha), but highly variable among stands (SD = 1,457 stems/ha) and among the plots within each transect.

Age-structure types 2 and 3 are similar to type 1 in the age distribution of shade-intolerant trees, but they differ from type 1 by the presence of charred bark on these trees in most stands and younger ages of shade-tolerant species (Figure 2.4a–c). In 89% of stands in age-structure types 1–3, all shade-intolerant trees form a single cohort initiated between 1470 and 1610. Remaining stands either contain older trees or have a second cohort represented by only one or two trees. Charred bark was recorded on the shade-intolerant trees in each stand of age-structure type 3 and 58% of stands of type 2. The

fires that charred these trees probably caused little mortality of shade-intolerant trees, as supported by the present density of shade-intolerant trees in age-structure types 2 and 3 (60 and 65 trees/ha, respectively), which is nearly identical to that in type 1 (62 trees/ha), where stands lack evidence of fire since stand initiation (Table 2.1, Figure 2.3).

In age-structure type 3, prolific regeneration of shade-tolerant species, presumably after the most recent of at least one NSR fire since stand initiation, produced a distinct cohort beneath the older cohort of shade-intolerant trees (Figure 2.4c). On average, 85% of establishment dates for shade-tolerant trees at each stand fall within a window < 40 years long. The initiation of these establishment pulses is staggered among stands, from the early 19th to the early 20th century, suggesting that similar overall age distributions developed in stands that burned in different events. Minimal survival of fire by shade-tolerant species is illustrated by intervals usually > 200 years long, separating cohorts of shade-intolerant and shade-tolerant species, where few, if any trees that established survived to the present. Fire-caused mortality and abundant post-fire regeneration of shade-tolerant trees has resulted in a higher density of shade-tolerant trees than in the unburned stands of age-structure type 1, but these trees are limited primarily to small size classes (Table 2.1, Figure 2.5).

Age-structure type 2 probably includes at least two developmental pathways that led to shade-tolerant tree age and size distributions intermediate between types 1 and 3 (Figures 2.4 and 2.5). One pathway is similar to that in type 3, where stands probably experienced at least one NSR fire that killed most shade-tolerant trees and enabled development of a new cohort, but the most recent fire may have been up to 100 years earlier than that in type 3. In another pathway, stands may have experienced 19th-century NSR fire of intensity low enough that several shade-tolerant trees survived. The resulting age distribution includes the cohort of shade-intolerant trees initiated primarily in the 16th century, an abrupt pulse of shade-tolerant tree establishment in the 19th century, and shade-tolerant trees at a density ≥ 20 trees/ha that predate this pulse. The role of fire in enabling initiation of the 19th-century establishment pulse is supported by a higher abundance of older western redcedar trees with an open catface than found in any other

age-structure type. Also, the initiation of the pulse usually coincides with a pulse of establishment at other slope positions along the same slope facet.

Stands of age-structure type 4 are characterized by two distinct cohorts of shade-intolerant trees, initiated primarily in the 15th and 19th centuries (Figure 2.4d). The older cohort is of similar age to the cohort of shade-intolerant trees in age-structure types 1–3. However, trees of this cohort have charred bark in every stand of type 4, and the average tree density in the old cohort (45 trees/ha) is only about 2/3 that in types 1–3 (60–65 trees/ha; Table 2.1, Figure 2.3). Thus, a portion of the shade-intolerant trees may have been killed either in a single fire or by cumulative effects of two or more NSR fires. With fewer trees that predate the most recent fire than in age-structure types 2 or 3, a more favorable post-fire light environment may be the prominent factor enabling post-fire regeneration of shade-intolerant trees in age-structure type 4. As a result, the younger of the two cohorts in each stand of type 4 is a mixed cohort of shade-intolerant and shade-tolerant species (Figure 2.4d).

Age-structure type 5 includes stands initiated following high-severity fire after 1780, and most stands lack evidence of additional fire to the present. All stands have a distinct cohort of shade-intolerant trees initiated after 1780, and trees that established before 1780 are present at a lower density (9 trees/ha) than in any other age-structure type (Figure 2.3). Two stands have two cohorts of shade-intolerant trees, probably initiated following two fires after 1780. These stands have two pulses of establishment separated by relatively short (21 and 42 years) intervals with no recorded establishment. In both cases, the gap in the age distribution may be attributed to fire based on healed-over fire scars in increment cores and the presence of charred bark only on trees in the older of the two establishment pulses.

Age-structure type 6 is characterized by three or more cohorts of shade-intolerant trees in most stands, suggesting the occurrence of several NSR fires that enabled establishment of shade-intolerant species while retaining older cohorts. Stands contain an average of 24 trees/ha that established before 1780, usually along with at least two

younger cohorts of shade-intolerant trees (Figures 2.3 and 2.4f). Shade-intolerant trees that established after 1780 have establishment dates spanning an average of 112 years per stand, compared to 35 and 37 years in age-structure types 4 and 5, respectively. The 112-year range includes a period averaging 44 years long with no recorded establishment. The gap in the age distribution most likely separates two cohorts initiated after different fires, as suggested by charred bark on only the older trees. Also, healed-over fire scars that coincide with the initiation of the younger cohort provide evidence of fire at 2/3 of the stands. Most shade-tolerant trees have establishment dates after the initiation of the youngest cohort of shade-intolerant trees, and their density (115 trees/ha) and basal area (11.8 m^2/ha), and the density of large shade-tolerant trees (3 trees/ha) are among the lowest of all age-structure types (Table 2.1).

Post-Fire Establishment

The majority of shade-intolerant trees established within 40 years of cohort initiation, and establishment intervals were relatively consistent regardless of when cohorts originated (Figure 2.6). Overall, the percentage of trees that established within 40 years of cohort initiation ranges from 91% using a 40-year interval with no establishment to distinguish multiple cohorts per stand, to 87% using an 80-year interval (Figure 2.6a).

Most cohorts originated in the intervals 1470–1610 and 1780–1940, corresponding to the two periods of region-wide, extensive fire identified in a synthesis of fire-history studies west of the crest of the Cascades (Weisberg and Swanson 2003). Using 40 years with no establishment as a threshold to distinguish multiple cohorts per stand, 35% of trees were in cohorts that initiated in the earlier period of extensive fire (1470–1610) and 54% in the more recent period (1780–1940). The percentage of trees that established within 40 years of cohort initiation in the earlier period (94%) was nearly identical to that in the later period (91%) (Figure 2.6b). After doubling the threshold for distinguishing multiple cohorts per stand to 80 years with no establishment dates, the percentage of trees that established within 40 years of cohort initiation for the intervals 1470–1610 and 1780–1940 was 89% and 90%, respectively (Figure 2.6c). Cohorts that

originated between 1610 and 1780 have longer establishment intervals than those originated at other times. However, only 9% of establishment dates for shade-intolerant trees were in cohorts originated between 1610 and 1780. Long establishment intervals during this period were driven by three stands of age-structure type 6, which have shallow, rocky soil, and one of them is located near the upper elevation limit for Douglas-fir.

DISCUSSION

Overview of Developmental Pathways Model

The use of age structure to classify stands into six groups (Figure 2.2), followed by a comparison of stand structure among the groups (Table 2.1, Figure 2.5), facilitated the construction of a conceptual model of fire-mediated pathways of stand development and forest dynamics in the central western Cascades of Oregon (Figures 2.7 and 2.8). Such an approach differs from most previous descriptions of stand development in the region, where inferences about stand development were drawn primarily from present stand structure (Franklin et al. 2002, Zenner 2005). Diameter distributions tend to be broader and flatter than age distributions, which may mask the effects of disturbances (Stewart 1986). Also, inferences about stand development based on comparison of tree-size distributions among stands may be complicated by site productivity (Larson et al. 2008), but the present study suggests that site differences had little effect on intervals of post-fire establishment except at the most extreme sites (Figure 2.6).

Developmental pathways are organized into three sub-models, representing stand and age structures likely to develop in the context of a mean interval > 250 years between SR fires, along with (1) no NSR fire, (2) episodic NSR fire at intervals generally < 150 years, and (3) chronic NSR fire at intervals rarely > 100 years (Figure 2.7). These fire frequencies are approximate values drawn from fire-history studies near the study area (Teensma 1987; Morrison and Swanson 1990; Weisberg 1998, 2009). Divisions between sub-models were set where changes in the frequency of NSR fire were likely to foster

substantial differences in the age distributions and successional roles of shade-intolerant and shade-tolerant species (Figure 2.7).

Three stages of stand development are represented in the model, where each stage is defined by the age of the youngest post-fire cohort: young (< ca. 60 years), mature (ca. 60–200 years), and old growth (> ca. 200 years), from left to right in Figure 2.8. These stages do not correspond with stand age, which commonly is defined by the age of the oldest cohort (e.g., Weisberg 2004). Each stage may be subdivided to more accurately describe long-term trends (Franklin et al. 2002). Differences in forest stand and age structure associated with different fires histories are represented by idealized drawings that depict the number and species of cohorts in each age class (young, mature, and old growth; Figure 2.8). A histogram is provided from a sampled stand representative of each set of conditions, although the range of ages associated with each developmental stage is broader than that represented by a single histogram. For example, the stand conditions in the upper right corner of Figure 2.8 denote stands with only old-growth cohorts present, which is most clearly represented by age-structure type 1 in the present study area, but older or younger stands, or stands with two old-growth cohorts of shade-intolerant trees also could be included, as long as there has been no fire for > 200 years. Histograms are not provided for the left column of Figure 2.8 because none of the sampled stands had burned within the last 60 years.

The model includes four levels of fire severity (underburn, low, moderate, and high; Figure 2.8), where severity is defined in terms of fire-caused mortality of overstory trees (consistent with Agee (1993, 1998), but see Keeley (2009) for other definitions). Underburn and low-severity fire are defined as fire that affects the stand primarily from below and leave the upper canopy largely intact, with the distinction that a greater number of shade-tolerant trees survive an underburn. Moderate-severity fire was defined as fire that partially opens the upper canopy and enables regeneration of shade-intolerant trees, whereas high-severity fire was assumed to kill the majority of trees in a stand. Inferences about fire severity were drawn by comparing the density and species composition of trees that predate a post-fire cohort to that averaged across unburned

stands of similar age (Figure 2.3). Because it is not known whether these differences represent effects of a single burn, cumulative effects of two or more fires, or the effects of non-fire disturbances acting before or after the most recent fire, the model includes several pathways that could lead to each developmental stage (Figure 2.8).

Although the six age-structure types represent the most common stand conditions of the study area, a broader range of conditions may be represented in other parts of the region or at different time periods within the present study area. Some of these conditions are illustrated by identifying groups of stands within several of the age-structure types that probably have slight differences in development (e.g., evidence of an additional NSR fire provided by a healed-over fire scar found within an increment core). Although such conditions are represented at too few stands to provide distinct groups in the clustering analysis, they are represented in Figure 2.8 to provide a more complete conceptual model and facilitate application to other parts of the region (or when considering other time periods) where these conditions may be more common.

Developmental Pathways

Sub-Model of Infrequent SR fire

Age-structure type 1 and the majority of stands in type 5 represent old-growth and mature stages, respectively, along a sequence of stand development following SR fire with no subsequent burning (Figure 2.8). In the absence of NSR fire, stands typically support a single cohort of shade-intolerant trees dating to the last SR fire (Figure 2.7; Franklin et al. 2002). Shade-tolerant species are likely to exhibit continuous regeneration, initiating either along with the shade-intolerant trees (Winter et al. 2002a), or lagged several decades behind the establishment of shade-intolerant species, possibly reflecting a loss of seed sources due to repeated burning (Wimberly and Spies 2001).

Zenner (2005) used the differences in the timing of initial post-fire colonization by shade-tolerant species to distinguish two pathways under his catastrophic/maturation model. The structural pathway (Figure 2.8) is equivalent to the early part of the succession sequence of Franklin et al. (2002). It represents an initial floristics model

(Connell and Slayter 1977), where shade-intolerant and shade-tolerant species establish concurrently, and early structural development reflects different growth and mortality rates among species. The successional pathway (Figure 2.8) follows a relay floristics model, where widespread establishment of shade-tolerant species is delayed until seed sources are available, and aggregated mortality of canopy trees and increasing availability of coarse woody debris provide suitable conditions for shade-tolerant tree regeneration (Zenner 2005). Given a long (ca. 200–300 year) fire-free interval, the two pathways are likely to converge (Figure 2.8), as canopy gap formation and regeneration of shade-tolerant species override structural differences associated with initial colonization (Kashian et al. 2005).

Both pathways of early development are evident in age-structure type 5 (Figure 2.8). Stands were grouped into the pathway they most likely followed based on the proportion of establishment dates for shade-tolerant species that fall within the pulse of establishment by shade-intolerant species. The largest portion of stands (53% of stands in type 5) most likely followed the structural/initial floristics pathway (type 5a of Figure 2.8). On average, shade-tolerant species account for 65% of the trees > 15 cm dbh in these stands, and 68% of their establishment dates fall within the pulse of establishment by shade-intolerant species. These stands currently represent the biomass accumulation/stem exclusion or maturation stages in the succession sequence of Franklin et al. (2002). Despite similar ages, the average dbh of shade-tolerant trees (35.0 cm) is only slightly more than half that of shade-intolerant trees (65.8 cm), illustrating that different growth rates among species have strongly influenced structural development to this point (Wierman and Oliver 1979).

Thirty-three percent of stands in age-structure type 5 probably followed the successional/relay floristics pathway of Zenner (2005) (type 5b in Figure 2.8). Shade-tolerant trees are present in low numbers in these stands (11% of trees > 15 cm dbh). On average, only 4% of their establishment dates fall within the pulse of establishment by shade-intolerant species. These stands are located on steep, south-facing slopes, where exposure to solar radiation may have hindered establishment or limited survival of shade-

tolerant species that established in the open after fire (Larson and Franklin 2005). They also lack live trees, snags, or logs carried over from the previous stand, which suggests the stands may have initiated following one or more fires at short intervals that could have removed local seed sources (Spies et al. 1988, Gray and Franklin 1997, Wimberly and Spies 2001). These stands have a dense canopy of relatively uniform-sized Douglas-fir trees at a density (342 trees/ha) about twice that of the stands that followed the structural/initial floristics pathway (141 trees/ha, or 185 trees/ha after excluding two stands near the upper elevation limit of Douglas-fir).

Most stands of age-structure type 1 (89%) initiated between 1470 and 1610 (Figure 2.4a), and their structure is representative of the horizontal diversification stage of Franklin et al. (2002). Distinctive structural features include large Douglas-fir trees with long, asymmetrical crowns (Van Pelt and Nadkarni 2004), shade-tolerant trees of all sizes (Figure 2.5), and high spatial variation in vegetation coverage in the mid- and lower-canopy. The oldest living shade-tolerant trees recorded at each stand established between 1527 and 1653, within the pulse of establishment by shade-intolerant trees at 17% of the stands. The time since stand initiation approaches the maximum ages reported for western hemlock trees in the region (Packee 1990), which precludes using a comparison of ages of shade-intolerant and shade-tolerant species to determine which early developmental pathway the stands followed. However, these stands were located in cooler sites (deep valley bottoms, benches, and cirques) than the younger stands of age-structure type 5 that followed the successional/relay floristics pathway, which suggests that only stands found in cool sites favorable for early post-fire establishment of shade-tolerant species are likely to reach old ages without fire.

The remaining 11% of stands in age-structure type 1 have a single cohort of Douglas-fir trees > 700 years old. The most notable difference from the younger stands of type 1 is the form of Douglas-fir trees. Almost every tree has a broken top, trunk reiterations, and large epicormic branches (Van Pelt and Sillett 2008).

Sub-Model of Episodic NSR Fire

Developmental pathways within the sub-model of episodic NSR fire account for age-structure types 2, 3, 4, and a small portion of the stands in type 5 (Figure 2.8). Episodic NSR fire interspersed with infrequent SR events is likely to foster development of multi-cohort stands where shade-intolerant and shade-tolerant species both form distinct age cohorts (Figure 2.7). Most old-growth stands sampled in the present study, and in previous fire-history studies in the central western Cascades of Oregon, have evidence of at least one NSR fire since stand initiation (Figure 2.4; Stewart 1986, 1989; Morrison and Swanson 1990; Weisberg 1998, 2004). However, the occurrence of NSR fire does not necessarily imply a high fire frequency. Many stands in the present study area probably have experienced at least one 100–200-year interval without fire (or where no fire left a detectable scar or enabled establishment of an age cohort that persists to the present) (Stewart 1986, 1989; Weisberg 2004).

Relatively long fire-free intervals may be important for the development of stand- and tree-level attributes that enable development of distinct age cohorts in response to subsequent NSR fire. For example, when fire-free intervals are longer than the time required for disturbed stands to develop canopy closure, recruitment of shade-intolerant species may be limited to discrete pulses following fire that opens the canopy (Figure 2.4d). Also, relatively long fire-free intervals (> ca. 100 years) enable vertical stratification of the canopy according to species shade-tolerance and resistance to fire-caused mortality (Figure 2.7). Continued regeneration only of shade-tolerant species following canopy closure and slow growth of these trees limits them primarily to the lower canopy, whereas faster-growing shade-intolerant trees are likely to be found only in the upper canopy. Development of thick bark and the pruning of shaded lower branches of these shade-intolerant trees render them relatively resistant to mortality by subsequent fire. As a result, the next fire of low intensity may kill most thin-barked, shade-tolerant trees of the lower canopy while leaving the upper canopy largely intact. Such patterns of mortality may be common in portions of most fires in Douglas-fir/western hemlock forests due to tremendous differences in resistance to fire-caused

mortality between Douglas-fir and its most abundant shade-tolerant associates (western hemlock, western redcedar, and Pacific silver fir).

NSR fire may either reduce structural complexity relative to unburned stands, or sustain complex structure throughout the development of younger cohorts. Simplification of forest structure is most likely after stands have reached canopy closure and the fire kills lower-strata vegetation while causing little mortality to upper-canopy trees. Persistence of complex structure following NSR fire is likely when the fire generates canopy openings of sufficient size to permit establishment of shade-intolerant trees, but numerous trees survive. The surviving trees persist as dominant structural features and strongly influence the density, spatial distribution, and growth rates of each species in the post-fire cohort (Goslin 1997, Rose and Muir 1997, Zenner 2000). The large numbers of trees that survive moderate-severity fire and their strong contribution to stand structure differs from the smaller number of live legacy trees that may persist following SR fire. For example, in the development sequence following SR fire described by Franklin et al. (2002), the structure of live vegetation in all but the disturbance/legacy creation stage was described only in terms of vegetation that established after the fire.

Simplification of forest structure by NSR fire is exemplified by age-structure type 3. Each stand has a 400–500-year-old cohort of shade-intolerant species and a younger post-fire cohort of shade-tolerant trees (Figure 2.4c). Unlike stands that develop in the absence of NSR fire and have vertically continuous foliage (Franklin et al. 2002), each of the two cohorts in age-structure type 3 forms a relatively distinct canopy layer. Van Pelt and Franklin (2000) have characterized such a two-layered canopy for an old-growth stand in the Blue River study area that contains a post-fire cohort of shade-tolerant trees initiated in the mid-1800s. The Douglas-fir trees were ca. 500 years old and 60–70-m tall, and their foliage volume peaked at a height of 40–45 m. Foliage of the shade-tolerant trees formed a dense layer 15–25-m high. Total leaf area was lower than that in a nearby unburned old-growth stand, but understory light levels were markedly reduced due to shading by the dense mid canopy (Van Pelt and Franklin 2000). Shading by a post-fire cohort of shade-tolerant trees may hinder understory development more than a century

after fire (Stewart 1986, 1989), as illustrated by the low abundance of small trees and shrubs (< 15 cm dbh) in age-structure type 3 (482 stems/ha) compared to that in the other age-structure types (Table 2.1).

Eventually, crown differentiation and thinning of the post-fire cohort of shade-tolerant trees, along with additional regeneration of shade-tolerant trees, is likely to generate complex mid- and lower-canopy structure similar to that in unburned stands. The time required for re-development of complex structure depends in part on stand age at the time of the fire. For example, the unburned old-growth stands of age-structure type 1 are in the horizontal diversification stage of Franklin et al. (2002), which is characterized by complex mid- and lower-canopy structure that developed in response to centuries of shade-tolerant tree regeneration under fine-scale canopy gaps. In age-structure type 3, the abrupt pulse of post-fire regeneration by shade-tolerant species provides mid- and lower-canopy structure that remains relatively uniform 1–2 centuries since the last fire. Even in the portion of stands of age-structure type 2 (23% of stands in this type) that have a cohort of shade-tolerant trees that most likely initiated following fire in the 18th century with no additional fire to the present (type 2b of Figure 2.8), the density of large shade-tolerant trees remains lower than that in age-structure type 1 (Figure 2.5).

Development of stand structure similar to that in unburned stands may occur more rapidly in stands that were of mature age (ca. 80–200 years old) at the time of the fire. For example, in 13% of the stands classified under age-structure type 5, a healed-over fire scar was found within an increment core, and an abrupt pulse of shade-tolerant tree establishment was initiated shortly after the scar year (type 5c of Figure 2.8). Because mature stands have relatively low structural complexity in the absence of NSR fire (Franklin et al. 2002), it did not take long for post-fire establishment by shade-tolerant species in the burned stands to generate mid- and lower-canopy structure resembling that in stands of age-structure type 5 that followed the structural/initial floristics pathway with no NSR fire.

The degree to which fire that kills understory vegetation while leaving the upper canopy intact simplifies stand structure may be reduced if fire intensity is low enough that a portion of the shade-tolerant trees survive. For example, several stands of age-structure type 2 (35%) most likely experienced fire in the 19th century, which did not reduce the density of shade-intolerant trees relative to that in age-structure type 1, and shade-tolerant trees at a density ≥ 20 trees/ha also predate the fire (type 2a of Figure 2.8). Shade-intolerant trees in each of these stands have charred bark, and western redcedar trees with an open catface were more common than in any other age-structure type. These trees predate a pulse of establishment by shade-tolerant trees within the stand, which corresponds to an establishment pulse of shade-intolerant trees at an adjacent slope position along the same slope facet. Shade-tolerant trees that survive fire can be seed sources that facilitate re-establishment (Keeton and Franklin 2005), and shading by these trees may promote heterogeneity in the post-fire cohort by reducing tree density and growth rates of younger trees that establish near them (Goslin 1997).

The potential for NSR fire to sustain complex forest structure throughout the development of younger cohorts most clearly is illustrated in age-structure type 4. Each stand of type 4 has a cohort of mature age (initiated after 1780) containing shade-intolerant and shade-tolerant species and an old-growth cohort of shade-intolerant trees, usually initiated in the 1500s (Figure 2.4d). Retention of large numbers of old-growth trees following the most recent fire enabled stands to forgo the otherwise low structural complexity characteristic of mature stands initiated after SR fire (Spies and Franklin 1988). At an average density (45 trees/ha) about 2/3 the density of shade-intolerant trees in unburned old-growth stands (62 trees/ha in age-structure type 1; Figure 2.3), the old cohort in type 4 has maintained a partially intact upper canopy since the last fire. Tree density in the old cohort essentially is equivalent to the density (40 trees/ha) described as optimal for enabling abundant Douglas-fir trees in the young cohort of two-cohort stands and maximizing a structural complexity index that accounts for spatial variation in tree dbh (Zenner 2000). Abundant old trees provide a heterogeneous environment that favors lower, more spatially heterogeneous tree density and greater variation in growth rates in

the post-fire cohort than typical of stands initiated following SR fire (Goslin 1997, Acker et al. 1998a, Zenner 2000).

A small portion (18%) of stands in age-structure type 4 has two cohorts of shade-intolerant trees and a third cohort of shade-tolerant trees, probably initiated after low-severity fire that allowed numerous shade-intolerant trees of the younger cohort to survive (type 4b of Figure 2.8). Charred bark was recorded on both cohorts of shade-intolerant trees, and an abrupt pulse of regeneration by shade-tolerant trees was initiated usually within 100 years of initiation of the younger cohort.

Sub-Model of Chronic NSR Fire

Stands of age-structure type 6 developed in the context of relatively frequent NSR fire, probably at intervals rarely > 100 years (Figure 2.8). At this relatively high frequency, NSR fire is likely to foster development of multi-cohort stands, where shade-intolerant species span a broad range of ages and are abundant in all canopy layers (Figure 2.7). Ages of shade-tolerant species are limited primarily to the interval since the most recent fire (Figure 2.4f), limiting these trees primarily to the smallest size classes (Figure 2.5).

NSR fire is likely to be a chronic occurrence only at particularly dry sites in the western Cascade Range (Means 1982). At extreme sites, too dry to support high canopy coverage, Douglas-fir may function as a climax species capable of regenerating and forming a broad age distribution in the absence of fire (e.g., the *Pseudotsuga/Holodiscus discolor* plant association of Franklin and Dyrness 1973), making it difficult to distinguish influences of fire on stand development from effects of the harsh environment. However, such dry conditions with a very low abundance of shade-tolerant trees apply to only 38% of stands classified as age-structure type 6, and charred bark was recorded in each of these stands (Figure 2.4f). In the remaining 62% of stands in types 6, shade-tolerant trees were common (> 20% of trees > 15 cm dbh), and the understory species composition was characteristic of slightly more mesic plant associations (the *Tsuga heterophylla/Castanopsis chrysophylla* or *Tsuga heterophylla/Rhododendrom*

macrophyllum/Gaultheria shallon associations of Franklin Dyrness 1973), suggesting western hemlock would likely replace Douglas-fir in the absence of fire.

Stand development under relatively frequent NSR fire may contribute to complex structure of live vegetation, including several attributes (large Douglas-fir trees and strong within-stand heterogeneity in tree size and density) commonly associated with stand development over centuries-long intervals without fire (Acker et al. 1998b). In age-structure type 6, trees with charred bark that survived at least one fire, and sometimes three or more fires, contribute to an average density of large (> 100 cm dbh) shade-intolerant trees (34 trees/ha) only 35% lower than that in type 1 (52 trees/ha), where stands lack evidence of fire for more than 400 years (Table 2.1). Tree size and tree density are highly variable in both age-structure types. However, in the context of relatively frequency NSR fire, this heterogeneity was driven primarily by fine-scale patchiness in fire-caused mortality and post-fire regeneration of shade-intolerant species, as opposed to gap-phase regeneration of shade-tolerant species in the absence of fire (Figure 2.7). For example, stem maps of aged trees in two stands (0.5 and 0.75 ha in area) in the central western Cascades of Oregon that had at least three cohorts of shade-intolerant trees illustrate that trees that survived at least one fire were clustered primarily in 0.1–0.3-ha patches, interspersed with denser patches of younger vegetation that established after the most recent fire (Means 1982).

Even in the context of relatively frequent NSR fire, stands may be subject to SR fire, especially in events driven by extreme fire weather (Turner and Romme 1994, Thompson and Spies 2009). All stands of age-structure type 6 have at least two cohorts of shade-intolerant trees initiated after 1780. Most stands (77%) also have an older cohort that initiated before 1780 (type 6a of Figure 2.8). The remaining stands lack an older cohort (type 6b of Figure 2.8). The absence of older trees in these stands may be due to a single SR fire before 1780, or to gradual removal of older trees over successive fires.

Post-Fire Establishment

Shade-intolerant species consistently formed distinct cohorts in almost all topographic settings, regardless of the time period that cohorts were initiated. Overall, 87% of establishment dates fell within pulses up to 40 years long, with multiple pulses per stand separated either by intervals longer than 80 years with no recorded establishment, or by healed-over fire scars within increment cores (10% of all cohorts were distinguished by scars and would not have been separated from the older cohort using only an 80-year interval with no establishment) (Figure 2.6a). Old-growth cohorts appear to have initiated over intervals similar to younger cohorts. For example, 87% of all establishment dates for shade-intolerant species fell within pulses initiated in the periods 1470–1610 or 1780–1940, and the proportion of trees that established within 40 years of cohort initiation during the earlier period (90%) was nearly identical to that in the later period (89%) (Figure 2.6c). The duration of cohort establishment also showed no strong differences in relation to elevation, slope position, or aspect, except in a small number of extreme sites mentioned below, with shallow, rocky soil or near the upper elevation limit of Douglas-fir.

Establishment primarily over the first four decades following fire is substantially longer than establishment periods for plantations and those likely to result from post-fire management aimed at hastening development of closed-canopy forest (Sessions et al. 2004). However, this study found no evidence that extended periods of post-fire establishment (lasting more than a century) were widespread in older stands, as suggested by several previous studies (Franklin and Hemstrom 1981, Tappeiner et al. 1997, Poage and Tappeiner 2002).

The previous interpretation of long (> 100 years) post-fire establishment periods in old-growth stands may have been influenced, at least in part, by errors associated with counting tree rings in the field. This was the method used to determine tree ages essentially in all studies supporting such findings (Franklin and Hemstrom 1981, Tappeiner et al. 1997, Poage and Tappeiner 2002, Poage et al. 2009). The cross-dating of

samples from 52, 90–440-year-old Douglas-fir trees previously aged in the field reveals that field-counted ages consistently were underestimated, by an average of 25 years, and errors increased with tree age (Weisberg and Swanson 2001). Even after excluding an outlier whose age was overestimated by 89 years, errors were spread over about 100 years, implying that counting errors alone could lead to the perception of a 100-year establishment period in old-growth stands, even if all trees established in a single year. Age underestimates, smearing of discrete recruitment events, and increasing errors with age also were evident in a comparison of counting vs. cross-dating of annual growth increments in a long-lived species of marine mollusk (Black et al. 2008).

The problem of aging old-growth trees in the field is illustrated by a re-evaluation of data for Watershed 10 at the H. J. Andrews Experimental Forest (within the Blue River study area), which was one of the first studies to report a long establishment period in old-growth forests (Franklin and Hemstrom 1981). Before the 10-ha watershed was harvested, in 1975, all trees > 15 cm dbh were mapped and tagged near ground level. Shortly after harvest, ages of about 600 trees were determined in the field. Pith dates for most old-growth Douglas-fir trees fell between 1455 and 1605, with no indication of multiple peaks of establishment over this period, and the ages of mapped old-growth trees did not appear to be related to site conditions or indicative of fine-scale disturbances (Franklin et al. 1979, Franklin and Waring 1980). In 1998, wedges were collected from five tagged stumps that still had sound heartwood (Winter, unpublished data). Cross-dating of these samples using the master chronology for the present study reduced the range of pith dates from 217 years (1443–1660) to 34 years (1497–1531). One tree had a fire scar in 1555. The fire could have enabled additional Douglas-fir establishment, contributing to the wide age range found in the field-counted data. However, field-counted pith dates for four of the five cross-dated trees were after the fire year, when in fact all five trees established before the fire. This discrepancy illustrates that the accuracy of field-counted data is too poor to distinguish a broad establishment period from multiple pulses in old-growth stands, even with a stem map of a large number of trees.

The finding of relatively short establishment pulses in the present study is consistent with studies of initial post-fire colonization spanning much of the climatic gradient in the Douglas-fir region of the PNW, and with the few retrospective studies that employed cross-dating. Douglas-fir seedlings were abundant within the first few years following fires in the Olympic Mountains of Washington (Agee and Huff 1980), the Coast Range and western Cascades of Oregon (Isaac and Meagher 1936, Larson and Franklin 2005), and the Klamath and Siskiyou Mountains of southwestern Oregon and northwestern California (Shatford et al. 2007, Donato et al. 2009). In stand reconstructions, 94 of 97 Douglas-fir trees sampled in a 10-ha stand near Mount St. Helens established in a 40-year period following fire in the early 1300s (Yamaguchi 1993), and all 58 Douglas-fir trees present in a 3.3-ha stand in the western Cascades of southwestern Washington established over a 21-year period following fire around 1500 (Winter et al. 2002a). Although fewer trees were sampled per stand in the present study, the consistency of relatively short establishment pulses across the majority of 124 stands and over time (Figure 2.6) suggests that relatively rapid post-fire establishment was widespread.

This study does not negate the existence of extended post-fire recruitment periods, but suggests they are much less common in the central western Cascades of Oregon than previously believed. Extended periods of post-fire establishment may occur on extremely dry sites or near the upper elevation limit of Douglas-fir. For example, Douglas-fir seedlings were still becoming established on dry slopes more than 50 years after a late 19th-century fire on Mount Rainier (Hemstrom 1979), and periods of post-fire establishment lasting 60–150 years have been reported at particularly dry sites in the central western Cascades of Oregon (Means 1982; but ages of large trees in this study were determined using regressions to extrapolate up to 20% of tree age beyond the end of increment cores). Three stands of age-structure type 6 were located on particularly dry sites and have a broad age distribution for cohorts initiated between 1610 and 1780 (Figure 2.6c). The broad age ranges found in these stands may represent gradual

establishment following a single fire or establishment following two or more fires that did not leave evidence in the data set.

Overlapping periods of post-fire recruitment produced by short-interval fires occasionally may reduce the distinctiveness of post-fire cohorts in the study area. For example, portions of the 1933 Tillamook Fire reburned in 1939, 1945, and 1951 (Pyne 1982). Similar short-interval fires may have contributed to the 10% of cohorts in the present study that were identified based on healed-over fire scars and would not have been distinguished from the older cohort using the criteria of no establishment dates in an 80-year window prior to cohort initiation. However, it was more common that multiple cohorts per stand were represented by discrete pulses of establishment separated by intervals > 80 years long (Figure 2.6c). This finding is consistent with the conventional interpretation that Douglas-fir regeneration in this region depends on disturbances that open the canopy (Munger 1930, Isaac 1943, Spies and Franklin 1989), and mean fire intervals (estimated at 95–149 years in three studies partially overlapping the Blue River study are; Teensma 1987, Morrison and Swanson 1990, Weisberg 1998) are longer than the time generally required for disturbed stands to develop canopy closure (ca. 20–50 years; Long 1977, Schoonmaker and McKee 1988, Yang et al. 2005). Overlapping post-fire recruitment periods leading to widespread occurrence of stands lacking distinct age cohorts is likely only in areas with consistently higher fire frequency, such as foothills along the Willamette Valley margin (Robbins 2004) and portions of the southern Klamath Mountains (Taylor and Skinner 2003).

A lack of seed sources (associated with large fires or reburns) and competition from shrubs probably played little role in delaying post-fire colonization of shade-intolerant species in the present study area. For a lack of seed sources to delay Douglas-fir colonization, areas of complete mortality would have to be larger than those commonly observed following fire (Turner et al. 1994). For example, Douglas-fir establishment occurred primarily within the first 60 years after the 1480 eruption of Mount St. Helens, except in portions of the complete mortality zone > 2 km from seed sources, where colonization proceeded gradually over more than 200 years (and may

have been complicated by infertile, freshly deposited, coarse tephra; Yamaguchi 1993). However, even after the 200,000-ha Biscuit Fire of 2002, which completely reburned the 38,000-ha Silver Fire of 1987, 71–90% of SR portions of the fire (excluding serpentine areas) was within 400 m of patches larger than 1 ha, where > 25% of overstory trees survived (Donato et al. 2009). Post-fire seedling density was high up to 400 m from these patches, and a peak in seedling abundance the second year after the fire indicates that surviving trees were important seed sources. Sprouting hardwoods and shrubs in SR portions of several fires in southwestern Oregon and northwestern California did not delay conifer establishment, and there was no evidence of growth suppression leading to mortality in conifers overtopped by hardwoods or shrubs (Shatford et al. 2007).

Conclusions and Management Implications

The diversity of forest stand and age structures found in this study (Figures 2.4 and 2.5) reflects the complexity of the fire regime and the numerous ways that fire of varying frequency and severity interacts with the dominant tree species (Figure 2.8). The organization of these diverse stand conditions into a conceptual model of fire-mediated developmental pathways, with three sub-models reflecting differences in the frequency of NSR relative to SR fire (Figures 2.7 and 2.8), provides a useful framework for interpreting the effects of regional and local variation in the fire regime on the distribution of different forest conditions across the landscape. At a regional scale, for instance, the dominant sub-model shifts from episodic NSR fire in the Fall Creek study area, where annual precipitation averages 182 cm (Daly et al. 2008) and 70% of sampled stands had two or more cohorts of shade-intolerant trees, to the sub-model of infrequent SR fire in the Bull Run watershed in the northernmost part of the western Cascades of Oregon, where annual precipitation averages 279 cm and only 10–25% of stands had more than one cohort of shade-intolerant trees (Agee and Krusemark 2001). However, all three sub-models may be represented to some extent in both study areas. At a local level, in the complex terrain characteristic of the western Cascade Range, I hypothesize that each sub-model may be most strongly associated with different parts of the landscape (chapter 3).

The characterization of developmental pathways associated with the mixed-severity regime in the central western Cascades of Oregon may facilitate comparisons to forest dynamics among other mixed-severity systems. Mixed-severity regimes commonly are associated with mixed-conifer forests of southwestern Oregon and northwestern California (Taylor and Skinner 1998), portions of the eastern Cascades of Washington and Oregon (Hessburg et al. 2007), and mid elevations throughout much of the Rocky Mountains (Schoennagel et al. 2004). Similar to the present study area, each of these systems supports mosaics of even-aged and multi-cohort stands, with a broad range of stand densities and stand structures. Several key differences are that drier mixed-conifer forests generally have higher fire frequency than the present study area, which may contribute to greater overlap in post-fire recruitment periods. Thus, shade-intolerant species may exhibit pulses of establishment associated with fires that cause substantial mortality (Sherriff and Veblen 2006), but there is not likely to be an absence of shade-intolerant tree regeneration in the intervening periods, as found in this study. Also, unlike the present study area, where dominant tree species are strongly differentiated along a continuum of shade tolerance and resistance to fire-caused mortality, intermediate values are better represented in most mixed-conifer systems. Therefore, the potential for fire to kill most shade-tolerant trees of the mid and lower canopy while leaving the upper canopy intact, followed by initiation of a post-fire cohort of shade-tolerant species (e.g., age-structure type 3) may be unique to this system.

The age-structure data including ages of all species complements previous fire-history work in the region based on field-counted fire scars and ages of Douglas-fir trees to further clarify the historic fire regime of the region and its effects on stand development. Such a characterization may be useful where there is interest in emulating historical disturbances (Cissel et al. 1999). Also, the differences between the range of forest stand and age structure characteristics common to the present study area and that found in wetter parts of the region that lack NSR fire (Huff 1995, Winter et al. 2002a and b) may contribute to a regional framework for guiding differences in management objectives and strategies, opposed to lumping all Douglas-fir/western hemlock forests

west of the crest of the Cascades under a single bin with a narrow range of management options.

LITERATURE CITED

Acker, S.A., E.K. Zenner, and W.H. Emmingham. 1998a. Structure and yield of two-aged stands on the Willamette National Forest, Oregon: implications for green tree retention. *Can. J. For. Res.* 28: 749–758.

Acker, S.A., T.E. Sabin, L.M. Ganio, and W.A. McKee. 1998b. Development of old-growth structure and timber volume growth trends in maturing Douglas-fir stands. *For. Ecol. Manage.* 104: 265–280.

Agee, J.K. 1993. *Fire Ecology of Pacific Northwest Forests*. Island Press. Washington, D.C. 493 pp.

Agee, J.K. 1998. The landscape ecology of western forest fire regimes. *Northwest Sci.* 72: 24–34.

Agee, J.K., and M.H. Huff. 1980. First year ecological effects of the Hoh fire, Olympic Mountains, Washington. pp. 175–181 *in* R.E. Martin, R.L. Edmonds, D.A. Faulkner, F.B. Harrington, D.M. Fuquay, B.J. Stocks, and S. Barr (eds.). Proceedings Sixth Conference on Fire and Forest Meteorology. Seattle, WA. April 22-24, 1980.

Agee, J.K., and F. Krusemark. 2001. Forest fire regime of the Bull Run watershed, Oregon. *Northwest Sci.* 75: 292–306.

Barrett, S.W., and S.F. Arno. 1988. Increment-borer methods for determining fire history in coniferous forests. USDA For. Serv. Gen. Tech Rep. INT-244. Ogden, UT. 15 pp.

Black, B.A., D.C. Gillespie, S.E. MacLellan, and C.M. Hand. 2008. Establishing highly accurate production-age data using the tree-ring technique of crossdating: a case study for Pacific geoduck (*Panopea abrupta*). *Can. J. Fish. Aquat. Sci.* 65: 2572–2578.

Cissel, J.H., F.J. Swanson, and P.J. Weisberg. 1999. Landscape management using historical fire regimes: Blue River, Oregon. *Ecol. App.* 9: 1217–1231.

Connell, J.H., and R.O. Slayter. 1977. Mechanisms of succession in natural communities and their role in community stability. *Amer. Natur.* 111: 1119–1144.

Daly, C., M. Halbeib, J.I. Smith, W.P. Gibson, M.K. Doggett, G.H. Taylor, J. Curtis, and P.P. Pasteris. 2008. Physiographically sensitive mapping of climatological temperature and precipitation across the conterminous United States. *Int. J. Climatol.* 28: 2031–2064.

Donato, D.C., J.B. Fontaine, J.L. Campbell, W.D. Robinson, J.B. Kauffman, and B.E. Law. 2009. Conifer regeneration in stand-replacement portions of a large mixed-severity wildfire in the Klamath-Siskiyou Mountains. *Can. J. For. Res.* 39: 823–838.

Duncan, R.P. 1989. An evaluation of errors in tree age estimates based on increment cores in Kahikatea (*Dacrycarpus cacrydioides*). *New Zealand Nat. Sci.* 16: 31–37.

Fox, J. 1997. *Applied Regression, Linear Models, and Related Methods.* Sage Publications. Thousand Oaks, CA. 624 pp.

Franklin, J.F., and C.T. Dyrness. 1973. Natural vegetation of Oregon and Washington. USDA For. Serv. Gen. Tech. Rep. PNW-GTR-8. 417 pp.

Franklin, J.F., and M.A. Hemstrom 1981. Aspects of succession in the coniferous forests of the Pacific Northwest. pp. 222–229 *in* D.C. West, H.H. Shugart, and D.B. Botkin (eds.). *Forest Succession.* Springer-Verlag. New York.

Franklin, J.F., A. McKee, F.J. Swanson, J. Means, and A. Brown. 1979. Age structure analyses of old-growth Douglas-fir stands: data versus conventional wisdom. *Bull. Ecol. Soc. Am.* 60: 102.

Franklin, J.F., T.A. Spies, R. Van Pelt, A.B. Carey, D.A. Thornburgh, D.R. Berg, D.B. Lindenmayer, M.E. Harmon, W.S. Keeton, D.C. Shaw, K. Bible, and J. Chen. 2002. Disturbances and structural development of natural forest ecosystems with silvicultural implications, using Douglas-fir forests as an example. *For. Ecol. Manage.* 155: 399–423.

Franklin, J F., and R.H. Waring. 1980. Distinctive features of the northwestern coniferous forest: Development, structure, and function. *In* Forests: Fresh perspectives from ecosystem analysis. R. H. Waring, ed. Proc. 40th Annu. Biol. Colloq. 1979: 59-86. Oreg. State Univ. Press, Corvallis.

Garza, E.S. 1995. Fire history and fire regimes of East Humbug and Scorpion Creeks and their relation to the range of *Pinus lambertiana* Dougl. M.S. Thesis. Oregon State University. Corvallis.

Gedalof, Z., D.L. Peterson, and N.J. Mantua. 2005. Atmospheric, climatic, and ecological controls on extreme wildfire years in the northwestern United States. *Ecol. App.* 15: 154–174.

Goslin, M.N. 1997. Development of two coniferous stands impacted by multiple, partial fires in the Oregon Cascades: establishment history and the spatial patterns of colonizing tree species relative to old-growth remnant trees. M.S. Thesis. Oregon State University. Corvallis.

Gray, A.N., and J.F. Franklin. 1997. Effects of multiple fires on the structure of southwestern Washington forests. *Northwest Sci.* 71: 174–185.

Hemstrom, M.A. 1979. A recent disturbance history of forest ecosystems at Mount Rainier National Park. Ph.D. Dissertation. University of Washington, Seattle.

Hemstrom, M.A., and J.F. Franklin. 1982. Fire and other disturbances of the forests in Mount Rainier National Park. *Quat. Res.* 18: 32–51.

Hessburg, P.F., R.B. Salter, and K.M. James. 2007. Re-examining fire severity relations in pre-management era mixed conifer forests: inferences from landscape patterns of forests structure. *Landscape Ecol.* 22: 5–24.

Huff, M.A. 1995. Forest age structure and development following wildfires in the western Olympic Mountains, Washington. *Ecol. App.* 5: 471–483.

Impara, P.C. 1997. Spatial and temporal patterns of fire in the forests of the central Oregon Coast Range. Ph.D. Dissertation. Oregon State University, Corvallis.

Isaac, L.A. 1943. Reproductive habits of Douglas-fir. Charles Lathrop Pack Forestry Foundation, Washington, DC.

Isaac, L.A., and G.S. Meagher. 1936. Natural reproduction on the Tillamook Burn two years after the fire. Pacific Northwest Experimental Station. USDA Forest Service, Portland, OR.

Kashian, D.M., M.G. Turner, W.H. Romme, and C.G. Lorimer. 2005. Variability and convergence in stand structural development on a fire-dominated subalpine landscape. *Ecology* 86: 643–654.

Keeley, J.E. 2009. Fire intensity, fire severity and burn severity: a brief review and suggested usage. *Int. J. Wildl. Fire* 18: 116–126.

Keeton, W.S., and J.F. Franklin. 2005. Do remnant old-growth trees accelerate rates of succession in mature Douglas-fir forests? *Ecol. Monogr.* 75: 103–118.

Larson, A.J., and J.F. Franklin. 2005. Patterns of conifer tree regeneration following an autumn wildfire event in the western Oregon Cascade Range, USA. *For. Ecol. Manage.* 218: 25–36.

Larson, A.J., J.A. Lutz, R.F. Gersonde, J.F. Franklin, and F.F. Hietpas. 2008. Potential site productivity influences the rate of forest structural development. *Ecol. App.* 18: 899–910.

Long, J.N. 1977. Trends in plant species diversity associated with development in a series of *Pseutotsuga menziesii/Gaultheria shallon* stands. *Northwest Sci.* 51: 119–130.

McCune, B., and J.B. Grace. 2002. Analysis of Ecological Communities. MJM Software Design. Gleneden Beach, OR.

Means, J.E. 1982. Developmental history of dry coniferous forests in the central western Cascade Range of Oregon. pp. 142–158 *in* J.E. Means (ed.), Forest Succession and Stand Development Research in the Northwest. Forest Research Laboratory, Oregon State University, Corvallis, Oregon, USA.

Morrison, P.H., and F.J. Swanson. 1990. Fire history and pattern in a Cascade Range landscape. USDA For. Serv. Gen. Tech. Rep. PNW-254.

Munger, T.T. 1930. Ecological aspects of the transition from old forests to new. *Science* 72: 327–332.

Munzel, U., and L.A. Hothorn. 2001. A unified approach to simultaneous rank test procedures in the unbalanced one-way layout. *Biometrical J.* 43: 553–569.

Oliver, C.D. 1981. Forest development in North America following major disturbances. *For. Ecol. Manage.* 3: 153–168.

Packee, E.C. 1990. *Tsuga heterophylla* (Raf.) Sarg. Western Hemlock. *In*: Burns, R.M., and B.H. Honkala (tech. eds.), Silvics of North America: 1. Conifers. Agriculture Handbook, vol. 654. USDA For. Serv. Washington, DC. pp. 613–622.

Peet, R.K., and N.L. Christensen, 1987. Competition and tree death. *BioScience* 37: 586–594.

Poage, N.J., and J.C. Tappeiner, III. 2002. Long-term patterns of diameter and basal area growth of old-growth Douglas-fir trees in western Oregon. *Can. J. For. Res.* 32: 1232–1243.

Poage, N.J., W.J. Weisberg, P.C. Impara, J.C. Tappeiner, and T.S. Sensenig. 2009. Influences of climate, fire, and topography on contemporary age structure patterns of Douglas-fir at 205 old forest sites in western Oregon. *Can. J. For. Res.* 39: 1518–1530.

Pyne, S. 1982. *Fire in America*. Princeton University Press. Princeton, N.J.

R Development Core Team. 2006. R: A language and environment for statistical computing. *In* R Foundation for Statistical Computing, Vienna, Austria.

Robbins, D. 2004. Temporal and spatial variability of historic fire frequency in the southern Willamette Valley foothills of Oregon. M.S. Thesis. Oregon State University, Corvallis.

Rose, C.R., and P.S. Muir. 1997. Green-tree retention: consequences for timber production in forests of the western Cascades, Oregon. *Ecol. App.* 7: 209–217.

Schoennagel, T., T.T. Veblen, and W.H. Romme. 2004. The interaction of fire, fuels, and climate across Rocky Mountain Forests. *BioScience* 54: 661–676.

Schoonmaker, P., and A. McKee. 1988. Species composition and diversity during secondary succession of coniferous forests in the western Cascade Mountains of Oregon. *For. Sci.* 34: 960–979.

Sessions, J., P. Bettinger, R. Buckman, M. Newton, and A. J. Hamann. 2004. Hastening the return of complex forests following fire: The consequences of delay. *J. For*. 102: 38–45.

Shatford, J. P. A., D. E. Hibbs, and K. J. Puettmann. 2007. Conifer regeneration after forest fire in the Klamath-Siskiyous: How much, how soon? *J. For.* 105: 139-146.

Sherriff, R.L., and T.T. Veblen. 2006. Ecological effects of changes in fire regimes in *Pinus ponderosa* ecosystems in the Colorado Front Range. *J. Veg. Sci.* 17: 705–718.

Skinner, C.N., and A.H. Taylor. 2006. Southern Cascades Bioregion. *In*: Fire in California's Ecosystems. Edited by N.G. Sugihara, J.W. van Wagtendonk, J. Fites-Kaufman, K.E Shaffer, A.E. Thode. University of California Press, Berkeley. pp. 195–224.

Spies, T.A., and J.F. Franklin. 1988. Old growth and forest dynamics in the Douglas-fir region of western Oregon and Washington. *Nat. Areas J.* 8: 190–201.

Spies, T.A., and J.F. Franklin. 1989. Gap characteristics and vegetation response in coniferous forests of the Pacific Northwest. *Ecology* 70: 543–545.

Spies, T.A., J.F. Franklin, and T.B. Thomas. 1988. Coarse woody debris in Douglas-fir forests of western Oregon and Washington. *Ecology* 69: 1689–1702.

Stewart, G.H. 1986. Population dynamics of a montane conifer forest, western Cascade Range, Oregon, USA. *Ecology* 67: 534–544.

Stewart, G.H. 1989. The dynamics of old-growth *Pseudotsuga* forests in the western Cascade Range, Oregon, USA. *Vegetatio* 82: 79–94.

Stokes, M.A., and T.L. Smiley 1996. An introduction to tree-ring dating. University of Arizona Press, Tucson.

Swetnam, T.W., and C.H. Baisan. 1996. Historical fire regime patterns in the southwestern United States since AD 1700. *In* C.D. Allen (tech. ed.). *Fire Effects in Southwestern Forests*. Proceedings of the second La Mesa Fire Symposium. March 29–31, 1994. Los Alamos, NM. USDA For. Serv. Gen. Tech. Report RM-GTR-286. pp. 11–32.

Swetnam, T.W., C.D. Allen, and J.L. Betancourt. 1999. Applied historical ecology: using the past to manage the future. *Ecol. App.* 9: 1189–1206.

Tappeiner, J.C., D. Huffman, H. Marshall, T.A. Spies, and J.D. Bailey. 1997. Density, ages, and growth rates in old-growth and young-growth forests in coastal Oregon. *Can. J. For. Res.* 27: 638–648.

Taylor, A.H., and C.N. Skinner. 1998. Fire history and landscape dynamics in a late-successional reserve, Klamath Mountains, California, USA. *For. Ecol. Manage.* 111: 285–301.

Taylor, A.H., and C.N. Skinner. 2003. Spatial patterns and controls on historical fire regimes and forest structure in the Klamath Mountains. *Ecol. App.* 13: 704–719.

Teensma, P.D.A. 1987. Fire history and fire regimes of the central Western Cascades of Oregon. Ph.D. Dissertation. Department of Geography. University of Oregon, Eugene.

Thompson, J.R., and T.A. Spies. 2009. Vegetation and weather explain variation in crown damage within a large mixed-severity wildfire. *For. Ecol. Manage.* 258: 1684–694.

Turner, M.G., W.W. Hargrove, R.H. Gardner, and W.H. Romme. 1994. Effects of fire on landscape heterogeneity in Yellowstone National Park, Wyoming. *J. Veg. Sci.* 6: 731–742.

Turner, M.G., and W.H. Romme. 1994. Landscape dynamics in crown fire ecosystems. *Landscape Ecol.* 9: 59–77.

Van Norman, K. 1998. Historical fire regime in the Little River watershed, southwestern Oregon. M.S. Thesis, Oregon State University. Corvallis.

Van Pelt, R., and J.F. Franklin. 2000. Influence of canopy structure on the understory environment in tall, old-growth, conifer forests. *Can. J. For. Res.* 30: 1231–1245.

Van Pelt, R., and N.M. Nadkarni. 2004. Development of canopy structure in *Pseudotsuga menziesii* forests in the southern Washington Cascades. *For. Sci.* 50: 326–341.

Van Pelt, R. and S.C. Sillett. 2008. Crown development of coastal *Pseudotsuga menziesii*, including a conceptual model for tall conifers. *Ecol. Monogr.* 78: 283–311.

Venables, W. N., and B. D. Ripley. 1997. Modern Applied Statistics with S-Plus, 2nd Edition. Springer-Verlag New York. 548 pp.

Ward, J.H. 1963. Hierarchical grouping to optimize an objective function. *J. Am. Stat. Assoc.* 58: 236–244.

Weisberg, P.J. 1998. Fire History, Fire Regimes, and Development of Forest Structure in the Central Western Oregon Cascades. Ph.D. Dissertation. Oregon State University. Corvallis.

Weisberg, P.J. 2004. Importance of non-stand-replacing fire for the development of forest structure in the Pacific Northwest, USA. *For. Sci.* 50: 245–258.

Weisberg, P.J. 2009. Historical fire frequency on contrasting slope facets along the McKenzie River, western Oregon Cascades. *W. North Am. Nat.* 69: 206–214.

Weisberg, P.J., and F.J. Swanson. 2001. Fire dating from tree rings in western Cascades Douglas-fir forests: an error analysis. *Northwest Sci.* 75: 145–156.

Weisberg, P.J., and F.J. Swanson. 2003. Regional synchroneity in fire regimes of western Oregon and Washington, USA. *For. Ecol. Manage.* 172: 17–28.

Wetzel, S.A., and R.W. Fonda. 2000. Fire history of Douglas-fir forests in the Morse Creek drainage of Olympic National Park, Washington. *Northwest Sci.* 74: 263–279.

Wierman, C.A., and C.D. Oliver. 1979. Crown stratification by species in even-aged mixed stands of Douglas-fir–western hemlock. *Can. J. For. Res.* 9: 1–9.

Wimberly, M.C., and T.A. Spies. 2001. Influences of environment and disturbance on forest patterns in coastal Oregon watersheds. *Ecology* 82: 1443–1459.

Winter, L.E., L.B. Brubaker, J.F. Franklin, E.A. Miller, and D.Q. DeWitt. 2002a. Initiation of an old-growth Douglas-fir stand in the Pacific Northwest: a reconstruction from tree-ting records. *Can. J. For. Res.* 32: 1039–1056.

Winter, L.E., L.B. Brubaker, J.F. Franklin, E.A. Miller, and D.Q. DeWitt. 2002b. Canopy disturbances over the five-century lifetime of an old-growth Douglas-fir stand in the Pacific Northwest. *Can. J. For. Res.* 32: 1057–1070.

Yamaguchi, D.K. 1991. A simple method for cross-dating increment cores from living trees. *Can. J. For. Res*. 21: 414–416.

Yamaguchi, D.K. 1993. Forest history, Mount St. Helens. *Natl. Geogr. Res. Explor*. 9: 294–325.

Yang, Z., W.B. Cohen, and M.E. Harmon. 2005. Modeling early forest succession following clear-cutting in western Oregon. *Can. J. For. Res.* 35: 1889–1900.

Zenner, E.K. 2000. Do residual trees increase structural complexity in Pacific Northwest coniferous forests? *Ecol. App.* 10: 800–810.

Zenner, E.K. 2005. Development of tree size distributions in Douglas-fir forests under differing disturbance regimes. *Ecol. App.* 15: 701–714.

Table 2.1. Comparison of stand-structure variables among six age-structure types in the central western Cascades of Oregon (values are means, SD is in parentheses, different letters indicate significant differences between groups based on the Tukey HSD test or the Behrens-Fisher test).

Variable[1]	Age-Structure Type					
	1 (n = 18)	2 (n = 26)	3 (n = 19)	4 (n = 33)	5 (n = 15)	6 (n = 13)
Density (trees/ha)						
All	$_{bc}$274 (62)	$_{c}$250 (62)	$_{ab}$368 (112)	$_{a}$397 (132)	$_{a}$452 (157)	$_{b}$351 (109)
Shade-intolerant	$_{b}$62 (34)	$_{b}$60 (26)	$_{b}$65 (26)	$_{a}$152 (94)	$_{a}$234 (158)	$_{a}$236 (111)
Large shade-intol.[2]	$_{a}$52 (27)	$_{a}$50 (20)	$_{a}$55 (21)	$_{a}$44 (17)	$_{b}$15 (17)	$_{a}$34 (24)
Shade-tolerant	$_{b}$212 (62)	$_{bc}$189 (57)	$_{a}$294 (95)	$_{ab}$230 (112)	$_{abc}$234 (213)	$_{c}$115 (103)
Large shade-tolerant[3]	$_{a}$39 (21)	$_{b}$19 (15)	$_{bc}$12 (16)	$_{c}$6 (11)	$_{c}$7 (14)	$_{c}$3 (8)
Small tree[4]	$_{a}$1,947 (1,457)	$_{ab}$1,007 (716)	$_{c}$482 (522)	$_{bc}$705 (462)	$_{ab}$1,285 (1,413)	$_{ab}$1,089 (585)
Basal Area (m^2/ha)						
All	$_{a}$133.2 (36.2)	$_{a}$129.7 (24.2)	$_{ab}$129.5 (35.0)	$_{ab}$118.9 (28.7)	$_{c}$89.5 (26.0)	$_{bc}$99.7 (25.8)
Shade-intolerant	76.3 (36.8)	88.9 (24.6)	92.7 (32.6)	88.3 (31.4)	69.4 (33.0)	88.4 (28.5)
Shade-tolerant	$_{a}$56.9 (22.3)	$_{b}$40.7 (15.3)	$_{bc}$36.2 (14.5)	$_{bc}$29.6 (16.0)	$_{cd}$25.2 (25.8)	$_{d}$11.8 (12.3)
DBH (cm)						
All mean	$_{a}$66.8 (11.0)	$_{a}$68.0 (12.4)	$_{b}$53.7 (10.7)	$_{b}$51.8 (9.7)	$_{b}$46.8 (11.7)	$_{b}$51.7 (10.4)
All SD	$_{ab}$42.4 (7.5)	$_{a}$48.4 (7.6)	$_{ab}$42.3 (7.9)	$_{bc}$36.9 (8.0)	$_{d}$23.6 (9.3)	$_{c}$33.5 (8.6)
Shade-intol. mean	$_{a}$123.5 (30.0)	$_{a}$142.5 (26.0)	$_{a}$134.8 (22.3)	$_{b}$82.9 (24.4)	$_{b}$62.8 (19.6)	$_{b}$64.6 (17.7)
Shade-intolerant SD	$_{d}$21.9 (9.5)	$_{bcd}$23.8 (10.2)	$_{bcd}$25.2 (11.2)	$_{d}$43.9 (17.5)	$_{cd}$15.3 (17.3)	$_{bc}$33.8 (24.3)
Shade-tolerant mean	$_{a}$50.2 (9.0)	$_{a}$46.1 (10.0)	$_{b}$36.2 (7.5)	$_{b}$36.4 (8.0)	$_{b}$30.9 (8.6)	$_{b}$31.3 (11.8)
Shade-tolerant SD	$_{a}$30.6 (8.0)	$_{a}$27.2 (8.8)	$_{b}$17.0 (6.6)	$_{b}$16.9 (6.3)	$_{b}$12.5 (7.6)	$_{b}$12.1 (8.6)

[1] Data are for trees ≥ 15.0 cm dbh unless otherwise noted.
[2] Large shade-intolerant trees are > 100.0 cm dbh.
[3] Large shade-tolerant trees are > 80.0 cm dbh.
[4] Small trees refers to trees and shrubs 1.5–14.9 cm dbh.

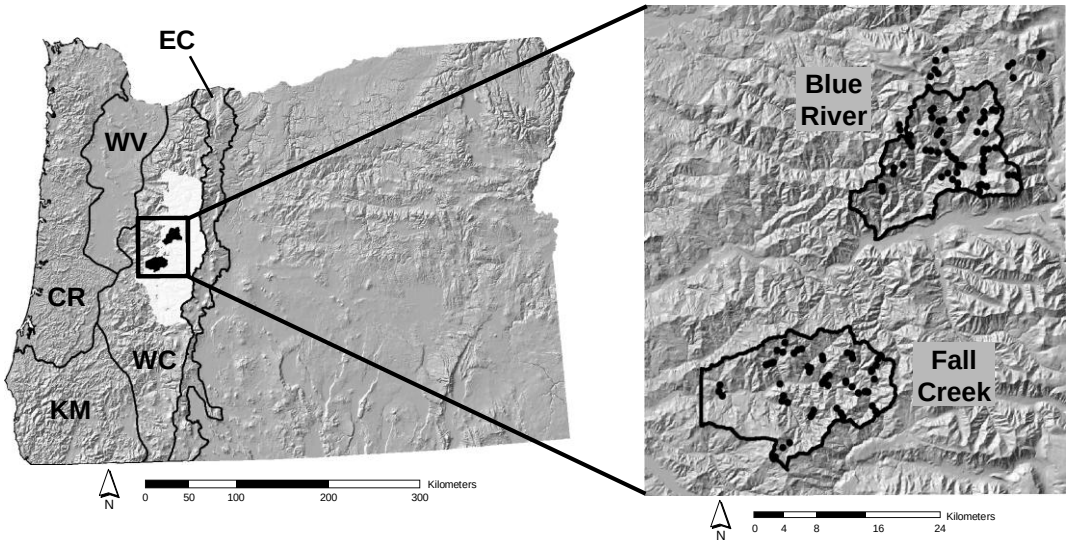

Figure 2.1. Study site locations in relation to the Willamette National Forest (white shading) and major physiographic provinces of western Oregon (WC = Western Cascades, EC = Eastern Cascades, WV = Willamette Valley, CR = Coast Range, KM = Klamath Mountains; Franklin and Dyrness 1973).

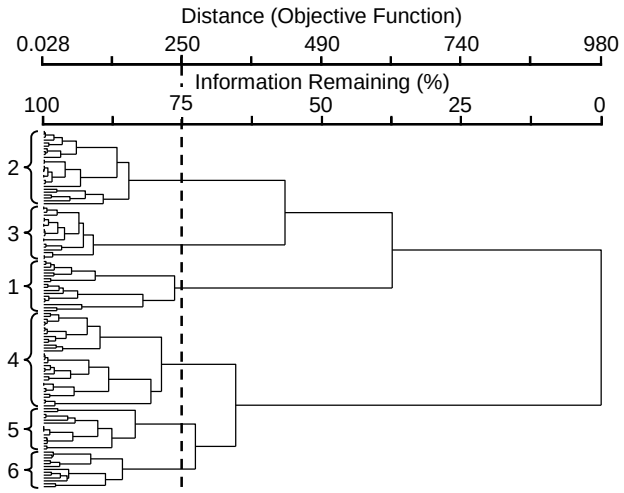

Figure 2.2. Dendrogram produced by hierarchical clustering of 124 transects by 8 variables describing the age distributions of shade-intolerant and shade-tolerant species. Group labels 1–6 denote age-structure types described in the text.

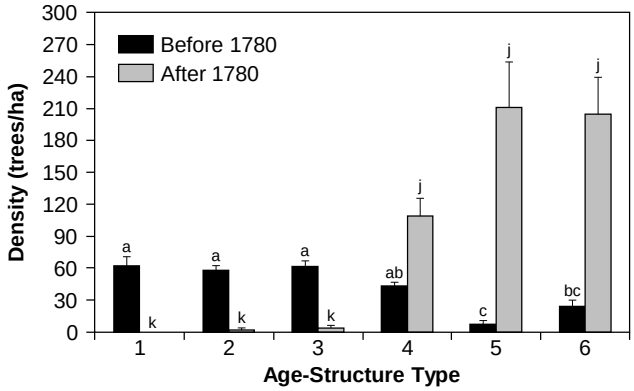

Figure 2.3. Comparison of the density of shade-intolerant trees that established before and after 1780 by age-structure type. Error bars represent 1 standard error. Letters a–c and j–k indicate significant differences between age-structure types for trees that established before and after 1780, respectively, based on Tukey's HSD test or the Behrens-Fisher test.

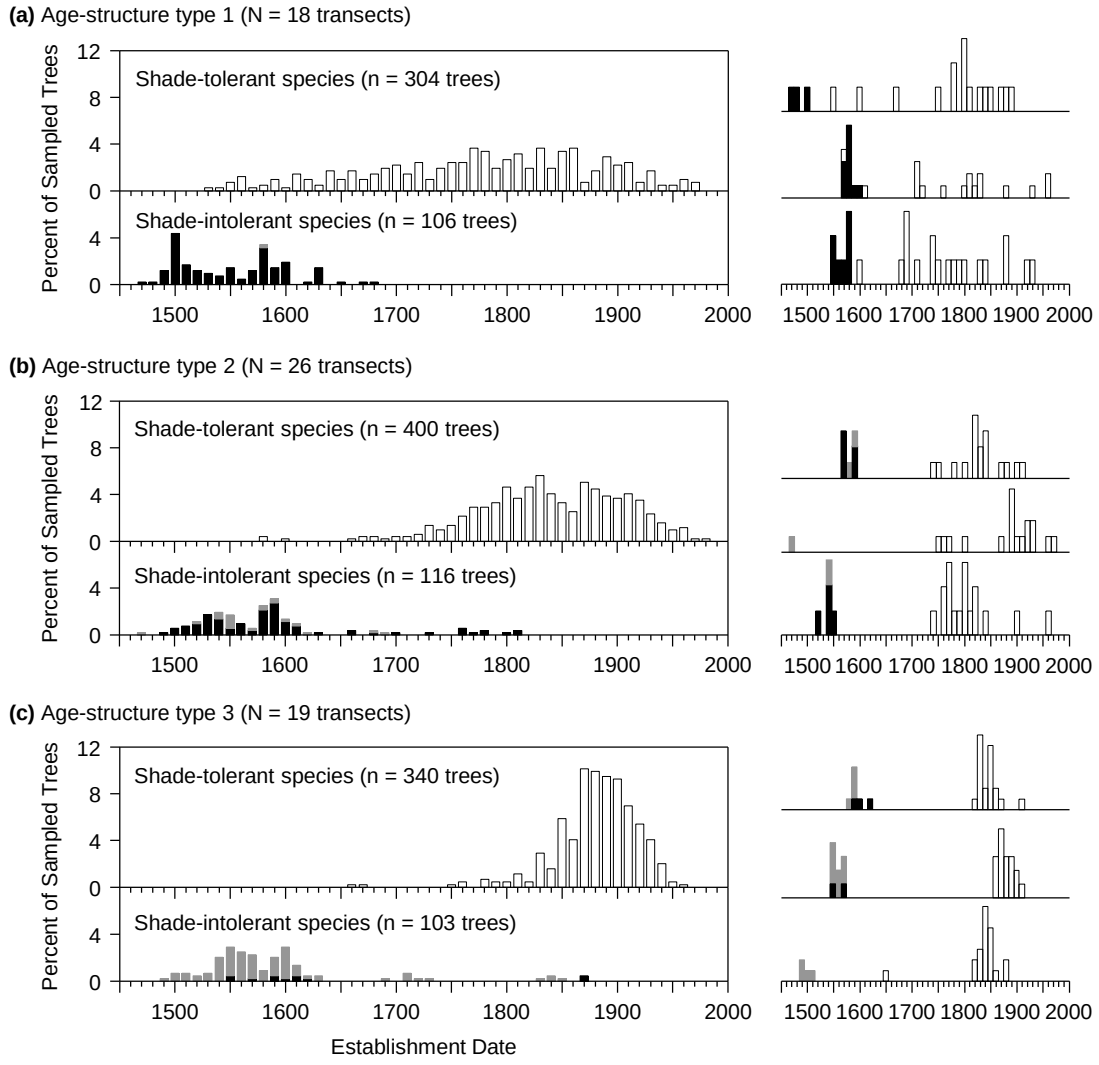

Figure 2.4. Comparison of the age distribution for shade-intolerant and shade-tolerant species among six age-structure types in the central western Cascades of Oregon. For each type, the composite histogram for all transects is shown on the left. Histograms for three representative sample sites are shown on the right to better illustrate the distinctiveness of establishment pulses in individual stands. Establishment dates for shade-intolerant species are shown in gray if the trees have charred bark and in black otherwise. White shading represents shade-tolerant species. Establishment dates prior to 1450 are not shown because they account for only 1% of all establishment dates.

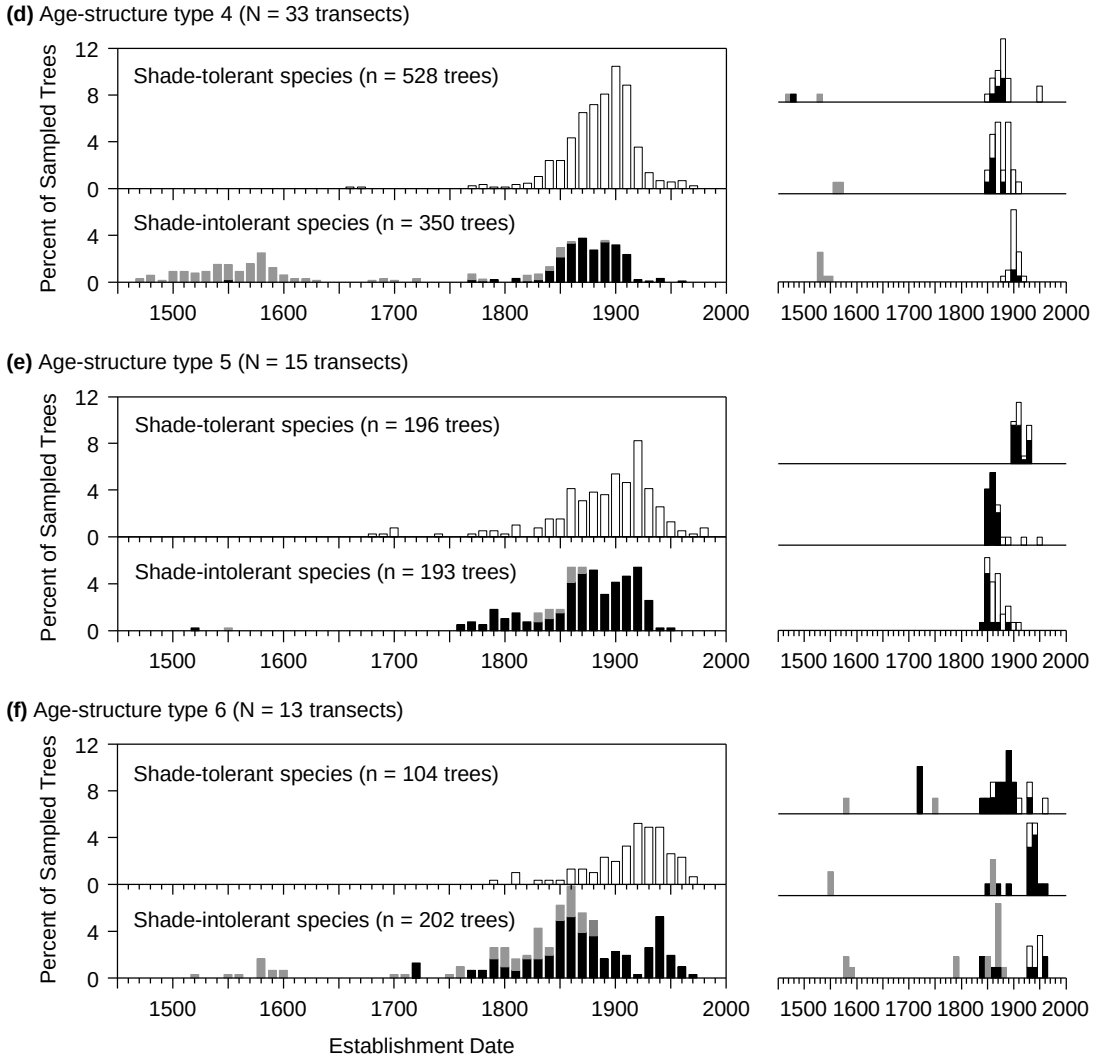

Figure 2.4. (continued)

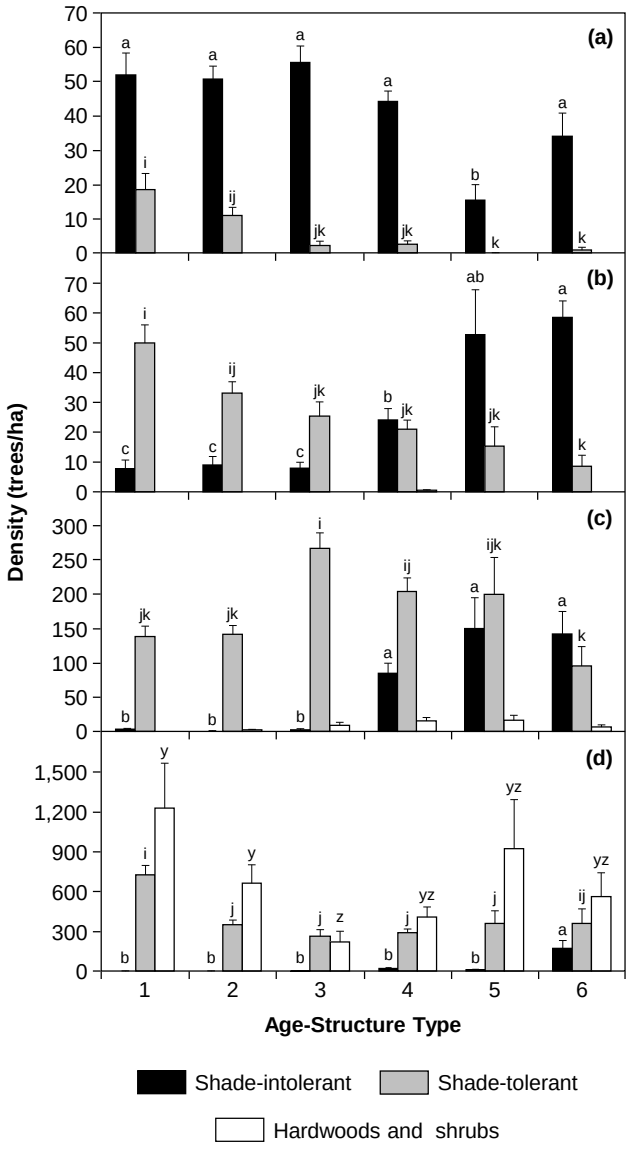

Figure 2.5. Comparison of tree density for shade-intolerant, shade-tolerant, and hardwood and shrub species by size class among six age-structure types in the central western Cascades of Oregon: (a) > 100 cm dbh, (b) 60–100 cm dbh, (c) 15–60 cm dbh, and (d) 1.5–14.9 cm dbh (error bars represent 1 standard error, letters a–c, i–k, and y–z indicate significant differences between age-structure types for shade-intolerant, shade-tolerant, and hardwoods and shrub species, respectively, as determined by Tukey's HSD test or the Behrens-Fisher test).

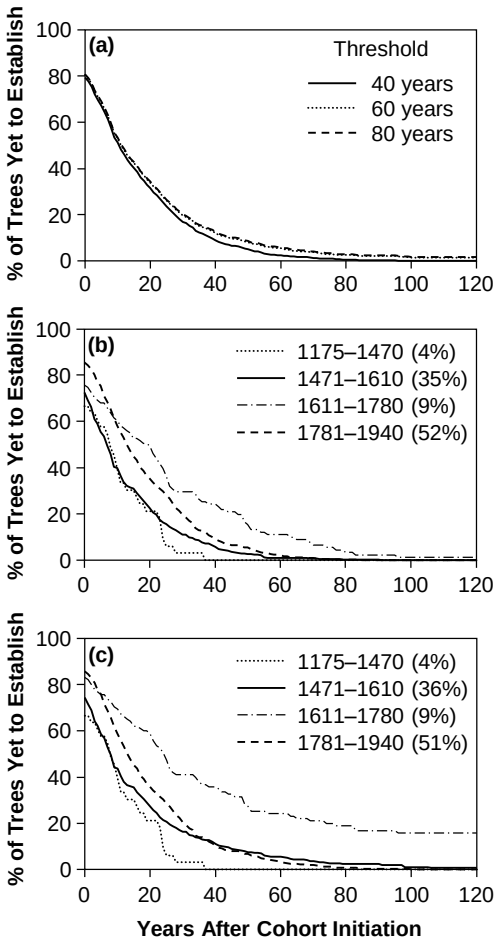

Figure 2.6. Comparison of (a) the duration of post-fire establishment periods for shade-intolerant trees for all cohorts in the central western Cascades of Oregon, in relation to thresholds for the interval prior to cohort initiation with no recorded establishment used to distinguish multiple cohorts per stand. Using thresholds of (b) 40 and (c) 80 years, the duration of cohort establishment intervals is compared for cohorts initiated in time periods roughly corresponding to previously-identified, alternating periods of region-wide extensive fire and limited burning (Weisberg and Swanson 2003). The percentage of trees present in cohorts initiated in each period is given in parentheses.

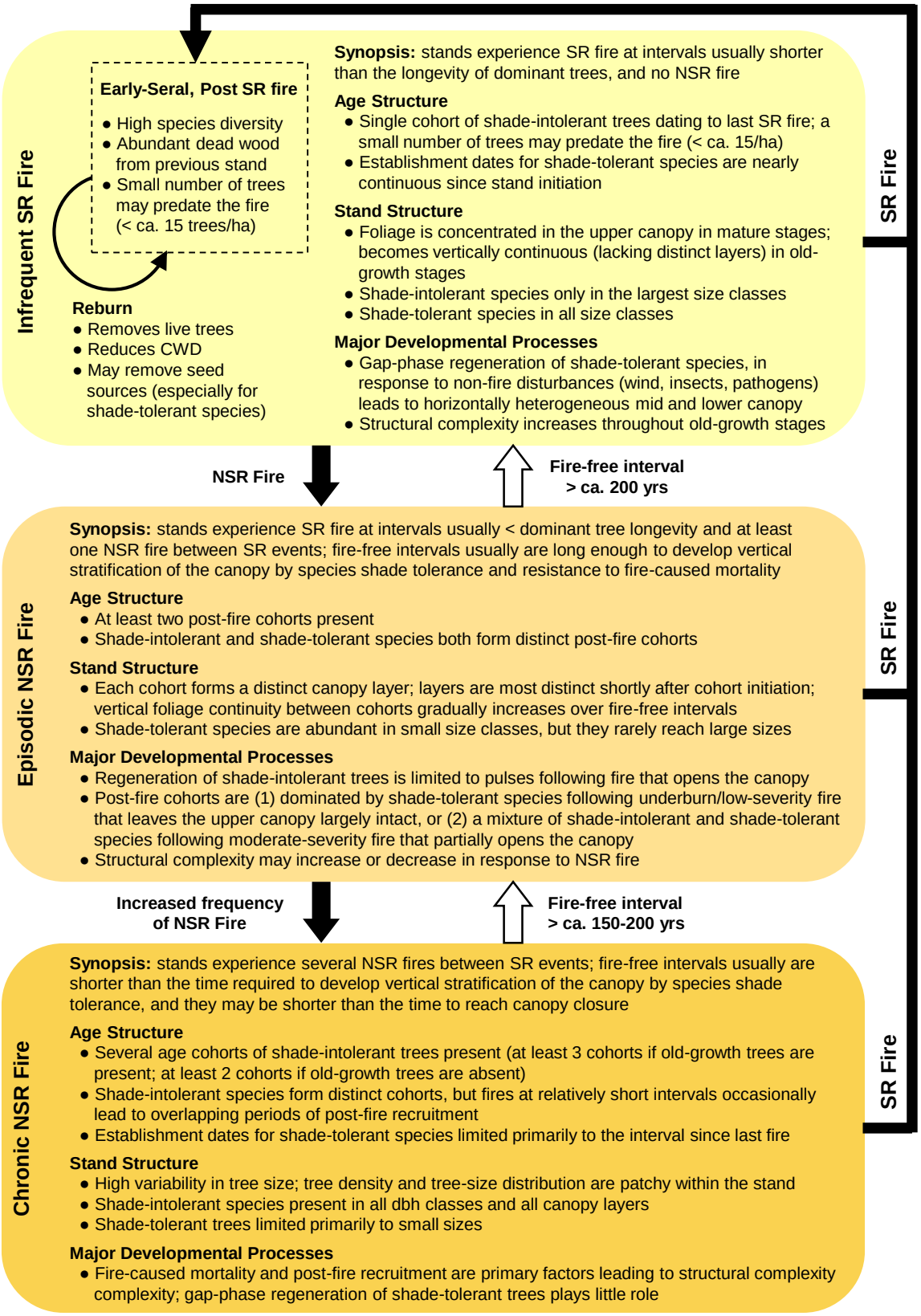
Infrequent SR Fire
Early-Seral, Post SR fire
• High species diversity
• Abundant dead wood from previous stand
• Small number of trees may predate the fire (< ca. 15 trees/ha)
Reburn
• Removes live trees
• Reduces CWD
• May remove seed sources (especially for shade-tolerant species)
Synopsis: stands experience SR fire at intervals usually shorter than the longevity of dominant trees, and no NSR fire
Age Structure
• Single cohort of shade-intolerant trees dating to last SR fire; a small number of trees may predate the fire (< ca. 15/ha)
• Establishment dates for shade-tolerant species are nearly continuous since stand initiation
Stand Structure
• Foliage is concentrated in the upper canopy in mature stages; becomes vertically continuous (lacking distinct layers) in old-growth stages
• Shade-intolerant species only in the largest size classes
• Shade-tolerant species in all size classes
Major Developmental Processes
• Gap-phase regeneration of shade-tolerant species, in response to non-fire disturbances (wind, insects, pathogens) leads to horizontally heterogeneous mid and lower canopy
• Structural complexity increases throughout old-growth stages
SR Fire
NSR Fire
Fire-free interval > ca. 200 yrs
Episodic NSR Fire
Synopsis: stands experience SR fire at intervals usually < dominant tree longevity and at least one NSR fire between SR events; fire-free intervals usually are long enough to develop vertical stratification of the canopy by species shade tolerance and resistance to fire-caused mortality
Age Structure
• At least two post-fire cohorts present
• Shade-intolerant and shade-tolerant species both form distinct post-fire cohorts
Stand Structure
• Each cohort forms a distinct canopy layer; layers are most distinct shortly after cohort initiation; vertical foliage continuity between cohorts gradually increases over fire-free intervals
• Shade-tolerant species are abundant in small size classes, but they rarely reach large sizes
Major Developmental Processes
• Regeneration of shade-intolerant trees is limited to pulses following fire that opens the canopy
• Post-fire cohorts are (1) dominated by shade-tolerant species following underburn/low-severity fire that leaves the upper canopy largely intact, or (2) a mixture of shade-intolerant and shade-tolerant species following moderate-severity fire that partially opens the canopy
• Structural complexity may increase or decrease in response to NSR fire
SR Fire
Increased frequency of NSR Fire
Fire-free interval > ca. 150-200 yrs
Chronic NSR Fire
Synopsis: stands experience several NSR fires between SR events; fire-free intervals usually are shorter than the time required to develop vertical stratification of the canopy by species shade tolerance, and they may be shorter than the time to reach canopy closure
Age Structure
• Several age cohorts of shade-intolerant trees present (at least 3 cohorts if old-growth trees are present; at least 2 cohorts if old-growth trees are absent)
• Shade-intolerant species form distinct cohorts, but fires at relatively short intervals occasionally lead to overlapping periods of post-fire recruitment
• Establishment dates for shade-tolerant species limited primarily to the interval since last fire
Stand Structure
• High variability in tree size; tree density and tree-size distribution are patchy within the stand
• Shade-intolerant species present in all dbh classes and all canopy layers
• Shade-tolerant trees limited primarily to small sizes
Major Developmental Processes
• Fire-caused mortality and post-fire recruitment are primary factors leading to structural complexity complexity; gap-phase regeneration of shade-tolerant trees plays little role
SR Fire

Figure 2.7. Comparison of the major stand- and age-structure attributes and developmental processes differentiating the three sub-models within the overall conceptual model of fire-mediated developmental pathways in Douglas-fir/western hemlock forests of the PNW.

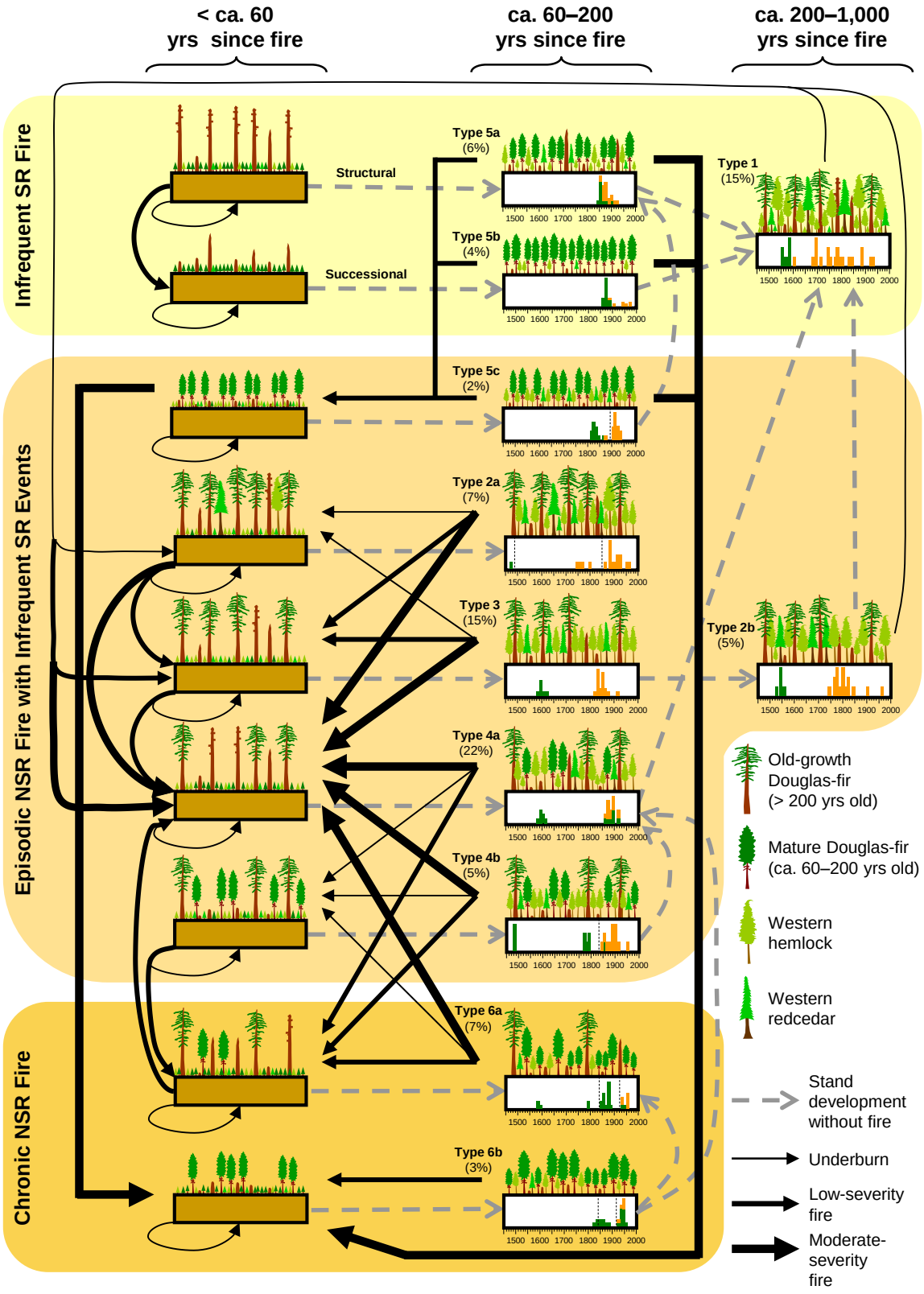
< ca. 60
yrs since fire
ca. 60–200
yrs since fire
ca. 200–1,000
yrs since fire
Infrequent SR Fire
Episodic NSR Fire with Infrequent SR Events
Chronic NSR Fire
Structural
Successional
Type 5a
(6%)
Type 5b
(4%)
Type 1
(15%)
Type 5c
(2%)
Type 2a
(7%)
Type 3
(15%)
Type 2b
(5%)
Type 4a
(22%)
Type 4b
(5%)
Type 6a
(7%)
Type 6b
(3%)
1500 1600 1700 1800 1900 2000
Old-growth Douglas-fir (> 200 yrs old)
Mature Douglas-fir (ca. 60–200 yrs old)
Western hemlock
Western redcedar
Stand development without fire
Underburn
Low-severity fire
Moderate-severity fire

Figure 2.8. Conceptual diagram of fire-mediated successional pathways in Douglas-fir/western hemlock forests in the central western Cascades of Oregon. Pathways leading to each age-structure type are shown (several types are subdivided to provide a more complete depiction of the effects of fire on stand development). Boxes represent differences in the ratio of NSR to SR fire, as in Figure 2.7. Dashed arrows represent stand development in the absence of fire, and solid arrows represent fire (to reduce complexity, arrows for high-severity fire are not shown, but high-severity fire is assumed to convert any stage to the upper left corner of the diagram). The three columns represent developmental stages when the youngest cohort is of young, mature, and old-growth age from left to right. For each stand condition in the center and right column, an idealized drawing of stand structure is shown along with an age-structure histogram from a representative transect. Histograms are not included in the left column because no sample sites had burned within the last 40–60 years. In the histograms, shade-intolerant trees are shown in orange and shade-tolerant trees in green. Fire-scar dates are indicated by dashed vertical lines. The x-axis represents establishment dates and the y-axis represents the percentage of sampled trees (the y-axis scale varies among transects). The percent of sample sites represented in each developmental stage is provided, but values do not sum to 100 because stands of age-structure type 2 that lack charred bark are excluded from the diagram due to uncertainty in their developmental history.

CHAPTER 3: TOPOGRAPHIC INFLUENCES ON THE FIRE REGIME AND FOREST AGE STRUCTURE IN DOUGLAS-FIR/WESTERN HEMLOCK FORESTS OF THE CENTRAL WESTERN CASCADES OF OREGON

ABSTRACT

Although broad trends in fire regimes along regional climatic gradients are fairly well understood, much remains unknown about the factors contributing to variation in fire regimes and associated forest structures across local landscapes. To better understand the contribution of topography to variation in the fire regime of Douglas-fir/western hemlock forests of the central western Cascades of Oregon, I evaluated relationships between forest age structure and topography. Ages of more than 3,000 trees were collected at 124 stands, located at upper, mid, and lower slope positions along randomly selected slope facets throughout two large (ca. 250 km^2) watersheds. Six discrete age-structure types, produced by clustering of age-structure variables in a previous study of fire-mediated developmental pathways, and a continuous age-structure gradient produced by Nonmetric Multidimensional Scaling of age-structure variables were related to topography by Non-Parametric Multiplicative Regression (NPMR). Age structure was most strongly related to topography at both ends of a continuum of fire influences on stand development. Old-growth stands with no evidence of fire for > 400 years were likely to be found only in concave landforms (lower slopes, benches, and cirques) beneath high ridgetops (> ca. 1,200 m). Stands with three or more post-fire cohorts of shade-intolerant trees were found in areas of highest exposure to solar radiation. A trend of increasing fire severity from lower to upper slope positions was supported by a tendency for the oldest cohorts to decrease in density toward the upper slope. However, the degree of differentiation in age structure by slope position was conditioned by local topographic relief. Age structure exhibited the greatest fidelity to terrain shape and slope position in areas of high relief, suggesting stronger influences of topographic shading and temperature inversions on microclimate and fuel moisture. Understanding these relationships and the variation of the strengths of topographic influences on the fire regime may aid in guiding landscape-level management influenced by historical disturbance regimes.

INTRODUCTION

Although broad trends in fire regimes along regional climatic gradients are fairly well understood, much remains unknown about the factors contributing to variation in fire regimes and associated forest structures across local landscapes. Recent fire-history research in the Douglas-fir (*Pseudotsuga menziesii* (Mirb.) Franco)/western hemlock (*Tsuga heterophylla* (Raf.) Sarg.) region of the Pacific Northwest (PNW) reveals a transition from infrequent, predominantly stand-replacement (SR) fires in northern parts of the region and coastal areas (Hemstrom and Franklin 1982, Impara 1997, Agee and Krusemark 2001) to a mixed-severity regime with higher fire frequency and greater representation of non-stand-replacement (NSR) fire in southern parts of the region and in rainshadows of coastal mountain ranges (Morrison and Swanson 1990, Wetzel and Fonda 2000, Weisberg 2004). Fire intervals and severity both are highly variable in drier parts of the region, which contributes to enormous diversity in stands structures and pathways of stand development (Weisberg 2004, Zenner 2005; chapter 2). However, the factors guiding spatial variation in forest conditions in these areas are poorly understood. To the extent that topography consistently influences fire patterns and behavior, an understanding of these influences may enable prediction of where different types of stand structures are most likely to occur. Such an understanding may provide guidance for management based on historical disturbance regimes (Cissel et al. 1999), and it could provide a baseline for evaluating the effects of recent and on-going changes in disturbance regimes by forest harvesting and landscape fragmentation, active fire suppression, and climatic warming.

Topography may have numerous direct and indirect influences on fire patterns and behavior. It influences fire behavior directly by increasing the efficiency of heat transfer to upslope fuel with increasing slope gradient (Rothermel 1983), and rocky, sparsely vegetated areas may directly affect fire patterns by providing physical barriers to fire spread (Iniguez et al. 2008). Topography affects fire indirectly by moderating microclimate (including diurnal and seasonal variation in temperature, relative humidity, precipitation amount and form, and snowpack persistence), which moderates the moisture

status of live foliage and dead woody fuel (Hayes 1941, Rothermel et al. 1986). In the Klamath Mountains and southern Cascades of northern California, fire severity was found to increase toward upper slopes, and fire frequency was higher on warm than cool aspects (Taylor and Skinner 1998, Beaty and Taylor 2001). Concave landforms in several regions have been found to have lower fire severity or were likely to remain unburned by fires that burned the adjacent terrain (Zackrisson 1977, Romme and Knight 1981, Camp et al. 1997, Keeton and Franklin 2004). In dry regions prone to frequent fire, topographically-moderated variation in site productivity may affect fire patterns by influencing the time required for burned areas to accumulate sufficient fuel to carry another fire (Rollins et al. 2002, Collins et al. 2009).

Douglas-fir/western hemlock forests of the central western Cascades of Oregon are well-suited to evaluating effects of topography on fire patterns and behavior. A single forest type with a small number of dominant tree species is widely distributed across highly complex terrain. Thus, patterns of fire behavior from the valley bottom to the ridgetop of most slope facets may be evaluated in relation to topography without the interaction of changes in species composition, and associated differences in fuelbeds and species resistance to fire-caused mortality found in other regions (Taylor 2000). Also, the deeply dissected terrain characteristic of the west side of the Cascade Range promotes substantial fine-scale variation in microclimate (Daly et al. 2007, 2009), and thus strong potential for topographic moderation of fuel moisture and fire behavior. Such fine-scale microclimatic variation may be particularly important in this highly productive region, where fuel is abundant essentially in all developmental stages, and fire extent and intensity probably are limited more by fuel moisture than fuel amount or connectivity (Rollins et al. 2002, Meyn et al. 2007).

The overall objective of this study is to provide a stronger understanding of the mechanisms and strengths of the influences of topography on local variation in the fire regime and associated variation in forest structure in the central western Cascades of Oregon. Effects of topography on fire patterns and behavior will be determined using forest age structure as a proxy for the cumulative effects of one or more NSR fires (or the

absence of NSR fire) on stand development over the time period represented by ages of the oldest trees in a stand. Specific objectives are to (1) evaluate the influences of site-level topographic variables, and determine if their influence is constant across the study area or varies with broader physiographic context, (2) determine if certain types of age structure have a strong association with their topographic settings, whereas other age-structure characteristics may be represented across a range of settings, and (3) evaluate trends in age structure from lower to upper slope positions and determine if the strength of these trends varies across the study area.

To address these objectives, six discrete age-structure types identified in a previous study of fire-mediated pathways of stand development in the study area (chapter 2) and a continuous age-structure gradient will be related to topography variables. Weather and fuel also are important drivers of fire patterns and behavior, and they may override influences of topography, particularly in fires burning under extreme values of either of these factors (Thompson and Spies 2009). However, topography is the only factor of the fire environment (weather, fuel, and topography) that does not vary over time. Thus, any relationships between age structure and topography found to be consistent over a broad area that includes stands burned in disparate events may provide a stronger basis for interpreting potential influences of topography on fire behavior than analysis of burn severity in a single event.

STUDY AREA

Sampling was conducted in two study areas, each centered on a large watershed in the central western Cascades of Oregon (Figure 3.1). The Blue River study area has steep, rugged terrain with high topographic relief representative of the eastern part of the western Cascade Range. It includes the 240-km^2 Blue River watershed and 3 smaller watersheds (totaling 33 km^2) to the north. Elevation ranges from 316 to 1,753 m. Most major ridges reach elevations above 1,200 m, and valley bottoms can be as much as 700–1,000 m below the ridgetop. Glacial landforms, including cirques and U-shaped valleys, are associated with some of the highest ridges.

The Fall Creek study area is the eastern 300 km^2 of the Fall Creek watershed (Figure 3.1). The terrain is generally steep and rugged, but most major ridges are lower than those in the Blue River study area. Elevation ranges from 254 to 1,519 m. Only the highest ridges along the southern perimeter of the study area are higher than 1,200 m, and evidence of glaciation is lacking except near these ridges. The elevation difference from ridgetop to valley bottom is less than 500 m on most slopes. Areas of higher relief are located primarily near the southern perimeter of the study area.

The climate of the central western Cascades of Oregon is transitional from Mediterranean to maritime temperate. Summers are warm and dry, and winters are mild and wet. Mean annual precipitation (1971–2000) averages 233 cm in the Blue River study area and 182 cm at Fall Creek (Daly et al. 2008). The majority of annual precipitation falls in the winter, and a persistent snowpack accumulates above about 900 m. Only about 10% of annual precipitation falls between June 1 and September 30, and the fire season typically occupies the latter part of this dry season.

Two vegetation zones comprise the majority of both study areas. The Western Hemlock zone (Franklin and Dyrness 1973) accounts for almost the entire Fall Creek study area and most of the Blue River study area, excluding ridgetops above about 1,200 m. Essentially all forests of this zone are dominated by Douglas-fir. Major shade-tolerant associates are western hemlock and western redcedar (*Thuja plicata* Donn ex D. Don). The Pacific Silver Fir zone is represented on ridges higher than about 1,200 m, including most major ridges in the Blue River study area and a few ridges in the southern part of Fall Creek. Abundant species of this zone are Douglas-fir, Pacific silver fir (*Abies amabilis* (Dougl. ex Loud.) Dougl. ex Forbes), noble fir (*Abies procera* Rehd.), western hemlock, and mountain hemlock (*Tsuga mertensiana* (Bong.) Carr.). The Mountain Hemlock zone is found in small patches on the highest ridgetops in the Blue River study area, and the Douglas-fir climax type occurs locally on the driest sites in both study areas.

METHODS

Field Methods

Age-structure data were collected in 124 stands: 71 in the Blue River study area and 53 at Fall Creek. Stands were selected using a stratified random method that distributes sampling intensity geographically throughout both study areas and captures most of the physiographic variation. To locate sample sites, a 5x5-km grid was overlaid on each study area, and sampling was conducted at upper, mid, and lower slope positions along a randomly selected slope facet in each 25-km^2 cell. Slope facets (contiguous areas of similar aspect extending from ridgetop to valley bottom) were delineated by applying a Gaussian filter to a 30-m Digital Elevation Model (DEM) to smooth features up to 240 m in extent (Daly et al. 2007). Aspect of the smoothed DEM was classified as northeast (0–90º), southeast (91–180º), southwest (181–270º), or northwest (271–360º), and areas of each class smaller than 40 ha were combined with the surrounding class. To select slope facets, a 1x1-km grid was overlaid on each study area and a random number generator was used to identify one, 1-km^2 cell in each 25-km^2 cell. The slope facet accounting for the majority of the random cell was selected for sampling.

Sample sites were determined by generating a random point at the upper, mid, and lower slope position of the selected slope facet. Slope positions were defined by dividing the elevation range of the slope facet into three equal portions. Aerial photos were used to draw polygons encompassing the forested area lacking 20^{th}-century anthropogenic disturbance at each slope position, excluding areas within 100 m of roads, perennial streams, harvested stands, and non-forest vegetation. Then, Universal Trans Mercator (UTM) coordinates were generated for a random point in the polygon at each slope position, and a GPS receiver was used to locate the point in the field. After sampling along one slope facet in each 25-km^2 grid cell, additional slope facets and landform types that were poorly represented in the dataset were selected for sampling. Sample locations within these landforms were identified as described above.

The point generated in the polygon of natural forest at each slope position served as the midpoint of a 120-m long transect consisting of 5, 0.02-ha circular plots at 30-m intervals between plot centers. Transects were oriented parallel to slope contours. The entire transect was treated as one sample unit. Sampling was conducted in five plots per transect rather than a single plot of equivalent area to ensure that age classes were spread over broad areas, and thus were likely to represent establishment in response to widespread disturbance rather than local treefall gaps. In each plot, the diameter at breast height (dbh) of all live and standing dead trees > 15 cm dbh was recorded. Evidence of fire, including charred bark and open wounds, or catfaces, was recorded for each tree.

Age-Structure Data

Age-structure data were collected by coring a subset of 3,279 trees > 15 cm dbh (or > 10 cm dbh for Pacific yew (*Taxus brevifolia* Nutt.)), representing an average of 27 trees per transect, or 76% of the live trees. The subset was determined by dividing each 0.02-ha plot into 4 quadrants and coring the largest tree of each species in each quadrant. The largest tree was selected to increase the likelihood that the oldest tree of each species was sampled, but sampling one tree per quadrant ensured that smaller trees also were cored. Trees were cored as close to the ground as possible, and the height of core extraction above the mineral soil surface was recorded for each tree. If trees had heartrot or were too large to reach the pith with an 81-cm increment borer, the area near the transect was searched for a tree of the same species and similar size to substitute for the tree in the plot. When no suitable trees were available, incomplete cores were collected from the tree in the plot as a minimum estimate of tree age, but establishment dates were not estimated for these trees.

Tree cores were mounted and sanded until cell structure was visible under a binocular microscope, and the majority (85%) of cores was cross-dated. Cross-dating was conducted using skeleton plotting and the list-year method (Yamaguchi 1991, Stokes and Smiley 1996). Then, master ring-width chronologies were developed by measuring ring width in more than 200 Douglas-fir and 50 western hemlock cores to the nearest 0.001

mm using a Velmex sliding-stage micrometer. The remaining cores were cross-dated by visual comparison to the master chronologies. Fifteen percent of the cores that could not be cross-dated were deciduous species, which were excluded from analyses due to representation in a small portion (23%) of stands. The remaining non-cross-dated cores were primarily from Pacific yew (16%), or from other shade-tolerant species that had suppressed growth within their first 100 years, which precluded accurate cross-dating of the innermost rings. These cores were retained in the analyses because they represent a small portion of the dataset, and possible dating errors were assumed to be minor relative to the timescale of stand development.

Establishment dates for 3,046 trees (89%) were estimated, limited to those that either intersected the pith, or where the innermost ring formed a complete arc and the number of years to the pith could be estimated without extrapolating beyond the end of the core. For these off-center cores, the geometric method of Duncan (1989) was applied to estimate an average of seven years to the pith. An additional four years, on average, was added to account for the time to reach coring height by applying the equation of Morrison and Swanson (1990) to all species and using the height of core extraction above the mineral soil surface.

Age-structure variables were developed to characterize the overall shape of age distributions of shade-intolerant and shade-tolerant species, where stands with similar overall age distributions are assumed to have followed similar succession trajectories. Variables were not defined to emphasize establishment in specific time periods (e.g., the proportion of establishment dates in each decade), because such an approach would likely group stands that responded to the same events (Taylor and Skinner 2003), but it is unlikely to group stands that followed similar succession trajectories after burning in different fires. Almost all (96%) shade-intolerant trees in the dataset were Douglas-fir. Additional shade-intolerant species were noble fir, incense-cedar (*Calocedrus decurrens* (Torr.) Florin), western white pine (*Pinus monticola* Dougl. ex D. Don), and sugar pine. The most abundant shade-tolerant species in the dataset were western hemlock (69%), western redcedar (14%), and Pacific silver fir (11%). Pacific yew, mountain hemlock,

grand fir (*Abies grandis* (Dougl. ex D. Don) Lindl.), and Alaska yellow-cedar (*Chamaecyparis nootkatensis* (D. Don) Spach) comprise the remaining 6% of cores from shade-tolerant species.

The dataset consists of four variables characterizing age distributions of shade-intolerant species and four for shade-tolerant species. For shade-intolerant species, the variables are the proportion of trees that established before 1780, the overall age range, the age range of trees that established after 1780, and the proportion of trees with charred bark. Variables characterizing age distributions of shade-tolerant species are the proportion of trees that established before 1780, and the range, mean, and standard deviation (SD) of shade-tolerant tree age. The year 1780 was used as a threshold distinguishing trees that predate the more recent of two region-wide periods of extensive burning identified in a synthesis of fire-history studies in western Oregon and Washington (Weisberg and Swanson 2003). The range of shade-intolerant tree age was calculated after excluding the oldest and youngest tree at each stand to minimize the influence of a single tree that predates a younger cohort or an individual young tree that may have established after a small-scale or low-intensity disturbance that otherwise did not open the canopy enough for widespread regeneration of shade-tolerant species. The oldest shade-tolerant tree at each stand was excluded from calculation of the range, mean, and SD of shade-tolerant age to minimize the influence of individual outlier trees that may have survived a fire and predate a post-fire cohort.

Topography Variables

Variables describing the physiographic context and site-level topography of sample sites were classified into seven categories (elevation, topographic relief, exposure to solar radiation, slope position, terrain shape, slope length, and slope gradient), and raster layers were generated for one or two variables in each category (Table 3.1). Topography variables for sampled stands were extracted from these layers at the center of each transect. The raster layers were generated using a 30-m DEM after applying a Gaussian filter to smooth features smaller than 120 m in extent while having minimal

influence on larger features (Daly et al. 2007). Smoothing of the DEM was conducted for two reasons. First, transect length (120 m) was larger than the cell size, and coarsening of the DEM resolution could over-generalize broad-scale features, such as major ridgetops and valley bottoms. Second, features smaller than 120 m in extent were assumed to have little influence on fire behavior. GIS methods for generating the raster layer for each variable are presented briefly in Table 3.1 and described in detail in Appendix A.

Analyses

A previous study of fire-mediated pathways of stand development (chapter 2) used hierarchical agglomerative cluster analysis of the age-structure dataset to identify six, relatively distinct age-structure types that are repeated across the study area (Figure 3.2). Each age-structure type represents a range of fire-history characteristics distinct from the other types. Most stands have a distinct age cohort of shade-intolerant species, presumably dating to the most recent high-severity fire. Many stands also have one or more younger cohorts of shade-intolerant or shade-tolerant species, probably dating to more recent NSR fire, based on charred bark on older trees (Figure 3.2) and consistency of the timing of cohort initiation among stands sampled at different slope positions along a slope facet. Relative differences in the severity of the most recent fire or cumulative effects of more NSR fire since stand initiation were inferred based on the density and species composition of trees that predate the youngest cohort, which usually was strongly related to the species composition of the younger cohort (chapter 2).

In the present study, age structure was related to topography in two ways. First, a continuous age-structure gradient through the sampled stands was related to topography. Then, analyses were conducted to determine if each of the discrete age-structure types could be distinguished from the remaining stands by its topographic context.

Relationships between age structure and topography were evaluated with Non-Parametric Multiplicative Regression (NPMR, McCune 2006), using HyperNiche version 2.54 beta (McCune and Mefford 2008). NPMR fits models locally to a particular region of sample space, allowing strengths of predictor variables and interactions among them to

vary across environmental space. It requires no assumptions regarding the shape of the response surface. The local model is a relationship for estimating the response at a target point, generated by weighting measured responses at other sample sites according to their environmental distance from the target point. Weight diminishes with environmental distance from the target point based on a Gaussian kernel centered on the target point. The SD of the Gaussian curve (referred to as the tolerance) is tuned for each topographic predictor to represent the rate at which weights diminish with environmental distance from the target point (McCune 2006).

The weight for each sample site was calculated as the product of the weights for each predictor (McCune 2006). Values range from 0, where environmental differences from the target point are so great that the response has no bearing on the estimated response, to 1.0, for sites environmentally identical to the target point. The Local Mean form of NPMR was applied, where sample site weights were utilized to estimate the response at the target point as the weighted average of response values across sample sites. The neighborhood size for each target point was calculated by summing weights across sample units as a measure of the amount of data bearing on the estimated response at each point (McCune 2006).

The continuous form of NPMR was applied to relate an age-structure gradient, developed by Nonmetric Multidimensional Scaling (NMS) (Kruskal 1964), to topography variables. NMS was conducted in PC-ORD version 5.04 (McCune and Mefford 2006). Ordinations were conducted with the complete set of eight, age-structure variables and with subsets of the dataset in order to develop a single ordination axis that provides an ecologically meaningful gradient through the sample sites and accounts for the majority of variation in age structure. NMS was selected over other ordination methods because it avoids assumptions of linearity and normality, which were not supported by a scatterplot matrix of age-structure variables. Prior to ordination, values of the age-structure variables were standardized by subtracting the mean and dividing by the SD of each variable to equalize variance among variables measured on different scales and in different units. Then, NMS was conducted using Euclidean distance to account for the negative values

generated by standardization. Starting from a random configuration, 500 runs were conducted with a maximum of 500 iterations per run and a stability criterion of 0.00001. Significance of the ordination axes was evaluated by a Monte Carlo test with 500 iterations.

Using NMS ordination scores as the response variable, NPMR was conducted by adding topographic predictor variables in a forward, stepwise fashion, where variables already in the model were evaluated for removal of adjustment in tolerance with the addition of each new predictor. The final model was selected as a compromise between minimizing the number of predictors and maximizing model fit (McCune 2006).

Model fit was evaluated using a leave-one-out, cross-validation approach. Similar to a traditional R^2, model fit is evaluated in terms of the ratio of residual sum of squares to total sum of squares. However, NPMR calculates a cross-validated measure (xR^2), where data for each target point is excluded from the estimated response at that point, providing a built-in method of cross-validation that helps guard against overfitting (McCune 2006). Significance was evaluated using a Monte Carlo test, where response variables were shuffled to destroy the relationship with predictors. Then, a forward, stepwise search through the predictors was conducted to find the best model fit. This procedure was repeated 1,000 times, and the proportion of runs resulting in equal or better fit was used as the *p*-value.

The relative contribution of each predictor was evaluated in terms of its tolerance and by sensitivity analysis. The tolerance (SD of the Gaussian weighting curve centered on the target point) of each predictor is inversely related to its influence on the response. High tolerance implies a broad range of responses associated with a particular value of a predictor. A low tolerance gives strong weight only to observations from sites environmentally similar to the target point. To enable comparison of the relative strengths of predictor variables measured on different scales and in different units, tolerance values were standardized proportionate to the range of each predictor. Sensitivity analysis was conducted by nudging values for each predictor by +/- 5% of their range individually and

measuring the resulting change in response. Changes in response were accumulated across points and scaled as a proportion of the observed range, providing a ratio measure of sensitivity that is independent of the scale or units of the original predictors (McCune 2006).

Binary NPMR was conducted to determine if stands of each age-structure type identified by clustering of age-structure variables could be distinguished from all other stands based only on topography. Analyses were conducted separately for each age-structure type, setting response values to 1 where the type was present and 0 otherwise. Binary NPMR was conducted in a similar manner to the continuous form, except model performance was evaluated with a log*B* statistic, representing the improvement over a "naïve model" where the probability of occurrence at each point is equal to its frequency of occurrence in the dataset (McCune 2006). Log*B* can be interpreted as the ratio of the likelihood of cross-validated estimates from the fitted model to estimates from the naïve model, expressed in powers of 10. It is linearly related to the deviance (or drop in deviance) statistic commonly used for model evaluation in logistic regression. Statistical significance of the likelihood ratio was tested using a Monte Carlo test as described for the continuous response variable.

RESULTS

Prediction of a Continuous Age-Structure Gradient

The strongest, ecologically interpretable gradient through the sample sites was developed by one-dimensional NMS ordination of sample sites by age structure variables after removing two variables (proportion of shade-intolerant trees with charred bark and age range of shade-intolerant trees) (Figure 3.3). This ordination was determined by conducting a two-dimensional ordination with the full age-structure dataset, and then removing two variables that were strongly correlated with the second axis, before conducting a one-dimensional ordination with the remaining variables. The ordination accounts for the majority of variation in the six age-structure variables ($R^2 = 0.91$, $p < 0.002$). It orders stands from old-growth stands with a single cohort of shade-intolerant

trees, old shade-tolerant trees, and no evidence (charred bark or age cohorts) of NSR fire since stand initiation (age-structure type 1), to stands with three or more cohorts of shade-intolerant trees and charred bark on all but the youngest cohort (age-structure type 6) (Figures 3.2 and 3.3). The gradient may approximate the cumulative effects of fire on stand development over the interval represented by ages of live trees, and it is used as a proxy for site fire-proneness in the following analysis.

Stepwise NPMR produced a five-predictor model where topography explained a moderate amount of variation in NMS scores ($xR^2 = 0.310$, $p < 0.002$). Estimated fire-proneness was most sensitive to variation in local relief, distance from the ridgetop, and the proxy for growing season insolation (sensitivity = 0.398, 0.315, and 0.262, respectively) (Table 3.2).

Estimated fire-proneness generally increased with increasing insolation, but the degree of increase varied depending on slope gradient, ridgetop proximity, and local relief (Figure 3.4). Fire-proneness was estimated to be relatively low under low insolation. However, above a threshold in the proxy for growing season insolation (ca. 4,600 WH/m^2), representing a switch from north to south aspect, fire-proneness was estimated to increase with increasing insolation, and the degree of increase was greater on steep than gentle slopes (Figure 3.4a). The increase in fire-proneness with insolation was similarly conditioned by ridgetop proximity, leading to a greater increase in fire-proneness with increasing insolation near the ridgetop than farther downslope (Figure 3.4b). Relationships between fire-proneness and insolation also were constrained by local relief, providing the greatest differentiation in fire-proneness between areas with low insolation and high local relief and areas with high insolation and low local relief (Figure 3.4c).

The relationship of estimated fire-proneness to vertical slope position was moderated by local relief, resulting in greater differentiation in fire-proneness by slope position in areas of high than low relief (Figure 3.4d). Lower slopes in areas of high local relief were estimated to be markedly less fire prone than those in areas of low relief.

Associations between age structure and topography may be strongest toward both extremes of the gradient of estimated fire-proneness and weakest in the middle, as suggested by changes in the relationship between residuals and neighborhood size along the gradient (Figure 3.5). Residuals show little relationship to neighborhood size near the middle of the gradient, meaning that increasing the amount of data bearing on an estimate did not improve the estimate. Thus, age-structure characteristic of the middle of the gradient (types 3 and 4; Figure 3.3) may be found across a range of topographic settings.

Toward both ends of the gradient, residuals generally decreased with decreasing neighborhood size (Figure 3.5), suggesting a counterintuitive tendency for improved estimates with less data bearing on the estimate at both extremes of the gradient. Such a tendency may indicate that age structure characteristic of both ends of the gradient of estimated fire-proneness (types 1 and 6; Figure 3.3) is associated with topographic settings that are uncommon in the study area (small neighborhood size), but predictions of age structure from topography may be fairly reliable in these settings. Given that NPMR excludes data from the target point in estimating its response, and that age-structure types 1 and 6 usually are represented only at one of the stands sampled along a slope facet, the low residuals for a small neighborhood size indicate that reasonably accurate responses were estimated based on a similar response at a small number of stands in similar topographic settings, but usually on different slope facets.

Applied across the landscape, the NPMR model produces a trend of increasing representation of less fire-prone portions of the NMS gradient and greater differentiation in estimated fire-proneness by slope position from west to east across the central western Cascades (Figure 3.6). The more fire-prone end of the gradient is predicted to be most widespread in areas of low local relief, including the northern part of the Fall Creek study area and the north-central part of the Blue River watershed. In these areas, fire-proneness was predicted to vary with aspect but have relatively little variation by slope position (Figure 3.6). The less fire-prone portion of the gradient is predicted to become increasingly abundant with higher local relief in the eastern part of the western Cascades. In the areas of highest local relief, almost the full range of the NMS gradient is predicted

to be represented along individual slope facets, with relatively strong differentiation by slope position (Figure 3.6).

Prediction of Discrete Age-Structure Types

The application of binary NPMR to determine if stands of each age-structure type could be distinguished from all other sample sites by their topographic context provided statistically significant models that were ecologically interpretable, only for age-structure types 1 and 6.

The stepwise procedure produced a two-predictor model using ridgetop elevation and terrain shape (topographic index over a 300-m radius) to distinguish stands of age-structure type 1 from the remaining sample sites ($logB = 3.54$, $p < 0.001$). The estimated probability of occurrence for age-structure type 1 was > 0.3 for 50% of stands classified as age-structure type 1, but only 8% of the remaining stands had an estimated probability of occurrence > 0.3. Concave landforms below high ridgetops had the highest estimated probability of occurrence (Figure 3.7a). The estimated probability of occurrence increased markedly with terrain concavity along slopes with ridgetops higher than ca. 1,000 m. Age-structure type 1 was unlikely to be found on slopes with lower ridgetops regardless of terrain shape (Figure 3.7a).

Stepwise NPMR produced a three-predictor model for age-structure type 6 ($logB = 4.85$, $p < 0.001$). The estimated probability of occurrence was > 0.3 for 69% of stands classified as type 6. Only 4% of the remaining stands had an estimated probability of occurrence > 0.3. The predictors were slope gradient, ridgetop elevation, and the proxy for growing season insolation. The estimated probability of occurrence was usually low on cool aspects (values below ca. 4,600 WH/m^2 in the proxy for growing season insolation; Figure 3.7b and c). On warmer aspects, however, the probability of occurrence increased markedly with increasing insolation on slopes with low ridgetops (< ca. 1,000 m). Increases in the probability of occurrence with increasing insolation were less pronounced on higher ridges (Figure 3.7b). In areas of high insolation, the estimated probability of occurrence also increased substantially with increasing slope gradient up to

moderate slope steepness (ca. 24–54%). Comparatively little increase in the probability of occurrence with increasing insolation was evident on the gentlest or the steepest slopes (Figure 3.7c). The relatively high estimated probability of occurrence at low insolation values on very steep slopes and with ridgetop elevation of about 1,050 m was driven by one sample site (Figure 3.7b and c), and it is unlikely to represent a consistent trend.

Application of the binary models across the landscape reveals that both age-structure types have their highest probability of occurrence in relatively small patches surrounded by areas with lower probability (Figures 3.8a and 3.9a). The estimated probability of occurrence for age-structure type 1 was highest in deep valley bottoms, benches, and cirques associated with high ridges in the eastern part of the western Cascades, including many high ridges of the Blue River study area (Figure 3.8b). It was unlikely to be found associated with lower ridges toward the western part of the western Cascades, including most of the Fall Creek study area (Figure 3.8c). The spatial distribution of areas with relatively high probability of occurrence is consistent with the observed distribution. Seventy-eight percent of the stands classified as age-structure type 1 were in the Blue River study area. Three of the 4 stands classified as type 1 at Fall Creek were located in a cirque, bench, and valley bottom of the highest peak in the watershed (Figure 3.8c).

Age-structure type 6 was estimated to have the greatest representation on south-facing slopes in areas of relatively low topographic relief toward the western part of the western Cascades (Figure 3.9a). Areas with a relatively high probability of occurrence are common in the northern part of the Fall Creek study area (Figure 3.9c). The highest probability of occurrence in the Blue River study area was in areas of relatively low topographic relief in the southwestern and north-central parts of the Blue River watershed (Figure 3.9b).

DISCUSSION

Relationships of Age Structure to Topography

Associations between age structure and topography were moderately strong across the study area. Age structures at both extremes of a gradient representing the degree of influence of fire on stand development had the strongest association with their topographic context, and the fidelity of age structure to terrain shape and slope position generally increased with increasing topographic relief (Figures 3.4 and 3.7). Thus, some influences of topography on patterns of fire spread and behavior probably have remained consistent across several fires over the time period represented by ages of live trees (400–500 years in many stands and occasionally > 800 years). Interactions of fire with weather and fuel, and possibly with the timing and locations of human ignitions, also undoubtedly have affected the distribution of age structure across the landscape (Thompson and Spies 2009). However, in contrast to several studies in landscapes with predominantly SR fire regimes, which describe spatially homogeneous fire regimes that are insensitive to topography (Johnson and Larsen 1991, Baker and Kipfmueller 2001), topography appears to exert some consistent influences on variation in the fire regime across the present study area (Figures 3.7 and 3.9).

Because fuel is abundant essentially in all developmental stages in the highly productive forests on the west side of the Cascade Range, fire spread and behavior are more likely limited by fuel moisture than fuel amount or connectivity (Rollins et al. 2002, Meyn et al. 2007). Below, the most consistent relationships between age structure and topography are related to likely roles of topography in moderating microclimate and fuel moisture that may affect fire patterns and behavior. First, the effects of a west-to-east trend of increasing orographic precipitation on broad-scale variation in the fire regime are inferred based on overall differences in age structure between the Blue River and Fall Creek study areas. Then, patterns of variation in age structure are compared along slope facets in areas of high and low topographic relief. Next, age structure is related to site-level variables (elevation, slope gradient, and aspect) commonly used in studies relating fire behavior to topography (Kushla and Ripple 1997, Thompson and Spies 2009).

Finally, the topographic context of sites that may function as fire-protected refugia for the oldest trees in the study area is compared to that of stands with the greatest influence of fire.

Broad-Scale Gradients

Broad patterns of variation in age structure across the study area are consistent with the central part of a west-to-east continuum of decreasing fire frequency and increasing representation of high-severity fire with increasing precipitation from the foothills toward the crest of the Cascades. However, substantial finer-scale variation in age structure within the study area illustrates that this is not a monotonic gradient.

Mean annual precipitation (1971–2000) in the Fall Creek study area (182 cm; Daly et al. 2008) is 51 cm less than that at Blue River (233 cm), and differences in age structure between the study areas suggest Fall Creek generally has higher fire frequency and less evidence of severe fire effects than at Blue River. Although most fire dates are unknown due to unavailability of complete tree cross-sections for sampling healed-over fire scars (Morrison and Swanson 1990, Skinner and Taylor 2006), relative differences in fire frequency between the study areas can be estimated by the proportion of stands with evidence of fire since 1780 (presence of a distinct cohort initiated after 1780 and either charred bark on trees that predate the cohort, or an absence of older trees; Figure 3.2). Post-1780 fire was evident at 89% of stands at Fall Creek, compared to 69% at Blue River. However, few stands at Fall Creek had evidence of high-severity fire after 1780. Only 6% of the stands at Fall Creek were classified as age-structure type 5 and support < 15 trees/ha that established before 1780, compared to 17% at Blue River.

The hypothesis that variation in annual precipitation is a primary factor driving broad-scale variation in the fire regime across the study area is supported by similar variation along precipitation gradients in other parts of the Douglas-fir/western hemlock region of the PNW. A fire-history study in the Oregon Coast Range spanned an annual precipitation gradient from 232 cm near the coast, to 151 cm near the Willamette Valley margin (Impara 1997). Fire frequency was higher and Douglas-fir was found in a broader

range of age classes in the eastern 1/3 of the study area than in wetter, coastal areas. On the Olympic Peninsula of Washington, stands lacking evidence of fire within the last 500 years were present on the wetter, coastal side (Huff 1995), but areas in the rainshadow of the Olympic Mountains had higher fire frequency and evidence of NSR fire (Wetzel and Fonda 2000).

Fire regimes also show variation along north-to-south precipitation gradients. For example, annual precipitation averages 279 cm in the Bull Run watershed, in the northernmost part of the western Cascades of Oregon (Daly et al. 2008). Only 10–25% of stands at Bull Run had more than one cohort of shade-intolerant trees (Agee and Krusemark 2001), compared to 50% at Blue River and 70% at Fall Creek, where annual precipitation averages 233 and 182 cm, respectively (cohorts were distinguished either by intervals > 80 years with no recorded establishment of any species, or by healed-over fire scars found within increment cores; chapter 2).

Some of the fine-scale variation in the fire regime within the broader west-to-east gradient may be related to local precipitation patterns, influenced by the height and orientation of major ridgelines. Direct effects of elevation on precipitation are minimal at scales finer than about 5–10 km (Sharples et al. 2004). Thus, valley bottoms adjacent to high ridges may receive higher precipitation than expected at equivalent elevations farther from major ridges (Daly et al. 1994). For example, the area adjacent to the high ridges along the perimeter of the Blue River watershed has higher estimated annual precipitation than that near the lower ridges in the north-central part of the watershed (Daly et al. 2008). Stands with two or more cohorts of shade-intolerant trees, including at least one cohort initiated after 1780 (age-structure types 4 and 6; Figure 3.2d and f), were found primarily in the drier, north-central part of the watershed (Figure 3.6b). Stands lacking evidence of fire since before 1780 (age-structure type 1; Figure 3.2a), and those that have burned, but where fire intensity probably was too low to generate canopy openings of sufficient size for regeneration of shade-intolerant species (types 2 and 3; Figure 3.2b and c), are most abundant near higher ridges along the perimeter of the watershed (Figure 3.6b).

The differences in age structure found between the wetter perimeter and the drier north-central part of the Blue River watershed are consistent with differences found between two, 2,000-ha study areas of Morrison and Swanson (1990). The Cook-Quentin study area, in the north-central part of the Blue River watershed, has a shorter estimated natural fire rotation (95 years) and more Douglas-fir cohorts per stand (2.2 on average) than the Deer Creek study area (149 years and 1.5 cohorts per stand), which includes high ridges along the eastern perimeter of the watershed.

Variation along Slope Facets

The NPMR model relating the continuous age-structure gradient to topography predicts that the range of age-structure characteristics represented along a given slope facet and the degree of differentiation in age structure by slope position vary with local relief (Figure 3.6). High ridges with deep valley bottoms are predicted to support a broader range of the age-structure gradient and have stronger fidelity of age structure to slope position and terrain shape than slope facets in areas of lower topographic relief (Figures 3.4d and 3.7a), possibly reflecting stronger microclimatic variation in areas of high than low topographic relief.

Wide microclimatic variation in areas of high relief may be influenced in part by stronger variation in exposure to solar radiation, which affects the moisture status of live foliage and dead woody fuel through its influence on daily maximum temperature (Rothermel et al. 1986). The contribution of local relief to variation in exposure to solar radiation is primarily through the amplification of insolation on steep slopes with direct exposure and the shading of deep valley bottoms by adjacent ridges (Pierce et al. 2005). For example, the range of values for the proxy for growing season insolation calculated within the area used to determine local relief (a circle of radius 2,340 m, representing the 90^{th} percentile for slope length of the sampled stands; Table 3.1), was strongly correlated with local relief ($r = 0.52$ for sample sites; $r = 0.61$ for all 30-m cells across both study areas), reflecting a trend of increasing maximum and decreasing minimum insolation values with increasing local relief.

Temperature inversions in areas of high topographic relief may contribute to strong differentiation in fuel moisture with terrain shape (Hayes 1941). Daily minimum temperatures in the steep, deeply-dissected terrain of the western Cascade Range are strongly influenced by temperature inversions and pooling of cold air in valleys and depressions (Daly et al. 2007, 2009). Temperature inversions were recorded on more than 80% of summer nights in a small (96 ha) catchment in the Blue River study area (Pypker et al. 2007). Under strong inversions, daily minimum temperatures in valley bottoms have been recorded to be as much as 10–15ºC cooler than those up to 800 m higher on nearby ridges (Daly et al. 2007, 2009).

Several factors may contribute to stronger temperature inversions, and thus greater differentiation in fuel moisture by terrain shape, with increasing topographic relief. Locally-driven, radiative cooling may account for a rapid decrease in temperature shortly after sunset, especially in concave landforms that are largely decoupled from the free atmosphere (Lundquist et al. 2008, Daly et al. 2009). Because air becomes denser as it cools, it drains downslope, enabling expansion and further cooling of cold-air pools in valleys and depressions (Gustavsson et al. 1998). To the extent that gravity-driven flow (advection) of cold air influences nocturnal cooling, nighttime minimum temperatures may be related to the source area and elevation within that area. For example, numerical simulations suggest that inversion layers build up to a greater depth in deep valleys than shallow valleys of the same width, and shading by surrounding terrain (which increases with valley depth) delays the morning breakup of the inversion layer (Colette et al. 2003).

Different patterns of fire spread and behavior along slope facets in areas of high and low topographic relief are illustrated by patterns of age structure along a representative slope facet in each context. Age structure along a north-facing slope in the Blue River study area with a ridgetop almost 800 m above the valley bottom illustrates that fire frequency and severity both vary with slope position (Figure 3.10a), a pattern represented along other ridges in areas of high topographic relief. The presence of three distinct age cohorts suggests the occurrence of at least three fires along the slope facet since the late 15th century. Trees of the oldest cohort are most abundant on the lower

slope. A trend of increasing fire frequency from lower to upper slope is supported by the presence only on the middle and upper slope, of two younger cohorts dating to probable fires in the late 18th and mid-19th century. There is no evidence of these fires on the lower slope, where the older Douglas-fir trees lack charred bark, and numerous fire-sensitive, shade-tolerant trees predate the younger cohorts present further up the slope. A trend of increasing fire severity from lower to upper slope is supported by gradually decreasing abundance of trees in the oldest cohort from the lower to the upper-mid slope position and the absence of the oldest cohort from upper slope (Figure 3.10a).

Variation in age structure along a west-facing slope in an area of lower relief in the Fall Creek study area represents a pattern of slight differences in fire severity by slope position, with no difference in fire frequency, characteristic of many slope facets in areas of low topographic relief (Figure 3.10b). The slope facet spans about 500 m from ridgetop to valley bottom. Age cohorts initiated in the 16th and 19th centuries are present at all slope positions. The younger cohort most likely initiated after a fire that burned the entire slope facet, as supported by the consistent timing of cohort initiation in each stand, and by the presence of charred bark on all trees that established before the 19th century, but not on any of the younger trees. The younger cohort was composed only of shade-tolerant trees at the lower slope, but shade-intolerant trees became increasingly abundant in the younger cohort toward the upper slope. Thus, the fire may have generated larger canopy openings conducive to regeneration of shade-intolerant trees at the mid and upper slope positions than on the lower slope (tree density in the older cohort on the lower slope is under-represented in the histogram of establishment dates because several older trees were too large to reach the pith with an 81-cm increment borer; Figure 3.10b).

Other fire-history studies in the PNW have reported variation in fire severity with slope position. However, few studies have found that trends in the degree of differentiation in fire effects with slope position were related to local topographic relief, as suggested in this study (possibly due to smaller extent and lower topographic complexity of many other study areas). Ages of Douglas-fir trees sampled by slope position in the Oregon Coast Range support a general trend of increasing fire severity

from lower to upper slopes (Impara 1997). Trees dating to fire episodes before the mid-17th century accounted for the majority of trees present on lower slopes, whereas trees dating to fire episodes after the mid-19th century outnumbered older trees on upper slopes. Similarly, in the Klamath Mountains and southern Cascades of northern California, lower slopes were inferred to have experienced lower fire severity based on higher densities of older trees than found on upper slopes (Taylor and Skinner 1998, Beaty and Taylor 2001). Temperature inversions have been suggested to contribute to this variation in burn severity by amplifying differences in fuel moisture and relative humidity among slope positions (Skinner et al. 2006). Fire severity did not vary by slope position in a study in the southern Klamath Mountains (Taylor and Skinner 2003), possibly due to gentler terrain and greater limitation of fire extent and intensity by fuel connectivity rather than fuel moisture in this drier study area.

Site-Level Variables

Although numerous fire-history studies in mountainous terrain have reported decreasing fire frequency with elevation (Swetnam et al. 1998, Taylor 2000, Sherriff and Veblen 2007), age structure in the present study showed no consistent relationship with elevation. Each age-structure type was found in stands spanning an elevation range > 700 m, and the interquartile range of elevation for all age-structure types overlapped between 860 and 1,100 m. The inverse relationship between fire frequency and elevation found in other studies probably is driven by cooler temperatures, greater precipitation, and longer snowpack persistence at higher elevations. Influences of slope position and temperature inversions may override these general trends in the rugged terrain of the present study. Other fire-history studies in the western Cascades of Oregon have reported fire frequency to decrease (Garza 1995, Van Norman 1998, Weisberg 1998), increase (Teensma 1987, Agee and Krusemark 2001), or show no relationship with elevation (Weisberg 2009).

The present analysis supports a general tendency for higher fire severity in high-elevation forest types (Pacific Silver Fir and Mountain Hemlock types) with low abundance of fire-resistant Douglas-fir trees, but there was no evidence suggesting fire

frequency in these forest types was lower than that in the Western Hemlock zone. Broad, contiguous areas of the high-elevation forest types near the crest of the Cascades may have lower fire frequency than montane forests (Simon 1991, Agee 1993). Within the study area, however, the high-elevation forest types are limited to small patches along the highest ridgetops (generally > 1,200 m), which are susceptible to fire spread from adjacent slopes and are unlikely to support fire frequency distinct from the adjacent slopes (Agee and Krusemark 2001). The age of the youngest cohort in almost all stands in Pacific Silver Fir or Mountain Hemlock zones corresponds to that in the Western Hemlock zone on the midslope position of the same slope facet, illustrating continuity of fire spread across forest types. However, older cohorts present further downslope commonly were lacking in the high-elevation forest types (Figure 3.10a), suggesting a greater probability of fires burning at high severity in these types.

In the productive Douglas-fir/western hemlock region of the PNW, where fire is probably limited more by fuel moisture than fuel amount or connectivity, high insolation on south aspects may enable higher fire frequency or greater fire intensity than on north aspects (Rollins et al. 2002). Both the fire-prone end of the NMS axis, inferred as a gradient of site fire-proneness, and the probability of occurrence for age-structure type 6 were associated with areas of high insolation (Figures 3.4 and 3.7).

Differences in aspect between age-structure types 3 and 4 support a tendency for higher fire severity on warmer aspects. Almost all stands of both types have a 400–500-year-old cohort of Douglas-fir trees with charred bark and a younger cohort of mature age (usually 80–200 years old; Figure 3.2c and d). Age-structure type 3 is located primarily on north aspects (mean transformed aspect = 1.3; 95% CI, 1.0–1.6; on a scale from 0 (southwest) to 2 (northeast)). It has a higher average density of trees that predate initiation of the younger cohort (65 trees/ha) than type 4 (45 trees/ha), which was found primarily on south aspects (mean transformed aspect = 0.8; 95% CI, 0.6–1.0). Lower tree density in the older cohort of type 4 and the association of type 4 with warmer aspects suggests either that severity of the most recent fire was higher, or that greater numbers of trees were killed over successive fires than in type 3. Otherwise, data from 29, 400–500-

year-old stands in the dataset of Spies and Franklin (1991) for the western Cascades of Oregon reveals a slightly higher density of large (> 100 cm dbh) Douglas-fir trees on south than north aspects, with no statistically significant difference in density by aspect class.

Slope gradient may affect fireline intensity and rates of fire spread by enhancing the efficiency of heat transfer to upslope fuel with increasing slope gradient (Rothermel 1983), but the strength of such a relationship may be conditioned by slope aspect. The inferred gradient of site fire-proneness, produced by NMS ordination of sample sites by age-structure variables, was unrelated to slope gradient on north aspects (areas of low insolation) (Figure 3.4a). On south aspects (areas of high insolation), however, the degree of increase in estimated fire-proneness with increasing insolation was amplified on steeper slopes. Steep slopes with south aspects may be especially fire prone due to rapid fuel desiccation under high insolation. However, lower portions of steep, V-shaped valleys may not be particularly fire-prone because temperature inversions and topographic shading may sustain relatively high fuel moisture (Hayes 1941).

Extremes of a Gradient of Fire-Proneness

Age structure most strongly was related to topography at both extremes of a continuum of fire influences on stand development. Old-growth stands with no evidence of fire for at least 400 years (age-structure type 1; Figure 3.2a) and stands containing three or more cohorts of shade-intolerant trees (age-structure type 6; Figure 3.2f) could be distinguished fairly reliably from the remaining stands based on their topographic context (Figure 3.7). These stands may occupy a small portion of the landscape, where strong topographic influences on microclimate and fuel moisture are likely to affect the probability of fire occurrence or moderate fire intensity. However, the majority of the landscape probably experiences a broader range of fire intervals and intensities, producing weaker relationships between age structure and topography (Figure 3.5).

The NPMR model for age-structure type 1 predicts the highest probability of occurrence in concave landforms below high ridgetops (Figure 3.7a), which may provide

the strongest topographic moderation of microclimate and fuel moisture. Annual precipitation is likely to be highest near high ridgetops, due to a trend of increasing orographic precipitation with increasing ridgetop elevation from the foothills toward the crest of the Cascades, and to influences of the height and orientation of major ridgelines on local storm patterns (Daly et al. 1994). Temperature inversions (Daly et al. 2007, 2009) and topographic shading by surrounding terrain (Pierce et al. 2005) are likely to contribute to cooler microclimate and higher soil and fuel moisture in concave landforms (lower slopes, benches, cirques) than on adjacent slopes. High moisture of live vegetation and dead woody fuel either may hinder fire spread or reduce fire intensity in these concave features relative to the surrounding terrain. In the western Cascades of southwestern Washington, for instance, fire-sensitive, shade-tolerant trees that predate the most recent fire consistently were associated with concave terrain shape (Keeton and Franklin 2004).

Stands supporting the old-age tail of the age distribution for shade-intolerant trees are likely to be associated with similar topographic settings as age-structure type 1, further supporting the role of topographic moderation of microclimate and fuel moisture in limiting fire spread and intensity. The oldest shade-intolerant trees in the study area are Douglas-fir trees that established between the late 12th and mid-14th century. They predate both periods of region-wide, extensive fire identified in a synthesis of fire-history studies west of the crest of the Cascades in Oregon and Washington (from the late 1400s to ca. 1650 and from ca. 1800 to ca. 1925; Weisberg and Swanson 2003). Cohorts dating to the earlier period of extensive burning are widespread across the study area (75% of stands have shade-intolerant trees that established between 1450 and 1610), but only 8% of stands include shade-intolerant trees that established before 1450. Most of these stands have evidence (charred bark and younger cohorts) of fire since establishment of the old trees. However, persistence of these trees through two periods of extensive fire that affected almost the full extent of both study areas suggests sites supporting these trees may be buffered from severe fire effects (Giglia 2004).

Similarity in topographic context between stands supporting the oldest shade-intolerant trees in the study area and those of age-structure type 1, which support the oldest shade-tolerant trees (Figure 3.2a) is suggested by the NPMR model for age-structure type 1 (Figure 3.7a). Although most stands supporting shade-intolerant trees that established before 1450 were not classified as age-structure type 1, the predicted probabilities of occurrence for age-structure type 1 based on topography of these stands were among the highest predictions of all sample sites. For example, the estimated probability of occurrence was > 0.3 only in 9 stands that were not classified as age-structure type 1, and 6 of these stands contain shade-intolerant trees that established before 1450. Of the remaining stands supporting such old trees, 3 were included in age-structure type 1, and only 2 had an estimated probability of occurrence < 0.3.

Stands of age-structure type 6, which usually have at least three cohorts of shade-intolerant trees (Figure 3.2f), are likely to be located in sites with the lowest fuel moisture across the study area. The highest probability of occurrence for type 6 is on moderately steep slopes with high insolation below low ridgetops (< ca. 1,100 m; Figure 3.7). Low ridgetop elevation generally is associated with low annual precipitation and little potential for moderation of microclimate by topographic shading or temperature inversions. In areas with low ridges, the probability of occurrence is high only in warm microsites with moderately steep slopes and high exposure to solar radiation (Figure 3.7). The moderate slope gradient and high exposure to solar radiation may render these sites susceptible to high daily maximum temperatures, and thus low fuel moisture (Hayes 1941, Rothermel et al. 1986).

Summary and Conclusions

The relationships between age structure and topography found here aid in developing a general picture of local variation in the fire regime and associated spatial variation in forest structure across the landscape. Age structure most strongly was related to topography at both extremes of a continuum of fire influences on stand development, in settings that represent extremes of a continuum of topographically moderated

microclimate and fuel moisture. Old-growth stands that have remained unburned for several centuries (age-structure type 1) are located in deep valley bottoms, benches, and cirques associated with ridgetops higher than about 1,200 m, which are limited almost exclusively to the eastern part of the western Cascades (Figure 3.8). Fire-prone stands supporting three or more cohorts of shade-intolerant trees are restricted to areas of high exposure to solar radiation, on relatively steep slopes beneath low ridgetops (Figure 3.9).

Age structure was not as strongly related to topography in other parts of the landscape, where microclimate and fuel moisture conditions are less extreme. For example, two-cohort stands (age-structure types 2, 3, and 4) account for the majority of sampled stands. Differences in the density of trees that predate the most recent fire in these stands may reflect differences in the severity of the most recent fire or cumulative effects of two or more fires. However, the inability to develop statistically significant NPMR models to distinguish these age-structure types from the remaining stands based on topography reflects that differences in fire behavior were not consistently influenced by topography. There are general tendencies for stands with higher densities of trees that predate the most recent fire (60 and 65 trees/ha in age-structure types 2 and 3, respectively; chapter 2) and a post-fire cohort of shade-tolerant trees to be located on cool aspects or on lower slope positions on warm aspects, and for stands with lower densities of trees that predate the most recent fire (45 trees/ha in type 4) and a post-fire cohort of shade-intolerant and shade-tolerant species to be located on warm aspects or upper slope positions. However, there was substantial overlap in the topographic settings supporting these age-structure types, which suggests that weather or stand conditions at the time of the fire may have overridden topographic influences in these areas of moderate microclimate.

This study supports a trend of increasing representation of older trees, and thus decreasing fire severity, toward lower slope positions and with increasing terrain concavity (Figure 3.10), as found in previous studies in the PNW (Impara 1997, Taylor and Skinner 1998, Keeton and Franklin 2004). However, across the present study area, the strength of this trend was conditioned by local topographic relief and ridgetop

elevation, providing a broader range of age structures and stronger fidelity of age structure to slope position and terrain shape in areas of high topographic relief than areas of lower relief (Figure 3.6). The strengthening of associations of age structure to terrain shape and slope position with increasing topographic relief most likely reflects an amplification of microclimatic and fuel moisture differences among different local topographic settings due to increasing importance of temperature inversions and topographic shading by adjacent ridges (Daly et al. 2007, 2009). Because ridgetop elevation and topographic relief tend to increase from west to east across the central western Cascades, the stronger of influences of terrain shape and slope position on fire behavior with higher relief contributes to a pattern of increasing diversity of stand structure and greater distinction in stand structure among slope positions in the eastern part of the western Cascades than in the western part (Figure 3.10).

The relationships between age structure and topography found here may help in developing guidelines for landscape-level management influenced by historical disturbance regimes. For example, a management plan in the Blue River study area uses previous fire-history research to divide the landscape into three zones, each with different harvest rotation lengths and tree-retention levels, developed to emulate effects of historical fires (Cissel et al. 1999). This study provides more specific guidance in locating areas for treatment and areas to leave untreated within those zones, and it may allow for greater tuning of management prescriptions to local topography. The relationships found here also may provide hypotheses for interpreting the contribution of topography to local variation in the fire regime in other landscapes, especially in productive regions where fire spread and behavior are limited primarily by fuel moisture rather than fuel amount or connectivity.

LITERATURE CITED

Agee, J.K. 1993. *Fire Ecology of Pacific Northwest Forests*. Island Press. Washington, D.C. 493 pp.

Agee, J.K., and F. Krusemark. 2001. Forest fire regime of the Bull Run watershed, Oregon. *Northwest Sci.* 75: 292–306.

Baker, W.L., and K.F. Kipfmueller. 2001. Spatial ecology of pre-Euro-American fires in a southern Rocky Mountain subalpine forest landscape. *Prof. Geog.* 53: 248–262.

Beaty, M.R., and A.H. Taylor. 2001. Spatial and temporal variation of fire regimes in a mixed conifer forest landscape, southern Cascades, California, USA. *J. Biogeogr.* 28: 955–966.

Beers, T.W., P.E. Beers, and L.C. Wensel, 1966. Aspect transformation in site productivity research. *J. For.* 64: 691–692.

Camp, A.E., C. Oliver, P. Hessburg, and R. Everett. 1997. Predicting late-successional fire refugia pre-dating European settlement in the Wenatchee Mountains. *For. Ecol. Manage.* 95: 63–77.

Cissel, J.H., F.J. Swanson, and P.J. Weisberg. 1999. Landscape management using historical fire regimes: Blue River, Oregon. *Ecol. App.* 9: 1217–1231.

Colette, A., F.K. Chow, and R.L. Street. 2003. A numerical study of inversion-layer breakup and the effects of topographic shading in idealized valleys. *J. Appl. Meteorol.* 42: 1255–1272.

Collins, B.M., J.D. Miller, A.E. Thode, M. Kelly, J.W. van Wagtendonk, and S.L. Stephens. 2009. Interactions among wildland fires in a long-established Sierra Nevada natural fire area. *Ecosystems* 12: 114–128.

Daly, C., D.R. Conklin, and M.H. Unsworth. 2009. Local atmospheric decoupling in complex topography alters climate change impacts. *Int. J. Clilmatol.* doi: 10.1002/joc.2007.

Daly, C., M. Halbeib, J.I. Smith, W.P. Gibson, M.K. Doggett, G.H. Taylor, J. Curtis, and P.P. Pasteris. 2008. Physiographically sensitive mapping of climatological temperature and precipitation across the conterminous United States. *Int. J. Climatol.* 28: 2031–2064.

Daly, C., R.P. Nielson, and D.L. Phillips. 1994. A statistical-topographic model for mapping climatological precipitation over mountainous terrain. *J. Appl. Meteorol.* 33: 140–158.

Daly, C., J.W. Smith, J.I. Smith, and R.B. McKane. 2007. High-resolution spatial modeling of daily weather elements for a catchment in the Oregon Cascade Mountains, United States. *J. Applied Meteorol. and Climatol.* 46: 1565–1586.

Duncan, R.P. 1989. An evaluation of errors in tree age estimates based on increment cores in Kahikatea (*Dacrycarpus cacrydioides*). *New Zealand Nat. Sci.* 16: 31–37.

Franklin, J.F., and C.T. Dyrness. 1973. Natural vegetation of Oregon and Washington. USDA For. Serv. Gen. Tech. Rep. PNW-GTR-8. 417 pp.

Garza, E.S. 1995. Fire history and fire regimes of East Humbug and Scorpion Creeks and their relation to the range of *Pinus lambertiana* Dougl. M.S. Thesis. Oregon State University. Corvallis.

Giglia, S.K. 2004. Spatial and temporal patterns of "super-old" Douglas-fir trees of the central western Cascades, Oregon. M.S. Thesis. Oregon State University. Corvallis.

Gustavsson, T., M. Karlsson, J. Bogren, and S. Lindqvist. 1998. Development of temperature patterns during clear nights. *J. Appl. Meteorol.* 37: 559–571.

Hayes, G.L. 1941. Influences of altitude and aspect on daily variations in factors of forest fire danger. USDA Circular 591. 38 pp.

Hemstrom, M.A., and J.F. Franklin. 1982. Fire and other disturbances of the forests in Mount Rainier National Park. *Quat. Res.* 18: 32–51.

Huff, M.A. 1995. Forest age structure and development following wildfires in the western Olympic Mountains, Washington. *Ecol. App.* 5: 471–483.

Impara, P.C. 1997. Spatial and temporal patterns of fire in the forests of the central Oregon Coast Range. Ph.D. Dissertation. Oregon State University, Corvallis.

Iniguez, J.M., T.W. Swetnam, and S.R. Yool. 2008. Topography affected landscape fire history patterns in southern Arizona, USA. *For. Ecol. Manage.* 256: 295–303.

Johnson, E.A., and C.P.S. Larsen. 1991. Climatically induced change in fire frequency in the southern Canadian Rockies. *Ecol*ogy 72: 194–201.

Keeton, W.S., and J.F. Franklin. 2004. Fire-related landform associations of remnant old-growth trees in the southern Washington Cascade Range. *Can. J. For. Res.* 34: 2371–2381.

Kushla, J.D., and W.J. Ripple. 1997. The role of terrain in a fire mosaic of a temperate coniferous forest. *For. Ecol. Manage.* 95: 97–107.

Kruskal, J.B. 1964. Multidimensional scaling by optimizing goodness of fit to a nonmetric hypothesis. *Psychometrika* 29: 1–27.

Lundquist, J.D, N. Pepin, and C. Rochford. 2008. Automated algorithm for mapping regions of cold-air pooling in complex terrain. *J. Geophys. Res.* 113: D22107.

Meyn, A., P.S. White, C. Buhk, and A. Jentsch. 2007. Environmental drivers of large, infrequent wildfires: the emerging conceptual model. *Prog. Phys. Geogr.* 31: 287–312.

McCune. B. 2006. Non-parametric habitat models with automatic interactions. *J. Veg. Sci.* 17: 819–830.

McCune, B., and M.J. Mefford. 2006. PC-ORD. Multivariate Analysis of Ecological Data. Version 5.04. MjM Software. Gleneden Beach, Oregon.

McCune, B. and M. J. Mefford. 2008. HyperNiche. Nonparametric Multiplicative Habitat Modeling. Version 2.54 beta. MjM Software, Gleneden Beach, Oregon, U.S.A.

Morrison, P.H., and F.J. Swanson. 1990. Fire history and pattern in a Cascade Range landscape. USDA For. Serv. Gen. Tech. Rep. PNW-254.

Pierce, K.B. Jr., T. Lookingbill, and D. Urban. 2005. A simple method for estimating potential relative radiation (PRR) for landscape-scale vegetation analysis. *Landscape Ecol.* 20: 137–147.

Pypker, T.G., M.H. Unsworth, A.C. Mix, W. Rugh, T. Ocheltree, K. Alstad, and B.J. Bond. 2007. Using nocturnal cold air drainage flow to monitor ecosystem processes in complex terrain. *Ecol. App.* 17: 702–714.

Rich, P.M., R. Dubayah, W.A. Hetrick, and S.C. Saving. 1994. Using viewsheds to calculate intercepted solar radiation: applications in ecology. American Society for Photogrammetry and Remote Sensing Technical Papers. pp. 524–529.

Rollins, M.G., P. Morgan, and T.W. Swetnam. 2002. Landscape-scale controls over 20th century fire occurrence in two large Rocky Mountain (USA) wilderness areas. *Landscape Ecol.* 17: 539–557.

Romme, W.H., and D.H. Knight. 1981. Fire frequency and subalpine forest succession along a topographic gradient in Wyoming. *Ecology* 62: 319–326.

Rothermel, R.C. 1983. How to predict the spread and intensity of forest and range fires. USDA For. Serv. Gen. Tech. Rep. INT-143.

Rothermel, R.C., R.A. Wilson, G.A. Morris, and S.S. Sackett. 1986. Modeling moisture content of fine dead wildland fuels input to the BEHAVE fire prediction system. USDA Forest Service, Research Paper INT-359.

Sharples, J.J., M.F. Hutchinson, and D.R. Jellett. 2004. On the horizontal scale of elevation dependence of Australian monthly precipitation. *J. Appl. Meteorol.* 44: 1850–1865.

Sherriff, R.L., and T.T. Veblen. 2007. A spatially-explicit reconstruction of historical fire occurrence in the Ponderosa Pine Zone of the Colorado Front Range. *Ecosystems* 10: 311–323.

Simon, S.A. 1991. Fire history in the Jefferson Wilderness area east of the Cascade Crest. Final report to the Deschutes National Forest Fire Staff.

Skinner, C.N., and A.H. Taylor. 2006. Southern Cascades bioregion. *In*: Fire in California's Ecosystems. Edited by N.G. Sugihara, J.W. van Wagtendonk, J. Fites-Kaufman, K.E Shaffer, A.E. Thode. University of California Press, Berkeley. pp. 195–224.

Skinner, C.N., A.H. Taylor, and J.K. Agee. 2006. Klamath Mountains bioregion. *In*: Fire in California's Ecosystems. Edited by N.G. Sugihara, J.W. van Wagtendonk, J. Fites-Kaufman, K.E Shaffer, A.E. Thode. University of California Press, Berkeley. pp. 170–194.

Spies, T.A., and J.F. Franklin. 1991. The structure of natural young, mature, and old-growth Douglas-fir forests in Oregon and Washington. *In* Ruggiero, L. (ed.), Wildlife and Vegetation of Unmanaged Douglas-fir Forests. USDA For. Serv. Gen. Tech. Rep. PNW-GTR-285. Pacific Northwest Research Station. Portland, OR. pp. 91–110.

Stokes, M.A., and T.L. Smiley 1996. An introduction to tree-ring dating. University of Arizona Press, Tucson.

Swetnam, T.W., C.H. Baisan, K. Morino, and A.C. Caprio. 1998. Fire history along elevational transects in the Sierra Nevada, California. Final Report to Sierra Nevada Global Change Research Program. University of Arizona, Laboratory of Tree-Ring Research.

Taylor, A.H. 2000. Fire regimes and forest changes in mid and upper montane forests of the southern Cascades, Lassen Volcanic National Park, California, USA. *J. Biogeogr.* 27: 87–104.

Taylor, A.H., and C.N. Skinner. 1998. Fire history and landscape dynamics in a late-successional reserve, Klamath Mountains, California, USA. *For. Ecol. Manage.* 111: 285–301.

Taylor, A.H., and C.N. Skinner. 2003. Spatial patterns and controls on historical fire regimes and forest structure in the Klamath Mountains. *Ecol. App.* 13: 704–719.

Teensma, P.D.A. 1987. Fire history and fire regimes of the central Western Cascades of Oregon. Ph.D. Dissertation. Department of Geography. University of Oregon, Eugene.

Thompson, J.R., and T.A. Spies. 2009. Vegetation and weather explain variation in crown damage within a large mixed-severity wildfire. *For. Ecol. Manage.* 258: 1684–694.

Van Norman, K. 1998. Historical fire regime in the Little River watershed, southwestern Oregon. M.S. Thesis, Oregon State University. Corvallis.

Weisberg, P.J. 1998. Fire History, Fire Regimes, and Development of Forest Structure in the Central Western Oregon Cascades. Ph.D. Dissertation. Oregon State University. Corvallis.

Weisberg, P.J. 2004. Importance of non-stand-replacing fire for the development of forest structure in the Pacific Northwest, USA. *For. Sci.* 50: 245–258.

Weisberg, P.J. 2009. Historical fire frequency on contrasting slope facets along the McKenzie River, western Oregon Cascades. *W. North Am. Nat.* 69: 206–214.

Weisberg, P.J., and F.J. Swanson. 2003. Regional synchroneity in fire regimes of western Oregon and Washington, USA. *For. Ecol. Manage.* 172: 17–28.

Wetzel, S.A., and R.W. Fonda. 2000. Fire history of Douglas-fir forests in the Morse Creek drainage of Olympic National Park, Washington. *Northwest Sci.* 74: 263–279.

Yamaguchi, D.K. 1991. A simple method for cross-dating increment cores from living trees. *Can. J. For. Res.* 21: 414–416.

Zackrisson, O. 1977. Influence of forest fires on the north Swedish boreal forest. *Oikos* 29: 22–32.

Zenner, E.K. 2005. Development of tree size distributions in Douglas-fir forests under differing disturbance regimes. *Ecol. App.* 15: 701–714.

Table 3.1. Description of topographic variables and their hypothesized influences on fire frequency or behavior.

Category Variable	Abbrev -iation	Units	Description	Hypothesized influence on fire frequency or behavior
Elevation				
Elevation	Elev	m	Pixel height above sea level.	Fire frequency decreases with elevation: cooler temperatures and longer snowpack persistence with increasing elevation lead to shorter fire seasons. Fire severity may increase at the highest elevations due to loss of fire-resistant tree species (Douglas-fir).
Ridgetop Elevation	RE	m	Elevation of the ridgetop immediately upslope from the focal pixel.	Fire frequency is lower near high than low ridges due to influences of major ridgelines on local precipitation. Microclimatic variation may be stronger on high than low ridges, contributing to stronger variation in fire frequency or behavior with terrain shape and slope position.
Topographic Relief				
Slope Relief	SR	m	Elevation difference along a straight line from ridgetop to valley bottom passing through the focal pixel.	Variation in fire frequency and/or behavior with terrain shape and slope position may be stronger in areas of high than low slope relief due to stronger influences of temperature inversions and topographic shading on microclimate and fuel moisture.
Local Relief	LR	M	Elevation range in a radius of 2,340 m, representing the 90th percentile of slope length for the sampled transects.	Similar to SR, but evaluated over a broader area to account for topographic relief over the entire width of a valley that potentially contributes to local microclimatic variation.
Exposure to Solar Radiation				
Trans-formed aspect	Asp	--	Transformation of aspect to a continuous variable ranging from 0 (southwest) to 2 (northeast) (Beers et al. 1966). Asp = 1 + cos(45° – aspect)	Exposure to solar radiation accelerates fuel desiccation, potentially leading to higher fire frequency or greater probability of severe fire effects on south than north aspects.
Growing Season Insolation	Insol	WH/ m^2	Incoming solar radiation (direct + diffuse) calculated hourly for the day of mean solar period in each month (May–September), and averaged across months (Rich et al. 1994).	Similar to Asp, but accounts for influences of slope gradient, shading by adjacent ridges, and changes in solar azimuth and zenith angle within a day and over the growing season.
Slope Position				
Vertical Slope Position	VSP	--	Height of the focal pixel above the valley bottom expressed as a proportion of slope relief. Values range from 0 (valley bottom) to 1 (ridgetop). VSP = (DEM – valley bottom elevation) / SR	Fire frequency and/or susceptibility to severe fire effects increase from lower to upper slopes due to increasing wind exposure and preheating of upslope fuel, and decreasing influences of topographic shading and temperature inversions on relative humidity and fuel moisture.
Slope Dist. from Ridgetop	SDR	m	Distance along the slope surface from the focal pixel upslope to the ridgetop.	Fire frequency and/or susceptibility to severe fire effects increase closer to the ridgetop. Similar to VSP, but account for slope length.
Terrain Shape				
Topo. Index 150 m	TI150	m	Focal pixel height above the minimum elevation in a neighborhood of radius 150 m (neighborhood diameter is ¼ the median slope length) (Daly et al. 2007, 2008).	Fire frequency and/or potential for severe fire effects decrease with increasing concavity due to cooler temperatures, higher relative humidity, and greater soil-water availability, which affect the moisture status of live foliage and dead woody fuel.
Topo. Index 300 m	TI300	m	Same as above, but neighborhood diameter is set to 300 m, representing ½ the median slope length.	Same as TI150 but evaluated over a larger area.

Table 3.1. (continued)

Category Variable	Abbrev -iation	Units	Description	Hypothesized influence on fire frequency or behavior
Slope Length				
Slope Length	SL	m	Horizontal distance from focal pixel to ridgetop plus horizontal distance to valley bottom. Approximately ½ valley width.	Long slopes may have stronger microclimatic variation, and thus greater variation in fire behavior and stronger association of behavior with topographic position than shorter slopes.
Slope Gradient				
Slope Gradient	Slp	%	Slope steepness measured as a percent.	Potential for severe fire effects increase with slope steepness due to greater fuel desiccation and greater efficiency of heat transfer, leading to faster spread rates on steep than gentle slopes.

Table 3.2. Comparison of predictor variable importance for a five-predictor NPMR model produced by forward stepwise NPMR with 12 original input variables ($xR^2 = 0.3104$, $p < 0.002$).

Variable	Raw Tolerance	Standardized Tolerance	Sensitivity
LR	64.98	0.15	0.398
SDR	505.53	0.15	0.315
Insol.	452.27	0.20	0.262
Slp	13.02	0.20	0.239
VSP	0.39	0.40	0.089

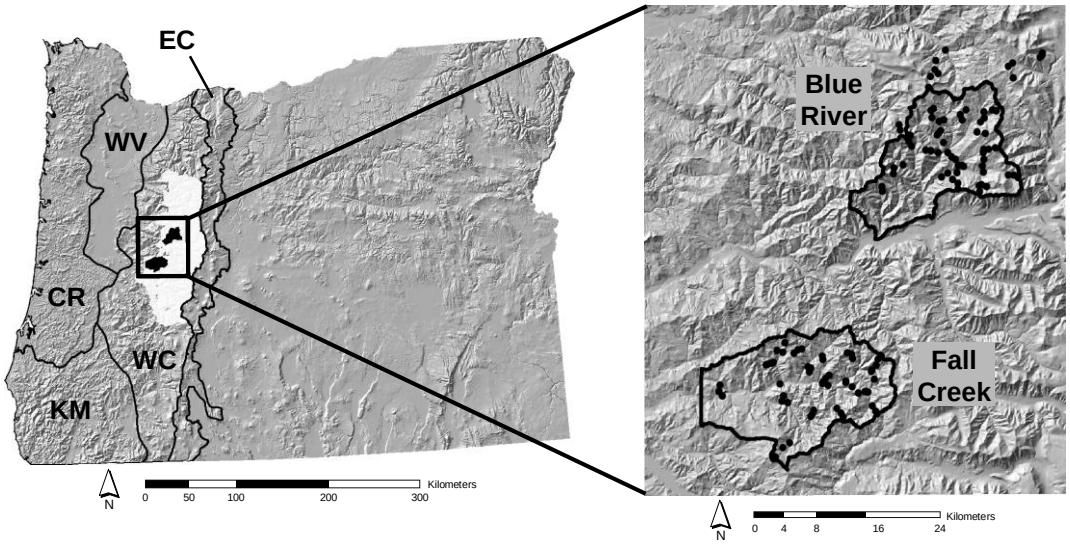

Figure 3.1. Study site locations in relation to the Willamette National Forest (white shading) and major physiographic provinces of western Oregon (WC = Western Cascades, EC = Eastern Cascades, WV = Willamette Valley, CR = Coast Range, KM = Klamath Mountains; Franklin and Dyrness 1973).

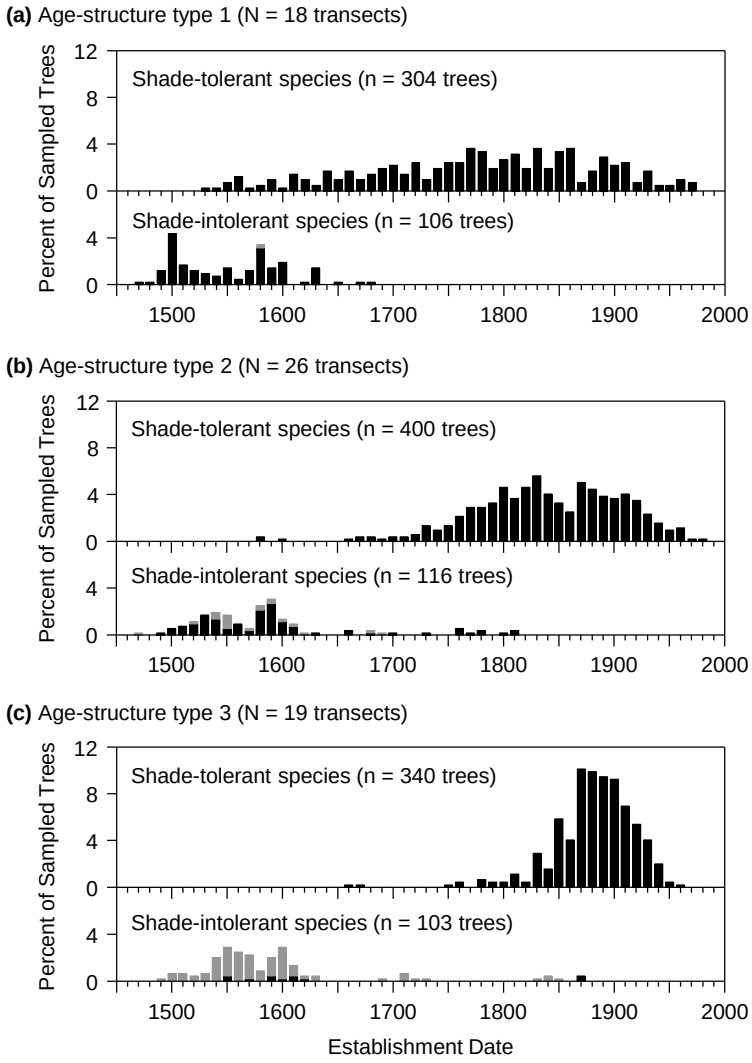

Figure 3.2. Comparison of the composite age distributions for shade-intolerant and shade-tolerant species among six age-structure types in the central western Cascades of Oregon. Age-structure types were identified by hierarchical clustering of eight age-structure variables, as described in chapter 2. Gray shading for shade-intolerant trees indicates trees with charred bark. Establishment dates prior to 1450 account for only 1% of establishment dates and are not shown.

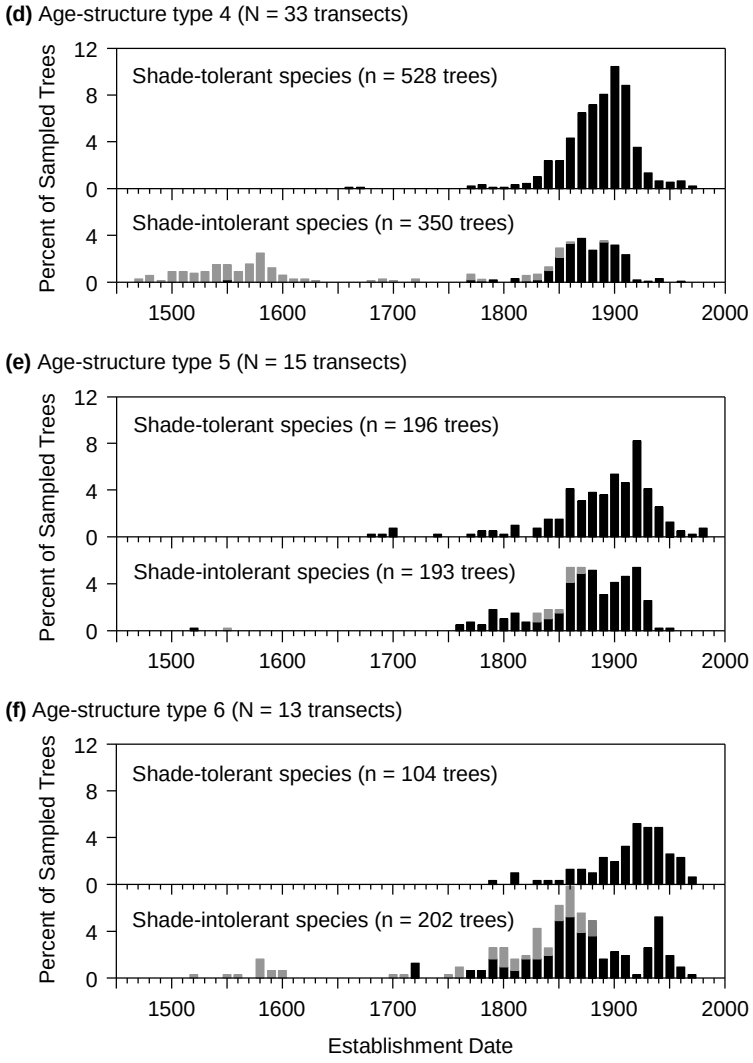

Figure 3.2. (continued)

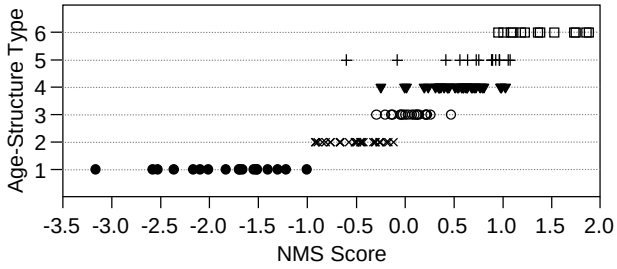

Figure 3.3. Ordination of 124 stands sampled in the central western Cascades of Oregon in the one-dimensional NMS ordination space of 6 age-structure variables (final stress = 13.412, $R^2 = 0.91$, final instability < 0.00001, $p < 0.002$)

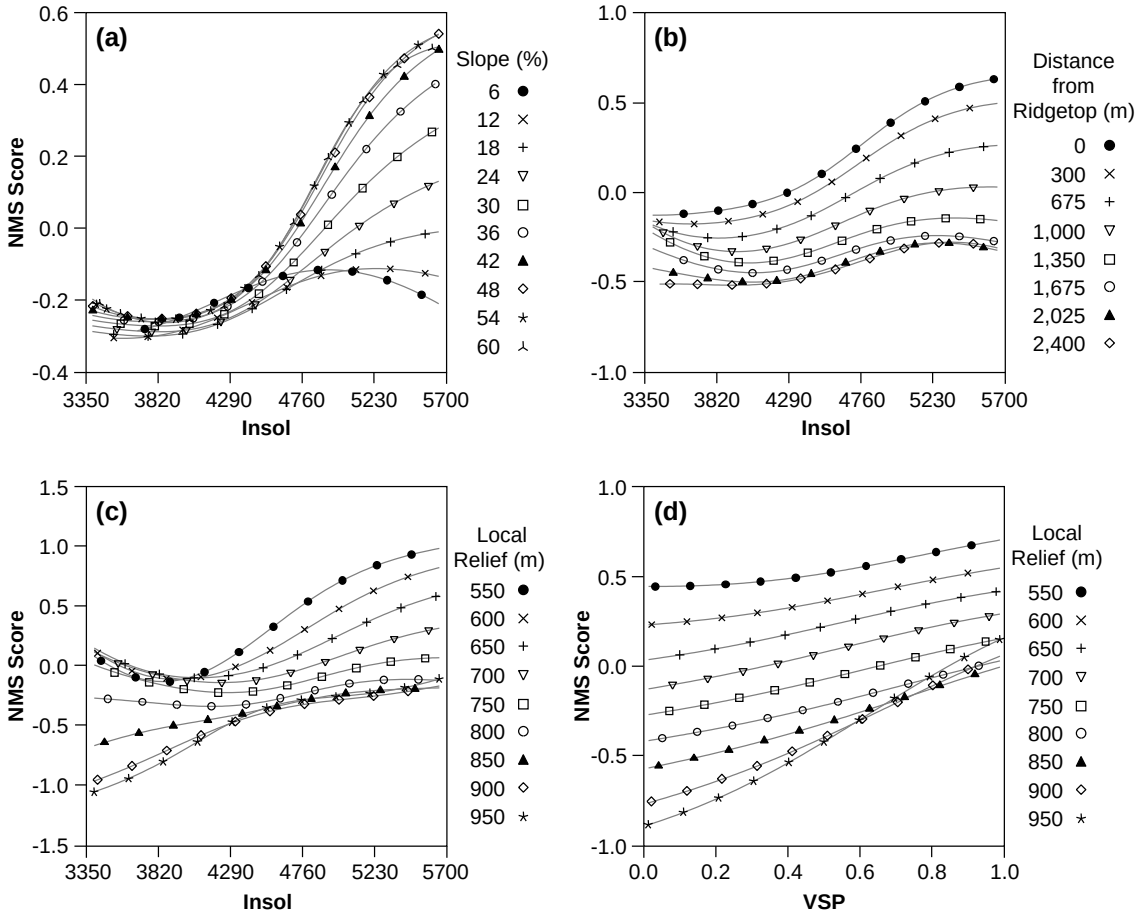

Figure 3.4. Selected interactions among topographic predictor variables used by NPMR to predict one-dimensional NMS ordination scores. Interactions include (a) slope gradient and growing season insolation (Insol), (b) distance from ridgetop and growing season insolation, (c) local relief and growing season insolation, and (d) local relief and vertical slope position (VSP).

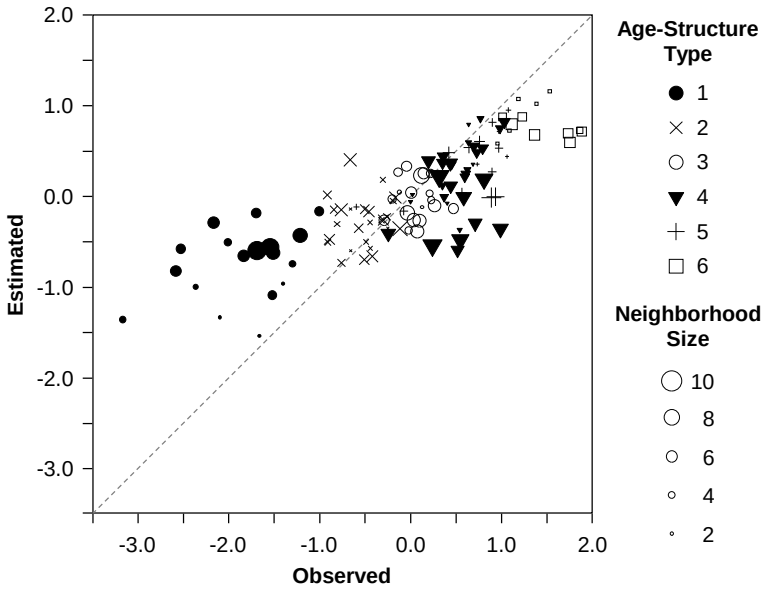

Figure 3.5. Comparison of estimated vs. observed values for the NPMR model predicting one-dimensional NMS ordination scores by five topographic variables. Points are coded by age-structure type as determined by hierarchical clustering of eight age-structure variables (Figure 3.2), and point size is scaled by neighborhood size. Neighborhood size is a measure of the amount of data bearing on the estimate at each point, calculated by summing the weights of all other sample sites, where sites receive a weight from 0 to 1 based on environmental similarity to the target point (McCune 2006). The dashed line is a one-to-one line representing estimates equal to observed values. Distances of each point from the line are residuals.

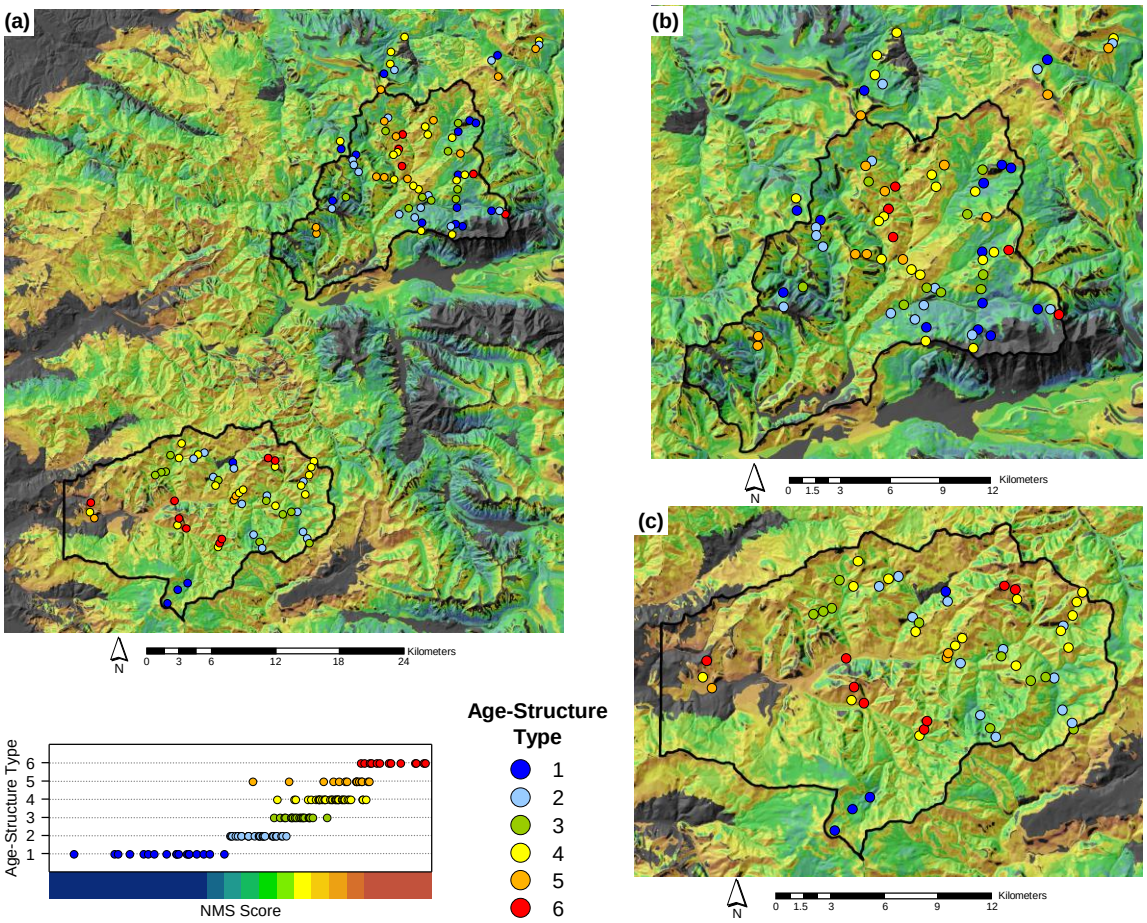

Figure 3.6. Map of the central western Cascades of Oregon developed by application of the relationships determined by the NPMR model to predict one-dimensional NMS ordination of 124 transects by 5 topographic variables. Maps show (a) the entire study area, and close-ups of the (b) Blue River, and (c) Fall Creek study areas. Points are transect locations, color-coded by age-structure type. Colors in the map are coded to the one-dimensional NMS ordination of Figure 3.3. Black shading represents topographic features not well represented by the sample sites, where the neighborhood size is too small for prediction.

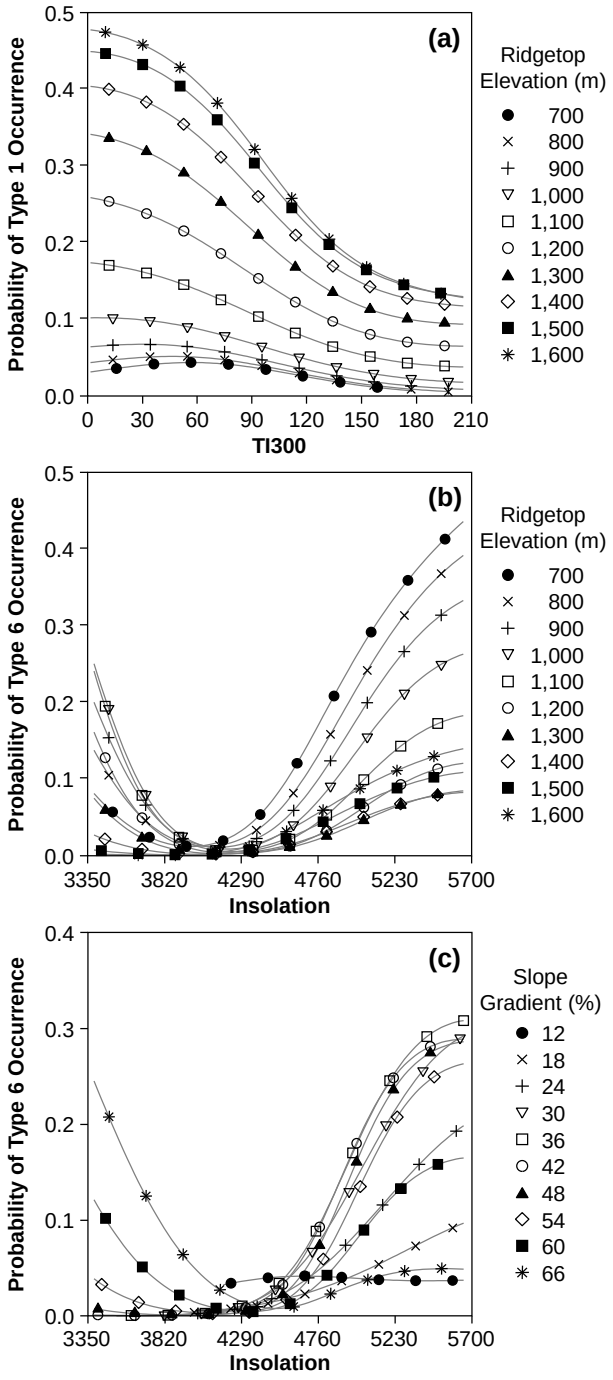

Figure 3.7. Interactions between topographic variables used in binary NPMR models to predict the probability of occurrence for age-structure type 1 based on (a) ridgetop elevation and terrain shape (TI300; low values are concave, high values are convex), and the probability of occurrence for age-structure type 6 based on interactions of the proxy for growing season insolation with (b) ridgetop elevation and (c) slope gradient.

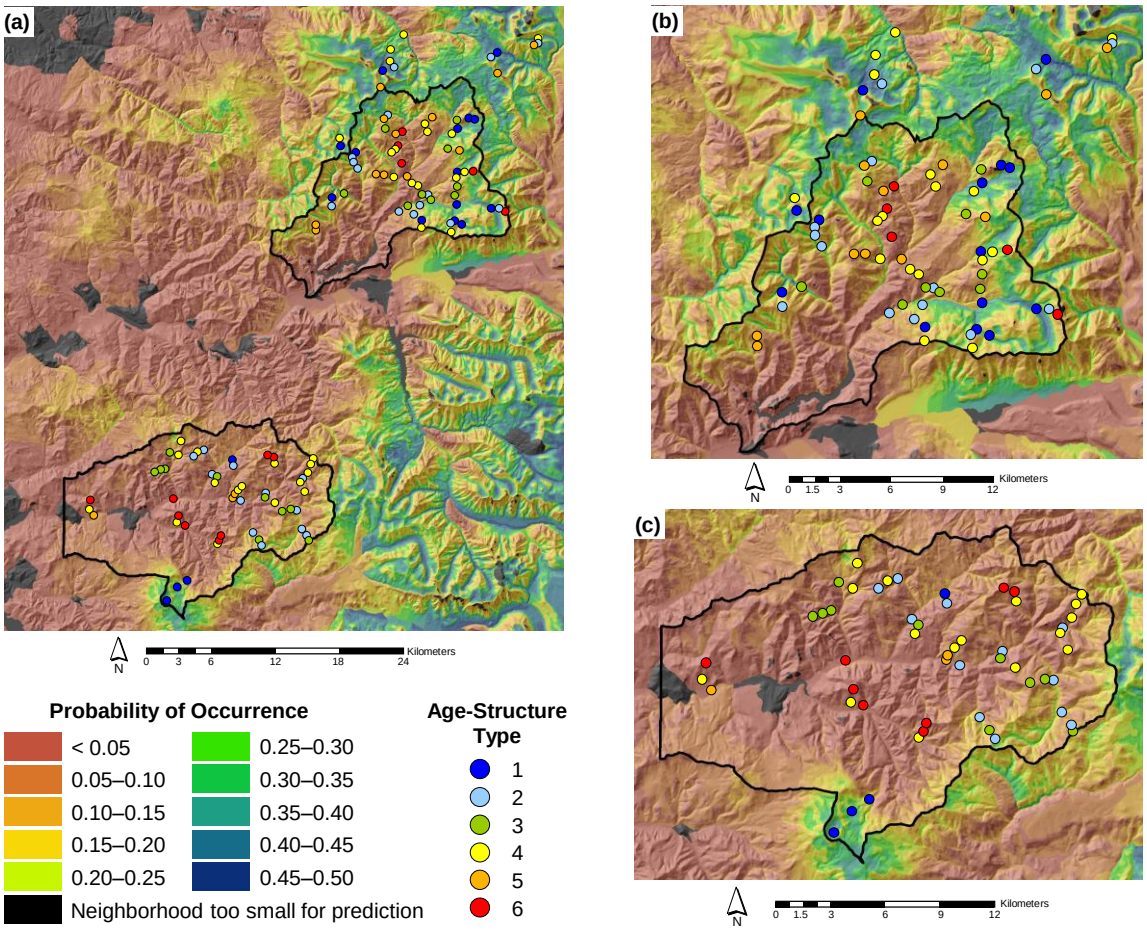

Figure 3.8. Map of the central western Cascades of Oregon developed by application of the relationships determined by the binary NPMR model to predict the probability of occurrence for age-structure type 1 by ridgetop elevation and terrain shape (TI300; Table 3.1). Maps show (a) the entire study area and close-ups of (b) the Blue River and (c) the Fall Creek study areas. Points are the locations of sample sites color-coded by age-structure type, corresponding to the histograms in Figure 3.2.

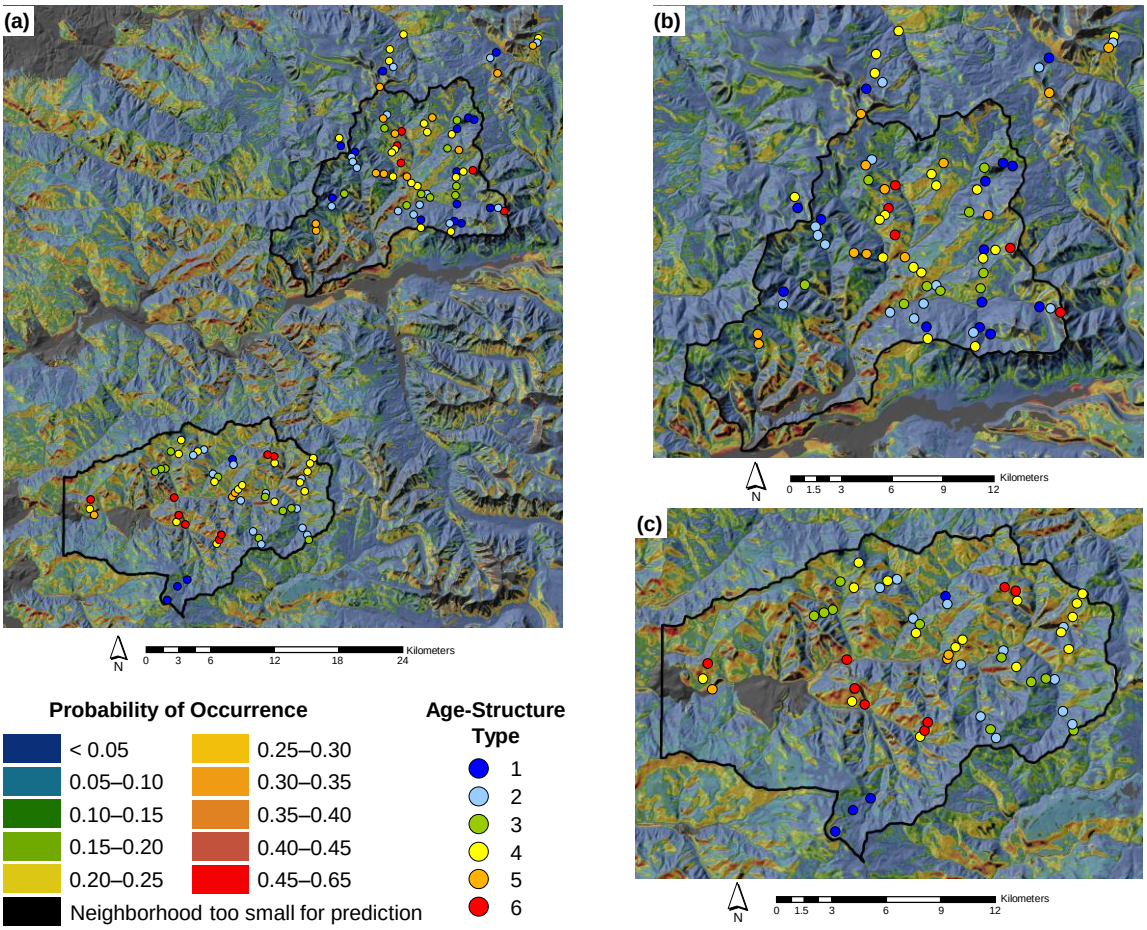

Figure 3.9. Map of the central western Cascades of Oregon developed by application of the relationships determined by the binary NPMR model to predict the probability of occurrence for age-structure type 6 by ridgetop elevation, slope gradient, and the proxy for growing season insolation. Maps show (a) the entire study area and close-ups of (b) the Blue River and (c) the Fall Creek study areas. Points are the locations of sample sites color-coded by age-structure type, corresponding to the histograms in Figure 3.2.

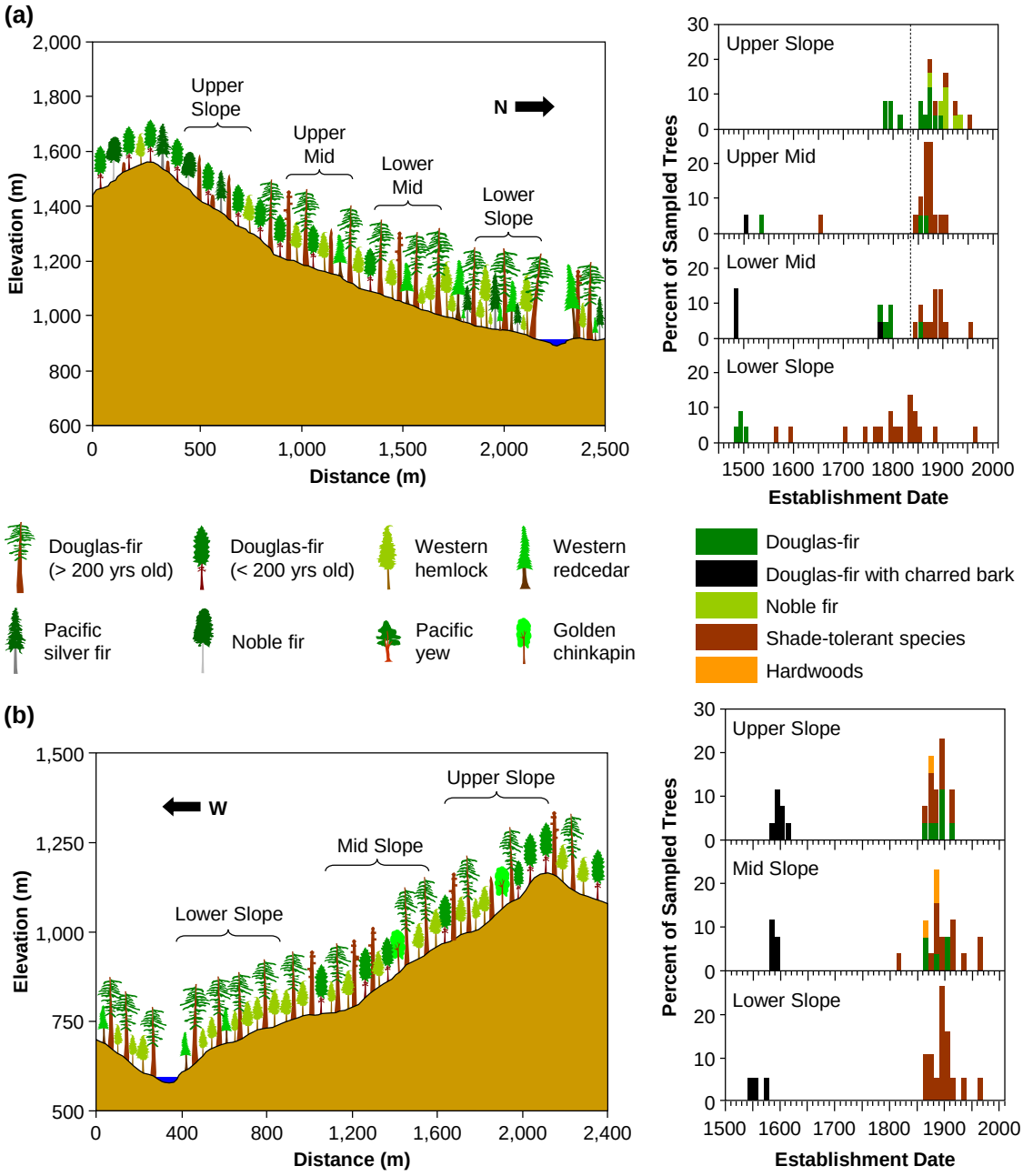

Figure 3.10. Comparison of age distributions for shade-intolerant and shade-tolerant species by slope position along slope facets representative of areas of (a) high and (b) low topographic relief in the central western Cascades of Oregon. The vertical dashed line in the histogram for (a) represents a healed-over fire scar in 1835, recorded in an increment core. Drawings are included to depict idealized trends along the slopes, but trees are not drawn to scale.

CHAPTER 4: ANALYTICAL APPROXIMATION OF A STOCHASTIC, SPATIAL SIMULATION MODEL OF FIRE AND FOREST DYNAMICS

ABSTRACT

Although stochastic, spatial simulation models of fire and forest dynamics commonly are applied to evaluate historical variability in landscape structure or predict potential changes under alternative climate or management scenarios, these models usually lack transparency into the effects of input parameters and modeling algorithms. Analytical models are an alternative approach, where equations directly specify the influence of each variable. However, application of such models usually has been limited to simple scenarios that lack feedbacks or spatial interactions more easily addressed by simulation. In this study, I develop an analytical approximation of a spatial simulation model initially developed and applied to the Oregon Coast Range. The model includes stochastic variation in the number of fires per year and the size of each fire, and there are two levels of fire severity, where the representation of high-severity fire increases with fire size. It was applied to a landscape composed of two provinces with different fire frequency and fire-size distributions. The analytically-determined equilibrium abundance of each of seven age classes was within 1.1% of the proportion of the landscape covered by each class averaged over time within model runs and across replications in a previous study. The equilibrium abundance of two stand-structure classes, defined by the time since the last high- and moderate-severity fire, also was determined analytically. The approximation provides an explicit representation of the effects of each input parameter and parameter interactions, and it enables direct evaluation of parameter effects rather than inferring these effects from model output in a sensitivity analysis. Analytical approaches probably may be applied to gain stronger insight into the functioning of other simulation models of fire and forest dynamics. The analytical approximation is not presented as an alternative to these models, but rather as a complementary approach that provides greater transparency into model function and may provide valuable insight in cases when analytical methods fail to produce the results produced by simulation.

INTRODUCTION

Numerous modeling approaches have been applied to expand upon insight gained from field studies of fire history and forest dynamics in order to better understand longer-term and broader-scale variation in landscape structure under inferred historical fire regimes, or to predict potential changes in landscape structure under future climate or management scenarios. Early approaches involved fitting mathematical models (e.g., exponential or Weibull) to stand-age distributions derived from time-since-fire map data (Van Wagner 1978, Johnson 1979) or fire-interval data from fire-scarred trees (Clark 1989). More recently, increasing computation power has enabled the use of spatial simulation modes to evaluate increasingly complex systems with greater representation of spatial processes (e.g., fire spread or seed dispersal) and feedbacks of stand structure and fuel on subsequent fire occurrence and severity (Keane et al. 2004, Scheller and Mladenoff 2007, He 2008). These models explicitly represent at least one spatial process, and various strategies are employed to simulate the ignition, spread, and effects of fire, and the interactions of fire with stand-level forest succession.

Stochastic, spatial simulation models of fire and forest dynamics have provided substantial insight into historical and potential future variability in forest landscapes by producing statistical distributions of key variables (e.g., the abundance and patch-size distribution of old-growth or early-seral forest). However, the complexity of many of these models leads to several criticisms. First, the inclusion of large numbers of interacting parameters may be needed to represent the processes believed to operate in the system, but such complexity makes it difficult to evaluate effects of individual parameters and algorithms (Oreskes 2003). The larger the number of input parameters and interactions among them, the greater the potential for uncertainty in parameter estimates to propagate in unpredictable ways (DeAngelis and Mooij 2003). Second, there may be a mismatch between the level of complexity in the model and that required for the question being addressed. For example, using a pre-existing model has practical advantages over developing a new model for each research question, but all of the detail in the original model formulation might not be necessary in each case that it is applied.

Third, the uncertainty associated with model output usually is not fully understood by the audience of ecologists, forest managers, and policy-makers interested in applying insight gained from modeling studies (Pielke 2003).

The above criticisms are not necessarily an impediment for using simulation models to evaluate historical or potential future fire regimes in forest landscapes. However, model users and those interested in applying the insight gained from these models would benefit from analytical approximations that reveal the fundamental mathematical relationships that underlie the behavior of the model. In many cases, it may be possible to produce the simulation results analytically. For scenarios involving substantial feedback on the spatial processes or complex landscape configurations, an analytical approximation may fail to reproduce the results of a simulation model. However, evaluation of the scenarios where the approximation can and cannot reproduce the results of the simulation may be highly useful in graining a greater understanding of thresholds and feedbacks guiding the spatial process (Ives et al. 1998).

In this study, I develop an analytical approximation of a stochastic, spatial simulation model of fire and forest dynamics (LADS) developed and initially applied to evaluate historical variation in forest age distribution and landscape patterns of the Oregon Coast Range (Wimberly et al. 2000, Wimberly 2002, Nonaka and Spies 2005). The primary objective is to use an understanding of model parameters and algorithms to generate an analytical approximation of the equilibrium age distribution (analogous to the proportion of the landscape covered by each age class when averaged over time within a long model run or across numerous replications), without explicitly modeling any spatial processes. By conducting such an exercise, I hope to provide greater transparency into model function, thereby enabling direct evaluation of the effects of individual input parameters and their interactions. Also, I hope to illustrate a general approach that may be applied to generate a better understanding of other stochastic models of fire and forest dynamics.

LADS was selected over other simulation models due to my familiarity with the forest system for which it initially was developed and applied, and because its strategies for modeling the ignition, spread, and effects of fire, and the interactions of fire with forest succession are representative of strategies commonly applied in other models (Keane et al. 2004, Scheller and Mladenoff 2007, He 2008). Many aspects of LADS provide complexity in the fire regime beyond that usually addressed analytically. These include (1) a heterogeneous landscape composed of two provinces with different fire-interval and fire-size distributions, (2) stochastic variation in the number of fires per year and the size of each fire, which leads to variation in the total area burned per year, and (3) two levels of burn severity (Wimberly 2002).

An overview of LADS, as parameterized and applied to the Oregon Coast Range, is provided below, followed by the development of analytical procedures to reproduce the equilibrium age distribution of the modeled landscape. A more complete description of the original version of LADS is provided by Wimberly et al. (2000). The more recent version of LADS that I evaluate here is described by Wimberly (2002), and results are compared to those produced by Nonaka and Spies (2005).

SIMULATION MODEL

The simulation model previously has been applied to evaluate fire and forest succession of the 23,420-km^2 Oregon Coast Range. Two hundred 1,000-yr simulations were conducted at 10-yr time steps on a grid of 9-ha cells (Nonaka and Spies 2005). The Coast Range was divided into Coastal and Willamette Valley Margin provinces (Table 4.1) to account for geographic variation in the fire regime described in a fire-history study (Impara 1997). The Coastal province has higher precipitation and cooler temperatures, and fires generally are less frequent, larger, and have greater representation of high burn severity than in the Valley Margin. Differences in fire frequency were represented by setting the natural fire rotation (NFR) of the Coastal province (200 years) twice as long as that of the Valley Margin (100 years) based on tree ring and lake

sediment studies (Impara 1997, Long et al. 1998). Fire-size distributions were derived from historical vegetation maps (Teensma et al. 1991).

The number of fires per 10-year timestep and the size of each fire were determined using random variables, which allowed the area burned per decade to fluctuate around a fixed mean (Wimberly 2002). Fires were simulated by first converting the overall rate of burning, specified by the reciprocal of the NFR, to the average number of fires initiated per timestep in each province, FF_j (Table 4.1). This was done by dividing the area of each province by the product of its NFR and its mean fire size (Boychuk et al. 1997). Then, the number of fires per timestep in each province was modeled as a Poisson random variable, with parameter $\lambda_j = 1/ FF_j$ (Table 4.1).

Each fire was initiated in a random cell, and it was allowed to spread stochastically until burning an area determined at the time of ignition. The probability of ignition was weighted geographically, providing the highest probability on upper slopes and in more flammable age classes. At the time of each ignition, fire size was drawn from a lognormal distribution with a mean and standard deviation of 73.0 and 320.5 km^2, respectively, for the Coastal province, and 22.2 and 51.0 km^2, respectively, for the Valley Margin (Table 4.1; Wimberly 2002).

The fire-spread algorithm is a cellular-automata-based subroutine designed to allow fire to spread most readily through cells in the most susceptible age classes and topographic positions, and thereby burn a greater proportion of these cells than those in other age classes or locations (Wimberly 2002). The algorithm also allows user-defined parameters for windspeed and wind direction to influence the rate and direction of fire spread. The susceptibility of each cell to fire spread from adjacent cells was calculated as the product of individual susceptibility scores based on stand age, topographic position, and wind variables (Wimberly 2002). For each of the eight cells surrounding a burning cell, a uniform random variable was drawn on the interval [0, 1], and the cell was burned if its overall susceptibility was greater than this value (Wimberly et al. 2000). The

algorithm was repeated, allowing fire to spread from each burning cell, until the total area burned reached the fire size determined at the time of ignition (Wimberly 2002).

Fire severity was classified as moderate or high, where the probability of burning at high severity increased with fire size (Wimberly 2002). To enable greater representation of high burn severity with increasing fire size, fire size was divided into three classes: small (< 100 km^2), medium (100–500 km^2), and large (> 500 km^2) (Table 4.1). For each burned cell, a uniform random variable was drawn on the interval [0.0, 0.5] for small fires, [0.1, 0.8] for medium fires, and [0.7, 0.95] for large fires. If a second uniform random variable on the interval [0, 1] was smaller than the first, the cell burned at high severity. Otherwise, it burned at moderate severity. The probability of burning at high severity also was weighted by topographic position and stand age (Wimberly 2002).

Each cell had two state variables representing the time since the last high-severity fire and the time since the last fire of any severity (Wimberly 2002). These variables determined stand age and successional stage, which influenced the probability of fire ignition, susceptibility to fire spread from adjacent cells, and fire severity. Stand age was equal to the time since the last high-severity fire and was reset only by high-severity fire. Moderate-severity fire converted a stand to a semi-open successional stage, from which it could proceed more rapidly to an old-growth stage than stands initiated following high-severity fire, but moderate-severity fire had no effect on stand age (Wimberly 2002). Susceptibility to fire spread was modeled as a U-shaped function of stand age, providing high susceptibility in young stands assumed to retain abundant dead wood produced by fire-caused mortality in the previous stand, and in old-growth stands with abundant fuel in all size classes (Agee and Huff 1987).

Simulations were initiated by assigning a random age to each cell and conducting a burn-in period, when simulations were run without recording output in order to overwrite initial stand ages. Simulations were conducted with a buffer around the Coast Range that allows fires initiated in the analysis area to spread into the buffer, and vice versa (Wimberly 2002).

ANALYTICAL APPROXIMATION

Background and Assumptions

Analytical evaluation of the equilibrium age distribution of a forested landscape may be conducted by determining the rate at which stands are burned and new stands initiated, and using this rate to calculate a probability density function for stand age. This rate of burning, referred to as the hazard of burning, or hazard rate, is the age-specific probability rate of fire within a given timestep (Johnson and Gutsell 1994). It is not strictly a probability (values are not constrained between 0 and 1), but rather a probability rate. However, when using an annual timestep, viewing the hazard rate as the annual probability of fire for stands of a given age provides an approximation almost identical to the actual probability of fire in that year (Reed 1994). The hazard rate, as used here, should not be confused with fire hazard, as used in fire ecology as a measure of potential fire behavior based on fuel loading.

The use of the hazard rate for high-severity fire to calculate the probability density function of stand age for individual stands is illustrated below. Then, the hazard rate for high-severity fire will be derived from the input parameters and algorithms of LADS, and it will be used to approximate the equilibrium age distribution of the Coast Range.

In the following equations, τ is a random variable representing the number of years between successive fires that burn an individual stand at high severity (regardless of the number of times it burned at moderate severity in the intervening period). In all equations, t represents stand age, which is reset only by high-severity fire, and thus is equivalent to the state variable defining stand age for each cell in LADS. The hazard rate for high-severity fire, $h_\tau(t)$, is defined as the probability rate of high-severity fire in a given cell on the interval $(t, t + \Delta t)$, provided the cell has reached age t without high-severity fire:

$$h_\tau(t) = \lim_{\Delta t \to 0} \left[P\{\tau \in (t, t+\Delta t) \mid \tau > t\} \right] \frac{1}{\Delta t}.$$

Regardless of the fire-interval distribution, the hazard rate for high-severity fire may be used to calculate several distributions useful in relating fire to stand-age distribution. The cumulative survivorship distribution, $S_\tau(t)$, is the probability of a cell reaching age *t* without high-severity fire:

$$S_\tau(t) = P\{\tau > t\} = \exp\left(-\int_0^t h_\tau(u)du\right). \quad [1]$$

In Equation 1 and in the following equations, *u* is a dummy variable used to clarify that $S_\tau(t)$ is a function of the upper level of integration, *t*, not a function of *u*. The interval distribution for high-severity fire (i.e., the distribution of intervals between fires when an individual cell burns at high severity regardless of the number of times it has burned at moderate severity in the intervening period), $f_\tau(t)$, is the probability of a cell reaching age *t* without high-severity fire (the cumulative survivorship distribution) multiplied by the probability of experiencing high-severity fire in the next timestep (the hazard rate for high-severity fire):

$$f_\tau(t) = P\{\tau \in [t, t+\Delta t]\} = S_\tau(t)h_\tau(t) = h_\tau(t)\exp\left(-\int_0^t h_\tau(u)du\right). \quad [2]$$

The above distributions are related to each other, as shown below:

$$h_\tau(t) = \frac{f_\tau(t)}{S_\tau(t)}.$$

The mean interval between fires that burn a given cell at high severity, $E(\tau)$, is determined by integrating the survivorship distribution, $S_\tau(t)$, over all stand ages:

$$E(\tau) = \int_0^\infty S_\tau(t)dt = \int_0^\infty \exp\left(-\int_0^t h_\tau(u)du\right)dt. \quad [3]$$

In a landscape where the hazard of burning at high severity follows the same function of stand age in all cells, $E(\tau)$ represents the NFR for high-severity fire, or the average

number of years required for a cumulative area equal to the extent of the landscape to be burned at high severity (Heinselman 1973).

Based on the above relationships, the hazard rate for high-severity fire may be used to determine the probability density function of stand age for individual cells under the following assumptions: (1) trees establish promptly after fire and tree longevity exceeds intervals between high-severity fires, such that stand age is equivalent to the time since the last high-severity fire, (2) only high-severity fire kills the existing forest and initiates a new stand, and (3) the landscape has undergone several fire rotations without changes in the hazard rate for high-severity fire. The first and second assumptions are equivalent to defining stand age as the number of years since the last high-severity fire for each cell and excluding non-fire disturbances in LADS. The third assumption is similar to the use of a burn-in period prior to recording model output in order to override the effects of initial stand ages.

In a landscape where the hazard rate for high-severity fire follows the same function of stand age for all stands, the probability density function for stand age in each stand represents the equilibrium age distribution of the landscape. To calculate the equilibrium age distribution of such a landscape, it is useful to recognize that the reciprocal of the mean interval between high-severity fires at each point, $1/E(\tau)$, represents the expected proportion of the landscape that experiences high-severity fire each year. Because landscape size is fixed, and by assumptions 1 and 2, a new stand is initiated only immediately after another stand is killed by high-severity fire, $1/E(\tau)$ also represents the frequency of stand establishment, or the average proportion of the landscape covered by stands initiated in each year.

The equilibrium probability density function for stand age, $a_\infty(t)$, is calculated by multiplying the frequency of stand establishment, $1/E(\tau)$, by the probability of stands reaching age t without high-severity fire, $S_\tau(t)$:

$$a_{\infty}(t) = \frac{1}{E(\tau)} S_{\tau}(t) = \frac{1}{\int_0^{\infty} \exp\left(-\int_0^{t} h_{\tau}(u)du \right) dt} \exp\left(-\int_0^{t} h_{\tau}(u)du \right). \quad [4]$$

Equation 4 specifies the probability that the age of a randomly selected cell is equal to *t* in a given year provided assumptions 1–3, above. If the assumptions are met in a landscape that is homogeneous with respect to the hazard rate for high-severity fire and large enough that there is little or no inter-annual variation in area burned, the observed age distribution in any year will approach $a_{\infty}(t)$. However, if landscape size is small enough relative to fire size that there is substantial stochastic variation in annual area burned, the observed age distribution in any year may depart widely from $a_{\infty}(t)$ (Turner and Romme 1994). This is the case for each province of the Oregon Coast Range, according to the fire-regime parameterization of LADS (Wimberly et al. 2000). Stochastic variation in the number of fires per year and fire size leads to variation around a fixed mean area burned per year. Therefore, the area covered by a given age class in any year is unlikely to equate to the equilibrium abundance of the age class. However, when the proportion of the landscape covered by each age class is averaged over time within a simulation or across model runs, it eventually should converge to values determined by Equation 4.

Calculation of the Equilibrium Age Distribution

Although the hazard rate for high-severity fire is not specified directly in LADS, it can be determined from the input parameters and model algorithms. Then, it may be used to approximate the equilibrium age distribution for each province and for the entire Coast Range. To illustrate a general approach for deriving the hazard rate for high-severity fire from the input parameters of a spatial simulation model, I first present a method for deriving the overall hazard of burning (regardless of fire severity). Then I expand upon this method to address the hazard rate for high-severity fire.

Analytical approximation of the equilibrium age distribution, as produced by LADS, requires the simplification that influences of stand age and topographic position on susceptibility to fire ignition and spread are not represented. The relationships in Equations 1–4 apply under an age-dependent or age-independent hazard of burning, and approaches are available to derive an age-dependent hazard rate from empirical data (e.g., Clark 1989). However, in LADS, influences of stand age and topographic position were incorporated into the fire-spread algorithm (Wimberly 2002), which means that the proportion of cells in each age class and topographic position burned by a given fire depends on the location of the ignition and the pattern of different age classes at the time of the fire. Therefore, differences between the equilibrium age distribution determined analytically without accounting for influences of stand age and topographic position and the average abundance of each age class determined by simulation may provide a measure of the strength of these influences.

Previously, Van Wagner (1978) has demonstrated that under the assumption that the probability of fire at any point in a given year is independent of stand age or geographic location, the hazard of burning is equivalent to the reciprocal of the NFR, which is supplied by the user in LADS (Table 4.1). However, it is useful to derive the hazard of burning from the number of fires per year and the fire-size distribution of each province, because this relationship can be expanded upon to determine the hazard rate for high-severity fire.

The overall hazard of burning for each cell in a given province, regardless of fire severity, is represented by $h^{(j)}(t)$, where the index, j, specifies a unique function for each province. The overall hazard rate for cells in a province may be calculated by multiplying the average number of fires per year in that province, FF_j (Table 4.1), by the probability that a randomly selected cell (the i^{th} cell) in the province is burned by each fire:

$$h^{(j)}(t) = FF_j \times P\{b_i = 1\}, \qquad [5]$$

where b_i, has a value of 1 if the i^{th} cell is burned by a given fire, and 0 otherwise.

When fire size is known, the probability that a random cell is burned can be determined by conditioning on fire size: $P\{b_i = 1 | X = x\} = x/A_j$ (Boychuk et al. 1997), where X represents the area burned by a particular fire and A_j represents the area of the j^{th} province (Table 4.1). This relationship simply states that if fire size is equivalent to 10% of province area, each cell in the province has a 10% chance of being burned.

If fire size is not known, but it is drawn from a known distribution, $f_j(x)$, then the probability that the i^{th} cell is burned in a particular fire also is calculated by conditioning on fire size as follows (Boychuk et al. 1997):

$$P\{b_i = 1\} = \int_0^\infty P\{b_i = 1 | X\} f_j(x)dx = \int_0^\infty \frac{x}{A_j} f_j(x)dx. \qquad [6]$$

Therefore, Equation 5 may be solved as

$$h^{(j)}(t) = FF_j \times P\{b_i = 1\} = FF_j \times \int_0^\infty \frac{x}{A_j} f_j(x)dx = FF_j \times \frac{MFS_j}{A_j} = \frac{1}{NFR_j},$$

where MFS_j and NFR_j, are user-defined parameters representing the mean fire size and the natural fire rotation, respectively, of the j^{th} province (Table 4.1). Thus, after assuming the probability of a cell burning in a given year is independent of stand age and its location, the above calculation illustrates that the overall hazard of burning is the reciprocal of the user-defined NFR for each province (0.005 for the Coastal Province and 0.01 for the Valley Margin; Table 4.2).

The hazard rate for high-severity fire, $h_\tau^{(j)}(t)$, can be calculated by expanding upon the relationships in Equations 5 and 6. The average number of fires initiated per year in each province, FF_j, is multiplied by the joint probability that a randomly selected cell is burned and fire severity is high:

$$h_\tau^{(j)}(t) = FF_j \times P\{b_i = 1, \omega_i = 1\}, \qquad [7]$$

where ω_i is given a value of 1 if the i^{th} cell is burned at high severity and 0 otherwise.

In LADS, fire severity is determined based on uniform random variables, U_k, drawn cell-by-cell on a different interval for each fire-size class (Table 4.1). Then, values of U_k are compared to a second uniform random variable, V, drawn on the interval [0, 1]. The cell is burned at high severity only if $V < U_k$. Therefore, given that the i^{th} cell is burned by a fire in the k^{th} size class, the probability that it experienced high-severity fire is provided by:

$$P\{\omega_i = 1\} = P\{V < U_k\} = E(U_k).$$

For each fire in the k^{th} size class, the average proportion of burned cells that experience high-severity fire, g_k, is calculated as the expected value of the uniform random variables, U_k, providing values of $g_1 = 0.25$, $g_2 = 0.45$, and $g_3 = 0.825$ (Table 4.2).

The joint probability that a random cell is burned ($b_i = 1$) and fire severity is high ($\omega_i = 1$) is calculated by multiplying the probability that the i^{th} cell is burned by a fire in each size class by the expected proportion of cells burned by a fire of that class that experience high-severity fire, and then summing across $m = 3$ fire-size classes:

$$P\{b_i = 1, \omega_i = 1\} = \sum_{k=1}^{m}\left(g_k \int_{Min_k}^{Max_k} \frac{x}{A_j} f_j(x)dx \right) \qquad [8]$$

$$= g_1 \int_0^{100} \frac{x}{A_j} f_j(x)dx + g_2 \int_{100}^{500} \frac{x}{A_j} f_j(x)dx + g_3 \int_{500}^{\infty} \frac{x}{A_j} f_j(x)dx.$$

In the above equation, Min_k and Max_k are the user-defined minimum and maximum area burned by fires of the k^{th} size class (Table 4.1).

Because fire size is drawn from a lognormal distribution, the fire-size distribution, $f_j(x)$, is calculated as,

$$f_j(x) = \frac{1}{x\sigma_j\sqrt{2\pi}} \exp\left[-\frac{1}{2}\left\{ \frac{\left(\ln(x) - \mu_j\right)^2}{\sigma_j^2} \right\} \right],$$

where parameters μ_j and σ_j are 2.786 and 1.735, respectively, for the Coastal province and 2.222 and 1.335, respectively, for the Valley Margin (Table 4.1). Each integral in Equation 8 can be solved as

$$g_k \int_{Min_k}^{Max_k} \frac{x}{A_j} f_j(x)dx = g_k \left[\frac{1}{A_j} \exp\left(\mu_j + \frac{1}{2}\sigma_j^2 \right) \times \left(Z_k - Y_k \right) \right],$$

where

$$Z_k = \Phi\left(\frac{\ln(Max_k) - (\mu_j + \sigma_j{}^2)}{\sigma_j} \right), \; Y_k = \Phi\left(\frac{\ln(Min_k) - (\mu_j + \sigma_j{}^2)}{\sigma_j} \right),$$

and $\Phi(x)$ represents the value of the standard normal distribution at x. The values, Z_k and Y_k, represent the proportion of fires expected to be smaller than the upper and lower bound, respectively of the k^{th} size class. Thus, the expected proportion of fires within the k^{th} class, Q_k, is determined by $Z_k - Y_k$ (Table 4.2).

Solutions to Equation 8 illustrate that for each fire initiated in the Coastal province, the probability that a randomly selected cell in that province is burned at high severity is 2.77×10^{-3} (Table 4.2). In the Valley Margin, the probability is 8.45×10^{-4}. Multiplying the above values by the average number of fires initiated per year in each province, FF_j, provides the hazard rate for high-severity fire in the respective province (Equation 7): $h_\tau^{(C)}(t) = 2.76 \times 10^{-3}$ and $h_\tau^{(V)}(t) = 3.34 \times 10^{-3}$ for the Coastal and Valley Margin provinces, respectively (Table 4.2). These hazard rates may be entered into Equation 3 to calculate the NFR for high-severity fire for each province: 362 years for the Coastal Province and 300 years for the Valley Margin.

Because I have assumed that stand age and topographic position do not influence the probability of a cell burning in a given year or fire severity, the hazard rate for high-severity fire in each province, $h_\tau^{(j)}(t)$, is equivalent to the proportion of the province expected to burn at high severity each year, $1/E(\tau)$ (Equation 3). Therefore, $h_\tau^{(j)}(t)$ may

replace $1/E(\tau)$ in Equation 4 to calculate the equilibrium age distribution of each province (Table 4.2).

To determine the equilibrium age distribution of the entire Coast Range, the landscape is conceived as a mixture of spatially distinct provinces (Coastal and Valley Margin) that are homogeneous with respect to fire-interval and fire-size distributions. Because each province has a unique hazard rate for high-severity fire, Equation 4 cannot be applied directly (Johnson and Gutsell 1994). Instead, the equilibrium age distribution is calculated by weighting the equilibrium age distribution in each province by the proportion of the total landscape represented by that province, as follows:

$$a_{\infty}(t) = \frac{A_1}{\sum_{j=1}^{n} A_j} a_{\infty}^{(1)}(t) + \ldots + \frac{A_n}{\sum_{j=1}^{n} A_j} a_{\infty}^{(n)}(t), \qquad [9]$$

where n is the number of provinces. Equation 9 is provided in a general form that may be applied to any number of provinces. For the two provinces of the Coast Range, Equation 9 is reduced to

$$a_{\infty}(t) = \frac{A_C}{A_C + A_V} a_{\infty}^{C}(t) + \frac{A_V}{A_C + A_V} a_{\infty}^{V}(t),$$

where A_C and A_V represent the area, and $a_{\infty}^{C}(t)$ and $a_{\infty}^{V}(t)$ represent equilibrium age distributions, of the Coastal and Valley Margin provinces, respectively.

The analytically-determined equilibrium proportion of the landscape covered by each of seven age classes was within 1.1% of the abundance of each age class averaged over time within model runs and across replications of the simulation model (Table 4.3). The equilibrium abundance of all but three age classes (Mature, Mid Old Growth, and Late Old Growth) was within 0.5% of their average abundance determined by simulation.

The analytical approximation also enabled direct evaluation of the response of the equilibrium age distribution to a change of each input parameter from its baseline value (Figure 4.1). Similar to the sensitivity analyses conducted on the simulation model

(Wimberly 2002), the abundance of each age class was most sensitive to changes in the overall NFR and the average proportion of cells that experience high-severity fire for a fire in the k^{th} size class (g_k). Changing the mean and SD of fire size individually by +/- 50% from the baseline values had little influence on the equilibrium age distribution (Figure 4.1).

Stand-Structure Classes

In addition to calculation of the equilibrium distribution of stand age, where stand age is defined by the time since the last high-severity fire (Table 4.3), the equilibrium abundance of different stand-structure classes can be determined by considering the hazard rate for moderate-severity fire, $h_M^{(j)}(t)$ (Table 4.2). Assuming the probability of fire occurrence in a given year and fire severity are independent of stand age, the hazard rate for moderate-severity fire in each province is determined as the difference between the overall hazard of burning and the hazard rate for high-severity fire:
$h_M^{(j)}(t) = h^{(j)}(t) - h_\tau^{(j)}(t)$.

Stands > 30 years old that have experienced moderate-severity fire within the last 30 years were classified as semi-open (Wimberly 2002; Table 4.4). Because the equilibrium age distribution has been calculated (Equation 9), the expected proportion of the landscape covered by stands in the semi-open class can be determined as the proportion of stands > 30 years old expected to have experienced at least one moderate-severity fire in the last 30 years. The probability of having gone a certain amount of time without moderate-severity fire is determined by the Survivorship distribution, $S(t)$ (Equation 1), using the hazard rate for moderate-severity fire. The probability of experiencing at least one moderate-severity fire over a given interval is determined by $1 - S(t)$, using the hazard rate for moderate-severity fire. Using these relationships, the equilibrium abundance of the semi-open class is calculated by multiplying the equilibrium abundance of stands of each age ($t > 30$), by the probability of experiencing at least one moderate-severity fire in the previous 30 years, and summing across ages:

$$\text{Semi-open} = \sum_{t=31}^{\infty}\left[a_{\infty}^{(j)}(t)\left\{1-\exp\left(-\int_{t-30}^{t} h_M^{(j)}(u)du \right)\right\}\right]. \qquad [10]$$

Based on this calculation, 6.0% of the Coastal Province and 16.4% of the Valley Margin is expected to be covered by stands in the semi-open class (Table 4.4).

Stands were classified as multi-story if the time since the last high-severity fire was > 80 years, and the time since the last moderate-severity fire was 30–80 years. The expected abundance of stands in the multi-story class is determined by finding the expected proportion of stands of age $t > 80$, which have experienced at least one moderate-severity fire in the last 80 years, but not within the last 30 years. The probability of no moderate-severity fire over the previous 30 years is determined by evaluating $S(t)$ over stand ages from $t - 30$ to t, using the hazard rate for moderate-severity. The probability that a stand has experienced at least one moderate-severity fire at least 30, but not more than 80 years ago is determined by evaluating $1 - S(t)$ over stand ages from $t - 80$ to $t - 30$, using the hazard rate for moderate-severity fire. Thus, the expected proportion of the landscape covered by stands in the multi-story class is

$$\text{Multi-story} = \sum_{t=81}^{\infty}\left[\begin{array}{c} a_{\infty}^{(j)}(t)\left\{1-\exp\left(-\int_{t-80}^{t-30} h_M^{(j)}(u)du \right)\right\} \\ \left\{\exp\left(-\int_{t-30}^{t} h_M^{(j)}(u)du \right)\right\} \end{array}\right]. \qquad [11]$$

The above calculation provides an expected 7.9% of the Coastal Province and 17.8% of the Valley Margin covered by stands in the multi-story class (Table 4.4).

DISCUSSION

Comparison of Modeling Approaches

The analytical approximation provides an equilibrium abundance of each of seven age classes that is almost identical to that produced by averaging the proportion of the

landscape covered by each class over time within a model run and across replications of the simulation model (Table 4.3). The ability to use the input parameters and algorithms of the spatial simulation model to reproduce the equilibrium age distribution without explicitly modeling the spread of each fire illustrates that simulation models are not always necessary to address questions relating to the relative abundance of different forest age classes. In addition, the analytical calculation of the equilibrium abundance of two stand-structure classes, influenced by high- and moderate-severity fire (Equations 10 and 11, Table 4.4), illustrates that analytical approaches are flexible enough for application under diverse fire regimes. The general approach presented in Equations 10 and 11 could be used to calculate the equilibrium abundance of any stand-structure class defined by the two state variables (time since the last high-severity fire and time since the most recent fire of any severity) tracked for each cell in LADS (Wimberly 2002)

The ability to produce the equilibrium age distribution and the abundance of different stand structures without explicitly modeling the spread of each fire is valuable because the fire-spread algorithm of stochastic, spatial models of fire and forest dynamics may be the most difficult algorithm to write, the most time-consuming part of running the model, and it may be highly difficult to evaluate relative to empirical data. Thus, for LADS, and possibly for other similar simulation models (Keane et al. 2004, He 2008), extensive calibration of the fire-spread algorithm may be necessary only if research questions are focused on landscape patterns or patch-size distributions of different age classes.

The high similarity between age distributions produced by the two modeling approaches, despite the simplification of not accounting for influences of stand age or topographic position on fire ignition and spread in the approximation, suggests that these factors had little influence on the proportion of the landscape covered by each age class. Several factors may have contributed to a weak degree of age dependence in the hazard rate for high-severity fire. For example, the overall susceptibility of each cell to fire spread from adjacent cells was calculated as the product of its susceptibility scores based on stand age, topographic position, windspeed, and wind direction, where the scores

based on wind variables were unrelated to stand age or topographic position (Wimberly 2002). Also, a random number was drawn for each cell adjacent to a burning cell, and fire could spread into the cell only if its overall susceptibility was greater than the random number (Wimberly et al. 2000). The use of random numbers provides an additional source of stochastic variation that can override the susceptibility to fire spread driven by stand age, topographic position, and wind variables.

Another factor that reduces the degree of age dependence in the hazard of burning for high-severity fire is that the expected area burned in a given year is fixed at the reciprocal of the overall NFR, regardless of the proportion of the landscape covered by different age classes in that year. Variation around this expected annual area burned was driven by stochastic variation in the number of fires per year and fire size. However, the number of fires initiated per year and the size of each fire were independent of the age distribution at the time of fire ignition. Thus, if the majority of the landscape was covered by age classes that are most susceptible to fire, the expected area burned in that year would be equivalent to that burned in a year when the majority of the landscape was covered by the least susceptible age classes. The use of a fixed mean area burned per year may have prevented unstable model behavior, such as continually increasing area burned per year under the model formulation for the Oregon Coast Range, where young stands were highly susceptible to fire while they retained large amounts of dead wood created by the stand-initiating event (Agee and Huff 1987, Wimberly 2002). However, avoiding this potentially unstable behavior by making the number of fire ignitions and fire size independent of the existing age distribution reduces the degree of age dependence in the overall hazard rate.

The small differences in age-class abundance produced by the two modeling approaches also may be related to the number of replications conducted in the simulation. The number of replications used to provide the average abundances of each age class in Table 4.3 (200, 1,000-year replicates), may have been insufficient for the average abundance of each age class to stabilize on its equilibrium abundance.

An additional component of the spatial simulation model that was not addressed analytically is that fires initiated in one province may spread into the other province. Because fire size was drawn at the time of ignition using parameters of the fire-size distribution for the province where the fire initiated, each province probably was not truly homogeneous with respect to its fire-size distribution. The fire-size distribution for cells located near a province boundary may have been different from that of cells farther from a boundary that were less likely to be burned by fires initiated in the other province. These differences are potentially important because the probability of a cell being burned at high severity is related to the size of the fire in which it burns. However, the effect of fires spreading across province boundaries on the equilibrium age distribution of the Oregon Coast Range may have been relatively minor because each province was a single polygon and there was relatively little common boundary between them. If the landscape were a finer-scale mosaic of smaller zones with different fire-regime parameters, failure to account for the effects of fire spread among zones could lead to greater divergence between age distributions determined analytically and by simulation. However, in the case where most fires spread among zones, drawing fire size at the time of ignition based on parameters of the zone where the fire was initiated might not provide a strong fit to empirical data.

The analytical approximation provides direct calculation of fire-regime descriptors, such as the NFR for high- and moderate-severity fire, which were not specified directly by the input parameters. For example, assuming the probability of fire occurrence in a given year and fire severity are independent of stand age, the overall rate of burning is equal to the sum of the rates of burning at moderate and high severity: $h(t) = h_\tau(t) + h_M(t)$, where $h(t)$ is the overall hazard rate and $h_\tau(t)$ and $h_M(t)$ are the hazard rates for high- and moderate-severity fire, respectively (Table 4.2). When the overall hazard rate is independent of stand age, it may be calculated as the reciprocal of the NFR, as specified by Wimberly (2002): 0.005 and 0.01 for the Coastal and Valley Margin provinces, respectively. Therefore, using the hazard rates for high-severity fire, as calculated analytically, the NFR for high- and moderate-severity fire is 362 and 447

years, respectively in the Coastal province, and 300 and 150 years, respectively in the Valley Margin. These values represent the mean intervals between fires of high and moderate severity for individual cells in each province, and the average number of years required for the cumulative area burned at high and moderate severity, respectively, in each province to reach the area of each province (Table 4.2).

Exponential Age Distributions

Under the simplification that the hazard rate for high-severity fire is independent of the time since the previous fire and geographic location within a province, the analytical approximation provides an equilibrium age distribution for each province that is exponential in form. Also, in the case of an age-independent hazard rate for high-severity fire, the hazard rate is equivalent to the reciprocal of the NFR for high-severity fire, $h_{\tau}^{(j)}(t) = 1/E^{(j)}(\tau)$ (Equation 3). Therefore, the interval distribution for high-severity fire in each province (Equation 2) is equivalent to the equilibrium age distribution (Equation 4), and both are exponential in form.

Van Wagner (1978) previously demonstrated that an exponential model describes the fire-interval distribution and equilibrium age distribution of a landscape under a simple fire regime. His model was applied to a uniform landscape where a fixed number of equal-sized stands burned one-at-a-time each year, fires burned only at high severity, and all stands had an equal probability of burning each year regardless of their age or location. Van Wagner (1978) suggested that incorporating variation in fire size and allowing the area burned per year to fluctuate around a fixed mean would not disqualify an exponential expected age distribution, as long as the temporal scale of fluctuation was short relative to the fire cycle. These suggestions are supported by the analytical approximation of the equilibrium age distribution for each province of the Oregon Coast Range, as modeled by LADS. Adding contagious fire spread and providing stochastic variation in the number of fires and area burned per year in LADS did not disqualify an exponential age distribution in each province. Also, allowing for two fire severities and a

relationship between fire size and the expected proportion of each fire that burns at high severity did not exclude an exponential age distribution.

The equilibrium age distribution for each province is exponential in form, but the observed age distribution produced in any year of the simulation fluctuates around the exponential distribution. The degree of variation is a function of the extent of the province relative to variation in area burned per year (Turner et al. 1993, Wimberly et al. 2000), as driven by variation in the number of fires per year and fire size. In this example, the expected number of fires per year was low (0.996 and 3.947 in the Coastal and Valley Margin provinces, respectively). Therefore, given that fire size was drawn from a lognormal distribution with a high SD (320.5 and 50 km^2 in the Coastal and Valley Margin provinces, respectively), the observed area burned per year fluctuates widely from the expected value, leading to substantial year-to-year variation in the observed age distribution. If province area (A_j) was extended indefinitely, the number of fires per year (FF_j) would increase according to the relationship: $FF_j = A_j/(NFR_j \times MFS_j)$ (Table 4.1). Thus, by the law of large numbers, with increasing numbers of fires per year, the mean fire size observed in a given year would approach MFS_j, which was specified as an input parameter. Also, the observed area burned per year would approach the expected annual area burned, and the observed age distribution in each year would approach the equilibrium age distribution. Averaging across a large number of replications would have a similar effect.

Despite an exponential form for the equilibrium age distribution of each province, the equilibrium age distribution of the entire Coast Range was not exponential. Calculating the equilibrium age distribution of a spatial mixture of fire regimes in the two provinces, each with different hazard rates for high-severity fire, requires first calculating the equilibrium age distribution of each province, and then averaging these distributions weighted by province area as a proportion of total area (Equation 9). This calculation is not equivalent to averaging the hazard rates between provinces and then using the average hazard rate to determine an equilibrium age distribution (McCarthy and Cary 2002). Similarly, under a temporally varying fire-regime, where the expected area burned

per year is not fixed, the expected age distribution in any year would not be exponential, even if the probability of fire in a given year was independent of stand age. This was demonstrated by a scenario examined in the simulation exercises of Boychuk et al. (1997). In their analysis, the expected area burned per year fluctuated between 4% of the landscape in 3 of 10 years, representing years of severe fire weather, and 0.43% in the remaining years of moderate fire weather. In this case, averaging at decadal or longer time scales would produce a constant average of 1.5% of the landscape burned per year. However, the age distribution averaged across model runs did not approach an exponential distribution with a parameter of 0.015, even when considered over large areas (Boychuk et al. 1997).

Direct Evaluation of Parameter Effects

The analytical approximation allows for direct evaluation of the effects of each input parameter on the equilibrium age distribution of the landscape. Such direct testing differs from sensitivity analysis of a simulation model in that equations specify the interactions among variables rather than having to infer these relationships based on model output. Also, direct testing of parameter effects using the analytical approximation is not dependent on the number of model replications used, and it can quickly be conducted over a broad range of parameter values.

After assuming the probability of fire ignition and spread were independent of stand age and topographic position, the equilibrium age distribution was highly sensitive to the overall NFR (Figure 4.1a), because with all other parameter values fixed, the hazard rate and NFR for high-severity fire both scale linearly with the overall NFR, as shown below. The relationship, $FF_j = A_j/(NFR_j \times MFS_j)$ (Table 4.1), illustrates that the expected number of fires per year in each province scales linearly with the overall NFR of the province. Equations 5 and 7 indicate that FF_j is the only term in the equations for the overall hazard rate and the hazard rate for high-severity fire affected by a change in the overall NFR, and both hazard rates scale linearly with this value. For example, when all other parameters are held at their baseline values (Table 4.1), the average number of

fires per year (FF_j) in the coastal province is 0.996, and the NFR for high-severity fire (362 years) is 1.81 times the overall NFR (200 years; Table 4.2). If the overall NFR is increased to 300 years, the expected number of fires per year in the Coastal Province is reduced to 0.663, and the NFR for high-severity fire increases to 543 years, which also is 1.81 times the overall NFR. With all other input parameters fixed, this linear scaling holds for any value of the overall NFR.

Increasing or decreasing the expected proportion of cells that burn at high severity for each fire in a given size class, g_k (Table 4.2), also has a substantial influence on the equilibrium age distribution (Figure 4.1b). Changing the probability that a cell burned by a fire of a given size experiences high-severity fire does not affect the expected number of fires or area burned per year. However, it changes the linear scaling between the overall NFR and the NFR for high-severity fire. For example, with all parameters at their baseline values (Table 4.1), reducing values of g_k for each fire-size class by 10% causes the NFR for high-severity fire in the Coastal Province to increase from 362 years (1.81 times the overall NFR) to 402 years (2.01 times the overall NFR). If values of g_k are held at 10% below their baseline values, the scaling of the NFR for high-severity fire in the Coastal Province as 2.01 times the overall NFR would persist for any value of the overall NFR.

Values of the fire-size distribution had little influence on the equilibrium age distribution (Figure 4.1c and d). Changing the mean fire size with all other parameters fixed has no effect on the expected area burned per year, because when mean fire size is increased or decreased, the relationship, $FF_j = A_j/(NFR_j \times MFS_j)$ (Table 4.1), illustrates that the expected number of fires per year will adjust to compensate for the larger or smaller fires, and thereby maintain the same average area burned per year. Different values of the mean fire size can influence the equilibrium age distribution only through the effect of mean fire size on the expected proportion of fires in each size class, Q_k (Table 4.2), which influences the probability that a cell will be burned at high severity for each fire initiated in its province (Equation 8). However, this influence is weak, as illustrated by increasing or decreasing the mean fire size of the Coastal Province by 50%

from its baseline value, which only caused the expected proportion of fires in the large size class to decrease to 0.397 or increase to 0.417, from its baseline value of 0.404 (Table 4.2). Thus, the effect of changing mean fire size on the equilibrium age distribution was minimal (Figure 4.1c). Changing the SD of fire size with the mean fire size fixed produced greater differences in the expected proportion of fires in the smallest and largest size class, which led to a slightly larger effect on the equilibrium age distribution than changing the mean fire size (Figure 4.1d).

Although the equilibrium abundance of each age class showed little sensitivity to parameters of the fire-size distribution (Figure 4.1c and d), changing parameters of the fire-size distribution is likely to have a substantial effect on the variation in the proportion of the landscape covered by each age class over time. If mean fire size is increased, the relationship, $FF_j = A_j/(NFR_j \times MFS_j)$ (Table 4.1), illustrates that the expected number of fires per year will decrease and thereby maintain the same expected area burned per year. However, this area will be burned by a smaller number of larger fires, on average, which means that year-to-year differences in the proportion of the landscape covered by each age class would increase. Therefore, a larger number of model replications would be needed to evaluate statistical distributions of age-class abundance or evaluate sensitivity to a change in parameters of the fire-size distribution. Without the explicit representation of the role of each parameter provided by the analytical approximation, changes in the average abundance of age classes found in a sensitivity analysis with too few replications may be misinterpreted as an effect of the parameter on the equilibrium abundance of each class.

Conclusions

It is likely that similar analytical approximations can be developed for other stochastic, spatial simulation models of fire and forest dynamics. The equations developed here illustrate general strategies that may be used to calculate the equilibrium age distribution (Table 4.2) and the equilibrium abundance of different stand-structure classes (Table 4.4) under a fire regime where non-stand-replacing fire can modify stand

structure. Specific approaches for the approximation of other simulation models will depend on the parameters and algorithms of each model. The assumption that the probability of fire ignition and the susceptibility to fire spread from adjacent cells were independent of stand age and topographic position were necessary given the ways these factors were incorporated into the fire-spread algorithm of LADS (Wimberly et al. 2000, Wimberly 2002). However, Equations 1–4 may be applied regardless of the form of the hazard rate, which illustrates that analytical modeling approaches are not limited only to the scenario of an age-independent hazard of burning.

With increasing degrees of feedback in simulation models and representation of more than one spatial process (e.g., fire spread and seed dispersal), analytical approximations may become increasingly difficult to develop. When it is not possible to reproduce the results of a spatial simulation model without explicitly modeling one of the spatial processes or representing all of the feedbacks in the model, it may be useful to compare results produced by the two approaches. Combining both modeling approaches in order to determine the range of conditions where the analytical approximation can reproduce the results of the simulation model and where it cannot may be highly useful in gaining insight into the roles of spatial processes and thresholds for parameters guiding these processes (Ives et al. 1998).

The analytical approximation is not suggested as a substitute for stochastic, spatial simulation models, but rather as a complementary approach that makes many aspects of these models more transparent to direct testing of the effects of input parameters and their interactions. Increasing the transparency of these models may clarify the degree of uncertainty in model output that can be attributed to input parameters that were estimated due to difficulty in determining exact values. For cases where averaged over a large number of replications the output of the simulation model eventually would converge to the results determined analytically, the approximation provides a basis for determining the minimum number of model runs necessary for evaluating statistical distributions of output values, and it provides a method for direct evaluation of the effects of each input parameter.

LITERATURE CITED

Agee, J.K., and M.H. Huff. 1987. Fuel succession in a western hemlock/Douglas-fir forest. *Can. J. For. Res.* 17: 697–704.

Boychuk, D., A.H. Perera, M.T. Ter-Mikaelian, D.L. Martell, and C. Li. 1997. Modelling the effect of spatial scale and correlated fire disturbances on forest age distribution. *Ecol. Modelling* 95: 145–164.

Clark, J.S. 1989. Ecological disturbance as a renewal process. *Oikos* 56: 17–30.

DeAngelis, D.L., and W.M. Mooij. 2003. In praise of mechanistically rich models. pp. 63–82 *In* C.D. Canham, J.J. Cole, and W.K. Lauenroth (eds.). *Models in Ecosystem Science*. Princeton University Press. Princeton, NJ.

He, H.S. 2008. Forest landscape models: definitions, characterization, and classification. *For. Ecol. Manage.* 254: 484–498.

Heinselman, M.L. 1973. Fire in the virgin forests of the Boundary Waters Canoe Area, Minnesota. *Quat. Res.* 3: 329–382.

Impara, P.C. 1997. Spatial and temporal patterns of fire in the forests of the central Oregon Coast Range. Ph.D. Dissertation, Oregon State University, Corvallis.

Ives, A.R., M.G. Turner, and S.M. Pearson. 1998. Local explanations of landscape patterns: can analytical approaches approximate simulation models of spatial processes? *Ecosystems* 1: 35–51.

Johnson, E.A. 1979. Fire recurrence in the subarctic and its implications for vegetation composition. *Can. J. Bot.* 57: 1374–1379.

Johnson, E.A., and S.L. Gutsell. 1994. Fire frequency models, methods, and interpretations. *Adv. Ecol. Res.* 25: 239–287.

Keane, R.E., G.J. Cary, I.D. Davies, M.D. Falnnigan, R.H. Gardner, S. Lavorel, J.M. Lenihan, C. Li, and T.S. Rupp. 2004. A classification of landscape fire succession models: spatial simulations of fire and vegetation dynamics. *Ecol. Modelling* 179: 3–27.

Long, C.J., C. Whitlock, P.J. Bartlein, and S.H. Millspaugh. 1998. A 9,000-year fire history from the Oregon Coast Range, based on a high-resolution charcoal study. *Can. J. For. Res.* 28: 774–787.

McCarthy, M.A., and G.J. Cary. 2002. Fire regimes in landscapes: models and realities. *In* R. Bradstock, J. Williams, and M. Gill. (eds.). *Flammable Australia: the Fire Regimes and Biodiversity of a Continent*. Cambridge University Press, Cambridge, UK, pp. 77–94.

Nonaka, E., and T.A. Spies. 2005. Historical range of variability in landscape structure: a simulation study in Oregon, USA. *Ecol. App.* 15: 1727–1746.

Oreskes, N. 2003. The role of quantitative models in science. pp. 13–31 *In* C.D. Canham, J.J. Cole, and W.K. Lauenroth (eds.). *Models in Ecosystem Science*. Princeton University Press. Princeton, NJ.

Pielke, R.A. Jr. 2003. The role of models in prediction for decision. pp. 111–138 *In* C.D. Canham, J.J. Cole, and W.K. Lauenroth (eds.). *Models in Ecosystem Science*. Princeton University Press. Princeton, NJ.

Reed, W.J. 1994. Estimating the probability of stand-replacing fire using the age-class distribution of undisturbed forest. *For. Sci.* 40: 104–119.

Scheller, R.M., and D.J. Mladenoff. 2007. An ecological classification of forest landscape simulation models: tools and strategies for understanding broad-scale forested ecosystems. *Landscape Ecol.* 22: 491–505.

Teensma, P.D., J.T. Rienstra, and M.A. Yoder. 1991. Preliminary reconstruction and analysis of change in forests stand age class of the Oregon Coast Range from 1850 to 1940. U.S. Bureau of Land Management, Portland, OR. Tech. Note T/N OR-9.

Turner, M.G., W.H. Romme, R.H. Gardner, R.V. O'Neill, and T.K. Kratz. 1993. A revised concept of landscape equilibrium: disturbance and stability in scaled landscapes. *Landscape Ecol.* 8: 213–227.

Turner, M.G., and W.H. Romme. 1994. Landscape dynamics in crown fire ecosystems. *Landscape Ecol.* 9: 59–77.

Van Wagner, C.E. 1978. Age-class distribution and the forest fire cycle. *Can. J. For. Res.* 8: 220–227.

Wimberly, M.C. 2002. Spatial simulation of historical landscape patterns in coastal forests of the Pacific Northwest. *Can. J. For. Res.* 32: 1316–1328.

Wimberly, M.C., T.A. Spies, C.J. Long, and C. Whitlock. 2000. Simulating historical variability in the amount of old forests in the Oregon Coast Range. *Conserv. Biol.* 14: 167–180.

Table 4.1. Input parameters for LADS, as parameterized for the Oregon Coast Range (Wimberly 2002). To facilitate comparison to equations used in the analytical approximation, values for the average number of fires per year (FF_j) and the parameter of the Poisson distribution used to simulate the number of fires per timestep (λ_j) were calculated assuming a one-year timestep. These values may be multiplied by 10 for a 10-year timestep, as used in LADS.

Variable	Notation/Equation	Coastal Province	Valley Margin
Area of the j^{th} province (km^2)	A_j	14,540	8,880
Natural fire rotation (years)	NFR_j	200	100
Mean fire size (km^2)	MFS_j	73	22.5
SD of fire size (km^2)	$SDFS_j$	320.5	50
Parameters for the lognormal fire-size distribution	$\mu_j = \ln[MFS_j^2 / \sqrt{(MFS_j^2 + SDFS_j^2)}]$	2.786	2.223
	$\sigma_j = \sqrt{[1 + (SDFS_j^2 / MFS_j^2)]}$	1.735	1.335
Average number of fires initiated in the j^{th} province (#/year)	$FF_j = A_j / (NFR_j \times MFS_j)$	0.996	3.947
Parameter for the Poisson distribution used to simulate the number of fires per timestep	$\lambda_j = 1/FF_j$	1.004	0.253
Minimum (Min_k) and maximum (Max_k) size (km^2) for fires in the k^{th} size class (k = 1, 2, or 3, for small, medium, and large fires, respectively)	(Min_1, Max_1) (Min_2, Max_2) (Min_3, Max_3)	(0, 100) (100, 500) (500, ∞)	(0, 100) (100, 500) (500, ∞)
Lower (l_k) and upper (u_k) bounds for the random variable (U_k) used to determine the probability of burning at high severity for a fire in the k^{th} size class	(l_1 , u_1) (l_2 , u_2) (l_3 , u_3)	(0, 0.5) (0.1, 0.8) (0.7, 0.95)	(0, 0.5) (0.1, 0.8) (0.7, 0.95)

Table 4.2. Calculations used to approximate the equilibrium age distribution produced by LADS, as parameterized for the Oregon Coast Range in studies of Wimberly (2002) and Nonaka and Spies (2005). Variables not defined below are input parameters defined in Table 4.1.

Variable	Equation	Coastal Province	Valley Margin
Average proportion of cells that experience high-severity fire for fires in the k^{th} size class	$g_k = (l_k + u_k)/2$	$g_1 = 0.250$ $g_2 = 0.450$ $g_3 = 0.825$	$g_1 = 0.250$ $g_2 = 0.450$ $g_3 = 0.825$
For each fire initiated in the j^{th} province, the joint probability that the i^{th} cell is burned ($b_i = 1$) and fire severity is high ($\omega_i = 1$)	$P\{b_i = 1, \omega_i = 1\} = \sum_{k=1}^{m}\left(g_k \int_{Min_k}^{Max_k} \frac{x}{A_j} f_j(x)dx \right)$ m is the number of fire-size classes	2.77×10^{-3}	8.45×10^{-4}
Expected proportion of fires smaller than the upper bound of the k^{th} size class[a]	$Z_k = \Phi\left(\frac{\ln(Max_k) - (\mu_j + \sigma_j^2)}{\sigma_j} \right)$	$Z_1 = 0.246$ $Z_2 = 0.596$ $Z_3 = 1.000$	$Z_1 = 0.674$ $Z_2 = 0.951$ $Z_3 = 1.000$
Expected proportion of fires smaller than the lower bound of the k^{th} size class[a]	$Y_k = \Phi\left(\frac{\ln(Min_k) - (\mu_j + \sigma_j^2)}{\sigma_j} \right)$	$Y_1 = 0.000$ $Y_2 = 0.246$ $Y_3 = 0.596$	$Y_1 = 0.000$ $Y_2 = 0.674$ $Y_3 = 0.951$
Proportion of fires expected to be in the k^{th} size class	$Q_k = Z_k - Y_k$	$Q_1 = 0.246$ $Q_2 = 0.349$ $Q_3 = 0.404$	$Q_1 = 0.674$ $Q_2 = 0.277$ $Q_3 = 0.049$
Overall hazard of burning	$h^{(j)}(t) = 1/NFR_j$	0.005	0.010
Hazard rate for high-severity fire	$h_\tau^{(j)}(t) = FF_j \times P\{b_i = 1, \omega_i = 1\}$	2.76×10^{-3}	3.34×10^{-3}
Hazard rate for moderate-severity fire	$h_M^{(j)}(t) = h^{(j)}(t) - h_\tau^{(j)}(t)$	2.24×10^{-3}	6.66×10^{-3}
Natural fire rotation for high-severity fire	$NFR_j^H = 1/h_\tau^{(j)}(t)$	362	300
Natural fire rotation for moderate-severity fire	$NFR_j^M = 1/h_M^{(j)}(t)$	447	150
Equilibrium age distribution for the j^{th} province	$a_\infty^j(t) = h_\tau^{(j)}(t) \times \exp\left(-\int_0^t h_\tau^{(j)}(u)du \right)$		
Overall equilibrium age distribution (n represents the number of provinces)	$a_\infty(t) = \frac{A_1}{\sum_{j=1}^{n} A_j} a_\infty^1(t) + \ldots + \frac{A_n}{\sum_{j=1}^{n} A_j} a_\infty^n(t)$	See Table 4.3	

[a] $\Phi(x)$ represents the value of the standard normal distribution at x.

Table 4.3. Comparison of the equilibrium age-class distribution for the Oregon Coast Range produced by LADS to that produced by an analytical approximation using the same fire-regime parameters.

Age Class	Age Range	Percentage of Landscape	
		Simulation[a]	Approximation
Very open	0–10	2.7	2.9
Patchy open	11–20	2.7	2.9
Young	21–80	15.3	15.4
Mature	81–200	23.0	23.6
Early old growth	201–450	28.3	28.8
Mid old growth	451–800	16.2	16.9
Late old growth	>800	10.5	9.4

[a] from Appendix A of Nonaka and Spies (2005). Values were averaged over time within each of 200, 1,000-year replications, then these values were averaged across replications.

Table 4.4. Equations used to calculate the expected proportion of the landscape covered by the semi-open and multi-story stand-structure classes, as defined by Wimberly (2002). Variables are defined in Table 4.2, and *u* is used as a dummy variable to clarify that the hazard rate for moderate-severity fire, $h_M^{(j)}(t)$ is a function of the limits of integration.

Stand-Structure Class	Equation	Coastal Province	Valley Margin
Semi-open[a] AGE > 30 TFIRE ≤ 30	$\sum_{t=31}^{\infty}\left[a_{\infty}^{(j)}(t)\left\{1-\exp\left(-\int_{t-30}^{t}h_M^{(j)}(u)du\right)\right\}\right]$	6.0	16.4
Multi-story[a] AGE > 80 30 < TFIRE ≤ 80	$\sum_{t=31}^{\infty}\left[a_{\infty}^{(j)}(t)\left\{1-\exp\left(-\int_{t-80}^{t-30}h_M^{(j)}(u)du\right)\right\}\left\{\exp\left(-\int_{t-30}^{t}h_M^{(j)}(u)du\right)\right\}\right]$	7.9	17.8

[a] AGE and TFIRE represent the time since the last high-severity fire and the time since the last fire of any severity, respectively, as used by Wimberly (2002) to define the semi-open and multi-open stand-structure classes.

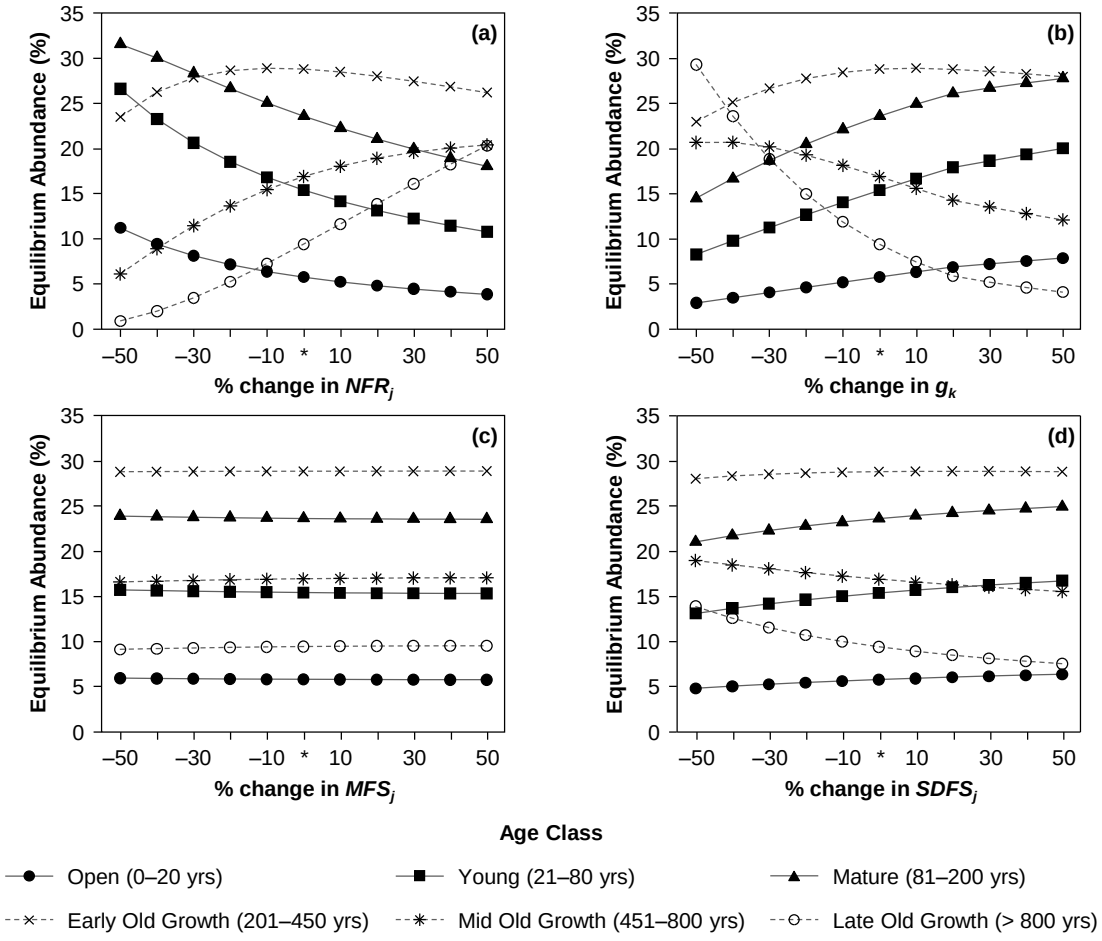

Figure 4.1. The expected proportion of the landscape covered by six age classes of the Oregon Coast Range over a range of values of (a) the overall NFR, (b) the expected proportion of fires that burn at high-severity for a fire of the k^{th} size class, g_k, (c) the mean fire size, and (d) the SD of fire size. Each parameter was adjusted in 10% increments to +/- 50% of its baseline value (the asterisk on the *x*-axis represents the baseline value for each parameter, as defined in Table 4.1). Age classes follow those of Nonaka and Spies (2005), as listed in Table 4.3, but the two youngest classes were combined due to narrow class width and similarity in response to changes in input parameters. Beyond a 20% increase in g_k, the value of g_3 was held constant at 0.99.

CHAPTER 5: TRAJECTORIES OF CHANGE IN FOREST AGE STRUCTURE UNDER A NON-STATIONARY FIRE REGIME

ABSTRACT

Although the potential for changes in climate or anthropogenic activities to alter forest disturbance regimes is well known, current understanding of long-term dynamics of forested landscapes under a non-stationary disturbance regime is limited. In this study, I present analytical methods for evaluating trajectories of change in forest age structure in response to changes in the fire regime. First, procedures for calculating the expected age distribution in any year following a change in fire frequency are presented, with and without allowing the time since the previous fire to feedback on susceptibility to subsequent fire. Then, I present a method to calculate the time required after a change in fire frequency for the expected age distribution to converge to the equilibrium age distribution of the new fire regime. Finally, the above methods are applied in a numerical example to track trajectories of change in forest age distribution and the abundance of different stand-structure types in response to changes in the rate of burning at three intensities in Douglas-fir/western hemlock forests of the Pacific Northwest. Two general properties were identified describing changes in forest age structure in response to a change in fire frequency. First, the expected proportion of a landscape covered by each age class is likely to change non-monotonically, rather than transition directly to its equilibrium abundance under the new fire regime. Second, under certain fire-interval models (exponential and some cases under a Weibull model), the time required for the expected age distribution to converge to the equilibrium age distribution of the new fire regime depends only on the magnitude of change in fire frequency, regardless of the initial frequency or the direction of change. These general properties are useful in interpreting the timing and magnitude of historical changes in the fire regime that would still have a legacy on contemporary landscapes, or for hypothesis exploration regarding forest response to future climate- or management-driven changes in disturbance regimes.

INTRODUCTION

Although assumptions of natural systems fluctuating within an unchanging envelope of variability were prevalent in ecological studies through the mid to late 20th century, many of these views recently have been modified or replaced by concepts of non-stationarity (Perry 2002, Milly et al. 2008). In particular, the potential for on-going climatic warming to affect ecosystems both directly, and indirectly through moderation of disturbance regimes (Westerling et al. 2006), has prompted substantial effort to better understand and predict ecosystem responses (Scheffer et al. 2001, Andersen et al. 2008). Also, tree ring and lake sediment based studies are increasingly elucidating the substantial and persistent effects of previous climatic variability on contemporary landscapes, largely due to climatic moderation of the dynamics of drought, fire, and insect outbreaks (Swetnam and Betancourt 1998, Whitlock et al. 2008, Marlon et al. 2009).

Climate-driven shifts in fire frequency at multi-decadal to multi-centennial timescales may be shorter than the time required for forest landscapes to adjust to the theoretical equilibrium conditions of the prevailing fire regime (Sprugel 1991). For example, a synthesis of ten fire-history studies west of the crest of the Cascade Mountains in Oregon and Washington suggests that existing old-growth forests developed under substantial, centennial-scale variation in the fire regime (Weisberg and Swanson 2003). Two periods of widespread burning, primarily in the 16th and 19th centuries, may have been separated by a long interval of reduced fire occurrence. In this region, Douglas-fir (*Pseudotsuga menziesii* (Mirb.) Franco) is a relatively shade-intolerant species whose regeneration depends on disturbances, such as fire, that open the canopy. Ages of more than 1,000 Douglas-fir trees distributed throughout two large watersheds (240 km^2) in the central western Cascades of Oregon produced a bimodal distribution, with peaks corresponding to each of the two putative periods of widespread fire (chapter 2).

Climatic changes on annual to decadal scales also may have broad-scale and long-lasting effects on forest landscapes, particularly in regions subject to frequent fire. For example, a period of substantially reduced fire frequency in the late 18th and early 19th centuries, possibly associated with increased precipitation and a dampening of interannual wet/dry oscillations, was identified in several fire-history studies in western North America and northern Argentina (Swetnam and Brown, in press). Age distributions of natural forests in some of these landscapes show a widespread pulse of establishment corresponding to this reduction in fire frequency (Brown and Wu 2005, Brown 2006).

Potential time lags and threshold responses of forest ecosystems to climate-driven changes in disturbance regimes make it difficult to predict responses under future climate and management scenarios. Also, tree-ring and lake-sediment data are not always available at sufficient spatial and temporal extent and resolution to evaluate effects of historical changes in disturbance regimes on present landscape structure. Thus, numerous modeling approaches may be applied to expand upon insight gained from field-based research regarding effects of historical or potential future changes in disturbance regimes on forest landscapes.

Modeling studies that evaluate changes in forest landscapes under changing climate and disturbance regimes commonly use stochastic, spatial simulation models (Chapin and Starfield 1997, He et al. 2002). Such an approach has the advantages of allowing for representation of numerous interacting processes believed to have important influences on the system and generating statistical distributions of key output variables over numerous model runs. However, including such complexity comes at the cost of a lack of transparency for the evaluation of the effects of individual variables and uncertainty in parameter estimates on model output (Oreskes 2003). Analytical models offer an alternative approach with greater potential for direct evaluation of effects of each input variable and algorithm. Although practical application of such approaches may be limited to simpler scenarios than can be evaluated by simulation, the analytical approach provides a more tractable representation of the system that may be helpful in identifying general relationships that apply in multiple contexts.

In this study, I develop analytical procedures for tracking trajectories of change in the age structure of a forested landscape in response to changes in the fire regime. Thus, the time-invariant density function of stand age used in previous analytical models (Van Wagner 1978, Johnson and Gutsell 1994) will be replaced by a density function that changes over historical time. In these exercises, model parameters that affect the rate of fire occurrence are changed in order to represent a response to changes in one or more external drivers that affect climate frequency. However, the external drivers are not modeled explicitly.

First, methods to determine the equilibrium age distribution of a landscape from fire frequency data under a stationary fire regime are summarized. Then, I expand upon these methods to calculate the expected age distribution of a landscape in any year following an abrupt change in fire frequency from a known initial age distribution. These calculations are developed initially for a scenario where all stands are equally likely to burn each year, and then they are modified to allow the time since the previous fire to feedback on susceptibility to subsequent fire. Then, an approach is presented to determine the time required for the expected age distribution of a landscape to converge to the equilibrium age distribution of the new fire regime following a change in fire frequency. Finally, the above methods are applied in a numerical example for Douglas-fir/western hemlock forests of the Pacific Northwest, where burning at three intensities affects the initiation and mortality of age cohorts of Douglas-fir and shade-tolerant species. Analytically-determined trajectories of change in the expected abundance of forest age classes and stand-structure types under two non-stationary scenarios are compared to those determined by simulation.

BACKGROUND

Equilibrium Age Distribution under a Stationary Fire Regime

The equilibrium age distribution of a forested landscape under a stationary fire regime can be determined by converting the rate at which stands are burned and new stands initiated into the expected proportion of the landscape covered by stands of each

age. This conversion is facilitated by three distributions, which provide a basis for calculating the mean fire interval and the probability density function of stand age for a given point in the landscape. In this section, I illustrate that each of these distributions may be specified by the hazard of burning, or hazard rate, which is defined as the age-specific probability rate of fire in a given year (Johnson and Gutsell 1994). It is not strictly a probability (e.g., values are not constrained between 0 and 1). However, when using an annual timestep, interpreting the hazard rate as the annual probability of fire for stands of a given age provides an approximation almost identical to the probability of fire in that year (Reed 1994). The hazard rate, as used here, should not be confused with the fire hazard, as used in fire ecology as a measure of potential fire behavior based on fuel loading.

The distributions used to calculate the mean fire interval and probability density function of stand age are presented in the context of only stand-replacing (SR) fire. However, they also may be used in evaluating age-cohort structure under a mixed-severity fire regime, where stands are subject to SR and non-stand-replacing (NSR) fire, as demonstrated in the numerical application in the final section of this chapter. In the equations below, τ is a random variable representing the number of years between successive SR fires at a given point in the landscape. The variable, *t*, represents stand age, which is reset only by SR fire, and thus is equivalent to the time since the last SR fire at a particular site. The hazard rate for SR fire, $h_\tau(t)$, is the probability rate of SR fire in a given stand during the interval (t, $t + \Delta t$), provided the stand has reached age *t* without SR fire:

$$h_\tau(t) = \lim_{\Delta t \to 0} \left[P\{\tau \in (t, t+\Delta t) \mid \tau > t\} \right] \frac{1}{\Delta t}.$$

Defining the hazard rate for SR fire as a function of stand age indirectly accounts for factors endogenous to a stand that change with time since fire and are hypothesized to affect the probability of subsequent fire occurrence (e.g., fuel loading). The Weibull model commonly has been used to specify fire-interval distributions with age-dependent

hazard rates (Clark 1989, Grissino-Mayer 1999), though a broader range of fire-interval models and associated hazard rates is possible (McCarthy et al. 2001). The exception to an age-specific hazard rate is the exponential fire-interval model, where all stands have the same probability of burning each year.

For any fire-interval model, the hazard rate for SR fire may be used to specify three distributions useful in determining the equilibrium age distribution. The cumulative survivorship distribution, $S_\tau(t)$, is the probability of a stand reaching age *t* without SR fire,

$$S_\tau(t) = P\{\tau > t\} = \exp\left(-\int_0^t h_\tau(u)du\right). \quad [1]$$

In Equation 1 and in the following equations, *u* is a dummy variable used to clarify that $S_\tau(t)$ is a function of the upper limit of integration, *t*, not a function of *u*.

The cumulative mortality distribution, $F_\tau(t)$, is the probability that a stand will experience SR fire before reaching age *t*,

$$F_\tau(t) = P\{\tau \le t\} = 1 - S_\tau(t) = 1 - \exp\left(-\int_0^t h_\tau(u)du\right). \quad [2]$$

The SR-fire-interval distribution, $f_\tau(t)$, represents the probability of a stand reaching age *t* without SR fire (the cumulative survivorship distribution) multiplied by the probability of experiencing SR fire in the next finite interval (the hazard rate for SR fire):

$$f_\tau(t) = P\{\tau \in [t, t+\Delta t]\} = S_\tau(t)h_\tau(t) = h_\tau(t)\exp\left(-\int_0^t h_\tau(u)du\right). \quad [3]$$

The distributions defined in equations 1–3 are related as follows:

$$h_\tau(t) = \frac{f_\tau(t)}{S_\tau(t)} = \frac{f_\tau(t)}{1 - F_\tau(t)}.$$

The mean interval between successive SR fires at a given point in the landscape, $E(\tau)$, is determined by integrating the cumulative survivorship distribution, $S_\tau(t)$, over all stand ages:

$$E(\tau) = \int_0^\infty S_\tau(t)dt = \int_0^\infty \exp\left(-\int_0^t h_\tau(u)du \right) dt. \qquad [4]$$

In a landscape that is homogeneous with respect to the hazard of burning (the hazard rate for SR fire follows the same function of stand age at each point), $E(\tau)$ represents the Natural Fire Rotation (NFR) for SR fire, or the average number of years required for a cumulative area equal to the extent of the landscape to experience SR fire (Heinselman 1973).

The relationships presented above may be used to specify the equilibrium probability density function of stand age for any point in the landscape under the following assumptions: (1) trees establish promptly after fire and tree longevity exceeds SR fire intervals, such that stand age is equivalent to time since the last SR fire, (2) only SR fire kills the existing forest and initiates a new stand, and (3) the landscape has undergone several fire rotations without changes in the hazard rate for SR fire. The first assumption may make this modeling approach invalid in surface fire regimes, where SR fire is very rare and stand age may have little meaning (e.g., White 1985). The third assumption implies that factors exogenous to a stand that affect the rate of burning across the landscape (e.g., climate or human ignitions) do not change over time. It also implies that the expected area burned is the same each year. There may be variation in the observed area burned per year, for instance, due to stochastic variation in the number of ignitions or fire size. However, variation in the expected area burned per year, even over short timescales, could invalidate the following methods of calculating the equilibrium age distribution (Boychuk et al. 1997). The third assumption will be dropped in the

following sections to evaluate trajectories of change in the expected age distribution of a landscape when the hazard rate varies as a function of historical time (with and without dependence on stand age).

To determine the equilibrium probability density function of stand age, it is useful to recognize that the reciprocal of the mean interval between successive SR fires at each point, $1/E(\tau)$, represents the expected proportion of the landscape that experiences SR fire each year. Because landscape size is fixed, and by assumptions 1 and 2 above, a new stand is initiated only immediately after another stand is killed by SR fire, the reciprocal of the NFR, $1/E(\tau)$, also represents the average proportion of the landscape covered by new stands initiated in each year. The proportion of the area of newly initiated stands that is expected to reach age *t* without experiencing SR fire is provided by the cumulative survivorship distribution, $S_\tau(t)$. Therefore, the equilibrium density function of stand age (the equilibrium age distribution of a landscape that is homogeneous with respect to the hazard rate for SR fire), $a_\infty(t)$, is calculated by multiplying the frequency of stand establishment, $1/E(\tau)$, by the probability of stands reaching age *t* without SR fire, $S_\tau(t)$:

$$a_\infty(t) = \frac{1}{E(\tau)} S_\tau(t) = \frac{1}{\int_0^\infty \exp\left(-\int_0^t h_\tau(u)du\right)dt} \exp\left(-\int_0^t h_\tau(u)du\right). \qquad [5]$$

Equation 5 specifies the probability that the age of a randomly selected stand is equal to *t* in a given year, provided assumptions 1–3, above. If the assumptions are met in a landscape that is homogeneous with respect to factors affecting fire occurrence, and large enough relative to fire size that there is little inter-annual variation in area burned, the observed age distribution in each year (i.e., the proportion of the landscape covered by stands of each age) will approach $a_\infty(t)$. However, the observed age distribution in any year may diverge from $a_\infty(t)$ if landscape size is small relative to the variation in fire size, leading to substantial stochastic variation in annual area burned around a fixed mean (Turner and Romme 1994). Under such a scenario, averaging the proportion of the

landscape covered by each age class over time eventually would approach the equilibrium age distribution, provided there are no changes in external factors (e.g., climate) affecting the overall probability of fire occurrence over this time period.

Under an age-independent hazard rate (exponential fire-interval distribution), the average proportion of the landscape represented by new stands initiated each year, $1/E(\tau)$, is equivalent to the hazard rate for SR fire, $h_\tau(t)$. Therefore, $h_\tau(t)$ may replace $1/E(\tau)$ in Equation 5, illustrating that the equilibrium age distribution is equivalent to the SR fire interval distribution (Equation 3). However, under an age-dependent hazard rate, $h_\tau(t)$ is not equivalent to $1/E(\tau)$, and the equilibrium age distribution is not equivalent to the SR fire-interval distribution. In Appendix B, Wald's Equation and the Renewal Theorem (Grimmett and Stirzaker 1992) are used to prove that Equation 5 provides the equilibrium age distribution regardless of the form of the hazard rate.

NON-STATIONARY FIRE REGIMES

Trajectories of Change under an Age-Independent Hazard Rate

In the previous section, the hazard rate for SR fire, $h_\tau(t)$, was presented as a function only of stand age. Hereafter, the time-invariant hazard rate is replaced by a hazard rate that varies over historical time to account for factors exogenous to a stand that affect the rate of burning across a landscape. The hazard rate for SR fire is now denoted by $h_\tau(t, s)$, to illustrate that it varies as a function of stand age, t, which is reset by SR fire, and historical time, s, which is continuous and not reset by fire. When the hazard rate for SR fire varies over historical time, the density of stands of age t in year s is represented by $a(t, s)$. The trajectory of change in the expected proportion of the landscape covered by stands of a given age can be evaluated by generating the time series for $a(t, s)$ with t fixed and allowing s to change incrementally. For simplicity, the descriptions below apply to a landscape that is homogeneous with respect to the hazard rate for SR fire, and only SR fire is considered here. Non-stand-replacing fire will be added in the numerical application provided in the final section.

The simplest scenario for evaluating the trajectory of change in the expected age distribution of a landscape under a non-stationary fire regime is after an abrupt change from one age-independent hazard rate to another. If time is divided into distinct epochs, each characterized by a different age-independent hazard rate for SR fire (e.g., Reed et al. 1998), the hazard rate for each epoch is defined as

$$h_\tau(t, s) = \begin{cases} \lambda_k & \text{if } s \le s_0 \\ \lambda_{k+1} & \text{if } s > s_0, \end{cases}$$

where s_0 denotes the time of an abrupt change in the overall rate of burning. The subscript, k, denotes the value of λ for the k^{th} epoch, ordered from past to present. Under an age-independent hazard rate, the mean interval between successive SR fires in a given stand (Equation 4) during the k^{th} epoch may be reduced to $E(\tau_k) = 1/\lambda_k$. The survivorship distribution (Equation 1) during the k^{th} epoch is represented by $S_{\tau_k}(t) = \exp(-\lambda_k t)$, recognizing that stands that originated in the previous epoch and survived into the k^{th} epoch would have faced two hazards of burning. Thus, Δs years after the change in the hazard rate (year $s_0 + \Delta s$), survivorship for stands that originated in the first epoch (i.e., stands of age $t > \Delta s$) is calculated as

$$S_{\tau_1}(t - \Delta s) S_{\tau_2}(\Delta s) = \exp[-\lambda_1 (t - \Delta s)] \exp(-\lambda_2 \Delta s).$$

The above simplifications are not valid when the hazard rate varies with stand age, as discussed in the next section.

In the evaluation of trajectories of change in the density function for stand age following an abrupt change in the hazard rate for SR fire, $a(t, s_0)$ will be used to represent the density function of stand age at time s_0, immediately before the change in the hazard rate. At a time Δs years after the change in the hazard rate, the density function of stand age is given by $a(t, s_0 + \Delta s)$. The above expressions represent the expected proportion of a homogeneous landscape covered by stands of age t in year s_0 and in year $s_0 + \Delta s$, respectively. The observed proportion of the landscape covered by stands of each

age may diverge from these values if landscape size is small enough relative to variation in fire size that there is substantial year-to-year variation in area burned in addition to the time-dependent change in the hazard rate.

By year $s_0 + \Delta s$, the landscape would be subject to the new hazard rate (λ_{k+1}) for Δs years. At this time, stands of age $t > \Delta s$ would have established in the first epoch (before year s_0). Stands of age $t \leq \Delta s$ would have established in the present epoch (after year s_0). The density of stands of age $t > \Delta s$ in year $s_0 + \Delta s$ is determined by multiplying the density of stands of age $t - \Delta s$ in year s_0 by the probability of surviving Δs years without SR fire under the prevailing fire regime, $S_{\tau_1}(\Delta s)$ (Equation 6a). The density of stands that established in the present epoch (after year s_0) is determined as in Equation 5, by multiplying the annual rate of stand establishment in the present epoch, $1/E(\tau_2)$, by the probability of reaching age $t \leq \Delta s$ without SR fire in the present epoch $S_{\tau_2}(t)$ (Equation 6b).

$$a(t, s_0 + \Delta s) = \begin{cases} a(t - \Delta s, s_0) S_{\tau_2}(\Delta s) & t > \Delta s \quad [6a] \\ \dfrac{1}{E(\tau_2)} S_{\tau_2}(t) & t \leq \Delta s \quad [6b] \end{cases}$$

Equation 6b is identical to Equation 5, which illustrates that if the hazard rate for SR fire is independent of stand age, following an abrupt change in the overall rate of burning, the expected proportion of the landscape that experiences SR fire each year immediately shifts to that specified by the new hazard rate: $1/E(\tau_2) = 1/\lambda_2$. Therefore, under an age-independent hazard of burning, at any time (Δs) after an abrupt change in the hazard rate for SR fire, the expected age distribution for stands of age $t \leq \Delta s$ is equal to the equilibrium density for stands of corresponding age under the new fire regime, regardless of the initial age distribution, $a(t, s_0)$.

When the initial age distribution is the equilibrium age distribution of the first epoch, $a(t, s_0) = a_{\infty}^{(1)}(t)$, after an abrupt change in the hazard rate for SR, fire, from λ_1 to λ_2, Equation 6a is solved as

$$a(t, s_0 + \Delta s) = a(t - \Delta s, s_0) S_{\tau_2}(\Delta s) = \lambda_1 \exp\left[-\lambda_1 (t - \Delta s)\right] \exp(-\lambda_2 \Delta s).$$

Regardless of the initial age distribution, Equation 6b is solved as

$$a(t, s_0 + \Delta s) = \frac{1}{E(\tau_2)} S_{\tau_2}(t) = \lambda_2 \exp(-\lambda_2 t).$$

In each year, integrating the density function of stand age, $a(t, s_0 + \Delta s)$, over all ages must be equal to 1, which is verified by

$$\int_0^{\infty} a(t, s_0 + \Delta s) dt = \frac{1}{E(\tau_2)} \int_0^{\Delta s} S_{\tau_2}(t) dt + \left(\int_{\Delta s}^{\infty} a(t - \Delta s, s_0) dt \right) S_{\tau_2}(\Delta s) = 1.$$

If the initial age distribution is the equilibrium age distribution of the first epoch, the above equation is solved as

$$\int_0^{\infty} a(t, s_0 + \Delta s) dt = \frac{1}{(1/\lambda_2)} \frac{1}{\lambda_2} \left[1 - \exp(-\lambda_2 \Delta s)\right] + \exp(-\lambda_2 \Delta s) = 1.$$

To clarify the above relationships, consider a landscape with an age distribution in equilibrium with a fire regime with an age-independent hazard of burning and an NFR of 100 years, (λ_1 = 0.01). Assume that a completely effective system of fire suppression was initiated in year s_0 = 1900, which eliminated all SR fire and provided a new hazard rate, λ_2 = 0. If fire is the only source of stand mortality and new stands are initiated only following SR fire, by year $s_0 + \Delta s$ = 1950, all stands would have aged by Δs = 50 years, and no new stands would have established since 1900 (Figure 5.1a).

Now, consider another scenario starting from the same initial conditions. Fire suppression was initiated in 1900, but it was not completely effective. Instead of eliminating all fire, it caused the NFR to double from 100 to 200 years (corresponding to

a reduction in the hazard rate from $\lambda_1 = 0.01$ to $\lambda_2 = 0.005$). By 1950, all stands of age $t > 50$ would have established in the first epoch, prior to the initiation of fire suppression, and their density is determined by Equation 6a. For example, the expected proportion of the landscape covered by stands of age $t = 100$ in year $s_0 + \Delta s = 1950$ is determined by multiplying the density of stands of age $t - \Delta s = 50$ in year $s_0 = 1900$ by the probability of surviving $\Delta s = 50$ years under the reduced hazard rate following fire suppression. Stands of age $t \leq 50$ in 1950 would have established after the initiation of fire suppression. Using Equation 6b, their density is calculated by multiplying the annual rate of SR fire (i.e., the annual rate of stand establishment = $1/E(\tau_2) = \lambda_2$) by the probability of stands surviving to age $t \leq 50$ without SR fire (Figure 5.1b). These relationships also apply for an abrupt change to a shorter NFR (Figure 5.1c).

Trajectories of Change under an Age-Dependent Hazard Rate

The above methods do not apply directly when the hazard rate for SR fire varies as a function of stand age (time since the previous fire) and historical time. Trajectories of change in the expected age distribution under a hazard rate that varies with stand age and historical time are more difficult to model analytically because the expected area burned in a given year depends on the expected age distribution in that year. Thus, the reciprocal of the NFR, $1/E(\tau)$ provides the expected proportion of the landscape that experiences SR fire in a given year only if the expected age distribution in that year is equivalent to the equilibrium age distribution. For example, if young stands that experienced SR fire within the last 2–3 decades are more susceptible to SR fire than older stands (e.g., Thompson and Spies 2010), and a larger fraction of the landscape is covered by young stands than expected under the equilibrium age distribution, the fraction of the landscape expected to experience SR fire in that year would be larger than that expected under the equilibrium age distribution. Therefore, unlike the case following an abrupt change from one age-independent hazard rate to another (Figure 5.1b and c), the density function for the ages of young stands that initiated after a change in the fire regime does not immediately adjust to the equilibrium density under the new fire regime.

Trajectories of change in the age distribution may be tracked year-by-year (Δs = 1) when the hazard rate for SR fire, $h_\tau(t, s)$, varies as a function of stand age, t, and historical time, s. For $t > 1$, a stand can reach age t in year $s + 1$ only if it was of age $t - 1$ in year s and did not experience SR fire during that year. The annual rate that stands of a given age experience SR fire is determined by multiplying the density function for stands of that age by the hazard rate for stands of that age. Thus, the density of stands of age $t > 1$ in year $s + 1$ can be calculated by subtracting the annual rate at which stands of age $t - 1$ are killed by SR fire in year s from the density of stands of age $t - 1$ in year s (Equation 7a). Assuming that landscape size is fixed and a new stand establishes only after another stand is killed by SR fire, the expected proportion of the landscape covered by new stands originated in each year is equal to the proportion of the landscape expected to experience SR fire that year. Therefore, the density function for stands of age $t = 1$ in year $s + 1$ is calculated by subtracting the fraction of the landscape expected to be covered by stands that were not killed by SR fire that year from 1, as shown in Equation 7b,

$$a(t, s+1) = \begin{cases} a(t-1, s) - [a(t-1, s) h_\tau(t-1, s)] & t > 1 \quad [7a] \\ 1 - \int_2^\infty a(t, s+1) dt & t = 1. \quad [7b] \end{cases}$$

The above equations may be solved iteratively, using the output, $a(t, s + 1)$, on the left-hand-side of Equation 7 as the input, $a(t - 1, s)$, on the right-hand-side for the next iteration. Although this approach involves a large number of calculations, it may easily be conducted using a variety of computational software or spreadsheet applications. Tracking the trajectory of change year-by-year has the advantage of allowing specification of a new hazard rate each year. Thus, Equations 7a and 7b may be applied using any time series of changes in one or more parameters of a hazard rate of any form at an annual timestep.

For any interval (Δs years) since a change in fire frequency, it is possible to determine the expected proportion of the landscape covered by stands of age $t > \Delta s$ using a single equation rather than solving Equations 7a and 7b iteratively. As long as the initial

age distribution, $a(t, s_0)$, is known, the expected proportion of the landscape covered by stands of age $t > \Delta s$, at time Δs years after the change in the fire regime is determined by:

$$a(t, s_0 + \Delta s) = a(t - \Delta s, s_0) \exp\left(- \int_{t-\Delta s}^{t} h(u, s) du \right).$$

The above equation does not account for the proportion of the landscape covered by stands of age $t \leq \Delta s$. Because the expected area burned in a given year under an age-dependent hazard rate depends on the age distribution in that year. Therefore, it is necessary to solve Equations 7a and 7b iteratively to determine the expected age distribution over the full range of stand ages under a non-stationary fire regime where the hazard rate depends on stand age.

The difficulty in calculating the proportion of the landscape of age $t \leq \Delta s$ at a time Δs years after a change in the fire regime is evident by examination of differences in the expected abundance of this portion of the age distribution at different intervals following an abrupt change in fire frequency under a Weibull fire-interval model where the hazard of burning increases with stand age. Immediately after an abrupt decrease in fire frequency, the landscape is expected to support more young stands and fewer old stands than expected under the equilibrium age distribution of the new fire regime (Figure 5.2a). Because young stands are less fire-prone than older stands in this example of a hazard rate that increases with stand age, the expected area burned per year shortly after the decrease in fire frequency is less than that under the equilibrium age distribution of the new fire regime. Thus, shortly after the change in fire frequency, the expected proportion of the landscape covered by young stands decreases below the new equilibrium density for these ages (Figure 5.2a).

Over time, the proportion of the landscape covered by stands of age $t \leq \Delta s$ gradually approaches the new equilibrium density, and the expected area burned per year approaches the equilibrium value of the new regime in accordance with the age distribution. In this example of a hazard rate that increases with stand age, after an abrupt increase in fire frequency, the expected proportion of the landscape covered by young age

classes initially increases above the new equilibrium density (Figure 5.2b) due to the burning of old, fire-prone stands that were abundant at the time of the change in fire frequency. However, as most of the older stands are eliminated the expected area burned per year approaches the equilibrium value under the new fire regime, and the density of stands of age $t \leq \Delta s$ decreases toward the new equilibrium value (Figure 5.2b).

The survivorship distribution (Equation 1) may be modified to account for an age-dependent hazard of burning that varies with historical time. For the case of two epochs, each characterized by a different hazard of burning, the probability of a stand reaching age t at a time Δs years after the change in the hazard of burning is provided by

$$S_\tau(t,s) = \exp\left(-\int_0^{\max(0,t-\Delta s)} h_\tau^{(1)}(u)du\right)\exp\left(-\int_{\max(0,t-\Delta s)}^{t} h_\tau^{(2)}(u)du\right), \qquad [8a]$$

where $h_\tau^{(1)}(t)$ and $h_\tau^{(2)}(t)$ are hazard rates of the first and second epochs, from past to present. The limits of integration represent the ages that a stand of age t in year $s_0 + \Delta s$ would have been subject to each hazard of burning.

If there is a second change in the hazard of burning, leading to three epochs, with changes in years s_1 and s_2, from past to present, the survivorship distribution Δs years after the most recent change is calculated as

$$S_\tau(t,s) = \exp\left(-\int_0^{\max[0,t-\Delta s-(s_2-s_1)]} h_\tau^{(1)}(u)du\right)\exp\left(-\int_{\max[0,t-\Delta s-(s_2-s_1)]}^{\max(0,t-\Delta s)} h_\tau^{(2)}(u)du\right), \qquad [8b]$$
$$\exp\left(-\int_{\max(0,t-\Delta s)}^{t} h_\tau^{(3)}(u)du\right)$$

where the limits of integration specify the range of ages that a stand of age t in year $s_2 + \Delta s$ would have been subject to each hazard of burning. Equations 8a and 8b apply to stands of all ages, regardless of the epoch in which they were originated. For stands that originated in one of the recent epochs and were not subject to the hazard of burning during previous epochs, the exponential terms representing epochs prior to stand origin

are reduced to, exp(0) = 1, because the lower limit of integration would be equal to the upper limit.

Because the limits of integration in Equations 8a and 8b specify the range of ages over which a stand would have been subject to each hazard rate, the equations may be applied regardless of the form of the hazard rate. This differs from a previous method to evaluate survivorship under a non-stationary fire regime, which counts backward from the present to determine the number of years that a stand would have been subject to each hazard rate, and therefore applies only under an age-independent hazard rate (Reed et al. 1998).

General Equation for Transitions in Stand-Age Distribution

Equations 6 and 7 solve a differential equation representing the probability density function for stand age, *t*, at time, *s*. The basis for the differential equation is a rule stating that in order for a stand to reach age *t* at time $s + \Delta s$, it has to have been of age $t - \Delta s$ at time *s*, and not experience SR fire during the interval $[s, s + \Delta s]$. Because the rate at which stands experience SR fire is given by the hazard rate for the age of the stand at time *s*, $h_\tau(t - \Delta s, s)$, multiplied by the fraction of the landscape in that class, $a(t - \Delta s, s)$, the above rule can be written as

$$a(t, s + \Delta s) \cong a(t - \Delta s, s) - a(t - \Delta s, s) h_\tau(t - \Delta s, s) \Delta s . \qquad [9a]$$

The above equation is an approximation for very small values of Δs, and it accounts only for the portion of the age distribution of age $t > \Delta s$ at time Δs years after a change in the fire regime.

Equation 9a may be rewritten as:

$$\frac{a(t, s + \Delta s) - a(t - \Delta s, s)}{\Delta s} = -a(t - \Delta s, s) h_\tau(t - \Delta s, s) . \qquad [9b]$$

Taking the limit as $\Delta s \to 0$ produces the following partial differential equation (PDE):

$$\frac{\partial a}{\partial s} + \frac{\partial a}{\partial t} = -a(t,s)h_\tau(t,s). \qquad [10]$$

The PDE requires that the initial age distribution, $a(t, 0)$, is known. It also has to satisfy that the density function of stand age integrates to 1 in each year (for each value of s),

$$\int_0^\infty a(t,s)dt = 1.$$

The above relationship is needed to calculate the proportion of the landscape covered by new stands that establish in a given year, as in Equation 7b. Also, it adjusts a boundary condition needed to solve the PDE in Equation 10.

For an age-independent hazard rate, $h_\tau(t,s) = h_\tau(s)$, and $\lim_{\Delta s \to \infty} h_\tau(s) = \lambda$. Thus, the PDE can be solved to show that as $s \to \infty, a(t,s) \to \lambda \exp(-\lambda t)$. Also, the equilibrium age distribution satisfies the ordinary differential equation:

$$\frac{da_\infty(t)}{dt} = -a_\infty(t)\lambda,$$

which can be solved to produce Equation 5.

Convergence to the Equilibrium Age Distribution

A useful question related to trajectories of change in the age distribution following a change in fire frequency is to determine the time required for the expected age distribution of a landscape to converge to the equilibrium age distribution of the new fire regime. As long as the initial age distribution, $a(t, 0)$, and the equilibrium age distribution under the new fire regime, $a_\infty^{(2)}(t)$, are known, Equations 7a and 7b (or 9a and 9b for an age-independent hazard rate) can be solved to determine the expected age distribution in each year following a change in fire frequency. The difference between the expected age distribution in each year and the equilibrium age distribution of the new fire regime, ρ, can be quantified as

$$\rho \geq \int_0^{\infty} \left| a(t,s) - a_{\infty}^{(2)}(t) \right| dt \, . \qquad [11]$$

The value, $(1 - \rho)$ x 100, is a measure of percent similarity between age distributions, similar to that used in previous studies (Baker 1989, Boychuk et al. 1997).

The use of Equation 11 to evaluate the time to converge to the equilibrium age distribution of a new fire regime following an abrupt shift from one age-independent hazard rate to another is illustrated in Figure 5.3. The number of years from the time of the change in the fire regime to the year when the expected age distribution reaches a specified degree of similarity to the equilibrium age distribution of the new regime is represented by $\Delta s(\rho)$, illustrating that the convergence time is a function of the desired degree of similarity, ρ. For a given value of ρ, finding the smallest value of s that satisfies Equation 11 provides the number of years to reach a specified degree of similarity to the equilibrium age distribution of the new fire regime (Figure 5.4a).

It would be valuable to determine if the convergence time can be calculated directly without having to calculate the density function of stand age each year following the change in fire frequency. To address this question, stand age, *t*, and historical time, *s*, will be converted from values in years, to non-dimensional (unitless) numbers. For example, I will calculate the time to converge to the equilibrium age distribution of the new fire regime as the number of fire rotations under the new fire regime. Under some scenarios (e.g., a shift from one age-independent hazard rate to another or a change in the NFR driven by a change in one parameter of a two-parameter Weibull distribution), I will demonstrate that the convergence time depends only on the degree of change in the NFR, regardless of the initial NFR or the direction of change.

In non-dimensional form, the probability density function for stand age is written as

$$\tilde{a}(x,y) = b_1 a(xb_1, yb_2) \, , \qquad [12]$$

where x and y are non-dimensional variables representing stand age, t, and historical time, s, respectively. In Equation 12 and in the following equations, $\tilde{a}$ specifies the non-dimensional form of the age distribution, and b_1 and b_2 are scaling parameters that convert stand age and historical time to unitless values. For example, dividing stand age, t, in years, by the scaling parameter, b_1, also in years, provides the unitless measure of stand age, $x = t/b_1$. Likewise, dividing historical time, s, by the scaling parameter, b_2, provides the unitless measure of historical time, $y = s/b_2$. Specific values of b_1 and b_2 can be determined based on the hazard rate of interest. For example, to evaluate the scenario of a change from one age-independent hazard rate to another, b_1 and b_2 may be defined as the NFR (the reciprocal of parameter, λ_k) for the first and second fire epoch, respectively.

It can be verified that integrating $\tilde{a}(x, y)$ with respect to x over all ages is equal to 1:

$$\int_0^\infty \tilde{a}(x, y)dx = \int_0^\infty b_1 a(xb_1, yb_2)dx = \int_0^\infty a(t, yb_2)dt = 1.$$

The PDE provided in Equation 10 also can be converted to non-dimensional form, as shown below. First, multiplying Equation 10 by b_1 and evaluating the equation at $(t, s) = (xb_1, yb_2)$, provides

$$b_1 \frac{\partial a}{\partial t}|_{(xb_1, yb_2)} + b_1 \frac{\partial a}{\partial s}|_{(xb_1, yb_2)} = -h_\tau^{(2)}(xb_1)a(xb_1, yb_2)b_1, \qquad [13]$$

where $h_\tau^{(2)}(xb_1)$ is the hazard rate for SR fire under the new fire regime. Then, using the chain rule from calculus, it can be shown that:

$$\frac{\partial \tilde{a}}{\partial x}|_{(x,y)} = b_1^2 \frac{\partial a}{\partial t}|_{(xb_1, yb_2)}, \text{ and}$$

$$\frac{\partial \tilde{a}}{\partial y}|_{(x,y)} = b_1 b_2 \frac{\partial a}{\partial s}|_{(xb_1, yb_2)}.$$

Using the above relationships, Equation 13 may be written in terms of $\tilde{a}(x, y)$, as

$$\frac{1}{b_1}\frac{\partial \tilde{a}}{\partial x}\Big|_{(x,y)} + \frac{1}{b_2}\frac{\partial \tilde{a}}{\partial y}\Big|_{(x,y)} = -h_\tau^{(2)}(xb_1)\tilde{a}(x,y).$$

Also, the non-dimensional form of the hazard rate, $\Lambda(x;\mu)$, may be written as a function of x with parameter, μ, where $\mu = b_2/b_1$,

$$\Lambda(x;\mu) \equiv b_2 h_\tau^{(2)}(xb_1). \qquad [14]$$

Then, the non-dimensional equivalent of the PDE provided in Equation 10 is given by

$$\mu\frac{\partial \tilde{a}}{\partial x} + \frac{\partial \tilde{a}}{\partial y} = -\Lambda(x;\mu)\tilde{a}(x,y). \qquad [15]$$

For specific hazard rates (e.g., exponential and some cases of a Weibull distribution), the function, Λ, depends only on x and μ, and not on individual values of b_1 and b_2. Therefore, Equation 15 can be solved for a given value of μ. Also, when starting with the equilibrium age distribution of an initial fire regime, the initial data,

$$\tilde{a}(x,0) = b_1 a(xb_1,0) = b_1 a_\infty^{(1)}(xb_1) \equiv \tilde{a}^{(1)}(x), \qquad [16]$$

is assumed to be a function only of x. For example, under an exponential fire-interval distribution (age-independent hazard rate) with $b_1 = 1/\lambda_1$ representing the NFR of the initial fire regime, $\tilde{a}(x,0) = \exp(-x)$.

Equation 11, which represents the degree of difference between the expected age distribution in year, s, and the new equilibrium age distribution after a change in fire frequency, can be converted to non-dimensional form, as shown below. Then, for specific hazard rates, the time to converge to the equilibrium age distribution of a new fire regime may be solved as a function of μ. In non-dimensional form, the amount of time, y (e.g., the number of fire rotations), to reach a specified degree of similarity to the equilibrium age distribution of a new fire regime is denoted by $y(\rho)$, where $y = s/b_2$. Equation 11 may be rewritten as:

$$\rho = \int_0^{\infty} \left| \frac{1}{b_1} \tilde{a}\left(\frac{t}{b_1}, \frac{s}{b_2} \right) - b_1 \frac{1}{b_1} a_{\infty}^{(2)}\left(b_1 \frac{t}{b_1} \right) \right| dt = \int_0^{\infty} \left| \tilde{a}\left(x, \frac{s}{b_2} \right) - b_1 a_{\infty}^{(2)}(x b_1) \right| dx .$$

Assuming that $b_1 a_{\infty}^{(2)}(x b_1) = \tilde{a}^{(2)}(x;\mu)$, the question of finding the time to converge to the equilibrium age distribution of the new fire regime is a problem of finding the smallest $y(\rho)$ such that for all $y > y(\rho)$, one has

$$\rho \geq \int_0^{\infty} \left| \tilde{a}(x,y) - \tilde{a}^{(2)}(x;\mu) \right| dx . \qquad [17]$$

The problem posed by solving Equation 15, with the initial data in Equation 16, and determining $y(\rho)$ satisfying Equation 17, has a solution that depends only on μ, not on specific values of b_1 and b_2. Thus, after an abrupt change from one age-independent hazard rate to another, where b_1 and b_2 are defined as the NFR of the initial fire regime and the new regime, respectively, parameter μ is defined as $b_2/b_1 = \text{NFR}_2/\text{ NFR}_1$. The time for the expected age distribution to converge to the equilibrium age distribution of the new fire regime is determined in multiples of b_2, or the number of fire rotations under the new fire regime. Therefore, starting from the equilibrium age distribution of the initial fire regime and following an abrupt change to a new, age-independent hazard rate, the number of fire rotations under the new fire regime for the expected age distribution to reach a specified degree of similarity to the new equilibrium age distribution depends only on the degree of change in the NFR, regardless of the initial NFR or the direction of change (Figure 5.4b).

Following an abrupt change in an age-independent hazard rate (exponential fire-interval distribution), with parameters b_1 and b_2 defined as the NFR of the initial and new fire regime, respectively, $y(\rho)$ may be determined satisfying the conditions in Equation 17 by

$$y(\rho) = \ln\left[\frac{2}{\rho} \left| (1/\mu)^{\mu/(\mu-1)} - (1/\mu)^{1/(\mu-1)} \right| \right]. \qquad [18]$$

Using Equation 18, following an abrupt 100% increase in the NFR ($\mu = b_2/b_1 = NFR_2/NFR_1 = 2$), it would take 1.6 fire rotations under the new fire regime for the expected age distribution to reach 90% similarity to the equilibrium age distribution of the new fire regime (Figure 5.4b). Thus, if the initial NFR was 100 years, it would require 322 years (using the relationship, $s = yb_2$) for the expected age distribution to reach 90% similarity to the new equilibrium age distribution.

Equation 18 also applies for certain scenarios using an age-dependent hazard rate. For example, if fire intervals are specified by a two-parameter Weibull distribution, the hazard rate is given by

$$h_\tau(t) = \frac{kt^{k-1}}{j^k},$$

where j is the scale parameter, measured in years, and k is the shape parameter. The scale parameter determines the fire interval that has the largest probability of occurrence, and therefore is likely to be influenced by environmental factors affecting fire ignition and spread that are regional in effect (Johnson 1979). The shape parameter determines the rate at which the probability of fire occurrence increases ($k > 1$) or decreases ($k < 1$) with stand age ($k = 1$ provides an age-independent hazard rate and an exponential fire-interval distribution). Parameter k describes variation in the shape of the distribution around the mean fire interval, probably reflecting influences of local factors that alter the frequency of fire occurrence from the regional average (Johnson 1979). Therefore, it may be reasonable to represent a change in a regional driver of the fire regime (e.g., climate) that produces a change in the NFR by changing the scale parameter (j) with the shape parameter (k) fixed.

For a given value of k, the NFR scales linearly with parameter j, which can be verified using Equation 4. Thus, starting from the equilibrium age distribution under an initial Weibull fire-interval distribution, the time to converge to the new equilibrium age distribution following a change in the NFR driven by a change only in the scale parameter (j) can be calculated using Equation 18, where b_1 and b_2 are defined as j_1 and j_2

of the initial and the new fire regime, respectively. In this case, Figure 5.4b also applies for a Weibull fire-interval distribution. However, if the change in fire frequency is driven by a change in both parameters of the Weibull distribution (e.g., Clark 1989), the NFR no longer scales linearly with parameter j. Therefore, parameters b_1 and b_2 would not scale linearly with NFR_1 and NFR_2, and Equation 18 and Figure 5.4b would not apply.

APPLICATION

Non-Stationary, Mixed-Severity Fire Regime

A stand-level model of age-cohort structure in Douglas-fir/western hemlock (*Tsuga heterophylla* (Raf.) Sarg.) forests under a mixed-severity fire regime was developed based, in part, on age-structure data collected in the central western Cascades of Oregon (chapter 2). It was developed as a simulation model with stochastic variation in fire intervals and intensity. Then, the analytical approach presented in Equations 1–5 was applied to calculate the equilibrium age distribution and the abundance of up to three stand-structure types within each of seven age classes under a stationary fire regime. The simulation model also was run under two scenarios of a non-stationary fire regime: an abrupt doubling of the NFR, and a doubling of the NFR followed by a return to the initial NFR 200 years later. For each scenario, trajectories of change in the expected age distribution were determined analytically using Equations 7a and 7b. Analytical methods also were applied to calculate the trajectory of change in the expected abundance of each stand-structure type using methods described briefly below and in more detail in Appendix C. Then the analytical results were compared to simulation values averaged across model runs. An overview of the model and the analytical methods for calculating the expected age distribution and the abundance of each stand-structure type is presented below. More detailed descriptions of the succession model and the methods for calculating trajectories of change are provided in Appendix C.

The model tracks the initiation and mortality of cohorts of Douglas-fir trees and shade-tolerant species in response to fire of three intensities. The only attributes represented for the cohorts are the species (Douglas-fir or shade-tolerant species) and age

(equivalent to the time since the fire that enabled cohort initiation, assuming cohorts are initiated immediately after fire and there is no upper bound to cohort age). Cohort age represents the maximum possible tree age within the cohort. Attributes of individual trees and changes in tree density due to fire-caused mortality or density-dependent thinning are not represented.

The input parameters are (1) the mean interval between successive fires regardless of intensity, (2) the expected proportion of fires that burn at low, moderate, and high intensity (q_1, q_2, and q_3, respectively), and (3) threshold ages beyond which Douglas-fir cohorts may survive fire of low and moderate intensity (r_1 and r_2, respectively). The overall rate of fire occurrence is assumed to be independent of the time since the previous fire and its intensity. Thus, the reciprocal of the user-supplied mean fire interval provides an age-independent hazard rate for all fire regardless of intensity, represented by λ. The intensity of each fire is assigned randomly based on the user-defined expected proportion of fires in each intensity class. Fire intensity is assumed to be driven by factors exogenous to the stand (e.g., weather) and is independent of stand conditions. However, the response of a stand to burning at a given intensity depends on cohort ages at the time of the fire, as described below.

At least one cohort of Douglas-fir trees is present at all times. Ages of Douglas-fir cohorts are represented by t_i ($i = 1,\ldots, n$). The subscript, i, is an index that sorts cohorts in the order they established since the last SR fire, and n represents the total number of Douglas-fir cohorts present. Thus, ages of the oldest and youngest Douglas-fir cohorts are represented by t_1 and t_n, respectively, where $t_n \leq t_1$. A single cohort of shade-tolerant trees is present at all times. Fire of all intensities kill this cohort, and a new cohort is assumed to be initiated immediately thereafter. Thus, the age of the cohort of shade-tolerant trees, t_0, represents the time since the last fire of any intensity.

Although the hazard rate for fire of any intensity is independent of the time since the previous fire, the hazard rate for stand-replacing (SR) fire depends on stand age, defined by the age of the oldest Douglas-fir cohort, t_1. The user-specified ages beyond

which a Douglas-fir cohort may survive fire of low and moderate intensity (r_1 and r_2, respectively) lead to a piecewise constant hazard rate for SR fire, where the annual probability of SR fire decreases each time the oldest cohort surpasses one of the thresholds (Figure 5.5). When the oldest cohort is younger than the first threshold ($t_1 \leq r_1$), fires of all intensities kill all existing cohorts, and the hazard rate for SR fire is equivalent to the overall hazard of burning: $h_\tau(t) = \lambda$. When the age of the oldest cohort is between the two thresholds ($r_1 < t_1 \leq r_2$), only moderate- or high-intensity fire removes all existing cohorts, and the hazard rate for SR fire decreases to $h_\tau(t) = (1 - q_1)\lambda$, where q_1 is the user-defined proportion of fires that burn at low intensity. After the oldest Douglas-fir cohort surpasses the second threshold ($t_1 > r_2$), only high-intensity fire kills the oldest cohort, and the hazard rate for SR fire decreases to $h_\tau(t) = q_3\lambda$, where q_3 is the user-defined proportion of fires that burn at high intensity (Figure 5.5).

Although high-intensity fire kills all existing cohorts and enables establishment of a single Douglas-fir cohort, non-stand-replacing (NSR) fire may increase the number of Douglas-fir cohorts in a stand. The number of Douglas-fir cohorts increases if fire intensity is moderate and the youngest Douglas-fir cohort is old enough to survive moderate-intensity fire ($t_n > r_2$). Moderate-intensity fire is assumed to generate canopy openings of sufficient size to enable regeneration of relatively shade-intolerant Douglas-fir, without completely removing cohorts older than the threshold age. If fire intensity is low or moderate, and the youngest Douglas-fir cohort is younger than the age required to survive low- or moderate-intensity fire ($t_n \leq r_1$ or $t_n \leq r_2$, respectively), the youngest cohort is killed and a new cohort is initiated, thereby retaining the same number of cohorts as before the fire, but erasing evidence of one of the previous cohorts. If fire intensity is low and the youngest Douglas-fir cohort is old enough to survive low-intensity fire ($t_n > r_1$), this cohort survives, but a new Douglas-fir cohort is not initiated because the fire is assumed not too have opened the canopy enough for Douglas-fir regeneration. Such a fire would kill the cohort of shade-tolerant trees regardless of its

age, and a new cohort of shade-tolerant trees would be the only cohort to establish after the fire.

Stand age, defined by the age of the oldest Douglas-fir cohort (t_1) was classified into seven classes (Table 5.1). A stand was classified into the j^{th} age class if the age of the oldest Douglas-fir cohort fell between the lower and upper age limits of the class, $R_L(j)$ and $R_U(j)$, respectively. Up to three stand-structure types were identified in each class based on ages of the youngest Douglas-fir cohort (t_n) and the cohort of shade-tolerant species (t_0), which reflect the timing and intensity of NSR fires since the last SR fire. Ages of these cohorts were compared to threshold ages, $t_n^*(j)$ and $t_0^*(j)$, for each cohort type in the j^{th} age class to determine the appropriate stand-structure type (Table 5.1).

The unburned structure type represents stand structures likely to develop in the absence of NSR fire. Stands that have experienced NSR fire early in development also may be included if the time since fire is long enough that present stand structure no longer is likely to be distinct from stands of similar age that have not experienced NSR fire. Stands in this class must have no Douglas-fir cohorts younger than the lower bound of the age class ($t_n \geq t_n^*(j) = R_L(j)$), and the cohort of shade-tolerant trees must be older than the threshold age for the class ($t_0 \geq t_0^*(j)$) (Table 5.1). These criteria can be met only in the absence of low-intensity fire for the last $t_0^*(j)$ years and moderate-intensity fire for the last $t_n^*(j)$ years.

The DF/Tol structure type represents stands with a Douglas-fir cohort over a younger cohort of shade-tolerant trees that established following low-intensity fire, which did not enable Douglas-fir regeneration. The youngest Douglas-fir cohort must be older than the lower bound of the age class ($t_n \geq t_n^*(j) = R_L(j)$), and the cohort of shade-tolerant trees must be younger than the threshold age for the age class ($t_0 < t_0^*(j)$) (Table 5.1). Thus, stands of the DF/Tol structure type must have experienced at least one low-

intensity fire within the last $t_0^*(j)$ years but no moderate-intensity fire in the last $t_n^*(j)$ years.

The DF/DF structure type refers to stands with Douglas-fir cohorts present in at least two of the age classes defined in Table 5.1. The youngest Douglas-fir cohort must be younger than the lower bound of the age class ($t_n < t_n^*(j) = R_L(j)$), indicating that the stand has experienced at least one moderate-intensity fire in the last $t_n^*(j)$ years (Table 5.1).

Under a stationary fire regime, the piecewise constant hazard rate for SR fire was entered into Equation 5 to determine the equilibrium age distribution (Appendix C). The equilibrium abundance of the stand-structure types within each age class was determined by evaluating the probability that a stand of a given age had or had not experienced low- or moderate-intensity fire over the preceding $t_n^*(j)$ or $t_0^*(j)$ years, respectively, as required to meet the criteria for each structure type (Table 5.1). The probability that a stand of age t_1 had not experienced low-intensity fire over the preceding $t_0^*(j)$ years was determined by evaluating the survivorship distribution (Equation 1) with the hazard rate for low-intensity fire, $q_1\lambda$, over stand ages ranging from $t_1 - t_0^*(j)$ to t_1. The probability that a stand has experienced at least one low-intensity fire over the preceding $t_0^*(j)$ years was determined by evaluating the mortality distribution (Equation 2) with the hazard rate for low-intensity fire over the same age range. Similar calculations were applied using the hazard rate for moderate-intensity fire, $q_2\lambda$, to determine the probability that a stand of a given age has or has not experienced at least one moderate-intensity fire over the preceding $t_n^*(j)$ years. The equilibrium abundance of each structure type was calculated by multiplying the density of each age in the j^{th} class by the probability of meeting the criteria for each structure type (e.g., no low- or moderate-intensity fire over the preceding $t_0^*(j)$ or $t_n^*(j)$ years, respectively, for the unburned type), and summing these values over all ages in the class (calculations are explained in greater detail in Appendix C).

The input parameters for the model were based on fire-history data for the Cook-Quentin study area of Morrison and Swanson (1990), within the central western Cascades of Oregon (Table 5.2). Under a stationary fire regime, the equilibrium age distribution and the equilibrium abundance of each stand-structure type determined analytically were almost identical to the proportion of model runs that a stand was classified in each age class and each stand-structure type in each year for 500 model runs that each were 4,000 years long after a 1,000-year burn-in period to override the effect of initial stand age (Figure 5.6).

The two scenarios for a non-stationary fire regime used the same input parameters as under the stationary fire regime (Table 5.2), except in the first scenario, the NFR was doubled abruptly from 95 to 190 years (corresponding to a change in the overall hazard of burning, from $\lambda_1 = 0.0105$ to $\lambda_2 = 0.0053$) in year 3,000 of a 5,000-year simulation (including a 1,000-year burn-in period). In the second non-stationary scenario, the NFR was doubled in year 3,000 of the simulation and then returned back to its initial value in year 3,200. Trajectories of change in the distribution of stand ages were determined by starting from the equilibrium age distribution of the initial fire regime and applying Equations 7a and 7b iteratively, using the piecewise constant hazard rate for SR fire described above. The expected abundance of each age class each year after the change in the fire regime was compared to the proportion of 250 model runs that the stand was classified under each age class in the respective year (fewer replicates were conducted than in the evaluation of the abundance of stand-structure types, in Figure 5.6, due to lower variability in the coarser classification of age classes). A comparison of results produced by the two modeling approaches for the first and second non-stationary scenarios is shown in Figures 5.7 and 5.8, respectively.

Trajectories of change in the expected proportion of the landscape covered by the stand-structure types within each age class under the non-stationary scenarios were determined as described for the stationary scenario. However, the time-invariant survivorship and mortality distributions (Equations 1 and 2) were replaced by the time-dependent distributions (Equation 8a for the first non-stationary scenario with a single

change in the hazard rate, and Equation 8b for the second scenario with two changes) to determine the probability that a stand of given age in year *s*, would have experienced low- or moderate-intensity fire over a preceding period that may include changes in the hazard rates for low- or moderate-intensity fire. Equations 8a and 8b provide the time-dependent survivorship distribution, $S(t, s)$, which may be applied to determine the probability that a stand has not experienced low- or moderate-intensity fire over a given period. The relationship, $F(t, s) = 1 - S(t, s)$, allows these equations to be applied to determine the probability that a stand of given age in year *s* has experienced at least one low- or moderate-intensity fire over the preceding period (see Appendix C for further explanation). The analytically-determined trajectories of change in the expected proportion of a landscape covered by each structure type of the Early and Mid Old Growth (EOG and MOG) age class are compared to the proportion of 1,000 model runs that a stand was classified in each structure type of these classes in 5.9 and 5.10 for the first and second non-stationary scenarios, respectively.

DISCUSSION

Use of Theoretical Models

The methods developed here are theoretical exercises aimed at promoting a stronger understanding of the response of forest age structure to changes in the disturbance regime. They are not intended for detailed historical reconstruction or projection of future change. Instead, the primary goal was to identify general patterns of change in the expected age distribution of a landscape that apply in relatively simple representations of non-stationary systems of fire and forest dynamics. These general patterns may serve as a baseline to aid in disentangling the effects of additional sources of variation under increasingly complex scenarios. The methods are illustrated by evaluating the response to changes in the fire regime, but they also may apply to other forest disturbances, such as harvesting (Wallin et al. 1994).

The analytically-derived expected age distribution in each year following a change in fire frequency, as determined by Equations 6 and 7, provides age-class

abundances equivalent to the proportion of simulation model runs that a stand was classified under each of seven age classes (Figures 5.7–5.10). The ability to determine trajectories of change in the expected age distribution without running a large number of simulations facilitated the identification of two general properties common to changes in forest age structure in response to an abrupt change in fire frequency. First, the expected proportion of the landscape covered by a discrete age class is likely to follow a non-monotonic trajectory of change (e.g., increase and then decrease in abundance; Figure 5.7) rather than transition directly to its equilibrium abundance under the new fire regime. Second, under an exponential fire-interval model and for some cases under a Weibull model, the time (number of fire rotations) required for the expected age distribution of a landscape to converge to the equilibrium age distribution of the new fire regime depends only on the magnitude of change in fire frequency, regardless of the initial value or the direction of change (Equation 18, Figure 5.4b).

The general properties are described below, but first a brief overview of the assumptions and limitations of the theoretical modeling exercises is provided. Finally, the numerical example is evaluated to illustrate how these theoretical exercises may be used to gain insight into potential historical changes in age structure in portions of the Douglas-fir/western hemlock region of the Pacific Northwest, where existing old-growth forests probably have developed under a changing fire regime (Weisberg and Swanson 2003).

Assumptions and Limitations

Application of the analytical methods presented here for evaluating trajectories of change in age structure under a non-stationary fire regime (Equations 6 and 7) requires the assumptions that only fire kills the existing forest and trees establish immediately thereafter, such that stand age is equivalent to time since fire, as also are required to evaluate the equilibrium age distribution under a stationary regime (Equation 5). In addition, the initial age distribution and a time-series of changes in the hazard of burning must be provided. The initial age distribution can be any known age distribution.

However, the relationship in Equation 18 describing the time for the expected age distribution to converge to the equilibrium age distribution of a new fire regime following a change in fire frequency applies only when starting from the equilibrium age distribution of the initial fire regime.

The changes in the hazard rate may range from an abrupt change in a single year, to continuous changes on a one-year timestep. These changes are assumed to represent a response to changes in one or more factors external to a stand that affect the overall rate of burning across the landscape (e.g., climate, human ignitions, or active fire suppression). However, the external factors are not modeled explicitly, and the mechanisms by which changes in them affect the fire regime (e.g., decreased snowpack and hastened spring snowmelt may lead to a longer fire season and greater area burned per year; Westerling et al. 2006) are not specified.

Accurate estimation of a historical time-series of changes in the hazard of burning from empirical data may be difficult, especially if the hazard rate varies as a function of stand age and historical time (Clark 1989). Methods for estimating such changes from time-since-fire map data under an age-independent hazard rate are addressed by Reed et al. (1998). However, it is important to recognize that exercises using a simulation model have shown that statistically significant differences in area burned per century may arise due only to stochastic variation in annual area burned (e.g., due to variation in the number of ignitions and fire size), with no underlying change in model parameters (Lertzman et al. 1998). Thus, inferred historical changes in fire frequency based on a single field study should be evaluated relative to an independent climate reconstruction or compared to other fire-history studies in the region before using the methods presented here for uses other than hypothesis exploration.

An additional assumption is that the landscape is treated as spatially homogeneous with respect to the hazard of burning. If a landscape can be divided into discrete zones, each with a different hazard rate, changes in the expected age distribution can be calculated separately for each zone. Then, the trajectory of change in the expected

age distribution of the landscape may be determined as the average of the trajectories in each zone, weighted by the proportion of the total area represented by each zone (McCarthy and Cary 2002). However, such an approach does not account for spatial interactions associated with fire spread across zones. For example, if sparsely vegetated areas function as fire breaks that protect leeward areas from fire only if fire frequency is high enough to prevent sufficient fuel to support fire spread across these areas (Taylor and Skinner 2003), susceptibility to fire in leeward areas will depend in part on recent fire frequency and forest conditions in the surrounding landscape.

The analytical modeling approach presented here does not directly account for changes in plant-species composition, either as a cause or response to changes in the fire regime. Although tree-ring and lake-sediment-based studies have identified substantial changes in fire frequency over several millennia while tree-species composition remained unchanged (Millspaugh et al. 2000, Carcaillet et al. 2001, Swetnam et al. 2009), it also is likely that the introduction of new species could alter fuel characteristics and rates of post-fire fuel accumulation, which in turn could affect fire frequency and intensity (Brooks et al. 2006). Shifts in species composition along with changes in climate or the fire regime can be represented indirectly by a change in the degree of age dependence in the hazard of burning. Otherwise, in the modeling approaches presented here, the changes in the fire regime are assumed to occur with no corresponding change in species composition.

Patterns in Age-Class Transitions

The identification of general patterns of change in forest age-class abundance under a non-stationary fire regime could be highly beneficial in estimating the historical range of variability in landscape structure or predicting changes under different climate or management scenarios. For example, given assumptions about the hazard of burning, lake-sediment data providing a record of changes in fire frequency over several millennia could be used along with Equations 6 or 7 to generate a time series of changes in age-class abundance, and thereby estimate the historical range of variability in forest age

distribution. An alternative approach that calculates the equilibrium age distribution across the range of identified fire intervals without accounting for trajectories of change in response to each change in fire frequency (e.g., Cyr et al. 2009) is likely to underestimate historical variability in age-class abundance.

The importance of evaluating trajectories of change in age class abundance is illustrated by the response of the Mid Old Growth (MOG) age class (351–650 years) in the numerical application to a doubling of the NFR (Figure 5.7). The equilibrium proportion of the landscape covered by this class under the initial NFR of 95 years (20.2%) was almost the same as that under an NFR of 190 years (20.9%). However, after doubling the NFR, the expected proportion of the landscape covered by this age class gradually increased to 34.5% over the first 350 years. Then it took just over 300 years to decrease to the equilibrium abundance under the new fire regime (Figure 5.7).

Following an abrupt change in fire frequency, the abundance of most age classes is likely to follow a non-monotonic trajectory of change similar to that of the MOG age class (Figure 5.7) rather than transitioning directly to their equilibrium abundance under the new fire regime (Figure 5.11). The reasons for non-monotonic trajectories are clarified by considering whether the stands recruited into a given age class were initiated before or after the change in fire frequency. The non-monotonic trajectories of change in age-class abundance are illustrated below under a simple scenario, where the age distribution at the time of the change in fire frequency is the equilibrium age distribution of the initial fire regime and the hazard of burning is independent of stand age (Figure 5.11). The lower and upper bounds of the j^{th} age class are represented by $R_L(j)$ and $R_U(j)$, respectively.

Starting at the time of the change in fire frequency (year s_0), and continuing for a number of years equal to the lower bound of the j^{th} age class (up to year $s_0 + R_L(j)$), all stands recruited into the j^{th} age class would have originated prior to the change in fire frequency. If fire frequency decreased in year s_0 ($\lambda_2 < \lambda_1$), all stands now would have a greater probability of aging into the next class (i.e., greater survivorship; Equation 1) than

they did under the initial fire regime. Thus, by Equation 6a, the proportion of the landscape covered by the j^{th} age class (excluding the youngest class, with $R_L(j) = 0$) is expected to increase relative to its initial abundance (Figure 5.11a). If the change in year s_0 was an increase in fire frequency ($\lambda_2 > \lambda_1$), young stands now would have a lower probability of recruitment into the j^{th} age class than under the initial fire regime. Therefore, over the interval up to year $s_0 + R_L(j)$, the proportion of the landscape covered by the j^{th} age class is expected to decrease relative to its initial abundance (Figure 5.11b), while recruitment into the class is from stands that originated prior to the increase in fire frequency.

After the number of years since the change in fire frequency (Δs) exceeds the lower bound of the j^{th} age class (after year $s_0 + R_L(j)$), recruitment into the class begins to include stands that originated after the change in fire frequency. Thus, the age class begins to include stands of age $t \leq \Delta s$, whose expected abundance is determined by Equation 6b. This equation multiplies the expected proportion of the landscape burned per year ($1/E(\tau_2) = \lambda_2$, for an age-independent hazard rate) by the probability of surviving to age $t \leq \Delta s$ under the prevailing fire regime ($S_{\tau_2}(t) = \exp(-\lambda_2 t)$, for an age-independent hazard rate). After a decrease in fire frequency ($\lambda_2 < \lambda_1$), the expected annual proportion of the landscape burned and that covered by new stands originated in a given year is less than that under the initial fire regime. Thus, by the time stands that originated after the decrease in fire frequency age into the j^{th} age class (after year $s_0 + R_L(j)$), the expected abundance of this age class begins to decrease (Figure 5.11a). After an increase in fire frequency ($\lambda_2 > \lambda_1$), the expected proportion of the landscape burned per year is greater than that under the initial fire regime. Thus, the expected proportion of the landscape covered by the j^{th} age class begins to increase after year $s_0 + R_L(j)$, when the age class begins to include stands originated after the increase in fire frequency (Figure 5.11b).

Excluding the oldest age class (with $R_U(j) = \infty$), each age class is expected to reach its new equilibrium abundance when the number of years since the change in fire

frequency (Δs) is equal to the upper bound of the class (by year $s_0 + R_U(j)$; Figure 5.11). After this time, all stands in the j^{th} age class would have originated after the change in fire frequency. Thus, under an age-independent hazard rate, the expected abundance for each age in the j^{th} age class would be determined by Equation 6b, which is equivalent to the equilibrium abundance for stands of that age in a given epoch (Equation 5).

The non-monotonic trajectories of change in age-class abundance following an abrupt change in fire frequency under an age-independent hazard of burning (Figure 5.11) may approximate trajectories of change under age-dependent hazard rates (Figure 5.7). However, the effect of the age-dependent hazard rate (i.e., the effect of the feedback of stand age on susceptibility to subsequent fire occurrence) is to extend the time required for an age class to reach its equilibrium abundance under the new fire regime. For example, using the piecewise constant hazard rate for stand-replacing fire described in the numerical application (Figure 5.5), after an abrupt decrease in fire frequency, the expected proportion of the landscape covered by each age class increased from year s_0 to year $s_0 + R_L(j)$, and then it decreased to year $s_0 + R_U(j)$ (Figure 5.7). Thereafter, it continued to decrease toward the equilibrium abundance of the new fire regime but at a more gradual rate than in preceding years. The difference from the pattern under an age-independent hazard rate is that each age class did not quite reach its new equilibrium abundance by year $s_0 + R_U(j)$, when all stands in the age class would have originated after the decrease in fire frequency. This difference arises because the expected area burned in a given year under an age-dependent hazard rate depends on the age distribution in that year (Figure 5.2). Thus, by the time all stands within a given age class originated after the change in fire frequency, the class is not necessarily at its equilibrium abundance.

Convergence to the Equilibrium Age Distribution

Although the potential for departure from theoretical equilibrium landscape structure as a function of spatial scale is reasonably well understood (Wimberly et al. 2000, Perry 2002), formal understanding of the development and persistence of non-equilibrium forest conditions as a function of changes in the disturbance regime is

limited. Under a stationary disturbance regime, landscape structure may be relatively stable over time only if disturbances are infrequent and small relative to landscape extent (Turner et al. 1993). If disturbances are infrequent and they affect a large portion of the landscape, the observed landscape structure in any year would diverge from equilibrium conditions, but the system may be stable in the sense that averaging the proportion of the landscape in each condition over time eventually would converge to a stable value. Otherwise, frequent disturbances that affect a large portion of the landscape could lead to unstable landscapes and possible shifts to alternate conditions (Turner et al. 1993). Under a non-stationary regime subject to periodic changes in disturbance frequency, there is potential for landscapes to be in perpetual disequilibrium, regardless of relationships between disturbance frequency, size, and landscape extent (Sprugel 1991). Landscape conditions at any point in time may be a collage of legacies from previous fire regimes.

The potential for development of an equilibrium forest age distribution under a non-stationary fire regime depends on a relationship between the magnitude of changes in fire frequency and the duration of intervening periods of relatively stable fire frequency. The length of such periods of stable fire frequency needed to achieve an equilibrium age distribution (scaled as the number of fire rotations under the prevailing fire regime) depends only on the magnitude of the most recent change in fire frequency (e.g., the present NFR divided by that of the preceding epoch), regardless of the initial NFR or the direction of change in fire frequency (Equation 18). This relationship applies when starting from the equilibrium age distribution of the initial fire regime under an age-independent hazard of burning or for certain cases under an age-dependent hazard rate (e.g., a change in fire frequency driven by a change only in the scale parameter of a Weibull distribution). If these conditions are met, following an abrupt 100% increase or a 50% decrease in fire frequency, an equilibrium age distribution could be expected only if there were no further changes in fire frequency for at least 1.6 fire rotations (Figure 5.4b).

The above relationships highlight that forest age distribution is likely to respond relatively quickly to an increase in disturbance frequency, but a much longer adjustment time is required following a decrease in disturbance frequency (Baker 1995). For

example, the initiation of dispersed patch forest harvesting at a rotation length shorter than the historical fire rotation, could greatly accelerate the rate that stands are lost and new stands established, and thus quickly remove much of the legacy of old-growth produced under a previous disturbance regime dominated by relatively infrequent fire. However, following a cessation of harvesting, it may take centuries to remove the legacy of stand ages and patch sizes produced by only a few decades of accelerated disturbance (Wallin et al. 1994).

Although the relationship illustrated in Equation 18 evaluates the response to a change in a single variable (the NFR under an age-independent hazard rate or the scale parameter of a Weibull distribution), the relationship may apply across a variety of scenarios that lead to such a change. For example, using a spatial simulation model, where changes in the NFR were driven by changes in the frequency of ignitions and the fire-size distribution, Baker (1995) concluded it would take from ½ to 2 fire rotations for both the stand-age distribution and the patch-size distribution to converge to the equilibrium conditions of the new regime. The analytical approach presented here supports this interpretation across a broad range of changes in fire frequency (Figure 5.4b), and it provides a simple method for direct calculation of the convergence time without having to run numerous simulations.

The conditions required for application of Equation 18 have been supported by numerous fire-history studies in boreal or subalpine landscapes with predominantly stand-replacement fire regimes and relatively long (generally ca. 50–200 years) fire rotations. For example, each study listed in Table 5.3 identified an abrupt decrease in fire frequency in the 18th or 19th century based on the age distribution of existing stands, and the authors of most studies suggested the change was likely due to climate. Given these interpretations, the age distributions of these landscapes would not have been stable over time prior to European settlement, regardless of the extent of the landscape considered. Also, even in the absence of harvesting, forest fragmentation, and changes in the fire regime driven by suppression activities or climate change, age distributions in most of

these study areas may still be adjusting to changes in the fire regime that occurred prior to European settlement (Table 5.3).

The studies in Table 5.3 illustrate the potential for forest age distribution to be in perpetual disequilibrium with the prevailing fire regime, especially following a reduction in fire frequency in regions where relatively low fire frequency leads to a long adjustment time. Five of the studies identified a third epoch with a longer NFR, beginning in the early 20th century (Masters 1990, Kipfmueller and Baker 2000, Weir et al. 2000, Bergeron et al. 2004, Van Wagner et al. 2006). To enable comparison with studies that identified only two epochs, the most recent change in fire frequency was not included in calculations of the similarity to the equilibrium age distribution of the prevailing fire regime or the time to reach 90% similarity with the new equilibrium age distribution (Table 5.3). However, the most recent change in fire frequency also may be included in these calculations even though the expected age distribution at the time of the most recent change was far from the equilibrium distribution of the second epoch. For example, Bergeron et al. (2004) concluded the NFR almost tripled after 1920, from 124 to 360 years. Without this change, the expected age distribution would have reached 90% similarity to the equilibrium age distribution of the second epoch by 1947 (Table 5.3). However, starting from the expected age distribution in 1920 and accounting for the additional reduction in fire frequency, by 2004 the expected age distribution would have reached only 31% similarity to the equilibrium distribution of the third epoch. With no further changes in the fire regime, an additional 700 years is needed to reach 90% similarity.

The ability to calculate the time for the expected age distribution to converge to the equilibrium age distribution following a change in fire frequency (Equation 18) provides limits on the timing and magnitude of historical changes in fire frequency that can be interpreted from the age distribution of existing stands. For instance, given the changes in fire frequency identified by three studies in Table 5.3 (Johnson et al. 1990, Johnson and Larsen 1991, Larsen 1997), the expected age distribution at the time of sampling nearly would have converged (95–97% similarity) to the equilibrium age

distribution of the prevailing fire regime, which may make the inferred changes questionable. For example, Johnson and Larsen (1991) suggested that after 1730 the NFR increased from 50 to 90 years, based on a map of stand ages as of 1980 (Δs = 250 years after the inferred reduction in fire frequency). The expected age calculated for 1980 (Equations 6a and 6b) reveals that only 6% of the study area (31 km^2), is expected to support stands of age $t > \Delta s$, which would have established in the first epoch and still persist. Estimation of the NFR for the first epoch based on stand ages in such a small area may be highly uncertain given stochastic variation in annual area burned and contagion in fire spread. Thus, differences in the age distribution of stands that established before and after 1730 may only reflect stochastic variation in area burned with no change in external drivers (Lertzman et al. 1998).

Recently, the data of Johnson and Larsen (1991) were re-evaluated, which resulted in a longer NFR of 145 years for the more recent epoch (Reed et al. 1998). The longer NFR would reduce the similarity to the equilibrium age distribution at the time of sampling from 97% to 87%. Also, with lower fire frequency in the more recent epoch, 18% of the study area (88 km^2), is expected to support stands of age $t > \Delta s$, which would have originated in the first epoch and survived to the time of sampling (Δs = 250 years). This area is closer to the observed area supporting stands > 250 years old in 1980 (15% of the forest area, or 75 km^2), as reported by Reed et al. (1998). Estimation of the NFR for the earlier epoch based on stand-age distribution in this larger area (compared to an expected area of 31 km^2 based on the original results), could provide greater confidence in the interpretation of an overall decrease in fire frequency in the early 1700s. The finding of similar reductions in fire frequency in several nearby study areas (Johnson et al. 1990, Masters 1990, Van Wagner et al. 2006) provide additional support for a broad-scale change in the fire regime.

Application to the Douglas-fir Region of the Pacific Northwest

The analytical approach presented here for evaluating trajectories of change in forest age distribution in response to changes in the fire regime provides insight to

historical variation in forest conditions of the Douglas-fir region of the Pacific Northwest (PNW). A synthesis of ten fire-history studies west of the crest of the Cascade Mountains in Oregon and Washington indicates the fire regime probably was not stationary during the development of existing old-growth forests (Weisberg and Swanson 2003). Two periods of region-wide, extensive fire (from the late 1400s to ca. 1650 and from ca. 1800 through the early 20th century) were identified, separated by a period of reduced fire frequency throughout much of the 17th and 18th centuries. Age-structure data collected in two large (ca. 240–300 km^2) watersheds in the central western Cascades of Oregon support this interpretation (Appendix D). Most old-growth stands established in the late 15th or 16th centuries, corresponding to the earlier period of widespread fire. The majority of these stands also had a younger post-fire cohort, dominated either by Douglas-fir or shade-tolerant species, which originated in the 19th century, corresponding to the more recent period of extensive fire (chapter 2).

Modeling fire and forest dynamics based only on mean fire intervals over the last several centuries without accounting for the likely changes in fire frequency over this period may poorly account for the present age distribution. For example, a field-based fire-history study that collected ages of more than 4,000 Douglas-fir trees in a 1,375-km^2 portion of the Oregon Coast Range found that only 8% of the trees were > 400 years old, with a maximum age of 516 years (Impara 1997). By contrast, the use of a stochastic, spatial simulation model to estimate the historical range of variability in landscape structure of the Coast Range, which was parameterized in part based on mean fire intervals found in the above study, predicted that the proportion of the Coast Range supporting forests > 450 years old would fluctuate around a mean of 27%, including an average of 11% of the area supporting forests > 800 years old (Nonaka and Spies 2005). Similarly, a fire-history study at Mount Rainier estimated an NFR of 434 years and found that only 8% of the forested area supported stands > 750 years old (Hemstrom and Franklin 1982). However, applying this NFR in an exponential fire-interval model predicts that 18% of the landscape would support stands > 750 years old (Sprugel 1991). Although several factors could contribute to these discrepancies, one possibility is that

modeling age distributions based on mean fire intervals without accounting for changes in fire frequency may provide inaccurate results.

Although too little is known about the timing and magnitude of inferred changes in the fire regime over the last several centuries in the Douglas-fir region of the PNW to reconstruct realistic historical changes in forest conditions, the changes in age-class abundance depicted in Figures 5.8 and 5.10 illustrate general patterns that may provide insight into likely changes in the region. The non-stationary scenario represented in these figures is a 50% reduction in fire frequency from an initial NFR of 95 years, which lasts for 200 years (simulation years 3,001–3,200) before returning to the initial NFR. The initial NFR was based on the fire-history study of Morrison and Swanson (1990), and the 200-year reduction in fire frequency may approximate the period of limited burning in the 17th and 18th centuries inferred from other fire-history studies throughout the region (Weisberg and Swanson 2003).

To the extent that the 200-year reduction in fire frequency in the modeled scenario (Figure 5.8) represents actual changes in the fire regime of the Douglas-fir region of the PNW, the resulting trajectories of change in age-class abundance may illustrate how the present bimodal age distribution may have developed in the central western Cascades of Oregon. Out of more than 1,000 Douglas-fir trees sampled in two watersheds, 36% had establishment dates between 1470 and 1610, and 54% established after 1780 (Appendix D), roughly corresponding to the Mid Old Growth (MOG) and Mature age classes, respectively (Table 5.1). However, only 6% of the trees established between 1610 and 1780, representing the Early Old Growth (EOG) age class. In the modeled scenario, the expected abundance of the MOG age class increased from 20 to 28% over the first 350 years (Figure 5.8). Over this interval, the expected abundance of the EOG age class increased from 19 to 27%, and then it decreased to 12% of the landscape by simulation year 3,350, when the MOG class was at its peak abundance of 28%. Thus, at this time the age distribution would have been strongly bimodal, with a peak at an age of 351 years and a prominent trough in the expected abundance of stands 151–350 years old. These trajectories also suggest that with no further changes in

disturbance regimes, the expected abundance of the MOG age class is likely to decrease from a peak of 28% to a trough of 15% by simulation year 3,650, largely through continued loss of stands in this class to fire and low recruitment into the class due to a paucity of stands in the EOG age class (Figure 5.8).

The oldest age classes showed relatively little sensitivity to a 200-year reduction in fire frequency followed by a return to the initial NFR (Figure 5.8). The proportion of the landscape supporting forests > 650 years old (Late Old Growth and Very Late Old Growth age classes; Table 5.1) was likely to exhibit only minor, gradual change in its expected coverage, because the period of reduced fire frequency was too short to enable substantial recruitment into these age classes. The relatively low sensitivity of the oldest age classes to such changes in the fire regime illustrates how the abundance of the oldest stands found in field studies may be lower than that expected based on mean fire intervals over the last several centuries without accounting for changes in the fire regime. For example, averaged over simulation years 3,001–3,400, the NFR is 143 years (corresponding to $\lambda = 0.007$). Under a stationary fire regime with this rate of burning, the expected proportion of the landscape covered by stands > 650 years old would be 9% higher than that expected based in simulation year 3,400 after accounting for the changes in fire frequency.

In addition to changes in forest age classes, a 200-year reduction in fire frequency was predicted to contribute to substantial variation in the expected abundance of different stand-structure types (Figure 5.10). For example, the initial increase in abundance of the EOG age class over the first 200 years following the reduction in fire frequency (Figure 5.8) was driven primarily by an increase in the expected abundance of the unburned stand-structure type, which increased from 5 to 13% while that of the other types remained relatively stable (Figure 5.10a). In the MOG age class, the DF/DF stand-structure type remained the most abundant structure type over the changes in fire frequency considered in this scenario (Figure 5.10b). However, the expected abundance of this type was highly variable, from a peak at 18% of the landscape in simulation year 3,350 to a trough of 11% in year 3,650.

Understanding the likely historical variability in the abundance of different stand-structure types may be highly relevant in setting management guidelines aimed at emulating effects of the historical fire regime, including non-stand-replacing (NSR) fire. However, the expected abundances of different stand-structure types in the succession model used here is sensitive to the user-defined expected proportion of fires that burn at low, moderate, and high intensity (q_1, q_2, and q_3, respectively). Due to a lack of information on changes in these parameters over time, each parameter was held at its baseline level, as interpreted for 19th-century fires in the Cook-Quentin study area of Morrison and Swanson (1990). Changes in these values over time could lead to markedly different trajectories of change in the expected abundance of each stand-structure types over time than shown in Figure 5.10. Thus, to better represent potential historical variability in the relative abundance of each stand-structure type, it may be useful to evaluate trajectories of change in the abundance of different stand-structure types across a range of values for these parameters.

Conclusions

Because theory describing long-term dynamics of forest landscapes under a non-stationary disturbance regime is limited, I developed analytical methods to evaluate the response of the age structure of a forest landscape to a change in the fire regime. By providing a means to directly calculate trajectories of change in forest age distribution in response to a change in fire frequency and excluding all stochastic sources of variation in forest age distribution, the analytical models provide a clear illustration of general patterns that may apply across a range of non-stationary scenarios. The methods are not intended to provide detailed historical reconstructions or projections of future change, but rather to identify general characteristics of the response to a change in the fire regime that may serve as a baseline for evaluating more complex scenarios with spatial interactions and feedbacks not represented in the analytical models.

There were two major findings describing changes in age structure in response to an abrupt change in fire frequency. First, when the age distribution is broken into discrete

age classes, the area covered by all but the oldest and youngest classes is likely to follow a non-monotonic trajectory of change (e.g., increase and then decrease in abundance), where inflection points can be determined based on the lower and upper bounds of each age class (Figure 5.11). Second, the time required for the expected age distribution of a landscape to reach a specified degree of similarity to the equilibrium age distribution of the new fire regime depends only on the magnitude of change in fire frequency, regardless of the initial value or the direction of change (Equation 18, Figure 5.4b). The above relationships apply to scenarios found in several fire-history studies (Table 5.3). Also, they may be useful for exploring theoretical questions, such as the time required to eliminate most of the legacy of old-growth forest after a climate- or management-driven shift to a higher rate of disturbance, or the time required to return to a level of old-growth forest similar to historical levels after a return to a lower rate of disturbance frequency (Wallin et al. 1994, Baker 1995).

The evaluation of the response of forest age structure under a non-stationary fire regime illustrates that forest conditions found at any point in time may be a collage of conditions produced under two or more fire regimes. Landscapes especially prone to retaining a legacy of previous disturbance regimes are those with relatively long fire rotations, such that the time required to reach the equilibrium conditions following a change in fire frequency may exceed the duration of periods with relatively stable fire frequency (Table 5.3). Also, in landscapes where tree longevity exceeds the fire rotation and non-stand-replacing disturbances are common, individual stands may contain legacies of several different disturbance regimes (Swetnam et al. 2009). The legacies may be represented by gaps in the age distribution or pulses of establishment that are synchronous among stands (Figures 5.7 and 5.8), or by substantial departure of the relative abundance of different stand-structure types from the equilibrium conditions of the prevailing fire regime (Figures 5.9 and 5.10). The methods presented here provide a relatively simple means for exploring hypotheses about the persistence of such legacies and other long-term changes in forest age distribution across a range of changes in the fire regime, and they may apply when considering other disturbance types.

LITERATURE CITED

Andersen, T., J. Cartensen, E. Hernández-García, and C.M. Duarte. 2008. Ecological thresholds and regime shifts: approaches to identification. *Trends Ecol. Evol.* 24: 49–57.

Baker, W.L. 1989. Effect of scale and spatial heterogeneity on fire-interval distributions. *Can. J. For. Res.* 19: 700–706.

Baker, W.L. 1995. Longterm response of disturbance landscapes to human intervention and global change. *Landscape Ecol.* 10: 143–159.

Bergeron, Y. 1991. The influence of island and mainland lakeshore landscapes on boreal forest fire regimes. *Ecology* 72: 1980–1992.

Bergeron, Y., S. Gauthier, M. Flannigan, and V. Kafka. 2004. Fire regimes at the transition between mixedwood and coniferous boreal forest in northwestern Quebec. *Ecology* 85: 1916–1932.

Boychuk, D., A.H. Perera, M.T. Ter-Mikaelian, D.L. Martell, and C. Li. 1997. Modelling the effect of spatial scale and correlated fire disturbances on forest age distribution. *Ecol. Modelling* 95: 145–164.

Brooks, M.L., C.M.D'Antonio, D.M. Richardson, J.B. Grace, J.E. Keeley, J. M. DiTomaso, R.J. Hobbs, M. Pellant, and D. Pyke. 2004. Effects of invasive alien plants on fire regime. *BioScience* 54: 677–688.

Brown, P.M. 2006. Climate effects on fire regimes and tree recruitment in Black Hills ponderosa pine forests. *Ecology* 87: 2500–2510.

Brown, P.M., and R. Wu. 2005. Climate and disturbance forcing of episodic tree recruitment in a southwestern ponderosa pine landscape. *Ecology* 86: 3030–3038.

Carcaillet, C., Y. Bergeron, P.J.H. Richard, B. Frechette, S. Gauthier, and Y.T. Prairie. 2001. Change of fire frequency in the eastern Canadian boreal forests during the Holocene: does vegetation composition or climate trigger the fire regime? *J. Ecol.* 89: 930–946.

Chapin, F.S., III., and A.M. Starfield. 1997. Time lags and novel ecosystems in response to transient climatic change in arctic Alaska. *Climatic Change.* 35: 449–461.

Clark, J.S. 1989. Ecological disturbance as a renewal process. *Oikos* 56: 17–30.

Cyr, D., S. Gauthier, Y. Bergeron, and C. Carcaillet. 2009. Forest management is driving the eastern North American boreal forest outside its natural range of variability. *Front. Ecol. Environ.* 7: 519–524.

Engelmark, O., L. Kullman, and Y. Bergeron. 1994. Fire and age structure of Scots pine and Norway spruce in northern Sweden during the past 700 years. *New Phytol.* 126: 163–168.

Grimmett, G.R., and D.R. Stirzaker. 1992. Probability and random processes. 2nd ed. Oxford University Press, Oxford.

Grissino-Mayer, H.D. 1999. Modeling fire interval data from the American Southwest with the Weibull distribution. *Int. J. Wildl. Fire* 9: 37–50.

He, H.S., D.J. Mladenoff, and E.J. Gustafson. 2002. Study of landscape change under forest harvesting and climate warming-induced fire disturbance. *For. Ecol. Manage.* 155: 257–270.

Heinselman, M.L. 1973. Fire in the virgin forests of the Boundary Waters Canoe Area, Minnesota. *Quat. Res.* 3: 329–382.

Hemstrom, M.A., and J.F. Franklin. 1982. Fire and other disturbances of the forests in Mount Rainier National Park. *Quat. Res.* 18: 32–51.

Impara, P.C. 1997. Spatial and temporal patterns of fire in the forests of the central Oregon Coast Range. Ph.D. Dissertation, Oregon State University, Corvallis.

Johnson, E.A. 1979. Fire recurrence in the subarctic and its implications for vegetation composition. *Can. J. Bot.* 57: 1374–1379.

Johnson, E.A., G.I. Fryer, and M.J. Heathcott. 1990. The influence of man and climate on frequency of fire in the Interior Wet Belt Forest, British Columbia. *J. Ecol.* 78: 403–412.

Johnson, E.A., and S.L. Gutsell. 1994. Fire frequency models, methods, and interpretations. *Adv. Ecol. Res.* 25: 239–287.

Johnson, E.A., and C.P.S. Larsen 1991. Climatically induced change in fire frequency in the southern Canadian Rockies. *Ecology* 72: 194–201.

Kipfmueller, K.F., and W.L. Baker. 2000. A fire history of a subalpine forest in south-eastern Wyoming, USA. *J. Biogeogr.* 27: 71–85.

Larsen, C.P.S. 1997. Spatial and temporal variations in boreal fire frequency in northern Alberta. *J. Biogeogr.* 24: 663–673.

Lauzon, E., D. Kneeshaw, and Y. Bergeron. 2007. Reconstruction of fire history (1680–2003) in Gaspesian mixedwood boreal forests of eastern Canada. *For. Ecol. Manage.* 244: 41–49.

Lertzman, K., J. Fall, and B. Dorner. 1998. Three kinds of heterogeneity in fire regimes: at the crossroads of fire history and landscape ecology. *Northwest Sci.* 72: 4–23.

Marlon, J.R., P.J. Bartlein, M.K. Walsh, S.P. Harrison, K.J. Brown, M.E. Edwards, P.E. Higuera, M.J. Power, R.S. Anderson, C. Brilles, A. Brunelle, C. Carcaillet, M. Daniels, F.S. Hu, M. Lavoie, C. Long, T. Minckley, P.J.H. Richard, A.C. Scott, D.S. Shafer, W. Tinner, C.E. Umbanhowar, Jr. and C. Whitlock. 2009. Wildfire responses to abrupt climate change in North America. *PNAS* 106: 2519–2524.

Masters, A.M. 1990. Changes in forest fire frequency in Kootenay National Park, Canadian Rockies. *Can. J. Bot.* 68: 1763–1767.

McCarthy, M.A., and G.J. Cary. 2002. Fire regimes in landscapes: models and realities. *In* R. Bradstock, J. Williams, and M. Gill. (eds.). *Flammable Australia: the Fire Regimes and Biodiversity of a Continent*. Cambridge University Press. Cambridge, UK. pp. 77–94.

McCarthy, M.A., A.M. Gill, and R.A. Bradstock. 2001. Theoretical fire-interval distributions. *Int. J. Wildl. Fire* 10: 73–77.

Millspaugh, S.H., C. Whitlock, and P.J. Bartlein. 2000. Variations in fire frequency and climate over the past 17,000 years in central Yellowstone Park. *Geology* 28: 211–214.

Milly, P.C.D., J. Betancourt, M. Falkenmark, R.M. Hirsch, Z.W. Kundewicz, D.P. Lettenmaier, and R.J. Stouffer. 2008. Stationarity is dead: whither water management? *Science* 319: 573–574.

Morrison, P.H., and F.J. Swanson. 1990. Fire history and pattern in a Cascade Range landscape. USDA For. Serv. Gen. Tech. Rep. PNW-254.

Nonaka, E., and T.A. Spies. 2005. Historical range of variability in landscape structure: a simulation study in Oregon, USA. *Ecol. App.* 15: 1727–1746.

Oreskes, N. 2003. The role of quantitative models in science. pp. 13–31 *In* C.D. Canham, J.J. Cole, and W.K. Lauenroth (eds.). *Models in Ecosystem Science*. Princeton University Press. Princeton, NJ.

Perry, G.L.W. 2002. Landscapes, space and equilibrium: shifting viewpoints. *Prog. Phys. Geogr.* 26: 339–359.

Reed, W.J. 1994. Estimating the probability of stand-replacing fire using the age-class distribution of undisturbed forest. *For. Sci.* 40: 104–119.

Reed, W.J., C.P.S. Larsen, E.A. Johnson, and G.M. MacDonald. 1998. Estimation of temporal variations in historical fire frequency from time-since-fire map data. *For. Sci.* 44: 465–475.

Scheffer, M., S. Carpenter, J.A. Foley, C. Folke, and B. Walker. 2001. Catastrophic shifts in ecosystems. *Nature* 413: 591–596.

Sprugel, D.G. 1991. Disturbance, equilibrium, and environmental variability: what is 'natural' vegetation in a changing environment? *Biol. Conserv.* 58: 1–18.

Swetnam, T.W., and J.L. Betancourt. 1998. Mesoscale disturbance and ecological response to decadal climatic variability in the American southwest. *J. Climate* 11: 3128–3147.

Swetnam, T.W, and P.M. Brown. In press. Climatic inferences from dendroecological reconstructions. *In* M.K. Hughes, H.F. Diaz, and T.W. Swetnam (eds.), Dendroclimatology: Progress and Prospects. Developments in Paleoenvironmental Research, Springer.

Swetnam, T.W., C.H. Baisan, A.C. Caprio, P.M. Brown, R. Touchan, R.S. Anderson, and D.J. Hallett. 2009. Multi-millennial fire history of the Giant Forest, Sequoia National Park, California, USA. *Fire Ecol.* 5: 120–150.

Taylor, A.H., and C.N. Skinner. 2003. Spatial patterns and controls on historical fire regimes and forest structure in the Klamath Mountains. *Ecol. App.* 13: 704–719.

Thompson, J.R., and T.A. Spies. 2010. Factors associated with crown damage following recurring mixed-severity wildfires and post-fire management in southwestern Oregon. *Landscape Ecol.* 25: 775–789.

Turner, M.G., and W.H. Romme. 1994. Landscape dynamics in crown fire ecosystems. *Landscape Ecol.* 9: 59–77.

Turner, M.G., W.H. Romme, R.H. Gardner, R.V. O'Neill, and T.K. Kratz. 1993. A revised concept of landscape equilibrium: disturbance and stability in scaled landscapes. *Landscape Ecol.* 8: 213–227.

Van Wagner, C.E. 1978. Age-class distribution and the forest fire cycle. *Can. J. For. Res.* 8: 220–227.

Van Wagner, C.E., M.A. Finney, and M. Heathcott. 2006. Historical fire cycles in the Canadian Rocky Mountain Parks. *For. Sci.* 52: 704–717.

Wallin, D.O., F.J. Swanson, and B. Marks. 1994. Landscape pattern response to changes in pattern generation rules: land-use legacies in forestry. *Ecol. App.* 4: 569–580.

Weir, J.M.H., E.A. Johnson, and K. Miyanishi. 2000. Fire frequency and the spatial age mosaic of the mixed-wood boreal forest in western Canada. *Ecol. App.* 10: 1162–1177.

Weisberg, P.J., and F.J. Swanson. 2003. Regional synchroneity in fire regimes of western Oregon and Washington, USA. *For. Ecol. Manage.* 172: 17–28.

Westerling, A.L., H.G. Hidalgo, D.R. Cayan, and T.W. Swetnam. 2006. Warming and earlier spring increases western U.S. forest wildfire activity. *Science* 313: 940–943.

White, A.S. 1985. Presettlement regeneration patterns in a southwestern ponderosa pine stand. *Ecology* 66: 589–594.

Whitlock, C., J. Marlon, C. Briles, A. Brunelle, C. Long, and P. Bartlein. 2008. Long-term relations among fire, fuel, and climate in the north-western US based on lake-sediment studies. *Int. J. Wildl. Fire* 17: 72–83.

Wimberly, M.C., T.A. Spies, C.J. Long, and C. Whitlock. 2000. Simulating historical variability in the amount of old forests in the Oregon Coast Range. *Conserv. Biol.* 14: 167–180.

Winter, L.E., L.B. Brubaker, J.F. Franklin, E.A. Miller, and D.Q. DeWitt. 2002. Initiation of an old-growth Douglas-fir stand in the Pacific Northwest: a reconstruction from tree-ting records. *Can. J. For. Res.* 32: 1039–1056.

Table 5.1. Age criteria for cohorts of Douglas-fir trees and shade-tolerant species used to classify a stand into one of up to three structure types within seven age classes.

Age Class Structure Type	Age range for oldest Douglas-fir cohort[a] $R_L(j) < t_1 \leq R_U(j)$	Youngest Douglas-fir cohort age relative to threshold age[b], $t_n^*(j)$	Shade-tolerant cohort age relative to threshold age[c], $t_0^*(j)$
Very Young			
Unburned	$0 < t_1 \leq 30$	$t_n = t_1$	$t_0 = t_0^* = t_1$
Young			
Unburned	$30 < t_1 \leq 80$	$t_n = t_1$	$t_0 = t_0^* = t_1$
DF/Tol	$30 < t_1 \leq 80$	$t_n = t_1$	$t_0 < t_0^* = t_1$
Mature			
Unburned	$80 < t_1 \leq 200$	$t_n = t_1$	$t_0 = t_0^* = t_1$
DF/Tol	$80 < t_1 \leq 200$	$t_n = t_1$	$t_0 < t_0^* = t_1$
DF/DF	$80 < t_1 \leq 200$	$t_n \leq t_n^*(j) = 120$	$t_0 < t_0^* = t_1$
Early Old Growth (EOG)			
Unburned	$200 < t_1 \leq 350$	$t_n > t_n^*(j) = 200$	$t_0 > t_0^* = 200$
DF/Tol	$200 < t_1 \leq 350$	$t_n > t_n^*(j) = 200$	$t_0 \leq t_0^* = 200$
DF/DF	$200 < t_1 \leq 350$	$t_n \leq t_n^*(j) = 200$	$t_0 \leq t_0^* = 200$
Mid Old Growth (MOG)			
Unburned	$350 < t_1 \leq 650$	$t_n > t_n^*(j) = 350$	$t_0 > t_0^* = 300$
DF/Tol	$350 < t_1 \leq 650$	$t_n > t_n^*(j) = 350$	$t_0 \leq t_0^* = 300$
DF/DF	$350 < t_1 \leq 650$	$t_n \leq t_n^*(j) = 350$	$t_0 \leq t_0^* = 300$
Late Old Growth (LOG)			
Unburned	$650 < t_1 \leq 1{,}000$	$t_n > t_n^*(j) = 650$	$t_0 > t_0^* = 400$
DF/Tol	$650 < t_1 \leq 1{,}000$	$t_n > t_n^*(j) = 650$	$t_0 \leq t_0^* = 400$
DF/DF	$650 < t_1 \leq 1{,}000$	$t_n \leq t_n^*(j) = 650$	$t_0 \leq t_0^* = 400$
Very Late Old Growth (VLOG)			
VLOG	$t_1 > 1{,}000$		

[a] t_1 is the age of the oldest Douglas-fir cohort. $R_L(j)$ and $R_U(j)$ are the lower and upper bounds, respectively, for the j^{th} age class.

[b] The age of the youngest Douglas-fir cohort, t_n, is compared to the threshold, $t_n^*(j)$, in order to classify stands into the appropriate structure type.

[c] The age of the cohort of shade-tolerant trees, t_0, is compared to the threshold, $t_0^*(j)$, to determine the appropriate structure type within each age class

Table 5.2. Fire-regime parameters used to calculate the equilibrium age distribution in the numerical application to Douglas-fir/ western hemlock forests of the central western Cascades of Oregon[a].

Parameter	Value	Source
NFR	95	Morrison & Swanson (1990)
q_1	0.31	Morrison & Swanson (1990)
q_2	0.42	Morrison & Swanson (1990)
q_3	0.27	Morrison & Swanson (1990)
r_1	30	Arbitrary
r_2	80	Arbitrary

[a] Morrison and Swanson (1990) estimated the percentage of fires that burn at low, moderate, and high severity based on field sampling and aerial photo interpretation. These proportions are used here as the proportion of fires that burn at low, moderate, and high intensity, represented by q_1, q_2, and q_3, respectively.

Table 5.3. Evaluation of 11 fire-history studies that identified at least 2 epochs with different fire rotations. Each study assumed an age-independent hazard rate (exponential fire-interval model), or the method used to calculate the NFR is valid only under an exponential model. Assuming the age distribution at the end of epoch 1 was the equilibrium age distribution of that epoch, for each study, the calendar year that the expected age distribution would reach 90% similarity to the equilibrium age distribution of epoch 2 was calculated using Equation 18 with $\rho = 0.1$. The expected age distribution in the year of sampling (the upper bound of epoch 2) was determined using Equations 6a and 6b. Then, the percent similarity of the expected age distribution to the equilibrium age distribution of epoch 2 was determined by Equation 11.

Location	Area (km^2)	Epoch 1	NFR 1	Epoch 2	NFR 2	Year of 90% sim	Sample Yr sim%	Reference
SE British Columbia	600	1520–1760	80	1761–1988	110	1853	97.1	Johnson et al. (1990)
SE British Columbia	1,400	1508–1788	60	1789–1928	130	2011[a]	80.9[a]	Masters (1990)
Canadian Rockies, East	8,555	1285–1760	70[b]	1761–1940	177[b]	2094[a]	76.2[a]	Van Wagner et al. (2006)
Canadian Rockies, West	1,624	1330–1840	94[b]	1841–1999	355[b]	2624	41.8	Van Wagner et al. (2006)
Southwestern Alberta	495	1600–1729	50	1730–1980	90	1861	97.3	Johnson & Larsen (1991)
Northern Alberta	44,870	1750–1859	38	1860–1989	63	1942	95.3	Larsen (1997)
Central Saskatchewan	1,563[c]	1745–1889	15	1890–1945	75	2068[a]	48.6[a]	Weir et al. (2000)
Northwestern Quebec	--	≤1870	63	1871–1988	99	1989	89.9	Bergeron (1991)[d]
Southwestern Quebec	15,000	≤1850	92	1851–1920	124	1947[a]	87.6[a]	Bergeron et al. (2004)
Southeastern Quebec	6,480	1680–1850	89	1851–2003	176	2130	79.4	Lauzon et al. (2007)
Southeastern Wyoming	32	≤1867	127	1868–1912	170	1997[a]	83.5[a]	Kipfmueller & Baker (2000)
Northern Sweden	--	≤1870	187	1871–1994	371	2463	54.5	Engelmark et al. (1994)

[a] A third epoch with a very long NFR was identified as initiating in the 20th century. Calculations assumed continuing under the fire regime of epoch 2.
[b] Averaged from Maximum Likelihood and theoretical estimates in Table 6 of Van Wagner et al. (2006).
[c] Data are for the northern region in the study of Weir et al. (2000). The southern region is not shown here.
[d] Data are only for the mainland lakeshore sites of Bergeron (1991). Islands are not included.

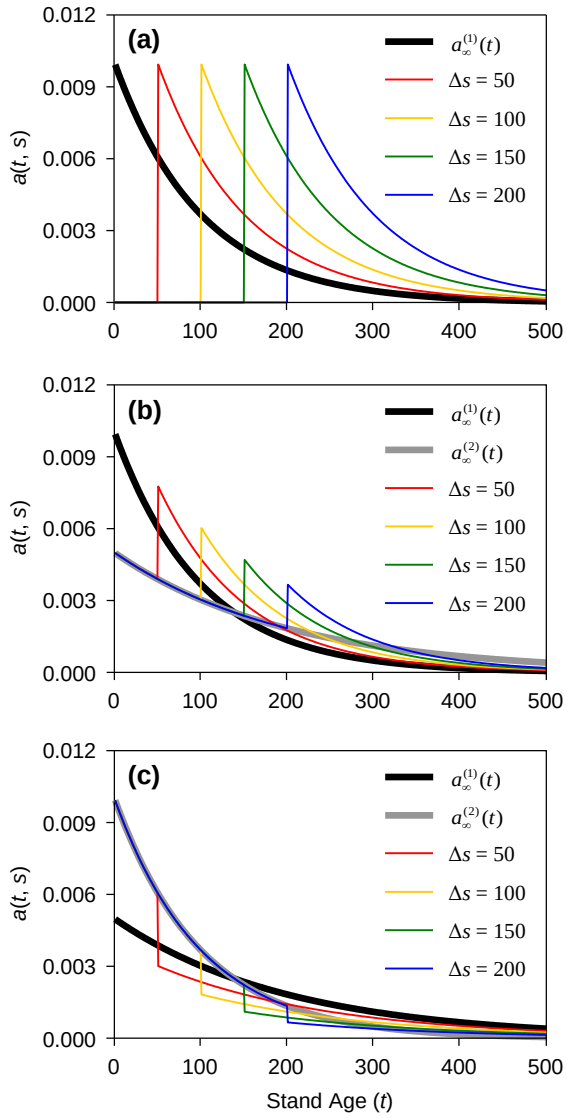

Figure 5.1. The expected age distribution of a landscape in 50-year increments following an abrupt (a) elimination of all fire, (b) decrease in fire frequency, and (c) increase in fire frequency under an age-independent hazard rate (exponential fire-interval model). The change in fire frequency was modeled by changing parameter λ from 0.01 to 0 in (a), from 0.01 to 0.005 in (b), and from 0.005 to 0.01 in (c). The equilibrium age distribution under the initial fire regime and that under the new regime are represented by $a_\infty^{(1)}(t)$ and $a_\infty^{(2)}(t)$, respectively, and Δs refers to the number of years since the change in fire frequency.

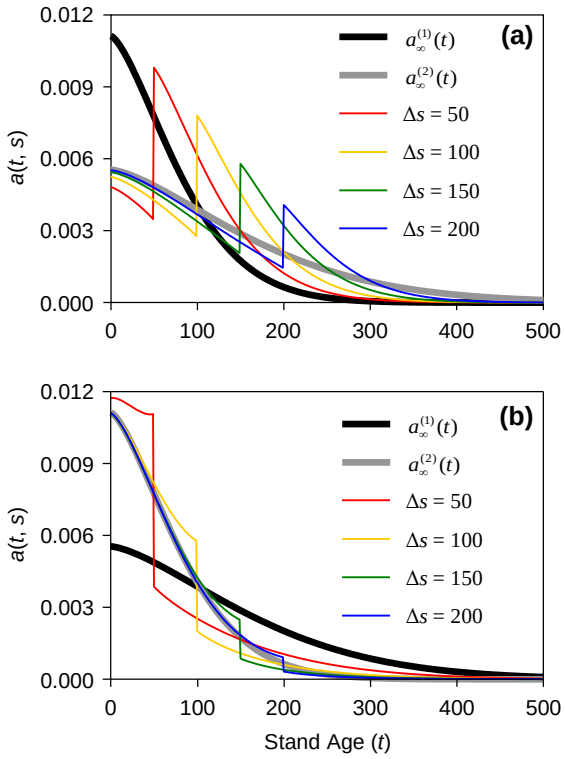

Figure 5.2. The expected age distribution of a landscape in 50-year increments following an abrupt (a) decrease, and (b) increase in fire frequency under an age-dependent hazard rate, modeled using a two-parameter Weibull distribution. The shape parameter was fixed at 1.2, and the changes in fire frequency were modeled by increasing the scale parameter to 200 from an initial value of 100 in (a), and by decreasing the scale parameter from 200 to 100 in (b). The equilibrium age distribution under the initial fire frequency and that under the new regime are represented by $a_\infty^{(1)}(t)$ and $a_\infty^{(2)}(t)$, respectively, and Δs refers to the number of years since the change in fire frequency.

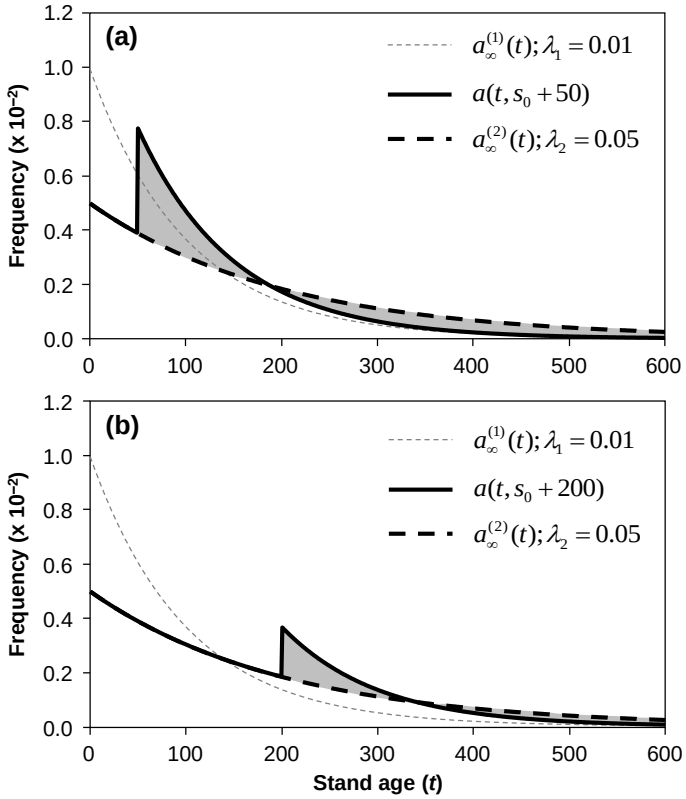

Figure 5.3. Comparison of the difference, ρ, between the expected age distribution at time (a) Δs = 50, and (b) Δs = 200 years after an abrupt doubling of the NFR from 100 to 200 years under an age-independent hazard rate (exponential fire-interval model). Equilibrium age distributions before and after the change in fire frequency are represented by $a_\infty^{(1)}(t)$ and $a_\infty^{(2)}(t)$, respectively, and the expected age distribution Δs years after the change in fire frequency is represented by $a(t, s_0 + \Delta s)$. The area of gray shading corresponds to values of ρ, calculated as 0.39 and 0.18 for (a) and (b), respectively, using Equation 11.

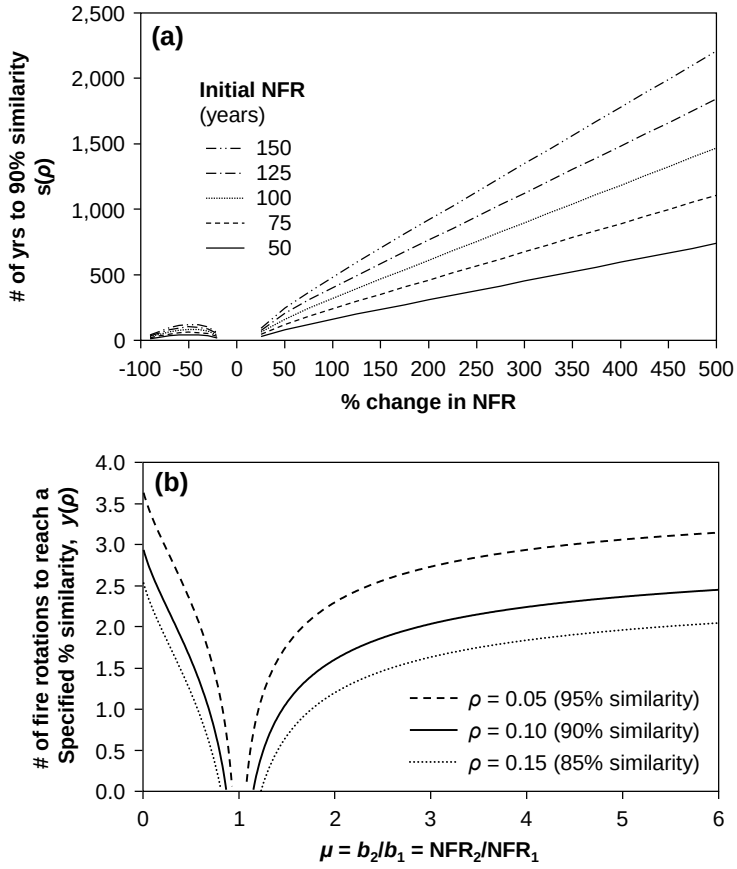

Figure 5.4. The time required for the expected age distribution to reach a specified percent similarity (% similarity = $(1 - \rho) \times 100$) to the equilibrium age distribution of a new fire regime after an abrupt change in fire frequency under an age-independent hazard rate. Values in (a) were determined using Equations 6a and 6b to calculate the expected age distribution in each year after the change in fire frequency. Then Equation 11 was applied with $\rho = 0.1$ to identify the year that similarity to the equilibrium age distribution reached 90%. In (b), values were determined using Equation 18, with three values of ρ (0.05, 0.10, and 0.15). Note that the *x*-axis in (a) corresponds to that in (b), and after converting the *y*-axis from years to the number of fire rotations, all curves in (a) collapse to the single curve for $\rho = 0.1$ in (b), as supported by Equation 18.

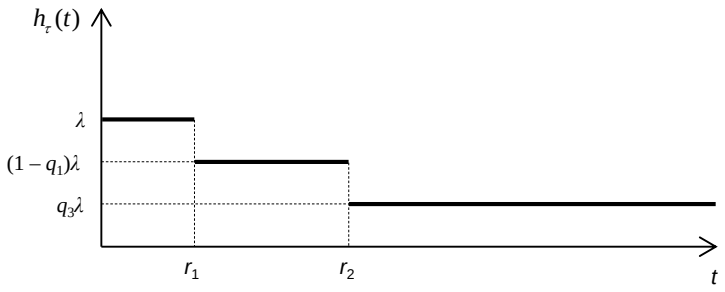

Figure 5.5. The piecewise constant hazard rate for SR fire, $h_\tau(t)$, as a function of the age of the oldest Douglas-fir cohort, t_1, as used in the numerical application to Douglas-fir/western hemlock forests of the central western Cascades of Oregon. The hazard rate for fire of any intensity is represented by λ. The user-defined expected proportion of fires that burn at low and high-intensity are given by q_1 and q_3, respectively. The variables, r_1 and r_2 are user-defined ages required for a Douglas-fir cohort to survive fires of low and moderate intensity, respectively. Values are provided in Table 5.2.

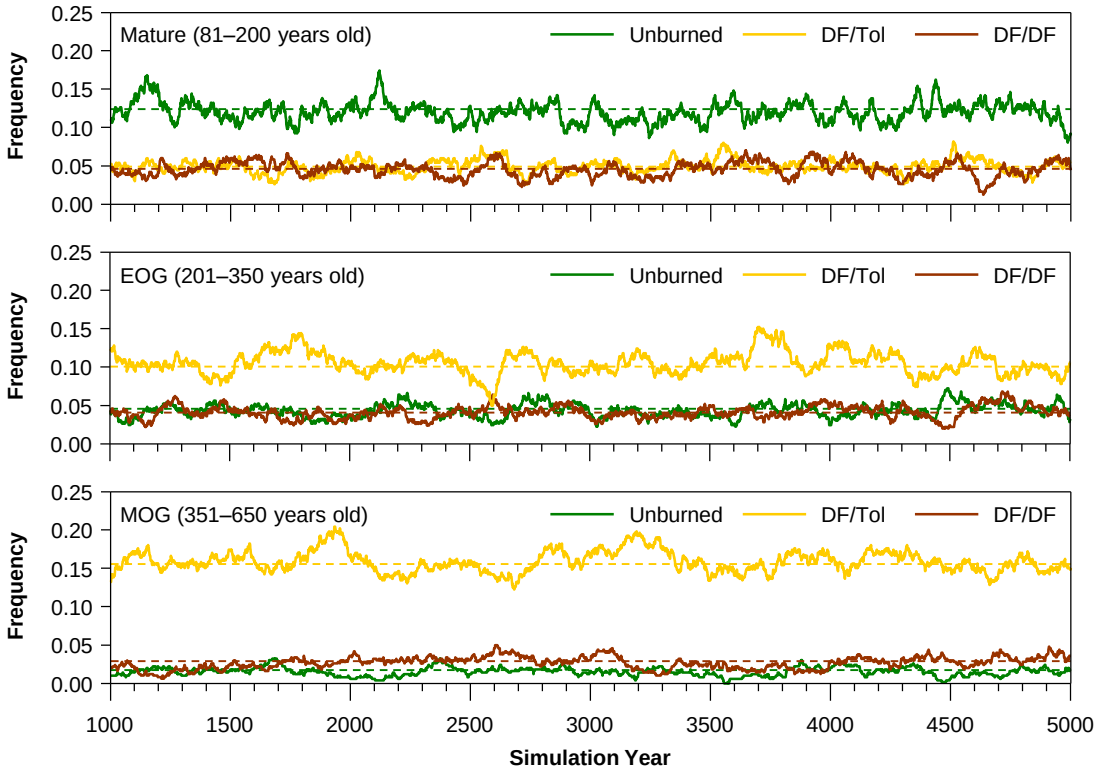

Figure 5.6. Comparison of the simulated abundance of each stand-structure type within the Mature, Early Old Growth (EOG), and Mid Old Growth (MOG) age classes (solid lines) to the analytical approximation of the equilibrium abundance of each class (dashed lines), using model parameters for the Cook-Quentin study area of Morrison and Swanson (1990) as shown in Table 5.2. The age classes and stand-structure types are defined according to Table 5.1. The *y*-axis represents the proportion of 500 model runs that the stand was classified under each stand-structure class. Other age classes are not shown.

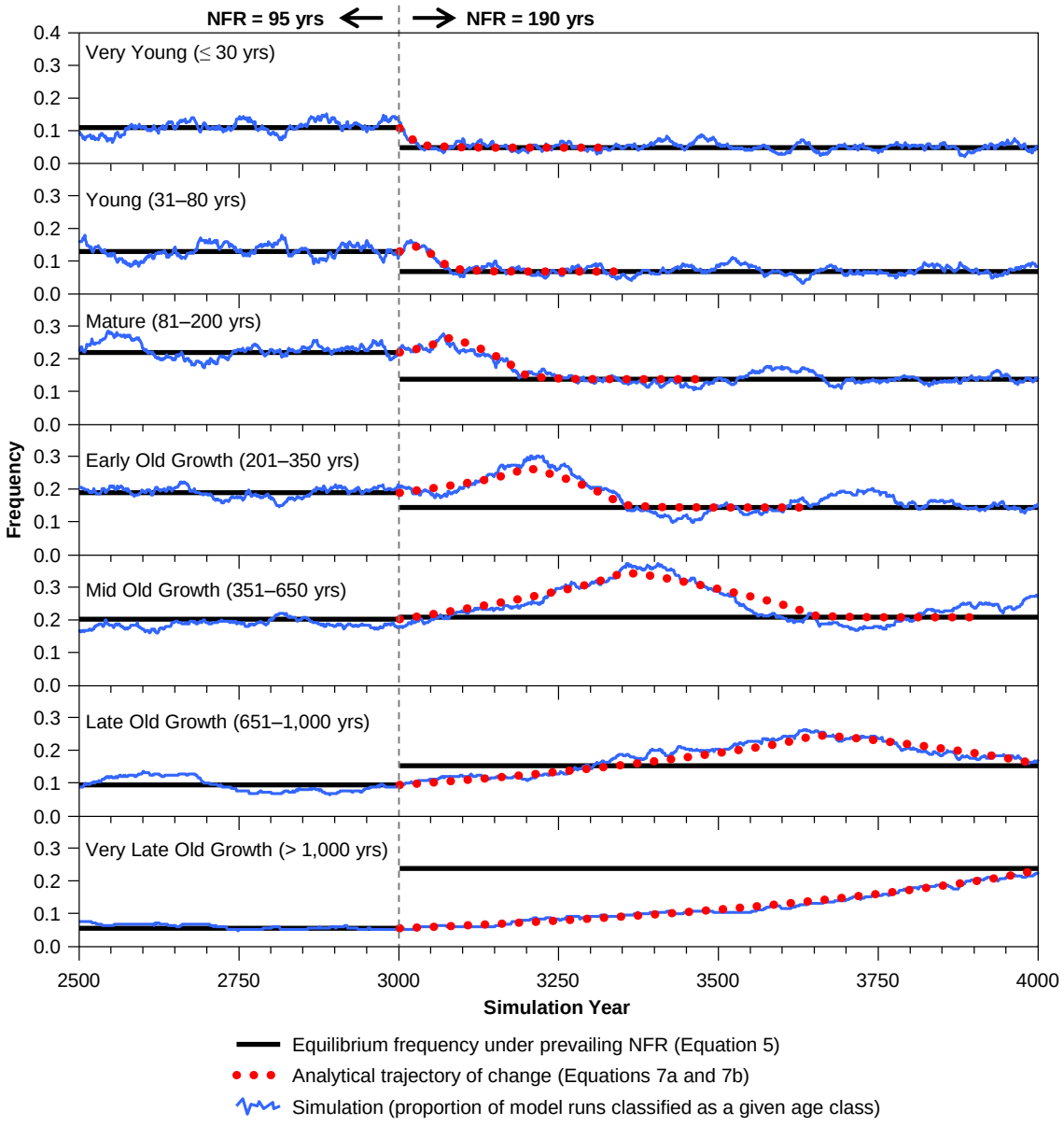

Figure 5.7. Comparison of analytically-determined trajectories of change in the expected proportion of a landscape covered by seven age classes (defined in Table 5.1), to the proportion of 250 simulation runs that a stand was classified in each class in each year following an abrupt doubling of the NFR for fire of all intensities. Trajectories were determined analytically using Equations 7a and 7b, assuming the expected age distribution in simulation year 2,999 was the equilibrium age distribution of the initial fire regime. All simulation input parameters were fixed at their baseline values (Table 5.2), except the NFR for fire of all intensities, ($1/\lambda$), which was increased from 95 to 190 years in simulation year 3,000.

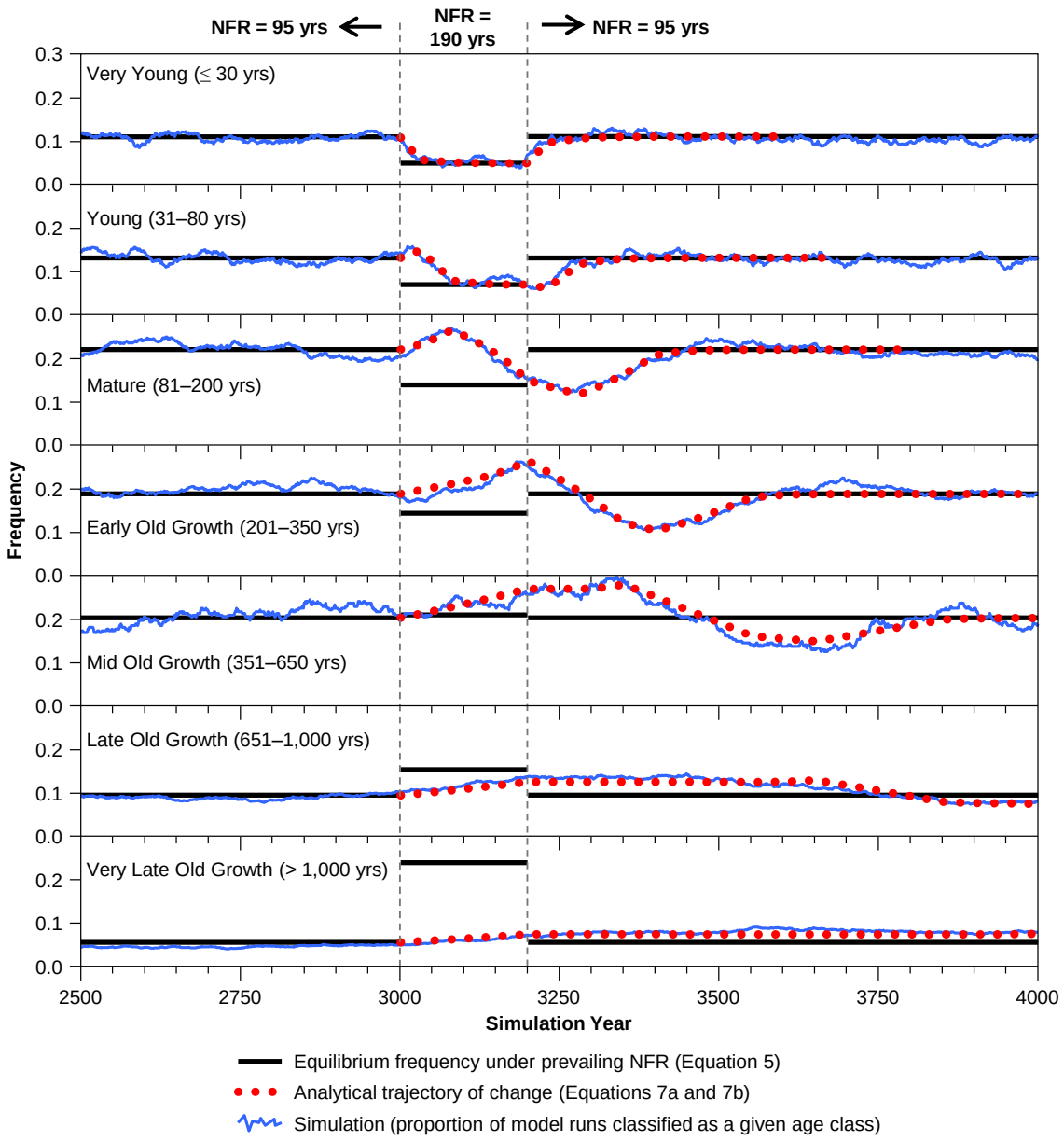

Figure 5.8. Comparison of analytically-determined trajectories of change in the expected proportion of a landscape covered by seven age classes (defined in Table 5.1), to the proportion of 250 simulation runs that a stand was classified in each class in each year after an abrupt doubling of the NFR for fire of all intensities, followed by a return to the initial NFR 200 years later. Trajectories were determined analytically using Equations 7a and 7b, assuming the expected age distribution in simulation year 2,999 was the equilibrium age distribution of the initial fire regime. Input parameters were fixed at their baseline values (Table 5.2), except the overall NFR, $1/\lambda$, which was doubled from 95 to 190 years in simulation year 3,000, and then returned to 95 years in year 3,200.

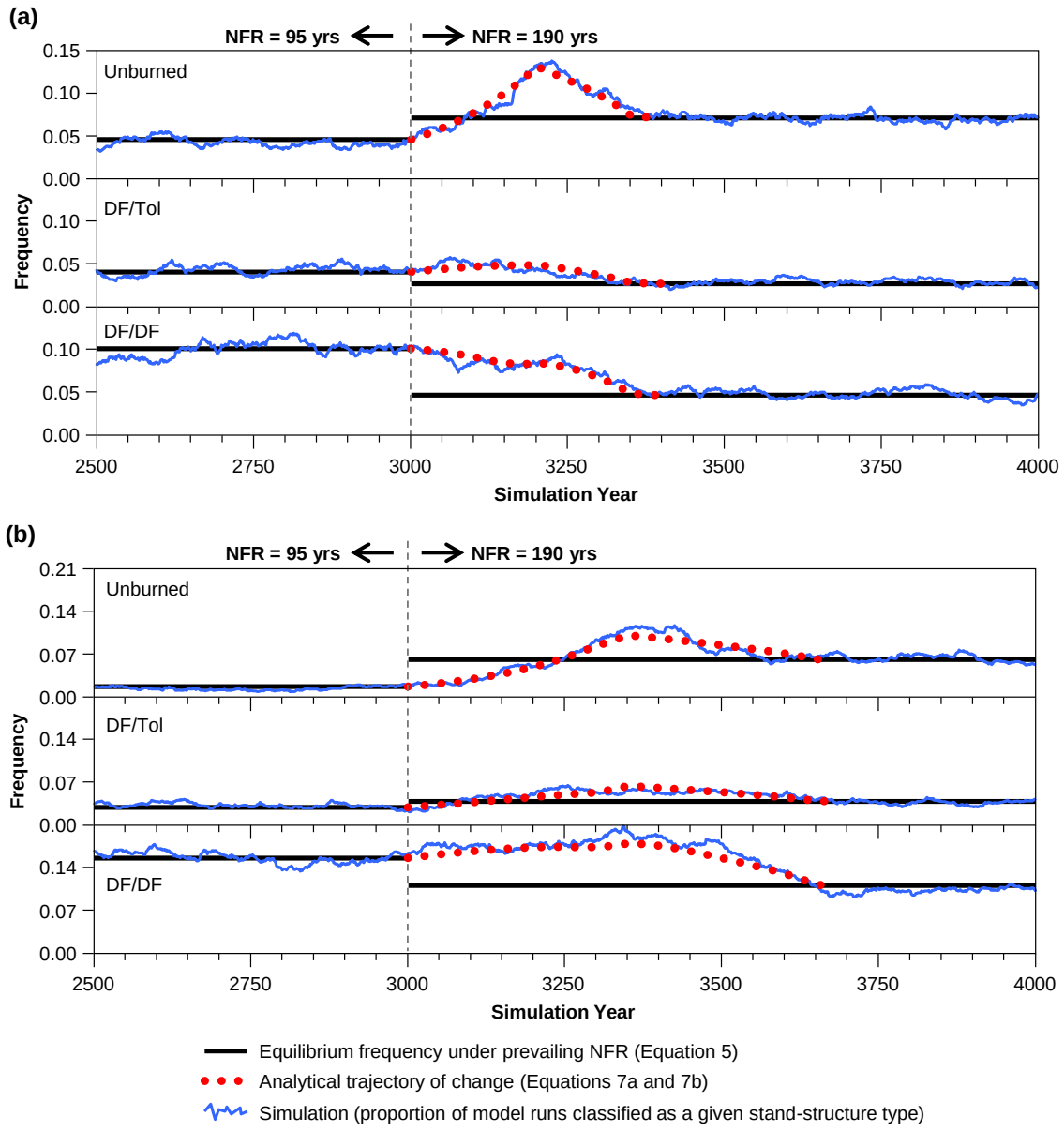

Figure 5.9. Comparison of analytically-determined trajectories of change in the expected proportion of the landscape covered by the unburned, DF/Tol, and DF/DF stand-structure types of the (a) Early Old Growth (201–350 years), and (b) Mid Old Growth (351–650 years) age classes to the proportion of 1,000 simulation runs that a stand was classified in each stand-structure type following an abrupt decrease in fire frequency (criteria defining the age classes and stand-structure types are provided in Table 5.1). Equations for analytically-determined trajectories are provided in Appendix C. In the simulation, all input parameters were fixed at the baseline values (Table 5.2), except the NFR for fire of all intensities, $1/\lambda$, which was increased from 95 to 190 years in simulation year 3,000.

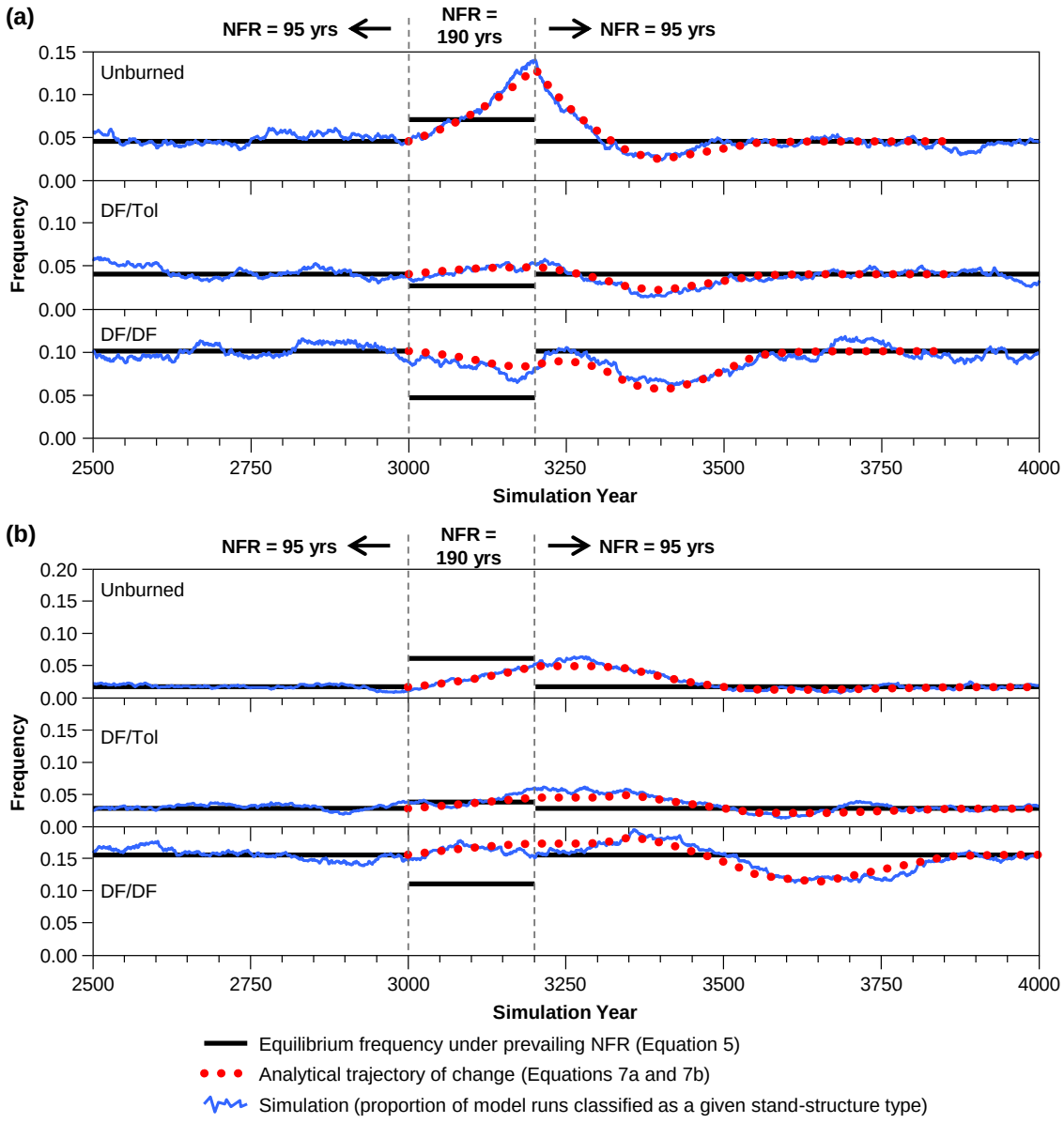

Figure 5.10. Comparison of analytically-determined trajectories of change in the expected proportion of a landscape covered by the unburned, DF/Tol, and DF/DF stand-structure types of the (a) Early Old Growth (201–350 years), and (b) Mid Old Growth (351–650 years) age classes to the proportion of 1,000 simulation runs that a stand was classified in each stand-structure type after a decrease in fire frequency, followed by a return to the initial fire frequency 200 years later (criteria defining age classes and stand-structure types are provided in Table 5.1). Equations for the analytically-determined trajectories are provided in Appendix C. All simulation input parameters were fixed at their baseline values (Table 5.2), except the overall NFR, ($1/\lambda$), which was increased from 95 to 190 years in simulation year 3,000, and returned to 95 years in year 3,200.

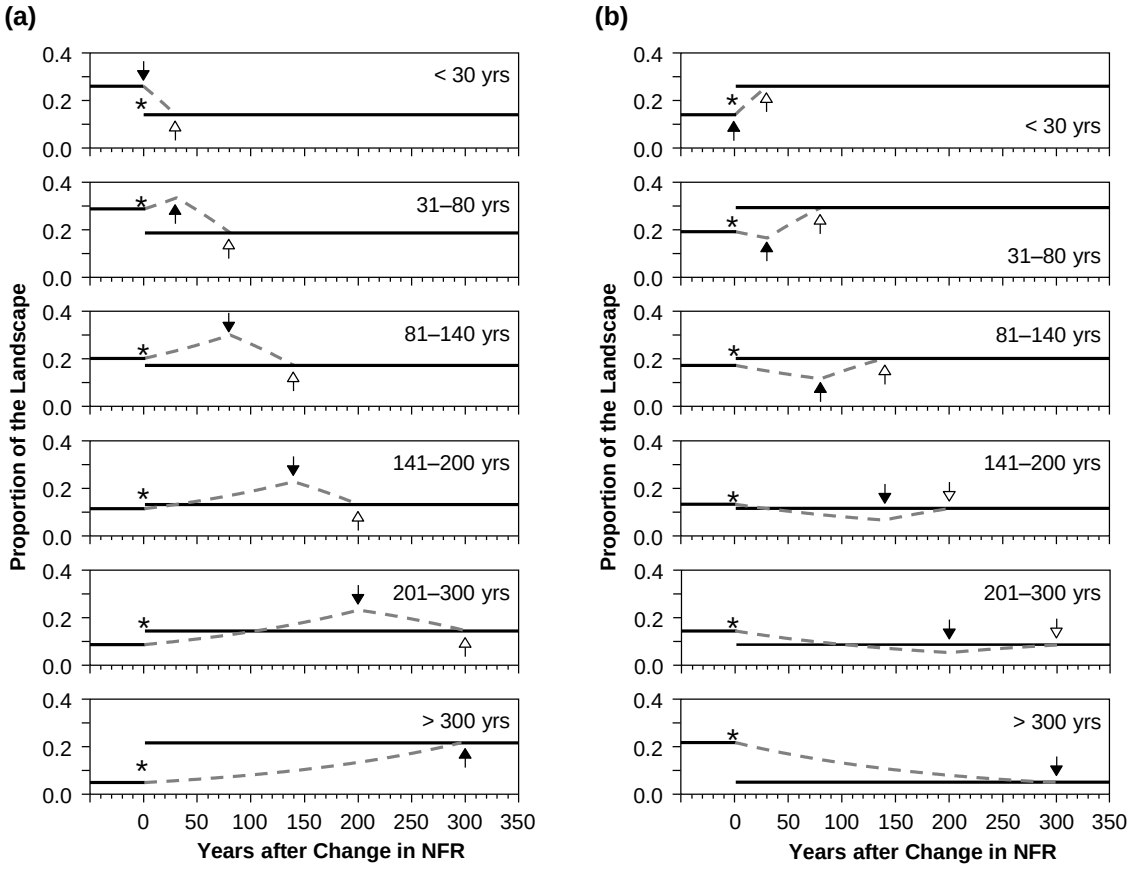

Figure 5.11. Analytically-determined trajectories of change in the expected proportion of the landscape covered by six age classes following an abrupt (a) decrease, and (b) increase in fire frequency under an age-independent hazard rate (exponential fire-interval model). Changes in fire frequency were modeled by changing parameter λ from 0.01 to 0.005 in (a), and from 0.005 to 0.01 in (b). Calculations assume the initial age distribution was the equilibrium age distribution of the initial fire regime. Solid horizontal lines represent the equilibrium abundance of each age class under the prevailing fire regime. Dashed lines represent the expected abundance of each age class, determined by Equations 6a and 6b. The year of the change in fire frequency (s_0) is indicated by an asterisk. The times that the number of years that have elapsed since the change in fire frequency are equal to the lower ($s_0 + R_L(j)$) and upper ($s_0 + R_U(j)$) bounds of each age class are indicated by arrows with black and white heads, respectively.

CHAPTER 6: CONCLUSIONS

Understanding historical disturbance regimes in forested landscapes is important for determining the range of disturbance effects and associated stand conditions that are sustainable in a particular setting. Recent fire-history research in the Douglas-fir/western hemlock region of the Pacific Northwest, demonstrates substantial variation in historical fire regimes along regional climatic gradients, with decreasing fire intervals and increasing representation of non-stand-replacing (NSR) fire toward drier parts of the region (Morrison and Swanson 1990, Weisberg 2004, Zenner 2005). The central western Cascades of Oregon has a complex fire regime, where some stands lack evidence of fire for > 400 years (Weisberg 1998), whereas other stands in close proximity show evidence of several fires over the past 400 years (Means 1982). To better understand this complex fire regime, including the diversity of developmental pathways and the influences of topography on spatial variation in fire behavior and associated stand conditions, I conducted field-based and modeling studies. Results of this research provide useful insight for managers interested in using knowledge of historical disturbance regimes as a basis for management, and they contribute to a stronger characterization of the poorly-understood, mixed-severity fire regime.

Field Component

In chapter 2, forest age-structure data, including ages of more than 3,000 trees collected in 124 stands throughout 2 study areas, each 240–300 km^2 in extent, were used to generate a conceptual model of fire-mediated pathways of stand development in Douglas-fir/western hemlock forests (Figure 2.8). Hierarchical clustering of variables describing the age distribution of shade-intolerant and shade-tolerant species produced six distinct age-structure types, each representing a different range of influences of fire on stand development (Figure 2.4). The age-structure types were organized into a conceptual model of forest developmental pathways that includes three sub-models reflecting differences in the frequency of NSR fire relative to stand-replacing (SR) fire. The model structure provides a useful framework for comparing forest stand and age structure

conditions in the present study area to that found in other portions of the Douglas-fir/western hemlock region (or at other time periods in the present study area) with different relative representation of NSR and SR fire effects.

NSR fire primarily was an episodic occurrence in the study area (Figure 2.8), where most stands have evidence of at least one NSR fire since initiation, but most old-growth stands probably experienced a fire-free period of at least 100–200 years during their development. The prominence of NSR fire is illustrated by the presence of at least two distinct age cohorts (where the youngest cohort is composed either of shade-intolerant or shade-tolerant species) in the majority (75%) of stands (Figure 2.4). Only the most fire-prone 10% of stands consistently experienced relatively short (< ca. 100 years) intervals between fires (Figure 2.8).

Shade-intolerant and shade-tolerant species both performed multiple successional roles rather than fitting neatly into traditional early- and late-seral roles. Shade-intolerant species formed even-aged stands following SR fire, or they formed up to four cohorts per stand in response to successive NSR fires. They were common in post-fire cohorts initiated beneath older trees at densities up to 2/3 the density of shade-intolerant trees found in unburned old-growth stands (Figure 2.3). When trees that predate the most recent fire were present at higher densities, the post-fire cohort was composed of shade-tolerant species. Shade-tolerant species could exhibit nearly continuous establishment in a shaded understory over centuries-long fire-free intervals (age-structure type 1; Figure 2.4a), form discrete cohorts along with shade-intolerant trees following fire that partially opened the canopy (age-structure type 4; Figure 2.4d), or form discrete cohorts composed only of shade-tolerant trees following fire that caused little mortality of upper-canopy trees (age-structure type 3; Figure 2.4c). Also, there was evidence that establishment of shade-tolerant trees either could occur along with, or lag behind that of shade-intolerant trees following SR fire, as previously described in the region (Zenner 2005).

In chapter 3, stand age structure was related to its topographic context as a means of gaining insight into the contribution of topography to spatial variation in the fire

regime and associated trends in the distribution of different types of stand structures across the landscape. Topography was found to have a moderately strong relationship with age structure overall, but relationships were strongest at both extremes of a continuum of the influences of fire frequency and severity on stand development, and relationships to topography were relatively weak in the middle of the continuum. The distinctive topographic contexts for stands that lack evidence of fire over the last 400 years (age-structure type 1) and fire-prone stands supporting at least three cohorts of shade-intolerant trees represent extremes in gradient of topographic moderation of microclimate and fuel moisture. The unburned old-growth stands were likely to be found only in the coolest microsites, including concave landforms (lower slopes, benches, and cirques) beneath ridges higher than ca. 1,200 m, which were found almost exclusively toward the eastern part of the western Cascades (Figure 3.8). Stands supporting at least three cohorts of shade-intolerant trees (age-structure type 6) were likely to be found in the warmest microsites, on relatively steep slopes with high exposure to solar radiation, and beneath ridgetops lower than ca. 1,100 m, which were most common toward the western part of the western Cascades (Figure 3.9).

This study supports a trend of decreasing fire severity toward lower slope positions and with increasing terrain concavity, as found in other studies in the Douglas-fir region of the Pacific Northwest (Impara 1997, Taylor and Skinner 1998, Keeton and Franklin 2001). However, in the present study area, the strength of this trend varied with local topographic relief and ridgetop elevation, providing a broader range of age structures and stronger fidelity of age structure to slope position and terrain shape in areas of high than low topographic relief (Figure 3.10). The increasing differentiation in age structure by terrain shape and slope position with increasing ridgetop elevation and local relief may reflect an amplification of microclimatic and fuel moisture differences among different topographic settings due to increasing importance of temperature inversions and topographic shading in steep, deeply dissected terrain (Daly et al. 2007, 2009). Because ridgetop elevation and topographic relief tend to increase from west to east across the central western Cascades, the strengthening of associations of age structure to its

topographic context with increasing topographic relief may contribute to a pattern of increasing diversity of stand and age structure and greater distinction of forest conditions among slope positions from west to east across the western Cascade Range (Figures 3.6 and 3.10).

Modeling Component

Field-based fire and forest history studies provide a snapshot of forest conditions, usually over a relatively small area (usually 1,000s to 100,000s of ha), as influenced by the specific events and contingencies operating within that area over a period usually of only 3–5 centuries. A detailed understanding of the contribution of the specific disturbance events that have acted within a local study area is highly valuable for understanding disturbance effects on forest dynamics and the factors guiding disturbance patterns, hence the distribution of local stand conditions. For the purpose of developing a regional framework guiding the range of disturbance effects and landscape conditions likely to be sustainable across a particular region, it is useful to expand the findings of local field studies to gain a stronger understanding of broader-scale landscape dynamics over a longer time period. Stochastic, spatial simulation models of fire and forest dynamics commonly are used to achieve such a broader understanding (Keane et al. 2004, Scheller and Mladenoff 2007, He 2008). The models usually represent several complex processes (e.g., fire spread and the factors contributing to fire severity), but the effects of modeling algorithms and parameter values are difficult to interpret by model output, which limits the insight that can be gained by such modeling exercises.

In chapter 4, I developed an analytical approximation of a stochastic, spatial simulation model of fire and forest dynamics (LADS; Wimberly 2002) previously applied to the Oregon Coast Range. The objective was to break the model down into a small number of equations that directly specify the effects of each input parameter and the interactions among them, and thereby strengthen the understanding of model output and uncertainty in it. Without explicitly modeling spatial processes, I was able to produce an equilibrium age distribution that was equivalent to the proportion of the landscape

covered by each age class averaged over time within model runs and across replications (Table 4.3). Also, I was able to calculate the expected abundance of different stand-structure conditions defined by the time since the last fires of high and moderate severity. The approximation demonstrates that the fire-spread algorithm had no effect on the equilibrium abundance of different age classes or stand-structure classes, and changing each parameter of the fire-size distribution individually had minimal effect (Figure 4.1). Thus, uncertainty in input parameters and the algorithms guiding fire spread and extent should not be a problem for questions related to the relative abundance of different forest conditions averaged over time or over a large area. However, such uncertainty will affect patch-size distributions, which were not produced analytically. The ability to break a spatial simulation model into relatively simple equations improves the basis for understanding model output and communicating the uncertainty associated with it. Such an approach may be applied to other spatial simulation models.

In chapter 5, I expanded upon the analytical modeling approaches of chapter 4 to develop methods to predict trajectories of change in the age structure of a landscape in response to changes in the fire regime or any other type of disturbance regime (e.g., due to factors such as climatic change or active fire suppression). Two useful properties were identified describing trajectories of change in landscape age structure, which may apply broadly to scenarios involving an abrupt change in fire frequency. First, when the age distribution is broken into discrete age classes, the area covered by all but the oldest and youngest class is likely to follow a non-monotonic trajectory (e.g., increase and then decrease in abundance) rather than transition directly to its equilibrium value under the new fire regime (Figure 5.11). Second, the time required for the expected age distribution of a landscape to reach a specified degree of similarity to the equilibrium age distribution of the new fire regime depends only on the magnitude of change in fire frequency, regardless of the initial frequency or the direction of change (Figure 5.4). These relationships apply to the findings of many field-based fire-history studies (Table 5.3), and they may be useful in addressing theoretical and practical questions, such as how long it would take after a climate- or management-driven shift to a higher frequency of

disturbances to eliminate most of the legacy of old-growth forest produced under a historical disturbance regime of lower fire frequency (Wallin et al. 1994). These relationships also help to determine the timing and magnitude of historical changes in the fire regime that still could be interpreted based on the age distribution of existing stands.

The long, gradual response of forest age structure to a change in fire frequency illustrates that forest conditions found at any point in time may be a collage of legacies remaining from past fire regimes. Landscapes particularly prone to retaining such legacies are those with relatively long fire rotations, such that the time to reach equilibrium conditions following a change in fire frequency exceeds the duration of periods with a relatively stable fire frequency (Table 5.3). Also, in landscapes where tree longevity exceeds the fire rotation and NSR disturbances are common, individual stands may retain legacies of several disturbance regimes.

The modeling approaches developed to evaluate trajectories of change in age-structure under a non-stationary fire regime were applied to gain a stronger understanding of likely changes in the relative abundance of different age classes and stand structures in the present study area over the last several centuries. A succession model that I developed to track the initiation, aging, and mortality of age cohorts of shade-intolerant and shade-tolerant species in response to fires of three intensities (Appendix C) was subjected to a non-stationary fire regime with a 200-year reduction in fire frequency followed by a return to the initial, higher fire frequency. The 200-year reduction in fire frequency was selected to represent the period of reduced burning in the region during much of the 17th and 18th centuries, as suggested by a synthesis of fire history studies (Weisberg and Swanson 2003), and by low numbers of stands that show cohort initiation during this period compared to that in the 16th or 19th centuries in the present study area (Appendix D). Modeling the trajectory of change in age structure under this scenario illustrates how the present, strongly bimodal age distribution of shade-intolerant trees may have developed (Figure 5.8), and it provides an estimate of how the representation of different stand-structure conditions may have changed over the last several centuries (Figure 5.10).

BIBLIOGRAPHY

Acker, S.A., E.K. Zenner, and W.H. Emmingham. 1998a. Structure and yield of two-aged stands on the Willamette National Forest, Oregon: implications for green tree retention. *Can. J. For. Res.* 28: 749–758.

Acker, S.A., T.E. Sabin, L.M. Ganio, and W.A. McKee. 1998b. Development of old-growth structure and timber volume growth trends in maturing Douglas-fir stands. *For. Ecol. Manage.* 104: 265–280.

Agee, J.K. 1993. *Fire Ecology of Pacific Northwest Forests*. Island Press. Washington, D.C. 493 pp.

Agee, J.K. 1997. The severe weather wildfire–too hot to handle? *Northwest Sci.* 71: 153–156.

Agee, J.K. 1998. The landscape ecology of western forest fire regimes. *Northwest Sci.* 72: 24–34.

Agee, J.K. 2005. The complex nature of mixed severity fire regimes. pp. 1–10 *in* L. Taylor, J. Zelnik, and B. Hughes (eds.). Mixed Severity Fire Regimes: Ecology and Management. Symposium Proceedings. The Association for Fire Ecology. November 17–19, 2004. Spokane, WA.

Agee, J.K., and M.H. Huff. 1980. First year ecological effects of the Hoh fire, Olympic Mountains, Washington. pp. 175–181 *in* R.E. Martin, R.L. Edmonds, D.A. Faulkner, F.B. Harrington, D.M. Fuquay, B.J. Stocks, and S. Barr (eds.). Proceedings Sixth Conference on Fire and Forest Meteorology. Seattle, WA. April 22-24, 1980.

Agee, J.K., and M.H. Huff. 1987. Fuel succession in a western hemlock/Douglas-fir forest. *Can. J. For. Res.* 17: 697–704.

Agee, J.K., and F. Krusemark. 2001. Forest fire regime of the Bull Run watershed, Oregon. *Northwest Sci.* 75: 292–306.

Allen, C.D., M. Savage, D.A. Falk, K.F. Suckling, T.W. Swetnam, T. Schulke, P.B. Stacey, P. Morgan, M. Hoffman, and J.T. Klingel. 2002. Ecological restoration of southwestern ponderosa pine ecosystems: a broad perspective. *Ecol. App.* 12: 1418–1433.

Andersen, T., J. Cartensen, E. Hernández-García, and C.M. Duarte. 2008. Ecological thresholds and regime shifts: approaches to identification. *Trends Ecol. Evol.* 24: 49–57.

Baker, W.L. 1989. Effect of scale and spatial heterogeneity on fire-interval distributions. *Can. J. For. Res.* 19: 700–706.

Baker, W.L. 1995. Longterm response of disturbance landscapes to human intervention and global change. *Landscape Ecol.* 10: 143–159.

Baker, W.L., and K.F. Kipfmueller. 2001. Spatial ecology of pre-Euro-American fires in a southern Rocky Mountain subalpine forest landscape. *Prof. Geog.* 53: 248–262.

Ballou, B. 2002. A chronology of wildland fire protection in Oregon. *In* S.A. Fitzgerald (ed.). Fire in Oregon's forests: Risks, effects, and treatment options. Oregon Forest Resources Institute. Portland, OR. pp. 67–77.

Barrett, S.W., and S.F. Arno. 1988. Increment-borer methods for determining fire history in coniferous forests. USDA For. Serv. Gen. Tech Rep. INT-244. Ogden, UT. 15 pp.

Beaty, M.R., and A.H. Taylor. 2001. Spatial and temporal variation of fire regimes in a mixed conifer forest landscape, southern Cascades, California, USA. *J. Biogeogr.* 28: 955–966.

Beers, T.W., P.E. Beers, and L.C. Wensel, 1966. Aspect transformation in site productivity research. *J. For.* 64: 691–692.

Bergeron, Y. 1991. The influence of island and mainland lakeshore landscapes on boreal forest fire regimes. *Ecology* 72: 1980–1992.

Bergeron, Y., S. Gauthier, M. Flannigan, and V. Kafka. 2004. Fire regimes at the transition between mixedwood and coniferous boreal forest in northwestern Quebec. *Ecology* 85: 1916–1932.

Bessie, W.C., and E.A. Johnson. 1995. The relative importance of fuels and weather on fire behavior in subalpine forests. *Ecology* 76: 747–762.

Black, B.A., D.C. Gillespie, S.E. MacLellan, and C.M. Hand. 2008. Establishing highly accurate production-age data using the tree-ring technique of crossdating: a case study for Pacific geoduck (*Panopea abrupta*). *Can. J. Fish. Aquat. Sci.* 65: 2572–2578.

Boychuk, D., A.H. Perera, M.T. Ter-Mikaelian, D.L. Martell, and C. Li. 1997. Modelling the effect of spatial scale and correlated fire disturbances on forest age distribution. *Ecol. Modelling* 95: 145–164.

Boyd, R. (ed.). 1999. Indians, Fire and the land in the Pacific Northwest. Oregon State University Press, Corvallis, OR.

Brooks, M.L., C.M.D'Antonio, D.M. Richardson, J.B. Grace, J.E. Keeley, J. M. DiTomaso, R.J. Hobbs, M. Pellant, and D. Pyke. 2004. Effects of invasive alien plants on fire regime. *BioScience* 54: 677–688.

Brown, P.M. 2006. Climate effects on fire regimes and tree recruitment in Black Hills ponderosa pine forests. *Ecology* 87: 2500–2510.

Brown, P.M., and R. Wu. 2005. Climate and disturbance forcing of episodic tree recruitment in a southwestern ponderosa pine landscape. *Ecology* 86: 3030–3038.

Brubaker, L.B. 1980. Spatial patterns of tree growth anomalies in the Pacific Northwest. *Ecology* 61: 798–807.

Burke, C.J. 1979. Historic fires in the central western Cascades, Oregon. M.S. Thesis. Oregon State University, Corvallis.

Camp, A.E., C. Oliver, P. Hessburg, and R. Everett. 1997. Predicting late-successional fire refugia pre-dating European settlement in the Wenatchee Mountains. *For. Ecol. Manage.* 95: 63–77.

Carcaillet, C., Y. Bergeron, P.J.H. Richard, B. Frechette, S. Gauthier, and Y.T. Prairie. 2001. Change of fire frequency in the eastern Canadian boreal forests during the Holocene: does vegetation composition or climate trigger the fire regime? *J. Ecol.* 89: 930–946.

Chapin, F.S., III., and A.M. Starfield. 1997. Time lags and novel ecosystems in response to transient climatic change in arctic Alaska. *Climatic Change.* 35: 449–461.

Cissel, J.H., F.J. Swanson, and P.J. Weisberg. 1999. Landscape management using historical fire regimes: Blue River, Oregon. *Ecol. App.* 9: 1217–1231.

Clark, J.S. 1989. Ecological disturbance as a renewal process. *Oikos* 56: 17–30.

Colette, A., F.K. Chow, and R.L. Street. 2003. A numerical study of inversion-layer breakup and the effects of topographic shading in idealized valleys. *J. Appl. Meteorol.* 42: 1255–1272.

Collins, B.M., J.D. Miller, A.E. Thode, M. Kelly, J.W. van Wagtendonk, and S.L. Stephens. 2009. Interactions among wildland fires in a long-established Sierra Nevada natural fire area. *Ecosystems* 12: 114–128.

Connell, J.H., and R.O. Slayter. 1977. Mechanisms of succession in natural communities and their role in community stability. *Amer. Natur.* 111: 1119–1144.

Coville, F. 1898. Forest growth and sheep grazing in the Cascade Mountains of Oregon. USDA Div. For. Bull. 15. Washington, DC. 54 pp.

Covington, W.W., and M.M. Moore. 1994. Southwestern ponderosa pine forest structure, changes since Euro-American settlement. *J. For.* 92: 39–47.

Cyr, D., S. Gauthier, Y. Bergeron, and C. Carcaillet. 2009. Forest management is driving the eastern North American boreal forest outside its natural range of variability. *Front. Ecol. Environ.* 7: 519–524.

Daly, C., D.R. Conklin, and M.H. Unsworth. 2009. Local atmospheric decoupling in complex topography alters climate change impacts. *Int. J. Clilmatol.* doi: 10.1002/joc.2007.

Daly, C., M. Halbeib, J.I. Smith, W.P. Gibson, M.K. Doggett, G.H. Taylor, J. Curtis, and P.P. Pasteris. 2008. Physiographically sensitive mapping of climatological temperature and precipitation across the conterminous United States. *Int. J. Climatol.* 28: 2031–2064.

Daly, C., R.P. Nielson, and D.L. Phillips. 1994. A statistical-topographic model for mapping climatological precipitation over mountainous terrain. *J. Appl. Meteorol.* 33: 140–158.

Daly, C., J.W. Smith, J.I. Smith, and R.B. McKane. 2007. High-resolution spatial modeling of daily weather elements for a catchment in the Oregon Cascade Mountains, United States. *J. Applied Meteorol. and Climatol.* 46: 1565–1586.

D'Arrigo, R., R. Villalva, and G. Wiles. 2001. Tree-ring estimates of Pacific decadal climate variability. *Climate Dynamics* 18: 219–224.

DeAngelis, D.L., and W.M. Mooij. 2003. In praise of mechanistically rich models. pp. 63–82 *In* C.D. Canham, J.J. Cole, and W.K. Lauenroth (eds.). *Models in Ecosystem Science*. Princeton University Press. Princeton, NJ.

Donato, D.C., J.B. Fontaine, J.L. Campbell, W.D. Robinson, J.B. Kauffman, and B.E. Law. 2009. Conifer regeneration in stand-replacement portions of a large mixed-severity wildfire in the Klamath-Siskiyou Mountains. *Can. J. For. Res.* 39: 823–838.

Duffy, P.A., J. Epting, J.M. Graham. T.S. Rupp, and A.D. McGuire. 2007. Analysis of Alaskan burn severity using remotely sensed data. *Int. J. Wildl. Fire* 16: 277–284.

Duncan, R.P. 1989. An evaluation of errors in tree age estimates based on increment cores in Kahikatea (*Dacrycarpus cacrydioides*). *New Zealand Nat. Sci.* 16: 31–37.

Engelmark, O., L. Kullman, and Y. Bergeron. 1994. Fire and age structure of Scots pine and Norway spruce in northern Sweden during the past 700 years. *New Phytol.* 126: 163–168.

ESRI. 2008. ArcMap version 9.3.

Fox, J. 1997. *Applied Regression, Linear Models, and Related Methods.* Sage Publications. Thousand Oaks, CA. 624 pp.

Franklin, J.F., and C.T. Dyrness. 1973. Natural vegetation of Oregon and Washington. USDA For. Serv. Gen. Tech. Rep. PNW-GTR-8. 417 pp.

Franklin, J.F., and M.A. Hemstrom 1981. Aspects of succession in the coniferous forests of the Pacific Northwest. pp. 222–229 *in* D.C. West, H.H. Shugart, and D.B. Botkin (eds.). *Forest Succession*. Springer-Verlag. New York.

Franklin, J.F., A. McKee, F.J. Swanson, J. Means, and A. Brown. 1979. Age structure analyses of old-growth Douglas-fir stands: data versus conventional wisdom. *Bull. Ecol. Soc. Am.* 60: 102.

Franklin, J.F., T.A. Spies, R. Van Pelt, A.B. Carey, D.A. Thornburgh, D.R. Berg, D.B. Lindenmayer, M.E. Harmon, W.S. Keeton, D.C. Shaw, K. Bible, and J. Chen. 2002. Disturbances and structural development of natural forest ecosystems with silvicultural implications, using Douglas-fir forests as an example. *For. Ecol. Manage.* 155: 399–423.

Franklin, J F., and R.H. Waring. 1980. Distinctive features of the northwestern coniferous forest: Development, structure, and function. *In* Forests: Fresh perspectives from ecosystem analysis. R. H. Waring, ed. Proc. 40th Annu. Biol. Colloq. 1979: 59-86. Oreg. State Univ. Press, Corvallis.

Garza, E.S. 1995. Fire history and fire regimes of East Humbug and Scorpion Creeks and their relation to the range of *Pinus lambertiana* Dougl. M.S. Thesis. Oregon State University. Corvallis.

Gedalof, Z., N.J. Mantua, and D.L. Peterson. 2002. A multi-century perspective of variability in the Pacific Decadal Oscillation: new insights from tree rings and coral. *Geophys. Res. Lett.* 29: 2204. doi:10.1029/2002GL015824, 2002.

Gedalof, Z., D.L. Peterson, and N.J. Mantua. 2005. Atmospheric, climatic, and ecological controls on extreme wildfire years in the northwestern United States. *Ecol. App.* 15: 154–174.

Giglia, S.K. 2004. Spatial and temporal patterns of "super-old" Douglas-fir trees of the central western Cascades, Oregon. M.S. Thesis. Oregon State University. Corvallis.

Goslin, M.N. 1997. Development of two coniferous stands impacted by multiple, partial fires in the Oregon Cascades: establishment history and the spatial patterns of colonizing tree species relative to old-growth remnant trees. M.S. Thesis. Oregon State University. Corvallis.

Gray, A.N., and J.F. Franklin. 1997. Effects of multiple fires on the structure of southwestern Washington forests. *Northwest Sci.* 71: 174–185.

Gray, S.T., L.J. Graumlich, J.L. Betancourt, and S.T. Pederson. 2004. A tree-ring based reconstruction of the Atlantic Multidecadal Oscillation since 1567 A.D. *Geophys. Res. Lett.* 31: L12205.

Grimmett, G.R., and D.R. Stirzaker. 1992. Probability and random processes. 2nd ed. Oxford University Press, Oxford.

Grissino-Mayer, H.D. 1999. Modeling fire interval data from the American Southwest with the Weibull distribution. *Int. J. Wildl. Fire* 9: 37–50.

Grissino-Mayer, H.D. 2001. FHX2–Software for analyzing temporal and spatial patterns in fire regimes from tree rings. *Tree-Ring Res.* 57: 113–122.

Gustavsson, T., M. Karlsson, J. Bogren, and S. Lindqvist. 1998. Development of temperature patterns during clear nights. *J. Appl. Meteorol.* 37: 559–571.

Hallett, D.J., and R.S. Anderson. 2010. Paleofire reconstruction for high-elevation forests in the Sierra Nevada, California, with implications for wildfire synchrony and climate variability in the late Holocene. *Quat. Res.* 73: 180–190.

Hayes, G.L. 1941. Influences of altitude and aspect on daily variations in factors of forest fire danger. USDA Circular 591. 38 pp.

He, H.S. 2008. Forest landscape models: definitions, characterization, and classification. *For. Ecol. Manage.* 254: 484–498.

He, H.S., D.J. Mladenoff, and E.J. Gustafson. 2002. Study of landscape change under forest harvesting and climate warming-induced fire disturbance. *For. Ecol. Manage.* 155: 257–270.

Heinselman, M.L. 1973. Fire in the virgin forests of the Boundary Waters Canoe Area, Minnesota. *Quat. Res.* 3: 329–382.

Hemstrom, M.A. 1979. A recent disturbance history of forest ecosystems at Mount Rainier National Park. Ph.D. Dissertation. University of Washington, Seattle.

Hemstrom, M.A., and J.F. Franklin. 1982. Fire and other disturbances of the forests in Mount Rainier National Park. *Quat. Res.* 18: 32–51.

Henderson, J.A., D.H. Peter, R.D. Lesher, and D.R. Shaw. 1989. Forested Plant Associations of the Olympic National Forest. USDA Forest Service Technical Paper R6 ECOL 001-88, Portland, OR, 502 pp.

Hessburg, P.F., R.B. Salter, and K.M. James. 2007. Re-examining fire severity relations in pre-management era mixed conifer forests: inferences from landscape patterns of forests structure. *Landscape Ecol.* 22: 5–24.

Hessl, A., D. McKenzie, and R. Schellhaas. 2004. Drought and Pacific Decadal Oscillation linked to fire occurrence in the inland Pacific Northwest. *Ecol. App.* 14: 425–442.

Heyerdahl, E.K., D. McKenzie, L.D. Daniels, A.E. Hessl, J.S. Littell, and N.J. Mantua. 2008. Climate drivers of regionally synchronous fires in the inland Northwest. *Int. J. Wildl. Fire* 17: 40–49.

Hofmann, J.V. 1924. Natural regeneration of Douglas-fir in the Pacific Northwest. USDA Bulletin 1200.

Huff, M.A. 1995. Forest age structure and development following wildfires in the western Olympic Mountains, Washington. *Ecol. App.* 5: 471–483.

Impara, P.C. 1997. Spatial and temporal patterns of fire in the forests of the central Oregon Coast Range. Ph.D. Dissertation. Oregon State University, Corvallis.

Iniguez, J.M., T.W. Swetnam, and S.R. Yool. 2008. Topography affected landscape fire history patterns in southern Arizona, USA. *For. Ecol. Manage.* 256: 295–303.

Isaac, L.A. 1940. Vegetative succession following logging in the Douglas-fir region with special reference to fire. *J. For.* 38: 716–721.

Isaac, L.A. 1943. Reproductive habits of Douglas-fir. Charles Lathrop Pack Forestry Foundation, Washington, DC.

Isaac, L.A., and G.S. Meagher. 1936. Natural reproduction on the Tillamook Burn two years after the fire. Pacific Northwest Experimental Station. USDA Forest Service, Portland, OR.

Ives, A.R., M.G. Turner, and S.M. Pearson. 1998. Local explanations of landscape patterns: can analytical approaches approximate simulation models of spatial processes? *Ecosystems* 1: 35–51.

Johnson, E.A. 1979. Fire recurrence in the subarctic and its implications for vegetation composition. *Can. J. Bot.* 57: 1374–1379.

Johnson, E.A., G.I. Fryer, and M.J. Heathcott. 1990. The influence of man and climate on frequency of fire in the Interior Wet Belt Forest, British Columbia. *J. Ecol.* 78: 403–412.

Johnson, E.A., and S.L. Gutsell. 1994. Fire frequency models, methods, and interpretations. *Adv. Ecol. Res.* 25: 239–287.

Johnson, E.A., and C.P.S. Larsen. 1991. Climatically induced change in fire frequency in the southern Canadian Rockies. *Ecol*ogy 72: 194–201.

Kashian, D.M., M.G. Turner, W.H. Romme, and C.G. Lorimer. 2005. Variability and convergence in stand structural development on a fire-dominated subalpine landscape. *Ecology* 86: 643–654.

Keane, R.E., G.J. Cary, I.D. Davies, M.D. Falnnigan, R.H. Gardner, S. Lavorel, J.M. Lenihan, C. Li, and T.S. Rupp. 2004. A classification of landscape fire succession models: spatial simulations of fire and vegetation dynamics. *Ecol. Modelling* 179: 3–27.

Keeley, J.E. 2009. Fire intensity, fire severity and burn severity: a brief review and suggested usage. *Int. J. Wildl. Fire* 18: 116–126.

Keeton, W.S., and J.F. Franklin. 2004. Fire-related landform associations of remnant old-growth trees in the southern Washington Cascade Range. *Can. J. For. Res.* 34: 2371–2381.

Keeton, W.S., and J.F. Franklin. 2005. Do remnant old-growth trees accelerate rates of succession in mature Douglas-fir forests? *Ecol. Monogr.* 75: 103–118.

Keeton, W.S., P.W. Mote, and J.F. Franklin. 2007. Climate variability, climate change, and western wildfire with implications for the urban–wildland interface. *In* A. Troy, and R. Kennedy (eds.) Living on the edge: Economic, institutional and management perspectives on wildfire hazard in the urban interface. Advances in the Economics of Environmental Resources, vol 6. Elsevier Sciences, New York, NY. pp. 223–255.

Kipfmueller, K.F., and W.L. Baker. 2000. A fire history of a subalpine forest in south-eastern Wyoming, USA. *J. Biogeogr.* 27: 71–85.

Kruskal, J.B. 1964. Multidimensional scaling by optimizing goodness of fit to a nonmetric hypothesis. *Psychometrika* 29: 1–27.

Kushla, J.D., and W.J. Ripple. 1997. The role of terrain in a fire mosaic of a temperate coniferous forest. *For. Ecol. Manage.* 95: 97–107.

Larsen, C.P.S. 1997. Spatial and temporal variations in boreal fire frequency in northern Alberta. *J. Biogeogr.* 24: 663–673.

Larson, A.J., and J.F. Franklin. 2005. Patterns of conifer tree regeneration following an autumn wildfire event in the western Oregon Cascade Range, USA. *For. Ecol. Manage.* 218: 25–36.

Larson, A.J., J.A. Lutz, R.F. Gersonde, J.F. Franklin, and F.F. Hietpas. 2008. Potential site productivity influences the rate of forest structural development. *Ecol. App.* 18: 899–910.

Lauzon, E., D. Kneeshaw, and Y. Bergeron. 2007. Reconstruction of fire history (1680–2003) in Gaspesian mixedwood boreal forests of eastern Canada. *For. Ecol. Manage.* 244: 41–49.

Lertzman, K., J. Fall, and B. Dorner. 1998. Three kinds of heterogeneity in fire regimes: at the crossroads of fire history and landscape ecology. *Northwest Sci.* 72: 4–23.

Littell, J.S., D. McKenzie, D.L. Peterson, and A.L. Westerling. 2009. Climate and wildfire area burned in western U.S. ecoprovinces, 1916–2003. *Ecol. App.* 19: 1003–1021.

Littell, J.S., D.L. Peterson, and M. Tjoelker. 2008. Douglas-fir growth in mountain ecosystems: water limits tree growth from stand to region. *Ecol. Monogr.* 78: 349–368.

Long, C.J., C. Whitlock, P.J. Bartlein, and S.H. Millspaugh. 1998. A 9,000-year fire history from the Oregon Coast Range, based on a high-resolution charcoal study. *Can. J. For. Res.* 28: 774–787.

Long, J.N. 1977. Trends in plant species diversity associated with development in a series of *Pseutotsuga menziesii/Gaultheria shallon* stands. *Northwest Sci.* 51: 119–130.

Lundquist, J.D, N. Pepin, and C. Rochford. 2008. Automated algorithm for mapping regions of cold-air pooling in complex terrain. *J. Geophys. Res.* 113: D22107.

MacDonald, G.W., and R.A. Case. 2005. Variations in the Pacific Decadal Oscillation over the past millennium. Geophys. Res. Lett. 32:L08703. doi 10.1029/2005GL022478.

Mackey, H. 1974. *The Kalapuyans: A Sourcebook on the Indians of the Willamette Valley*. Mission Hill Museum Association. Salem, OR.

Marlon, J.R., P.J. Bartlein, M.K. Walsh, S.P. Harrison, K.J. Brown, M.E. Edwards, P.E. Higuera, M.J. Power, R.S. Anderson, C. Brilles, A. Brunelle, C. Carcaillet, M. Daniels, F.S. Hu, M. Lavoie, C. Long, T. Minckley, P.J.H. Richard, A.C. Scott, D.S. Shafer, W. Tinner, C.E. Umbanhowar, Jr. and C. Whitlock. 2009. Wildfire responses to abrupt climate change in North America. *PNAS* 106: 2519–2524.

Masters, A.M. 1990. Changes in forest fire frequency in Kootenay National Park, Canadian Rockies. *Can. J. Bot.* 68: 1763–1767.

McCarthy, M.A., and G.J. Cary. 2002. Fire regimes in landscapes: models and realities. *In* R. Bradstock, J. Williams, and M. Gill. (eds.). *Flammable Australia: the Fire Regimes and Biodiversity of a Continent*. Cambridge University Press. Cambridge, UK. pp. 77–94.

McCarthy, M.A., A.M. Gill, and R.A. Bradstock. 2001. Theoretical fire-interval distributions. *Int. J. Wildl. Fire* 10: 73–77.

McCune. B. 2006. Non-parametric habitat models with automatic interactions. *J. Veg. Sci.* 17: 819–830.

McCune, B., and J.B. Grace. 2002. Analysis of Ecological Communities. MjM Software Design. Gleneden Beach, OR.

McCune, B., and M.J. Mefford. 2006. PC-ORD. Multivariate Analysis of Ecological Data. Version 5.04. MjM Software. Gleneden Beach, Oregon.

McCune, B. and M. J. Mefford. 2008. HyperNiche. Nonparametric Multiplicative Habitat Modeling. Version 2.54 beta. MjM Software, Gleneden Beach, Oregon, U.S.A.

Means, J.E. 1982. Developmental history of dry coniferous forests in the central western Cascade Range of Oregon. pp. 142–158 *in* J.E. Means (ed.), Forest Succession and Stand Development Research in the Northwest. Forest Research Laboratory, Oregon State University, Corvallis, Oregon, USA.

Meyn, A., P.S. White, C. Buhk, and A. Jentsch. 2007. Environmental drivers of large, infrequent wildfires: the emerging conceptual model. *Prog. Phys. Geogr.* 31: 287–312.

Millspaugh, S.H., C. Whitlock, and P.J. Bartlein. 2000. Variations in fire frequency and climate over the past 17,000 years in central Yellowstone Park. *Geology* 28: 211–214.

Milly, P.C.D., J. Betancourt, M. Falkenmark, R.M. Hirsch, Z.W. Kundewicz, D.P. Lettenmaier, and R.J. Stouffer. 2008. Stationarity is dead: whither water management? *Science* 319: 573–574.

Minor, R. and A.F. Pecor. 1977. Cultural resource overview of the Willamette National Forest. University of Oregon, Anthropological Paper No. 12.

Morris, W.G. 1934. Forest fires in western Oregon and western Washington. *Oregon Historical Quarterly*. 35: 313–339.

Morrison, P.H., and F.J. Swanson. 1990. Fire history and pattern in a Cascade Range landscape. USDA For. Serv. Gen. Tech. Rep. PNW-254.

Munger, T.T. 1930. Ecological aspects of the transition from old forests to new. *Science* 72: 327–332.

Munger, T.T. 1940. The cycle from Douglas-fir to hemlock. *Ecology* 21: 451–459.

Munzel, U., and L.A. Hothorn. 2001. A unified approach to simultaneous rank test procedures in the unbalanced one-way layout. *Biometrical J.* 43: 553–569.

Nonaka, E., and T.A. Spies. 2005. Historical range of variability in landscape structure: a simulation study in Oregon, USA. *Ecol. App.* 15: 1727–1746.

Noss, R.F., J.F. Franklin, W.L. Baker, T. Schoennagel, and P.B. Moyle. 2006. Managing fire-prone forests in the western United States. *Front. Ecol. Environ.* 4: 481–487.

Oliver, C.D. 1981. Forest development in North America following major disturbances. *For. Ecol. Manage.* 3: 153–168.

Oreskes, N. 2003. The role of quantitative models in science. pp. 13–31 *In* C.D. Canham, J.J. Cole, and W.K. Lauenroth (eds.). *Models in Ecosystem Science*. Princeton University Press. Princeton, NJ.

Packee, E.C. 1990. *Tsuga heterophylla* (Raf.) Sarg. Western Hemlock. *In*: Burns, R.M., and B.H. Honkala (tech. eds.), Silvics of North America: 1. Conifers. Agriculture Handbook, vol. 654. USDA For. Serv. Washington, DC. pp. 613–622.

Peet, R.K., and N.L. Christensen, 1987. Competition and tree death. *BioScience* 37: 586–594.

Perry, G.L.W. 2002. Landscapes, space and equilibrium: shifting viewpoints. *Prog. Phys. Geogr.* 26: 339–359.

Peterson, D.W., and D.L. Peterson. 2001. Mountain hemlock growth response to climatic variability at annual and decadal time scales. *Ecology* 82: 3330–3345.

Pielke, R.A. Jr. 2003. The role of models in prediction for decision. pp. 111–138 *In* C.D. Canham, J.J. Cole, and W.K. Lauenroth (eds.). *Models in Ecosystem Science*. Princeton University Press. Princeton, NJ.

Pierce, K.B. Jr., T. Lookingbill, and D. Urban. 2005. A simple method for estimating potential relative radiation (PRR) for landscape-scale vegetation analysis. *Landscape Ecol.* 20: 137–147.

Poage, N.J., and J.C. Tappeiner, III. 2002. Long-term patterns of diameter and basal area growth of old-growth Douglas-fir trees in western Oregon. *Can. J. For. Res.* 32: 1232–1243.

Poage, N.J., W.J. Weisberg, P.C. Impara, J.C. Tappeiner, and T.S. Sensenig. 2009. Influences of climate, fire, and topography on contemporary age structure patterns of Douglas-fir at 205 old forest sites in western Oregon. *Can. J. For. Res.* 39: 1518–1530.

Pyne, S. 1982. *Fire in America*. Princeton University Press. Princeton, N.J.

Pypker, T.G., M.H. Unsworth, A.C. Mix, W. Rugh, T. Ocheltree, K. Alstad, and B.J. Bond. 2007. Using nocturnal cold air drainage flow to monitor ecosystem processes in complex terrain. *Ecol. App.* 17: 702–714.

R Development Core Team. 2006. R: A language and environment for statistical computing. *In* R Foundation for Statistical Computing, Vienna, Austria.

Reed, W.J. 1994. Estimating the probability of stand-replacing fire using the age-class distribution of undisturbed forest. *For. Sci.* 40: 104–119.

Reed, W.J., C.P.S. Larsen, E.A. Johnson, and G.M. MacDonald. 1998. Estimation of temporal variations in historical fire frequency from time-since-fire map data. *For. Sci.* 44: 465–475.

Rich, P.M., R. Dubayah, W.A. Hetrick, and S.C. Saving. 1994. Using viewsheds to calculate intercepted solar radiation: applications in ecology. American Society for Photogrammetry and Remote Sensing Technical Papers. pp. 524–529.

Robbins, D. 2004. Temporal and spatial variability of historic fire frequency in the southern Willamette Valley foothills of Oregon. M.S. Thesis. Oregon State University, Corvallis.

Rollins, M.G., P. Morgan, and T.W. Swetnam. 2002. Landscape-scale controls over 20th century fire occurrence in two large Rocky Mountain (USA) wilderness areas. *Landscape Ecol.* 17: 539–557.

Romme, W.H., and D.H. Knight. 1981. Fire frequency and subalpine forest succession along a topographic gradient in Wyoming. *Ecology* 62: 319–326.

Rose, C.R., and P.S. Muir. 1997. Green-tree retention: consequences for timber production in forests of the western Cascades, Oregon. *Ecol. App.* 7: 209–217.

Ross, S. 2002. A First Course in Probability. 6th ed. Prentice Hall. Upper Saddle River, NJ.

Rothermel, R.C. 1983. How to predict the spread and intensity of forest and range fires. USDA For. Serv. Gen. Tech. Rep. INT-143.

Rothermel, R.C., R.A. Wilson, G.A. Morris, and S.S. Sackett. 1986. Modeling moisture content of fine dead wildland fuels input to the BEHAVE fire prediction system. USDA Forest Service, Research Paper INT-359.

Scheffer, M., S. Carpenter, J.A. Foley, C. Folke, and B. Walker. 2001. Catastrophic shifts in ecosystems. *Nature* 413: 591–596.

Scheller, R.M., and D.J. Mladenoff. 2007. An ecological classification of forest landscape simulation models: tools and strategies for understanding broad-scale forested ecosystems. *Landscape Ecol.* 22: 491–505.

Schoennagel, T., T.T. Veblen, and W.H. Romme. 2004. The interaction of fire, fuels, and climate across Rocky Mountain Forests. *BioScience* 54: 661–676.

Schoonmaker, P., and A. McKee. 1988. Species composition and diversity during secondary succession of coniferous forests in the western Cascade Mountains of Oregon. *For. Sci.* 34: 960–979.

Sessions, J., P. Bettinger, R. Buckman, M. Newton, and A. J. Hamann. 2004. Hastening the return of complex forests following fire: The consequences of delay. *J. For*. 102: 38–45.

Sharples, J.J., M.F. Hutchinson, and D.R. Jellett. 2004. On the horizontal scale of elevation dependence of Australian monthly precipitation. *J. Appl. Meteorol.* 44: 1850–1865.

Shatford, J. P. A., D. E. Hibbs, and K. J. Puettmann. 2007. Conifer regeneration after forest fire in the Klamath-Siskiyous: How much, how soon? *J. For.* 105: 139-146.

Sherriff, R.L., and T.T. Veblen. 2006. Ecological effects of changes in fire regimes in *Pinus ponderosa* ecosystems in the Colorado Front Range. *J. Veg. Sci.* 17: 705–718.

Sherriff, R.L., and T.T. Veblen. 2007. A spatially-explicit reconstruction of historical fire occurrence in the Ponderosa Pine Zone of the Colorado Front Range. *Ecosystems* 10: 311–323.

Simon, S.A. 1991. Fire history in the Jefferson Wilderness area east of the Cascade Crest. Final report to the Deschutes National Forest Fire Staff.

Skinner, C.N., and A.H. Taylor. 2006. Southern Cascades bioregion. *In*: Fire in California's Ecosystems. Edited by N.G. Sugihara, J.W. van Wagtendonk, J. Fites-Kaufman, K.E Shaffer, A.E. Thode. University of California Press, Berkeley. pp. 195–224.

Skinner, C.N., A.H. Taylor, and J.K. Agee. 2006. Klamath Mountains bioregion. *In*: Fire in California's Ecosystems. Edited by N.G. Sugihara, J.W. van Wagtendonk, J. Fites-Kaufman, K.E Shaffer, A.E. Thode. University of California Press, Berkeley. pp. 170–194.

Spies, T.A., and J.F. Franklin. 1988. Old growth and forest dynamics in the Douglas-fir region of western Oregon and Washington. *Nat. Areas J.* 8: 190–201.

Spies, T.A., J.F. Franklin, and T.B. Thomas. 1988. Coarse woody debris in Douglas-fir forests of western Oregon and Washington. *Ecology* 69: 1689–1702.

Spies, T.A., and J.F. Franklin. 1989. Gap characteristics and vegetation response in coniferous forests of the Pacific Northwest. *Ecology* 70: 543–545.

Spies, T.A., and J.F. Franklin. 1991. The structure of natural young, mature, and old-growth Douglas-fir forests in Oregon and Washington. *In* Ruggiero, L. (ed.), Wildlife and Vegetation of Unmanaged Douglas-fir Forests. USDA For. Serv. Gen. Tech. Rep. PNW-GTR-285. Pacific Northwest Research Station. Portland, OR. pp. 91–110.

Sprugel, D.G. 1991. Disturbance, equilibrium, and environmental variability: what is 'natural' vegetation in a changing environment? *Biol. Conserv.* 58: 1–18.

Stahle, D.W., F.K. Fye, E.R. Cook, and R.D. Griffin. 2007. Tree-ring reconstructed megadroughts over North America since A.D. 1300. *Climatic change* 83: 133–149.

Stambaugh, M.C., and R.P. Guyette. 2008. Predicting spatio-temporal variability in fire return intervals using a topographic roughness index. *For. Ecol. Manage.* 254: 463–473.

Stewart, G.H. 1986. Population dynamics of a montane conifer forest, western Cascade Range, Oregon, USA. *Ecology* 67: 534–544.

Stewart, G.H. 1989. The dynamics of old-growth *Pseudotsuga* forests in the western Cascade Range, Oregon, USA. *Vegetatio* 82: 79–94.

Stokes, M.A., and T.L. Smiley 1996. An introduction to tree-ring dating. University of Arizona Press, Tucson.

Swetnam, T.W., C.D. Allen, and J.L. Betancourt. 1999. Applied historical ecology: using the past to manage the future. *Ecol. App.* 9: 1189–1206.

Swetnam, T.W., and C.H. Baisan. 1996. Historical fire regime patterns in the southwestern United States since AD 1700. *In* C.D. Allen (tech. ed.). *Fire Effects in Southwestern Forests*. Proceedings of the second La Mesa Fire Symposium. March 29–31, 1994. Los Alamos, NM. USDA For. Serv. Gen. Tech. Report RM-GTR-286. pp. 11–32.

Swetnam, T.W., C.H. Baisan, K. Morino, and A.C. Caprio. 1998. Fire history along elevational transects in the Sierra Nevada, California. Final Report to Sierra Nevada Global Change Research Program. University of Arizona, Laboratory of Tree-Ring Research.

Swetnam, T.W., C.H. Baisan, A.C. Caprio, P.M. Brown, R. Touchan, R.S. Anderson, and D.J. Hallett. 2009. Multi-millennial fire history of the Giant Forest, Sequoia National Park, California, USA. *Fire Ecol.* 5: 120–150.

Swetnam, T.W., and J.L. Betancourt. 1998. Mesoscale disturbance and ecological response to decadal climatic variability in the American southwest. *J. Climate* 11: 3128–3147.

Swetnam, T.W, and P.M. Brown. In press. Climatic inferences from dendroecological reconstructions. *In* M.K. Hughes, H.F. Diaz, and T.W. Swetnam (eds.), Dendroclimatology: Progress and Prospects. Developments in Paleoenvironmental Research, Springer.

Tappeiner, J.C., D. Huffman, H. Marshall, T.A. Spies, and J.D. Bailey. 1997. Density, ages, and growth rates in old-growth and young-growth forests in coastal Oregon. *Can. J. For. Res.* 27: 638–648.

Taylor, A.H. 2000. Fire regimes and forest changes in mid and upper montane forests of the southern Cascades, Lassen Volcanic National Park, California, USA. *J. Biogeogr.* 27: 87–104.

Taylor, A.H., and C.N. Skinner. 1998. Fire history and landscape dynamics in a late-successional reserve, Klamath Mountains, California, USA. *For. Ecol. Manage.* 111: 285–301.

Taylor, A.H., and C.N. Skinner. 2003. Spatial patterns and controls on historical fire regimes and forest structure in the Klamath Mountains. *Ecol. App.* 13: 704–719.

Teensma, P.D.A. 1987. Fire history and fire regimes of the central Western Cascades of Oregon. Ph.D. Dissertation. Department of Geography. University of Oregon, Eugene.

Teensma, P.D., J.T. Rienstra, and M.A. Yoder. 1991. Preliminary reconstruction and analysis of change in forests stand age class of the Oregon Coast Range from 1850 to 1940. U.S. Bureau of Land Management, Portland, OR. Tech. Note T/N OR-9.

Thompson, J.R., and T.A. Spies. 2009. Vegetation and weather explain variation in crown damage within a large mixed-severity wildfire. *For. Ecol. Manage.* 258: 1684–694.

Thompson, J.R., and T.A. Spies. 2010. Factors associated with crown damage following recurring mixed-severity wildfires and post-fire management in southwestern Oregon. *Landscape Ecol.* 25: 775–789.

Trouet, V., A.H. Taylor, A.M. Carleton, and C.N. Skinner. 2006. Fire-climate interactions in forests of the American Pacific coast. *Geophys. Res. Lett.* 33: L18704.

Turner, M.G., W.W. Hargrove, R.H. Gardner, and W.H. Romme. 1994. Effects of fire on landscape heterogeneity in Yellowstone National Park, Wyoming. *J. Veg. Sci.* 6: 731–742.

Turner, M.G., and W.H. Romme. 1994. Landscape dynamics in crown fire ecosystems. *Landscape Ecol.* 9: 59–77.

Turner, M.G., W.H. Romme, R.H. Gardner, R.V. O'Neill, and T.K. Kratz. 1993. A revised concept of landscape equilibrium: disturbance and stability in scaled landscapes. *Landscape Ecol.* 8: 213–227.

Vale, T.R. (Ed.). 2002. *Fire, Native Peoples, and the Natural Landscape*. Island Press. Washington, D.C. 238 pp.

Van Norman, K. 1998. Historical fire regime in the Little River watershed, southwestern Oregon. M.S. Thesis, Oregon State University. Corvallis.

Van Pelt, R., and J.F. Franklin. 2000. Influence of canopy structure on the understory environment in tall, old-growth, conifer forests. *Can. J. For. Res.* 30: 1231–1245.

Van Pelt, R., and N.M. Nadkarni. 2004. Development of canopy structure in *Pseudotsuga menziesii* forests in the southern Washington Cascades. *For. Sci.* 50: 326–341.

Van Pelt, R. and S.C. Sillett. 2008. Crown development of coastal *Pseudotsuga menziesii*, including a conceptual model for tall conifers. *Ecol. Monogr.* 78: 283–311.

Van Wagner, C.E. 1978. Age-class distribution and the forest fire cycle. *Can. J. For. Res.* 8: 220–227.

Van Wagner, C.E., M.A. Finney, and M. Heathcott. 2006. Historical fire cycles in the Canadian Rocky Mountain Parks. *For. Sci.* 52: 704–717.

Venables, W. N., and B. D. Ripley. 1997. Modern Applied Statistics with S-Plus, 2nd Edition. Springer-Verlag New York. 548 pp.

Wallin, D.O., F.J. Swanson, and B. Marks. 1994. Landscape pattern response to changes in pattern generation rules: land-use legacies in forestry. *Ecol. App.* 4: 569–580.

Ward, J.H. 1963. Hierarchical grouping to optimize an objective function. *J. Am. Stat. Assoc.* 58: 236–244.

Weir, J.M.H., E.A. Johnson, and K. Miyanishi. 2000. Fire frequency and the spatial age mosaic of the mixed-wood boreal forest in western Canada. *Ecol. App.* 10: 1162–1177.

Weisberg, P.J. 1998. Fire History, Fire Regimes, and Development of Forest Structure in the Central Western Oregon Cascades. Ph.D. Dissertation. Oregon State University. Corvallis.

Weisberg, P.J. 2004. Importance of non-stand-replacing fire for the development of forest structure in the Pacific Northwest, USA. *For. Sci.* 50: 245–258.

Weisberg, P.J. 2009. Historical fire frequency on contrasting slope facets along the McKenzie River, western Oregon Cascades. *W. North Am. Nat.* 69: 206–214.

Weisberg, P.J., and F.J. Swanson. 2001. Fire dating from tree rings in western Cascades Douglas-fir forests: an error analysis. *Northwest Sci.* 75: 145–156.

Weisberg, P.J., and F.J. Swanson. 2003. Regional synchroneity in fire regimes of western Oregon and Washington, USA. *For. Ecol. Manage.* 172: 17–28.

Weiss, A.D. 2001, Topographic position and landform analysis. Environmental Systems Research Institute, Inc. International User Conference, San Diego, CA, USA, 9-13 July 2001.

Westerling, A.L., H.G. Hidalgo, D.R. Cayan, and T.W. Swetnam. 2006. Warming and earlier spring increases western U.S. forest wildfire activity. *Science* 313: 940–943.

Wetzel, S.A., and R.W. Fonda. 2000. Fire history of Douglas-fir forests in the Morse Creek drainage of Olympic National Park, Washington. *Northwest Sci.* 74: 263–279.

White, A.S. 1985. Presettlement regeneration patterns in a southwestern ponderosa pine stand. *Ecology* 66: 589–594.

Whitlock, C., and M.A. Knox. 2002. Prehistoric burning in the Pacific Northwest: Human versus climatic influences. *In* T.R. Vale (ed.). Fire, native peoples, and the natural landscape. Island Press. Washington, DC. pp. 195–231.

Whitlock, C., J. Marlon, C. Briles, A. Brunelle, C. Long, and P. Bartlein. 2008. Long-term relations among fire, fuel, and climate in the north-western US based on lake-sediment studies. *Int. J. Wildl. Fire* 17: 72–83.

Wierman, C.A., and C.D. Oliver. 1979. Crown stratification by species in even-aged mixed stands of Douglas-fir–western hemlock. *Can. J. For. Res.* 9: 1–9.

Wimberly, M.C. 2002. Spatial simulation of historical landscape patterns in coastal forests of the Pacific Northwest. *Can. J. For. Res.* 32: 1316–1328.

Wimberly, M.C., and T.A. Spies. 2001. Influences of environment and disturbance on forest patterns in coastal Oregon watersheds. *Ecology* 82: 1443–1459.

Wimberly, M.C., T.A. Spies, C.J. Long, and C. Whitlock. 2000. Simulating historical variability in the amount of old forests in the Oregon Coast Range. *Conserv. Biol.* 14: 167–180.

Winter, L.E., L.B. Brubaker, J.F. Franklin, E.A. Miller, and D.Q. DeWitt. 2002a. Initiation of an old-growth Douglas-fir stand in the Pacific Northwest: a reconstruction from tree-ting records. *Can. J. For. Res.* 32: 1039–1056.

Winter, L.E., L.B. Brubaker, J.F. Franklin, E.A. Miller, and D.Q. DeWitt. 2002b. Canopy disturbances over the five-century lifetime of an old-growth Douglas-fir stand in the Pacific Northwest. *Can. J. For. Res.* 32: 1057–1070.

Yamaguchi, D.K. 1991. A simple method for cross-dating increment cores from living trees. *Can. J. For. Res*. 21: 414–416.

Yamaguchi, D.K. 1993. Forest history, Mount St. Helens. *Natl. Geogr. Res. Explor*. 9: 294–325.

Yang, Z., W.B. Cohen, and M.E. Harmon. 2005. Modeling early forest succession following clear-cutting in western Oregon. *Can. J. For. Res.* 35: 1889–1900.

Zackrisson, O. 1977. Influence of forest fires on the north Swedish boreal forest. *Oikos* 29: 22–32.

Zenner, E.K. 2000. Do residual trees increase structural complexity in Pacific Northwest coniferous forests? *Ecol. App.* 10: 800–810.

Zenner, E.K. 2005. Development of tree size distributions in Douglas-fir forests under differing disturbance regimes. *Ecol. App.* 15: 701–714.

APPENDICES

APPENDIX A. GIS METHODS FOR GENERATING RASTER LAYERS FOR TOPOGRAPHY VARIABLES

Elevation was hypothesized to influence fire frequency and severity through its influences on temperature, precipitation amount and form, and snowpack persistence. Cooler temperatures and more precipitation at high elevations may lead to shorter fire seasons and higher fuel moisture during the fire season, contributing to an inverse relationship between fire frequency and elevation (Table 3.1). However, many topographic features may be too small to affect precipitation, and temperature inversions may complicate relationships between elevation and temperature (Daly et al. 1994, 2007). Therefore, in addition to sample site elevation, the elevation at the ridgetop directly upslope from the sample site (GIS methods for determining ridgetop elevation are described below in relation to calculation of vertical slope position and illustrated in Figure A-1) was determined to account for influences of major ridgelines on precipitation patterns and as an index of the broader topographic context that may contribute to temperature inversions (Table 3.1).

Slope gradient influences fire behavior by enabling fuel preheating and greater efficiency of heat transfer with increasing slope steepness, leading to faster rates of fire spread on steep than gentle slopes (Rothermel 1983). Also, in areas productive enough that fuel amount and connectivity are unlikely to limit fire spread, steep slopes (especially with south aspects) may have greater fuel desiccation, and thus greater potential for severe fire effects than gentler slopes.

Topographic relief (the elevation range within a fixed area) was hypothesized to foster spatial variation in fire behavior through its influence on microclimatic variation, which moderates the moisture status of live foliage and dead woody fuel (Table 3.1). Areas of high topographic relief were hypothesized to have broader microclimatic variation and stronger association of microclimate with terrain shape and slope position than areas of lower relief due to stronger influences of topographic shading and temperature inversions. Slope relief was calculated as the elevation difference from

ridgetop to valley bottom (methods for assigning ridgetop and valley bottom elevations to each pixel are described below in relation to calculation of vertical slope position, and shown in Figure A-1). At a broader scale, local relief was calculated as the elevation range within an area of radius 2,340 m, representing the 90^{th} percentile of slope length (horizontal distance from ridgetop to valley bottom) for the sample sites. The radius was selected so that local relief would be calculated over an area including the entire width of a valley that potentially influences the local microclimate.

Exposure to solar radiation was hypothesized to increase the likelihood of severe fire effects by accelerating fuel desiccation. Indices of insolation were generated in two ways (Table 3.1). First, aspect was transformed to a continuous variable emphasizing the difference between northeast and southwest facing slopes (Beers et al. 1966). The second approach modeled direct and diffuse solar radiation under uniform sky as a function of surface orientation (slope gradient and aspect) relative to solar position (azimuth and zenith angle) (Rich et al. 1994). Shading by surrounding terrain was represented based on upward-looking hemispherical viewsheds generated for each pixel. As a proxy for growing season insolation, the algorithm was applied hourly over one day per month (May through September), and values were averaged across months. Because solar path changes in a continuous manner, the day of each month with daylength closest to the monthly mean was selected, thereby accounting for trends within a day and over the growing season while minimizing computation time (Pierce et al. 2005).

Terrain shape was hypothesized to influence fire behavior through its influences on microclimate and soil moisture, which affect the moisture status of live foliage and dead woody fuel. Concave landforms may have higher soil-water availability, cooler temperatures, and greater relative humidity than adjacent terrain, potentially reducing fire frequency or the probability of severe fire effects relative to adjacent terrain. Terrain shape was quantified using a Topographic Index previously used to map temperature data from weather stations across complex terrain (Daly et al. 2007, 2008). Topographic Index was calculated as the height of a focal pixel above the minimum elevation in neighborhoods of radius 150 and 300 m. The diameters of these neighborhoods

correspond to ¼ and ½ the median slope length (distance from ridgetop to valley bottom) of the sample sites, thereby enabling identification of fine-scale features (e.g., benches or cirques) within each slope facet.

Derivation of the remaining variables required delineation of major ridgelines and valley bottoms (Figures 3.A-1 and 3.A-2). The Hydrology Tools of ArcGIS 9.2 (ESRI 2008) were used to delineate a stream network, excluding first-and second-order streams as a first approximation of the location of major valley bottoms. Then, this network was revised by adding a small number of second-order stream segments, located on relatively flat terrain at bottoms of major slopes, and removing third-order stream segments that were located on steeply sloping terrain. The resulting layer was used to represent major valley bottoms (Figure A-1a). To guide delineation of major ridgelines, a watershed was generated around each stream segment in the valley bottom layer. Then, watershed divides located along major ridgecrests were traced to generate the layer of major ridgetops (Figure A-1a).

Differentiation in fire effects by slope position was hypothesized to be more pronounced on long than short slopes due to stronger microclimatic variation (Table 3.1). A slope length raster was developed by adding the horizontal distances from each pixel to the ridgetop and the distance from each pixel to the valley bottom. Both distances were measured using cost-weighted distance and setting a prohibitively high cost for crossing a ridgetop or valley bottom. The cost barriers ensured that distance was measured to the ridge at the top of the slope (valley at the bottom of the slope) rather than measuring to the ridge on the opposite side of the valley (valley on the other side of a ridge) where this distance was shorter (Figure A-2).

The potential for severe fire effects was hypothesized to increase closer to ridgetops due to factors supporting high rates of fire spread on upper slopes (e.g., wind exposure, preheating of upslope fuels, and little nighttime recovery of fuel moisture and relative humidity) (Table 3.1). The distance along the slope surface from each pixel to the ridgetop was measured by first calculating the slope surface length of each pixel as the

hypotenuse of the angle formed by its slope (Stambaugh and Guyette 2008). Next, a cost layer was developed by scaling surface lengths by the original cell size and adding a prohibitively high cost to cells on the valley bottom in order to prevent measuring to the ridge on the opposite side of the valley. Cost distance was then used to measure the distance along the slope surface from each pixel to the ridgetop.

Slope position was hypothesized to influence fire behavior due to factors promoting high spread rates on upper slopes (wind exposure and preheating of fuel) and cooler microclimate on lower slopes (topographic shading and temperature inversions) (Table 3.1). Vertical Slope Position (VSP) was measured as the height of a focal pixel above the valley bottom, scaled as a proportion of slope relief (where slope relief is defined as the elevation difference from ridgetop to valley bottom; Figure A-1d). Unlike other measures, which evaluate focal pixel elevation relative to elevation in an area of fixed horizontal radius (e.g., Topographic Position Index (TPI); Weiss 2001), VSP is scaled vertically to the slope relief of the focal pixel, which varies continuously across the study area. Scaling to slope relief provides a consistent measure of slope position across a range of slope sizes and shapes and valley widths. VSP is compared to TPI in Figure A-1e and f.

To determine the elevation at the ridgetop immediately upslope from each pixel, points were generated at 10-m intervals along each major ridgeline, and elevations were extracted to the points from a 10-m DEM. Then, spline interpolation was applied, using valley bottoms as barriers, to assign each pixel the elevation of the nearest ridgetop (Figure A-1b). The interpolation algorithm uses elevations of the 12 closest points (ESRI 2008), which were spread over a distance (120 m) equivalent to the transect length. It produces an output layer that is smooth relative to subtle variation in elevation along the ridgetop. Although spline interpolation may produce values above or below values of the input points, this was minimal due to the high density of input points with similar elevation values, and because interpolation was conducted over relatively short distances. Using valley bottoms as barriers ensured that pixels were assigned the elevation at the ridgetop immediately upslope rather than on the opposites side of the valley. To assign

the valley bottom elevation to each pixel (Figure A-1c), elevation values were extracted to points generated at 10-m intervals along the major valley bottoms. Then, spline interpolations was conducted using these points as the input and using the major ridgetops as barriers. VSP was then calculated by subtracting the valley bottom layer from the DEM and then dividing by the slope relief layer (Table 3.1, Figure A-1e).

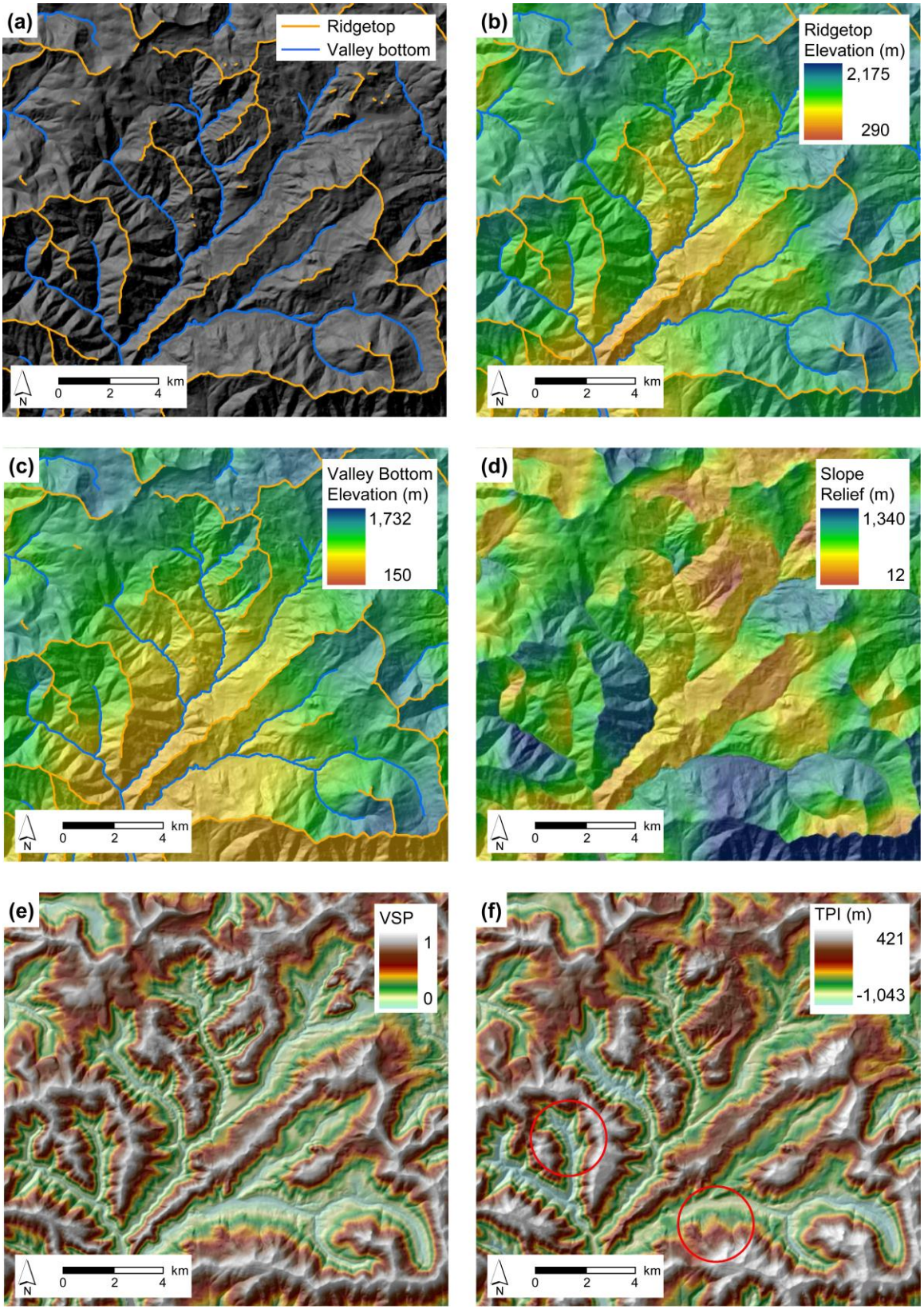
(a)
Ridgetop
Valley bottom
N
0 2 4 km
(b)
Ridgetop Elevation (m)
2,175
290
N
0 2 4 km
(c)
Valley Bottom Elevation (m)
1,732
150
N
0 2 4 km
(d)
Slope Relief (m)
1,340
12
N
0 2 4 km
(e)
VSP
1
0
N
0 2 4 km
(f)
TPI (m)
421
-1,043
N
0 2 4 km

Figure A-1. Illustration of the output layers produced by the GIS analyses to generate methods raster layers for ridgetop elevation, slope relief, and vertical slope position. The southern part of the Blue River study area is shown with layers representing (a) major ridgelines and valley bottoms, (b) ridgetop elevation (RE), (c) valley bottom elevation (VE), (d) slope relief (SR = RE – VE), (e) vertical slope position (VSP = (elevation – VE)/SR), and (f) the topographic position index (TPI) of Weiss (2001), calculated using an outer radius of 1,000 m and an inner radius of 850 m. TPI is shown to illustrate the difference between this method that evaluates focal pixel elevation relative to a circle of fixed radius (red circles represent the outer radius) and the method of developing vertical slope position, where the focal pixel height above the valley bottom is scaled as a proportion of slope relief, which varies continuously across the study area.

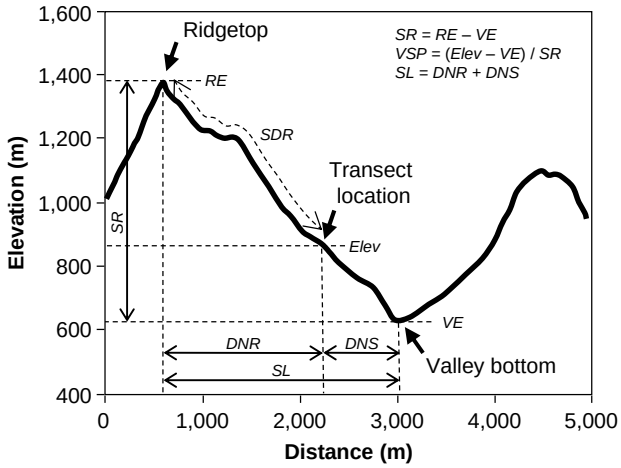

Figure A-2. Idealized topographic cross-section between two major ridges illustrating how several of the topographic variables were defined (*RE* = ridgetop elevaiton, *VE* = valley bottom elevation, *Elev* = transect elevation, *DNR* = horizontal distance to ridgetop at the top of the slope, *DNS* = horizontal distance to the valley bottom at the bottom of the slope, *SL* = slope length, *SR* = slope relief, *VSP* = vertical slope position).

APPENDIX B. PROOF OF THE EQUILIBIRUM AGE DISTRIBUTION UNDER A STATIONARY FIRE REGIME

Wald's Equation and the Elementary Renewal Theorem (Grimmett and Stirzaker 1992) are used to verify that Equation 5 of chapter 5 represents the equilibrium age distribution regardless of the form of the hazard rate for SR fire. To evaluate the use of Equation 5 to calculate the equilibrium age distribution, a forest divided into j non-overlapping age classes, where $R_L(j)$ and $R_U(j)$ represent lower and upper bounds, respectively, of the j^{th} age class. The length of the l^{th} interval between stand-replacing (SR) fires is represented by τ_l, and the number of years in that interval that the age of a particular stand is greater than $R_L(j)$ is represented by $X_l(j)$:

$$X_l(j) = [\tau_l - R_L(j)]^+ = \begin{cases} \tau_l - R_L(j) & \text{if } \tau_l > R_L(j) \\ 0 & \text{if } \tau_l \le R_L(j). \end{cases}$$

The upper bound of one age class is equal to the lower bound of the next oldest age class: $R_U(j) = R_L(j + 1)$. Therefore, the number of years in interval τ_l spent in the j^{th} age class can be calculated as $X_l(j) - X_l(j + 1)$.

If an analysis is conducted over a period of T years, $N(T)$ represents the number of SR fires occurring on the interval [0, T]. The proportion of time on the interval [0, T] that a particular stand is older than age $R_L(j)$ is given by:

$$\frac{1}{T} E\left(\sum_{l=1}^{N(T)} X_l(j) \right).$$

However, the above expression cannot be calculated accurately for a finite time period ($T < \infty$) because $N(T)$ and X_l are not independent and the interval before the first SR fire $[0, \tau_1]$ and the interval from the last SR fire to the end of the analysis period $[\tau_{N(T)}, T]$ are not necessarily complete intervals between SR fires.

Over a finite time period, the interval before the first SR fire [0, τ_1] is a complete fire interval only when starting with an initial stand age of 0, representing the age immediately after a SR fire. The problem of the interval from the last SR fire to the end of the analysis [$\tau_{N(T)}$, T] not representing a complete interval between SR fires can be addressed by using stopping time, $M = N(T) + 1$, representing the number of SR fires that have occurred at the time of the first SR fire after time T. If an initial stand age of 0 is assumed, then Wald's Equation (Grimmett and Stirzaker 1992) gives:

$$\frac{1}{T}E\left(\sum_{l=1}^{M} X_l(j)\right) = \frac{1}{T}E[X_1(j)]E(M), \qquad \text{[B-1]}$$

where the expected value of the number of years that the age of a stand is above $R_L(j)$ on the first interval between SR fires, X_1, replaces the number of years above $R_L(j)$ on the l^{th} fire interval, X_l, because X_l is an independent, identically distributed random variable.

The equilibrium age distribution is determined by calculating the proportion of time spent above the age threshold, $R_L(j)$, over an infinite time period. As T increases, the influence of incomplete fire intervals for the time up to the first SR fire and from the last SR fire to the end of the analysis period decreases. Eventually, as $T \to \infty$, these incomplete fire intervals become irrelevant. Therefore, it can bees seen by the Elementary Renewal Theorem (Grimmett and Stirzaker 1992) that

$$\lim_{T\to\infty}\frac{1}{T}E(M) = \lim_{T\to\infty}\frac{1}{T}E[N(T)] = \frac{1}{E(\tau)}$$

Therefore, as $T \to \infty$, $1/E(\tau)$ can be substituted into Equation B-1 to calculate the proportion of time on interval T spent above age $R_L(j)$:

$$\lim_{T\to\infty}\frac{1}{T}E\left(\sum_{l=1}^{N(T)} X_l(j)\right) = \lim_{T\to\infty}\frac{1}{T}E[N(T)]E[X_1(j)] = \frac{1}{E(\tau)}E[X_1(j)]. \qquad \text{[B-2]}$$

The expected amount of time on a given fire interval that stand age is above $R_L(j)$, $E[X_1(j)]$, is calculated as the probability that the interval between SR fires, τ_l, is longer than $R_L(j) + t$ (Ross 2002):

$$E[X_1(j)] = \int_0^\infty P\{X_1(R_L(j)) > u\}du = \int_0^\infty P\{(\tau_1 - R_L(j))^+ > u\}du$$

$$= \int_0^\infty P\{\tau_1 > R_L(j) + u)\}du,$$

where u is a dummy variable.

The equilibrium proportion of the landscape covered by the j^{th} age class is determined by evaluating Equation B-2 for $X_1(j + 1)$ and subtracting it from the result of Equation B-2 for $X_1(j)$. So far, j has been used to indicate a relatively small number of age classes. However, to calculate the equilibrium age distribution, it is useful to consider a large number of age classes of equal width, where R represents the lower bound of an age class and ΔR represents age-class width. Using this notation, the proportion of time spent in a particular age class is given by:

$$E[X_1(R) - X_1(R + \Delta R)] = \int_0^\infty P\{\tau_1 > (R + u)\}du - \int_0^\infty P\{\tau_1 > (R + \Delta R + u)\}du.$$

For simplification, v will be set equal to $R + u$, and the above equation is reduced to

$$E[X_1(R) - X_1(R + \Delta R)] = \int_R^\infty P\{\tau_1 > v\}dv - \int_{R+\Delta R}^\infty P\{\tau_1 > v\}dv =$$

$$= \int_R^{R+\Delta R} P\{\tau_1 > v\}dv \cong P\{\tau_1 > R\}\Delta R.$$

Now, it is possible to divide by ΔR and let $\Delta R \to 0$.

$$\lim_{\Delta R \to 0} \frac{1}{\Delta R} \int_R^{R+\Delta R} P\{\tau_1 > v\}dv = P\{\tau_1 > R\}$$

The right hand side of the above equation is equivalent to the survivorship distribution, $S_\tau(t)$ (Equation 1 of chapter 5). Therefore, $S_\tau(t)$ can replace $E[X_l(j)]$ in Equation B-2, which reproduces Equation 5 of chapter 5 for calculating the proportion of time on interval T that a stand is of age t as $T \to \infty$.

APPENDIX C. MODEL OF AGE-COHORT STRUCTURE IN DOUGLAS-FIR/WESTERN HEMLOCK FORESTS UNDER A MIXED-SEVERITY FIRE REGIME

EMPIRICAL BASIS

A multi-pathway model of forest development was constructed to evaluate the age-cohort structure of Douglas-fir (*Pseudotsuga menziesii* (Mirb.) Franco)/western hemlock (*Tsuga heterophylla* (Raf.) Sarg.) forests of the PNW under a mixed-severity fire regime. The model is based in part on forest age-structure data collected in the central western Cascades of Oregon (chapter 2), and it incorporates insight from other fire-history and stand reconstruction studies in the region (Stewart 1986, 1989; Morrison and Swanson 1990; Weisberg 2004). However, the model was developed as a relatively simple tool to contribute to a stronger understanding of fire-regime parameters and their interactions rather than for detailed historical reconstructions or projections of future change.

Douglas-fir is a long-lived (ca. 750–1,200 years; Franklin and Waring 1980), relatively shade-intolerant species. Its regeneration may be prolific following fire that opens the canopy, but small canopy gaps (< 0.1 ha) produced by mortality of individual or small groups of trees are not conducive to Douglas-fir establishment and recruitment (Spies and Franklin 1989). Thus, Douglas-fir forms even-aged stands following stand-replacing (SR) fire, and it may form a distinct cohort beneath older trees following non-stand-replacing (NSR) fire that partially opens the canopy, but it is not likely to regenerate following low-intensity fire that leaves the upper canopy largely intact (Stewart 1986; chapter 2). Douglas-fir may be common in post-fire cohorts beneath surviving trees at densities up to 2/3 the density of Douglas-fir trees in unburned old-growth stands, but it usually was not found in post-fire cohorts that established beneath higher densities of older trees (chapter 2).

The episodic regeneration of Douglas-fir following disturbances that open the canopy, and the general inability of Douglas-fir to regenerate following canopy closure

was evident in the age distribution of Douglas-fir trees in 124 stands throughout 2 large watersheds in the central western Cascades of Oregon. Almost all trees had establishment dates clustered within discrete pulses (usually < 40 years long), with multiple pulses per stand usually separated by intervals > 80 years long with no establishment dates recorded for any species (chapter 2).

The major shade-tolerant associates, western hemlock and western redcedar (*Thuja plicata* Donn ex D. Don), are able to establish almost continuously in the absence of fire. They may persist in the shaded understory for decades to centuries until they either die or are recruited to the forest canopy through small canopy gaps (Winter et al. 2002). Thin bark, retention of shaded lower branches, and shallow rooting render these species highly susceptible to fire-caused mortality, even following low-intensity fire (Agee 1993). However, where seed sources are available, they usually are able to regenerate across the full range of densities of surviving trees following fire (Agee and Huff 1980, Larson and Franklin 2005).

Although the major shade-tolerant species may reach ages > 400 years old in undisturbed forests (Winter et al. 2002), shade-tolerant trees > 200 years old were lacking from most old-growth stands sampled in the central western Cascades of Oregon (chapter 2). Instead, most stands had a distinct pulse of establishment in a 40–60-year window, presumably following fire in the 19th or early 20th century. These establishment pulses either coincide with establishment of Douglas-fir following fire that opened the canopy, or they were composed only of shade-tolerant species following fire that caused little mortality to upper-canopy trees. Stands also may contain a small number of shade-tolerant trees that predate the most recent fire (Keeton and Franklin 2005), but the density of these trees usually is low, and they are not represented in the model.

SIMULATION MODEL

The model represents a small stand (ca. 1 ha). The input parameters are (1) the NFR for all fire regardless of intensity (equivalent to the mean interval between

successive fires at a stand), (2) the proportion of fires that burn at low, moderate, and high intensity at the stand level, and (3) thresholds ages for cohorts of Douglas-fir trees required to survive burning at low and moderate intensity. The state variables are the ages of post-fire cohorts of Douglas-fir and shade-tolerant species. The only attributes of cohorts represented in the model are the species (Douglas-fir or shade-tolerant species) and age (equivalent to time since the cohort-initiating fire, assuming that cohorts are initiated only following fire and there is no upper bound to cohort age). The model does not track attributes of individual trees or changes in tree density over time due to fire-caused mortality or density-dependent thinning.

Fire Occurrence and Intensity

Fire is assumed to have a fixed probability of occurrence each year (a constant hazard rate) that is independent of time since previous fires or their intensities. Fire intensity is assumed to be driven by factors exogenous to the stand (e.g., wind, relative humidity, and weather-driven antecedent fuel moisture) rather than conditions within the stand at the time of the fire (e.g., fuel amount or connectivity). However, the response of a stand to burning at a given intensity depends on stand age structure at the time of the fire, as explained below.

The interval between successive fires in a stand regardless of intensity is represented by a sequence of independent identically distributed random variables, θ_l, that have an exponential distribution with parameter, λ, equal to the reciprocal of the user-defined NFR. If a stand is burned in the l^{th} fire, it burns with intensity, μ_l, where μ takes on values of 1, 2, or 3, for low, moderate, or high intensity, respectively. The proportion of fires expected to burn at low, moderate, and high intensity (q_1, q_2, and q_3, respectively) is defined by the user, where $q_1 + q_2 + q_3 = 1$. Each time a stand is burned, a uniform random variable, U_l, is drawn on the interval [0, 1], and fire intensity, μ_l, is determined as follows:

$\mu_l = 1$ if $U_l \leq q_1$

$\mu_l = 2$ if $q_1 < U_l \leq q_1 + q_2$

$\mu_l = 3$ if $U_l > 1 - q_3$.

Cohort Initiation and Mortality

Cohorts are assumed to be initiated or removed from a stand only by fire. Non-fire disturbances (e.g., wind, insects, or diseases) and mortality associated with competition are not represented. There is no maximum age of cohorts, meaning cohorts are assumed never to be lost from a stand in the absence of fire, even in the rare case of a fire-free interval exceeding the typical maximum longevity of each species.

At least one cohort of Douglas-fir trees is present at all times. Ages of Douglas-fir cohorts are represented by t_i ($i = 1,\ldots, n$). The subscript i is an index that sorts cohorts in the order they established following SR fire, and n represents the total number of Douglas-fir cohorts present in the stand. Thus, ages of the oldest and youngest cohorts are represented by t_1 and t_n, respectively, where $t_n \leq t_1$. SR fire is assumed to eliminate all pre-existing cohorts from a stand and enable establishment of a single Douglas-fir cohort, whose age, t_1, is equal to the number of years since the last SR fire. Although field data indicate that establishment dates within cohorts usually are spread over ca. 40-year windows following fire (chapter 2), each cohort in the model is represented by a single age, corresponding to the number of years since cohort initiation (i.e., time since fire) or the maximum possible tree age within the cohort.

Following NSR fire, the number of Douglas-fir cohorts either remains unchanged or increases, depending on fire intensity and cohort ages at the time of the fire. A Douglas-fir cohort may survive fire of low or moderate intensity when its age exceeds user-defined thresholds, r_1 and r_2, respectively. The thresholds enable the following rules guiding Douglas-fir cohort initiation and mortality: (1) if fire intensity is low ($\mu_l = 1$) and the youngest Douglas-fir cohort is too young to survive low-intensity fire ($t_n \leq r_1$), the cohort is removed from the stand and a new cohort establishes, regardless of the presence of older cohorts, (2) if fire intensity is moderate ($\mu_l = 2$) and the youngest Douglas-fir

cohort is too young to survive moderate-intensity fire ($t_n \leq r_2$), it is killed and a new cohort establishes, regardless of the presence of older cohorts, (3) if fire intensity is high ($\mu_l = 3$), all Douglas-fir cohorts are killed regardless of their age, and a single cohort is established, and (4) if fire intensity is moderate ($\mu_l = 2$), and the youngest Douglas-fir cohort is old enough to survive moderate-intensity fire ($t_n > r_2$), it survives and a new cohort is initiated, resulting in an increase in the total number of Douglas-fir cohorts in the stand. Although tree density is not tracked, moderate-intensity fire is assumed to thin existing cohorts and generate gaps of sufficient size for Douglas-fir regeneration, while retaining enough surviving trees that the older cohort remains an important structural component of the stand.

The above rules lead to three key points regarding the initiation and mortality of Douglas-fir cohorts. First, the only way to increase the number of Douglas-fir cohorts in a stand is following moderate-intensity fire when the youngest Douglas-fir cohort is old enough to survive the fire ($\mu_l = 2$ and $t_n > r_2$). Second, all high-intensity fires are SR fires, which kill all cohorts and lead to a new stand with a single cohort of Douglas-fir trees. However, low- and moderate-intensity fire also are SR fires when the oldest Douglas-fir cohort is too young to survive the fire ($\mu_l = 1$ and $t_1 \leq r_1$, or $\mu_l = 2$ and $t_1 \leq r_2$). Third, there may be erasure of cohorts when stands containing two or more cohorts experience low- or moderate-intensity fire. For example, if a stand with Douglas-fir cohorts of ages $t_1 > r_2$ and $t_2 = t_n \leq r_1$ experiences low-intensity fire, the older cohort would survive, the younger cohort would be killed, and a new cohort would be initiated. The number of Douglas-fir cohorts would be the same ($n = 2$) before and after the fire, but there would no longer be a cohort representing the timing of the fire prior to the most recent fire. Thus, the number of Douglas-fir cohorts present at any time provides only a minimum estimate of the number of cohorts that have been initiated since the last SR fire.

A single cohort of shade-tolerant trees is present at all times. Its age, t_0, represents the initiation of a period with potential for nearly continuous establishment to the present (Winter et al. 2002). Delayed post-fire establishment of shade-tolerant species

has been attributed to elimination of seed sources by repeated burning (Wimberly and Spies 2001) or a harsh post-fire environment for survival of shade-tolerant trees on dry, exposed sites (Larson and Franklin 2005). Thus, the age of the cohort of shade-tolerant trees represents the maximum possible age within the cohort, but it does not necessarily indicate actual tree ages. The cohort of shade-tolerant trees is assumed to be killed by all fire, regardless of intensity and cohort age. Similar to Douglas-fir cohorts, there may be erasure of cohorts of shade-tolerant trees from a stand (the age of the cohort of shade-tolerant trees dates to the most recent fire of any intensity, and cohorts initiated following previous fires do not survive to the present).

Age Classes and Stand-Structure Types

Stand age is classified into one of seven classes based on the age of the oldest Douglas-fir cohort, t_1, which is equivalent to the time since the last SR fire (Table 5.1). A stand is classified into the j^{th} age class if the age of the oldest Douglas-fir cohort falls between the lower and upper age limits of the class, represented by $R_L(j)$ and $R_U(j)$, respectively.

Within each age class, stands are classified into one of up to three stand-structure types, representing effects of NSR fires or a lack of burning on stand development since the last SR fire. Rules for classifying stands into structure types are based on comparison of the age of the youngest Douglas-fir cohort and the cohort of shade-tolerant trees to age thresholds, $t_n^*(j)$ and $t_0^*(j)$, respectively, for the j^{th} age class (Table 5.1). Ages of these cohorts reflect the timing and intensity of the most recent fire, or the most recent fire that generated canopy openings of sufficient size to enable initiation of a new cohort of Douglas-fir trees. The time since such fires is likely to have a strong influence on present stand structure, and thus comparison of cohort ages to the threshold ages determines that structure type within each age class.

The "unburned" stand-structure type of each age class represents stand structures likely to develop in the absence of NSR fire since the last SR fire (Franklin et al. 2002). This structure type also may include stands that experienced NSR fire early in their

development, as long as the time since the most recent fire is long enough that forest structure no longer is likely to be distinct from stands of the j^{th} age class that have not experienced NSR fire. To be in the unburned structure type, the cohort of shade-tolerant trees must exceed an age threshold, $t_0^*(j)$, equal to, or only slightly younger than the lower bound of the age class, $R_L(j)$. Thus, the stand could not have experienced fire of any intensity in the last $t_0^*(j)$ years (Table 5.1). Also, stands must have a single cohort of Douglas-fir trees, or, if more than one cohort is present, all cohorts must be within the j^{th} age class: $t_n > t_n^*(j) = R_L(j)$. In other words, the stand may have experienced moderate-intensity fire leading to a second Douglas-fir cohort early in its development, but it could not have experienced moderate-intensity fire within the last $t_n^*(j)$ years (Table 5.1).

The "DF/Tol" stand-structure type represents a Douglas-fir cohort over a younger cohort of shade-tolerant trees that initiated following low-intensity fire that did not open the canopy enough for Douglas-fir regeneration. Similar to the unburned structure type, the DF/Tol type has either a single Douglas-fir cohort, or if two cohorts are present, the younger cohort must exceed the lower age limit of the j^{th} age class: $t_n > t_n^*(j) = R_L(j)$ (Table 5.1). The DF/Tol structure type is distinguished from the unburned type by the age of the cohort of shade-tolerant trees. This cohort must be younger than the threshold age ($t_0 \leq t_0^*(j)$), indicating the stand has experienced at least one low-intensity fire in the last $t_0^*(j)$ years. Because the age of the youngest Douglas-fir cohort must exceed a threshold age equivalent to the lower bound of the age class, $t_n > t_n^*(j) = R_L(j)$, stands in this structure type could not have experienced moderate-intensity fire within the last $t_n^*(j)$ years (Table 5.1). Stands of the DF/Tol structure type may transition to the unburned structure type in the absence of fire, as continued establishment and recruitment of shade-tolerant species is likely to generate stand structure increasingly similar to that of stands that have not experienced low-intensity fire (Figure C-1).

The "DF/DF" stand-structure type refers to stands with Douglas-fir cohorts present in at least two of the age classes defined in Table 5.1. Because the age of the youngest Douglas-fir cohort must be younger than the minimum age for the j^{th} age class ($t_n \leq t_n^*(j) = R_L(j)$), stands in the DF/DF structure type must have experienced at least one moderate-intensity fire within the last $t_n^*(j)$ years. For example, if a stand containing a single, 100-year-old Douglas-fir cohort ($t_1 = t_n = 100$) experiences moderate-intensity fire, this cohort would survive and a new Douglas-fir cohort would establish. Ten years later, the stand would contain two Douglas-fir cohorts (ages $t_1 = 110$ and $t_2 = t_n = 10$), and the stand would be classified as the DF/DF structure type of the Mature age class (Table 5.1). At this point, stand structure is likely to be distinct from mature stands that have not experienced NSR fire. If the stand remains unburned until the Douglas-fir cohorts reach ages of 400 and 500 years, both cohorts would be in the Mid Old Growth (MOG) age class. Based on stand structure, it may be difficult to tell that the stand had experienced NSR fire 400 years ago. Therefore, with no additional fire, this stand would transition to the DF/Tol and then to the unburned structure type (Figure C-1). If it experiences additional moderate-intensity fire, it would remain in the DF/DF structure type, and if it experiences only additional low-intensity fire, it would transition to the DF/Tol structure type.

ANALYTICAL APPROXIMATION

Equilibrium Age Distribution

The rules described above for determining fire occurrence and intensity and cohort initiation and mortality can be used to identify the hazard rate for SR fire, $h_\tau(t)$, which in turn may be used to calculate the probability density function of stand age or the equilibrium age distribution of a landscape (Equation 5 of chapter 5). Because the model specifies intervals between fires of any intensity, θ, using an exponential variable with parameter, λ, equal to the reciprocal of the user-defined NFR, the hazard rate for fire of any intensity, $h_\theta(t) = \lambda$, is constant (not dependent on stand age). However, intervals

between successive SR fires in each stand, τ, do not follow an exponential distribution because low- and moderate-intensity fires may be SR fires when the oldest Douglas-fir cohort is younger than age thresholds r_1 and r_2, respectively, but only high-intensity fires are SR fires at ages beyond r_2.

Because the range of fire intensities that kill the oldest Douglas-fir cohort decreases each time the age of the cohort surpasses one of the user-defined thresholds (r_1 and r_2), the hazard rate for SR fire, $h_\tau(t)$, is piecewise constant (Figure 5.5). That is, when the oldest cohort is young enough to be killed by fire of any intensity ($t_1 \le r_1$), the hazard rate for SR fire is equivalent to the hazard rate for fire of any intensity, $h_\tau(t) = h_\theta(t) = \lambda$. When the oldest cohort exceeds age r_1, it no longer is killed by low-intensity fire, and the hazard rate for SR fire decreases to $h_\tau(t) = (1-q_1)\lambda$, where q_1 is the user-defined proportion of fires that burn at low intensity. After the age of oldest cohort exceeds r_2, it is killed only by high-intensity fire, and the hazard rate for SR fire decreases to $h_\tau(t) = q_3\lambda$, where q_3 is the user-defined proportion of fires that burn at high intensity (Figure 5.5).

$$h_\tau(t) = \begin{cases} \lambda & \text{if} \quad t_1 \le r_1 \\ (1-q_1)\lambda & \text{if} \quad r_1 < t_1 \le r_2 \\ q_3\lambda & \text{if} \quad t_1 > r_2 \end{cases}$$

The mean interval between fires of any intensity, $E(\theta)$, is specified directly by the user. The mean interval between successive SR fires, $E(\tau)$ (Equation 4 of chapter 5), may be derived from the hazard rate for SR fire using the cumulative survivorship distribution, $S_\tau(t)$ (Equation 1 of chapter 5), and accounting for the piecewise constant hazard rate, as illustrated below:

$$E(\tau) = \int_0^{r_1} S_\tau(t)dt + \int_{r_1}^{r_2} S_\tau(t)dt + \int_{r_2}^{\infty} S_\tau(t)dt ,$$

where

$$S_\tau(t) = P\{\tau > t_1\} = \begin{cases} \exp(-t_1\lambda) & t_1 \le r_1 \\ \exp\left[-\lambda\{r_1 + (1-q_1)(t_1 - r_1)\}\right] & r_1 < t_1 \le r_2 \\ \exp\left[-\lambda\{r_1 + (1-q_1)(r_2 - r_1) + q_3(t_1 - r_2)\}\right] & t_1 > r_2. \end{cases}$$

Therefore, using Equation 4 of chapter 5, the mean interval between SR fires is calculated as:

$$E(\tau) = \frac{1}{\lambda}\left[\begin{array}{l} [1-\exp(-r_1\lambda)] + \dfrac{1}{(1-q_1)}\left[\exp(-r_1\lambda) - \exp[-(r_2\lambda) + (q_1\lambda)(r_2 - r_1)]\right] \\ + \dfrac{1}{q_3}\exp[(-r_1\lambda) - (1-q_1)\lambda(r_2 - r_1)] \end{array}\right].$$

The equilibrium age distribution can be determined by multiplying the cumulative survivorship distribution, $S_\tau(t)$, by the reciprocal of the mean interval between SR fires, $1/E(\tau)$, as presented in Equation 5 of chapter 5 and supported in Appendix B.

The equilibrium age distribution for a landscape parameterized by data collected at the Cook-Quentin study area of Morrison and Swanson (1990) in the central western Cascades of Oregon is presented in Figure C-2, using the input parameters presented in Table 5.2. The use of this data set is primarily to illustrate that the succession model can be parameterized based on data commonly collected in fire-history research. It is not intended to represent the actual age distribution of this study area because (1) the extent of the study area (2,000 ha) is much too small relative to fire size to expect an equilibrium age distribution, (2) the thresholds, r_1 and r_2, and the constant hazard rates for low- and moderate-intensity fire (described below) have not been validated, and (3) this area is likely to have had substantial centennial-scale variation in fire frequency within the lifetime of existing old-growth stands based on a synthesis of 10 fire-history studies west of the crest of the Cascades in Oregon and Washington (Weisberg and Swanson 2003).

Approximation of Stand-Structure Type Abundance

Hazard rates for low- and moderate-intensity fire are needed to evaluate the abundance of up to three structure types within each age class. The hazard rate for SR fire, $h_\tau(t)$, is piecewise constant, decreasing when stand age reaches thresholds r_1 and r_2 (Figure 5.5). Hazard rates for low- and moderate-intensity fire are indicated by $h_L(t) = q_1\lambda$ and $h_M(t) = q_2\lambda$, respectively, where q_1 and q_2 are user-defined constants, and the hazard rates for low- and moderate-intensity fire are independent of time since the last fire and its intensity. These constant hazard rates for low- and moderate-intensity fire are simple formulations that do not require assumptions regarding the effects of fire on fuel profiles and feedbacks on subsequent fire occurrence and intensity. However, the methods for approximating the abundance of each structure type presented below in Equations C1–C3 also apply for more complex hazard rates that account for such feedback.

Determining the equilibrium abundance of the stand-structure types within each age class requires first calculating equilibrium age distribution, and then evaluating the proportion of stands within each age class where ages of the youngest Douglas-fir cohort and the shade-tolerant cohort meet criteria for each structure type (Table 5.1). For example, the equilibrium abundance of stands in the Early Old Growth (EOG) age class is determined by integrating the equilibrium density function of stand age, $a_\infty(t)$ (Equation 5 of chapter 5), over ages between $R_L(j) = 200$ and $R_U(j) = 350$ (Table 5.1). Within this age class, the unburned stand-structure type requires that the youngest Douglas-fir cohort and the cohort of shade-tolerant trees exceed threshold ages of $t_0^*(j) = t_n^*(j) = 200$ (Table 5.1). Exceeding these thresholds is possible only without low- or moderate-intensity fire over a 200-year interval before the present. Thus, given stand age, $t_1 = 300$, the probability of going without low- or moderate-intensity fire over the previous 200 years is calculated as the probability of no low- or moderate-intensity fire over the interval from age $t_1 - 200$ to t_1 (Figure C-3a).

The probability that no low- or moderate-intensity fire has occurred over the preceding 200 years must be calculated after conditioning on stand age (the probability of reaching age t_1 with no SR fire). The need for conditioning on stand age is evident toward the younger end of the age class. For example, a stand could reach age t_1 = 210 years only with no low-intensity fire up to age $t_1 = r_1$ = 30 years, no moderate-intensity fire to age $t_1 = r_2$ = 80 years, and no high-intensity fire to age t_1 = 210 years. Therefore, the probability of no low-intensity fire over the previous 200 years, given stand age, t_1 = 210, is the probability of no low-intensity fire over the interval from age $t_1 = r_1$ = 30 to age t_1 = 210 (Figure C-3b). In this case, the interval [r_1, t_1] is only 180 years, because a stand could reach an age of 210 years only if there had not been low-intensity fire within the first r_1 = 30 years following stand initiation. An additional 180 years without low-intensity fire would be required for the cohort of shade-tolerant trees to exceed an age of $t_0 = t_0^*(j)$ = 200 years. Likewise, the probability of no moderate-intensity fire over the previous 200 years, given stand age, t_1 = 210, is the probability of no moderate-intensity fire over the interval from age r_2 = 80 to age t_1 = 210 (Figure C-3b).

In general form, the criteria for each stand-structure type within a given age class can be determined by considering the following events:

*E*1. No SR fire for at least $R_L(j)$ and up to $R_U(j)$ years.

*E*2. No low-intensity fire during the preceding $t_0^*(j)$ years.

*E*3. No moderate-intensity fire during the preceding $t_n^*(j)$ years.

*E*4. At least one low-intensity fire within the last $t_0^*(j)$ years.

*E*5. At least one moderate-intensity fire within the last $t_n^*(j)$ years.

Joint probabilities of exceeding the age thresholds for each stand-structure type of the age classes listed in Table 5.1 can be stated in terms of conditional probabilities of the above events:

Unburned: $P\{R_L(j) \le t_1 \le R_U(j), t_n \ge t_n^*(j), t_0 \ge t_0^*(j)\} = P\{E2 \cap E3 \mid E1\}P\{E1\}$

DF/Tol: $P\{R_L(j) \le t_1 \le R_U(j), t_n \ge t_n^*(j), t_0 < t_0^*(j)\} = P\{E4 \cap E3 \mid E1\}P\{E1\}$

DF/DF: $P\{R_L(j) \le t_1 \le R_U(j), t_n < t_n^*(j)\} = P\{E5 \mid E1\}P\{E1\}$

The probability of $E1$ is calculated by integrating the density function of stand age (Equation 5 of chapter 5) over the interval $[R_L(j), R_U(j)]$. The probability of having gone a certain amount of time without low- or moderate-intensity fire ($E2$ and $E3$, respectively) is evaluated using the survivorship distribution (Equation 1 of chapter 5) with the hazard rate for low- or moderate-intensity fire ($q_1\lambda$ or $q_2\lambda$, respectively). The probability of experiencing at least one low- or moderate-intensity fire in a given interval ($E4$ and $E5$) is evaluated using the cumulative mortality distribution (Equation 2 of chapter 5) with the hazard rate for low- or moderate-intensity fire. Stand age is used as the upper limit of integration. Conditioning on stand age leads to setting the lower limit of integration for the survivorship and mortality distributions as the maximum of r_1 or $t_1 - t_0^*(j)$ for low-intensity fire and the maximum of r_2 or $t_1 - t_n^*(j)$ for moderate-intensity fire (Figure C-3). The equilibrium abundance of each stand-structure type is calculated by multiplying the probability of $E1$ by the probabilities of the other events necessary for that structure type and summing over all ages in the age class:

$$\text{Unburned} = \sum_{t_1=R_L(j)}^{R_U(j)} \left[a_\infty(t_1) \exp\left(- \int_{\max[r_1, t_1 - t_0^*(j)]}^{t_1} h_L(u)du \right) \exp\left(- \int_{\max[r_2, t_1 - t_n^*(j)]}^{t_1} h_M(u)du \right) \right] \quad \text{[C-1]}$$

$$\text{DF/Tol} = \sum_{t_1=R_L(j)}^{R_U(j)} \left[a_\infty(t_1) \left\{ 1 - \exp\left(- \int_{\max[r_1, t_1 - t_0^*(j)]}^{t_1} h_L(u)du \right) \right\} \exp\left(- \int_{\max[r_2, t_1 - t_n^*(j)]}^{t_1} h_M(u)du \right) \right] \quad \text{[C-2]}$$

$$\text{DF/DF} = \sum_{t_1=R_L(j)}^{R_U(j)} \left[a_\infty(t_1) \left\{ 1 - \exp\left(- \int_{\max\{r_2, t_1 - t_0^*(j)}^{t_1} h_M(u)du \right) \right\} \right]. \quad \text{[C-3]}$$

The equilibrium abundance of each stand-structure type within the Mature, EOG, and MOG age classes, determined by Equations C-1, C-2, and C-3, using the fire-regime parameters shown in Table 5.2 for the Cook-Quentin study area of Morrison and Swanson (1990), is compared to the output of a simulation model using the same parameters in Figure 5.6. The simulation model was run for 500 replicates (5,000 years each), starting from an initial stand age of 1. Only simulation years 1,000–5,000 are shown to minimize the influence of initial stand age on model output.

Trajectories of Change under a Non-Stationary Fire Regime

Because stand age is equal to the age of the oldest Douglas-fir cohort, t_1, which represents the number of years since the last SR fire, the expected proportion of a landscape covered by stands of each age in a given year depends only on the time since the last-SR fire. Thus, for any known initial age distribution, the expected age distribution in any year following an abrupt change in the hazard rate for SR fire can be determined by applying Equations 7a and 7b of chapter 5 iteratively, using the piecewise constant hazard rate for SR fire (Figure 5.5).

After the expected age distribution in a given year is determined, the expected proportion of the landscape covered by each stand-structure type within each age class may be determined by modifying Equations C-1, C-2, and C-3. First, the equilibrium abundance of each stand age, $a_\infty(t_1)$, must be replaced by the expected abundance of each age in a particular year, $a(t_1, s)$, as determined by Equations 7a and 7b of chapter 5, using the piecewise constant hazard rate for SR fire. Then the probabilities that a stand of a given age in year s would or would not have experienced low- or moderate-intensity fire over a preceding interval, as required to meet the criteria for each stand-structure type (Table 5.1), are determined by replacing the time-invariant survivorship and mortality distributions (Equations 1 and 2 of chapter 5) with the time-dependent distribution (Equations 8a and 8b of chapter 5). The limits of integration for each term in the equations below ensure that for a stand of given age in year s, the probability that it has or has not experienced low- or moderate-intensity fire over the preceding $t_0^*(j)$ or $t_n^*(j)$

years, respectively, is determined by conditioning on stand age. Also, for stands that either initiated in the present epoch or were younger than the ages necessary to survive fire of low- or moderate-intensity fire at the beginning of the present epoch, the lower limit of integration for the terms evaluating survivorship or mortality under the hazard rate for the first epoch, and the exponential of the integrals is equal to 1. Therefore, under a non-stationary fire regime, the expected proportion of the unburned, DF/Tol, and DF/DF stand-structure types within a given age class in any year is determined by Equations C-4, C-5, and C-6, below:

Unburned:

$$\sum_{t_1=R_L(j)}^{R_U(j)} \left[\begin{array}{l} a(t_1,s) \exp\left(- \int_{\max[r_1,t_1-t_0^*(j)]}^{\max[t_1-\Delta s,\max\{r_1,t_1-t_0^*(j)\}]} h_L^{(1)}(u)du \right) \exp\left(- \int_{\max[t_1-\Delta s,\max\{r_1,t_1-t_0^*(j)\}]}^{t_1} h_L^{(2)}(u)du \right) \\ \exp\left(- \int_{\max[r_2,t_1-t_n^*(j)]}^{\max[t_1-\Delta s,\max\{r_2,t_1-t_n^*(j)\}]} h_M^{(1)}(u)du \right) \exp\left(- \int_{\max[t_1-\Delta s,\max\{r_2,t_1-t_n^*(j)\}]}^{t_1} h_M^{(2)}(u)du \right) \end{array} \right] \quad \text{[C-4]}$$

DF/Tol:

$$\sum_{t_1=R_L(j)}^{R_U(j)} \left[\begin{array}{l} a(t_1,s) \left[1 - \left\{ \begin{array}{l} \exp\left(- \int_{\max[r_1,t_1-t_0^*(j)]}^{\max[t_1-\Delta s,\max\{r_1,t_1-t_0^*(j)\}]} h_L^{(1)}(u)du \right) \\ \exp\left(- \int_{\max[t_1-\Delta s,\max\{r_1,t_1-t_0^*(j)\}]}^{t_1} h_L^{(2)}(u)du \right) \end{array} \right\} \right] \\ \exp\left(- \int_{\max[r_2,t_1-t_n^*(j)]}^{\max[t_1-\Delta s,\max\{r_2,t_1-t_n^*(j)\}]} h_M^{(1)}(u)du \right) \exp\left(- \int_{\max[t_1-\Delta s,\max\{r_2,t_1-t_n^*(j)\}]}^{t_1} h_M^{(2)}(u)du \right) \end{array} \right] \quad \text{[C-5]}$$

$$\text{DF/DF:}\quad \sum_{t_1=R_L(j)}^{R_U(j)} a(t_1,s)\left[1-\left\{\exp\left(-\int_{\max[t_1-\Delta s,\max\{r_2,t_1-t_n^*(j)\}]}^{\max[r_2,t_1-t_n^*(j)]} h_M^{(1)}(u)du\right)\right\}\left\{\exp\left(-\int_{\max[t_1-\Delta s,\max\{r_2,t_1-t_n^*(j)\}]}^{t_1} h_M^{(2)}(u)du\right)\right\}\right] \qquad \text{[C-6]}$$

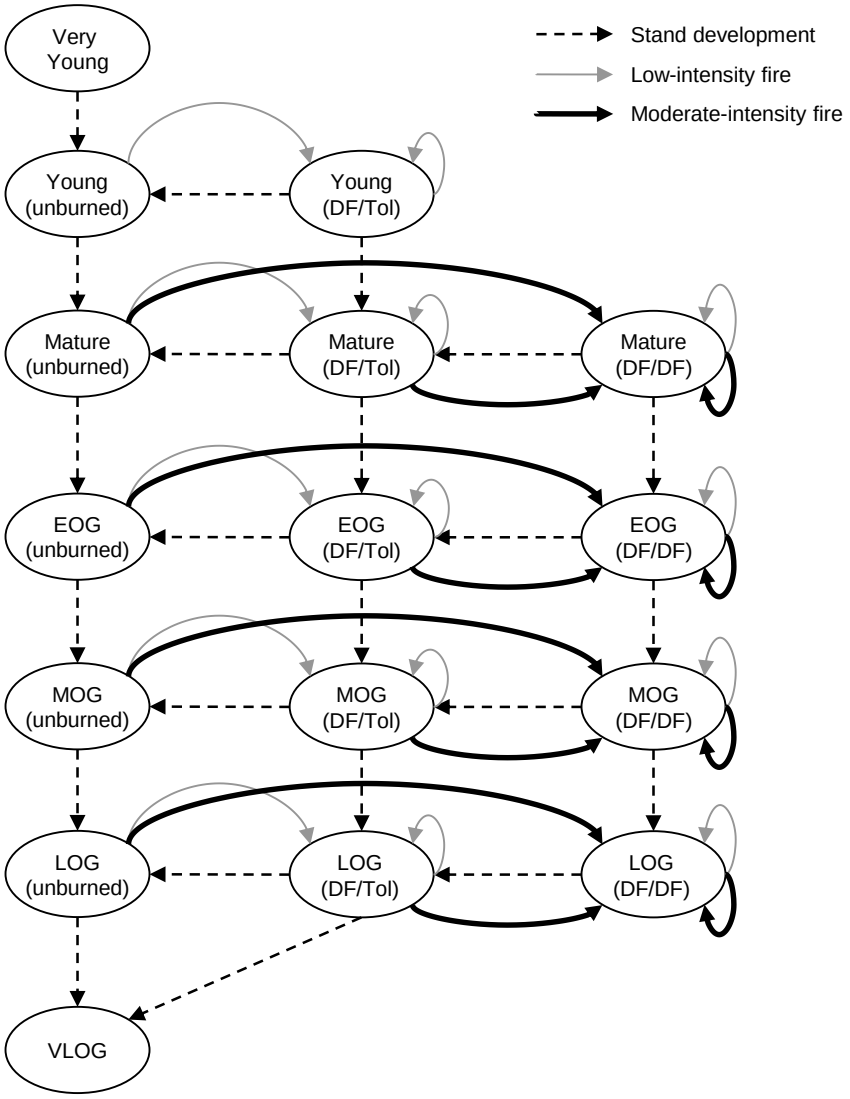

Figure C-1. Successional pathway diagram for Douglas-fir forests of the Pacific Northwest arranged by age class, from youngest (top) to oldest (bottom), and showing up to three structure types within each age class, with increasing influence of non-stand-replacing fire from left to right. Solid arrows indicate transitions following fire of moderate and high intensity. Dashed arrows indicate stand development in the absence of fire. High-intensity fire converts any stage to the Open age class. Age classes and structure types correspond to Table 5.1.

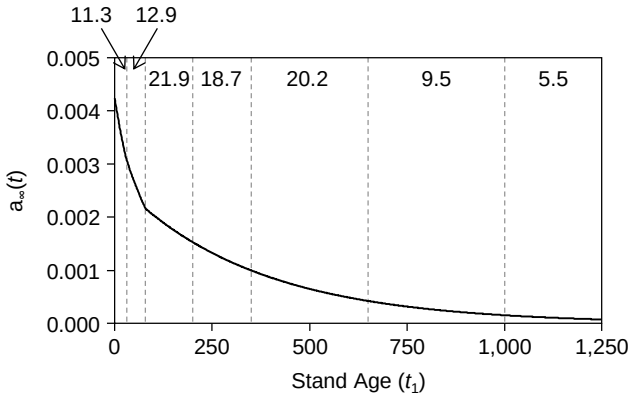

Figure C-2. Equilibrium age distribution for the Cook-Quentin study area of Morrison and Swanson (1990) produced using fire-regime parameters in Table 5.2. Vertical dashed lines represent divisions between age classes as defined in Table 5.1, and the numbers indicate the equilibrium density (percentage of the landscape) represented in each class.

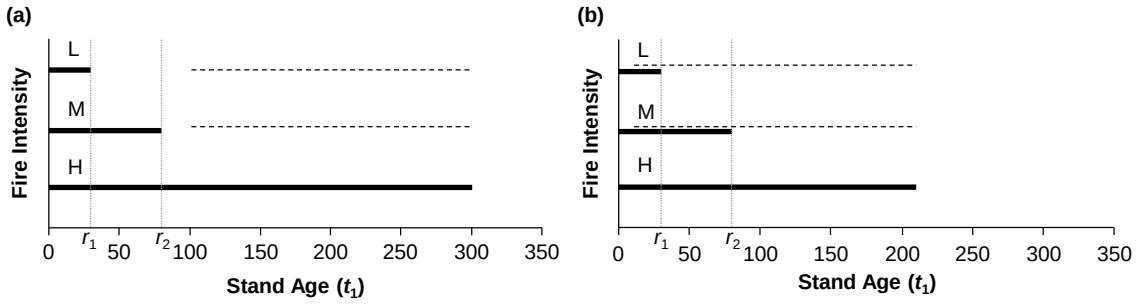

Figure C-3. Comparison of the time period when it is known that there has been no stand-replacing fire (thick lines) and the interval when no low- or moderate-intensity fires could have occurred for a stand to be classified as the classic structure type of the Mid Old Growth age class for stand age of (a) 300, and (b) 210 years (L, M, and H, refer to low, moderate, and high-intensity fire, and r_1 and r_2 are user defined age thresholds required for Douglas-fir cohorts to survive fires of low and moderate intensity, respectively).

APPENDIX D: TEMPORAL VARIATION IN THE FIRE REGIME

Aggregated across all sample sites, establishment dates for shade-intolerant trees (96% of which were Douglas-fir) produced a bimodal age distribution that was synchronous between the Blue River and Fall Creek study areas (Figure D-1), and the peaks of establishment dates coincide with the two periods of region-wide, extensive fire previously identified in a synthesis of ten fire-history studies west of the crest of the Cascades in Oregon and Washington (Weisberg and Swanson 2003). In the Blue River study area, 31% of establishment dates for shade-intolerant trees fell between 1470 and 1610, and 54% were after 1780, but only 8% fell between 1610 and 1780 (Figure D-1a). Similarly, at Fall Creek, 42% of the establishment dates were between 1470 and 1610, and 54% were after 1780, but only 4% fell between 1610 and 1780 (Figure D-1b). At individual stands, establishment dates for shade-intolerant species were clustered in discrete pulses, usually < 40 years long (Figure 2.6), most likely initiated shortly after fire that generated substantial openings in the canopy. The initiation of these pulses was staggered over time within each of the two periods of widespread establishment (1470–1610 and 1780–1940), suggesting that both study areas were affected by several fires during these periods. Only 21% of stands had cohorts initiated between 1610 and 1780, compared to 75% between 1470 and 1610 and 51% after 1780.

The period from the late 12th century to the mid 14th century may represent a third period of region-wide, extensive fire not previously identified in the synthesis of Weisberg and Swanson (2003). None of the sampled trees had establishment dates between 1360 and 1450, but 7% of the trees established in the interval 1170–1360 Figure D-1a). Establishment dates for these old trees formed relatively abrupt pulses (< 40 years long) that were staggered among stands in different parts of the study area, suggesting the occurrence of at least four fires during this period. Evidence of widespread burning in the early to mid 1200s and around 1300 AD also was suggested by studies in the Bull Run watershed in the northernmost part of the western Cascades of Oregon (Agee and Krusemark 2001), and at Mount St. Helens (Yamaguchi 1993), Mount Rainier

(Hemstrom and Franklin 1982), and the Olympic Peninsula (Henderson et al. 1989) of Washington. The widespread occurrence of Douglas-fir trees initiated from the late 12th century to the mid-14th century may indicate that drought during the "Medieval Warm Period" contributed to widespread fire in this period, as has been found in studies in the Sierra Nevada (Swetnam et al. 2009, Hallett and Anderson 2010).

To evaluate the role of climate in synchronizing the alternating periods of widespread burning and limited fire suggested within the present study area (Figure D-1) and more broadly across the region (Weisberg and Swanson 2003), the pattern of establishment dates for shade-intolerant trees was related to a reconstruction of the Pacific Decadal Oscillation (PDO) (MacDonald and Case 2005). Previous analyses of documented fires in the 20th century (Trouet et al. 2006, Keeton et al. 2007) and tree-ring-based reconstructions of fire in the 18th and 19th century (Hessl et al. 2004, Heyerdahl et al. 2008) suggest that warm phases of the PDO may contribute to widespread fire occurrence across the Pacific Northwest. The mechanism for such a relationship most likely relates to the role of warm sea surface temperatures in bringing warmer than average winters with less snow than typically found in cool phases of the PDO. Thus, warm phases may have longer fire seasons with a longer time for fuel to dry. Warm phases of the PDO also are associated with slightly cooler summers with more precipitation on the west side of the Cascade Range than found in cool phases. These summer conditions might suggest a decreased likelihood of widespread fire during the warm phase. However, the importance of winter conditions in driving large fire years in the Pacific Northwest is supported by the finding that annual area burned across the region had a statistically significant relationship with the winter PDO index, but not with the summer index (Keeton et al. 2007).

Because fire dates in the present study area only can be approximated, using the establishment date of the oldest tree in a cohort as the closest estimate of the fire year, and the number of trees sampled per stand might be too small to include the first trees to establish following fire, estimated fire years probably can be resolved only within 1–2 decades. However, given the multi-decadal pattern of oscillation in the PDO, the

relatively poor resolution in estimated fire years may be sufficient to identify a relationship with the PDO. Other climate indices, such as El Nino/Southern Oscillation (ENSO) and the Palmer Drought Severity Index (PDSI) may contribute to fire occurrence in the study area (Littell et al. 2009), but the high-frequency variation in these indices does not allow for comparison to the poorly resolved estimates of fire years in the present study. The Atlantic Multidecadal Oscillation (AMO) also may contribute to long-term patterns of drought in the Pacific Northwest, and thereby contribute to the synchrony of widespread burning across the study area (Kitzberger et al. 2007), but reconstructions of the AMO extend only to 1567 (Gray et al. 2004), which is not long enough to evaluate its influence on the fire regime over the time period of interest in this study.

Relationships between temporal patterns of cohort initiation and the PDO were evaluated using Superposed Epoch Analysis (SEA; Grissino-Mayer 2001). The decade containing the earliest establishment date within a cohort was used as an estimate of the decade of fire occurrence. Multiple cohorts per stand were defined using the criteria of a pulse of establishment of shade-intolerant trees following an interval at least 80 years long with no establishment dates recorded for any species, or a healed-over fire scar within an increment core (chapter 2). Values of the reconstructed PDO index (MacDonald and Case 2005) were averaged by decade. Then, SEA was conducted to determine if decades when cohort initiation was recorded at two or more stands had different relationships with the PDO than decades when cohort initiation was lacking or recorded at only one stand.

Relationships between cohort initiation and the PDO support the interpretation that warm phases of the PDO synchronize widespread fire occurrence across the Pacific Northwest, as found for 20th-century fires (Trouet et al. 2006, Keeton et al. 2007). The periods of widespread cohort initiation in the late 1400s, mid 1500s, and mid 1800s correspond to some of the warmest values of the PDO index over the last 800 years, as reconstructed by MacDonald and Case (2005) (Figure D-2a). Decades with widespread cohort initiation were associated multi-decade warm periods of the PDO (Figure D-3). Values of the PDO index were warmer than expected by chance during the decade of

cohort initiation and in each of the four decades preceding cohort initiation. Thus, even if the fire occurred earlier than estimated by the decade of cohort initiation, it was likely to be within the warm phase of the PDO. Decades that lacked cohort initiation, or when cohort initiation was found at only one stand, were associated with cool phases of the PDO and were preceded by four decades when values of the PDO index were cooler than expected by chance (Figure D-3).

The interpretation that the PDO has been an important factor contributing to the periods of widespread fire occurrence in the study area over the last 550 years should be interpreted with caution due to substantial differences among the tree-ring based reconstructions of the PDO. The reconstruction of MacDonald and Case (2005) was used in this study because it is the only one long enough to evaluate the period of widespread establishment that initiated in the late 15th century. However, this reconstruction is strongly out of phase with the instrumental record in the period from about 1915 to 1924. For example, the highest reconstructed value during the period of overlap with the instrumental record is in 1920, but this year was in the lowest 10% of values in the instrumental record. The reconstruction by D'Arrigo et al. (2001) has been related to fire in other studies (e.g., Heyerdahl et al. 2008), but it extends only to 1700. Over the period of overlap between the reconstructions by MacDonald and Case (2005) and D'Arrigo et al. (2001) the correlation between the two reconstructions is only 0.19. Thus, one or both of these reconstructions may be inaccurate, or the PDO may have had a weaker influence on the North Pacific climate system prior to the 20th century (Gedalof et al. 2002).

Tree-ring width measured in some of the oldest trees in the study area support an interpretation that periods of widespread establishment by shade-intolerant species may have been associated with summer drought, thus supporting a role for long-term climate variation in synchronizing periods of widespread fire occurrence across the study area. Ring width was measured in 58 trees > 650 years old sampled at 4 stands in the northern part of the Blue River study area (including 12 trees from a stand adjacent to one of the sample sites provided by Bryan Black). Ring-width data from all of these trees were combined into a single chronology. Detrending was conducted with an exponential curve

and then with a 250-year cubic smoothing spline in an effort to reduce long-term trends associated with bole geometry but retain a low-frequency climate signal.

Relationships between ring width and 20th century climate variables show limitation primarily by growing-season moisture, as found for another study of Douglas-fir in the region (Littell et al. 2008). For example, ring width was positively correlated with growing season precipitation and PDSI during the year of ring formation and in the preceding year (Figure D-4a and b). The positive correlation with growing season PDSI extended into the late fall of the year prior to ring formation. Thus, narrow ring width may indicate dry summer conditions conducive to widespread fire. However, this relationship was complicated by a positive correlation of ring width with temperature during the winter and early spring of the year of ring formation, and with late-spring temperature of the preceding year (Figure D-4c). Thus, narrow ring width also may be an indication of cold winters and relatively short growing seasons that might not be conducive to widespread fire. The positive response of Douglas-fir radial growth to winter temperature found in the relatively high-elevation sites supporting these old trees (1,016–1,151 m) is consistent with a trend toward a limitation of growing season length on Douglas-fir growth near its upper elevation limit as found in other studies in this region (Brubaker 1980, Littell et al. 2008). In addition to the climate signals in tree-ring width, there were several disturbance signals, including likely outbreaks of the western spruce budworm (*Choristoneura occidentalis* Freeman) inferred by periods of decade-long growth reduction in Douglas-fir (e.g., around 1400 and the 1740s in Figure D-2a) that did not correspond with reduced growth in western hemlock. Also, fire sometimes was associated with a growth release or less often a growth reduction.

Despite the complications in the tree-ring record, it appears that portions of the periods of widespread establishment of shade-intolerant trees are associated with long periods of reduced ring-width, which may be an indication of drought. In particular, a long period of substantially reduced growth was found in the mid-to late 1400s (Figure D-2a). This period coincides with a long, warm phase in the PDO reconstruction of MadDonald and Case (2005) and with the 15th-century megadrought (1444–1481),

identified by Stahle et al. (2007). The 15th-century megadrought is one of three "megadroughts" identified over the last 700 years in the western United States by using gridded, tree-ring reconstructed PSDI data to find decadal droughts more severe and prolonged than those witnessed in the instrumental record. The 15th-century megadrought was centered primarily over the Central Plains and Front Range of the Rocky Mountains, but dry conditions also were suggested in the Pacific Northwest, particularly in the later part of this interval (Stahle et al. 2007). Thus, extensive fire during and following this long dry period may have contributed to the widespread distribution of shade-intolerant trees initiated in the late 15th and 16th centuries and the low abundance of trees that predate this period (Figure D-2b).

Several additional data sources could contribute to a stronger evaluation of the contribution of climatic fluctuation to the centennial-scale pattern of variation in the fire regime. Higher-resolution dating of fire events by fire scars is needed to determine whether areas with synchronous decades of cohort initiation were burned in a single fire or by several fires within a window of 1–2 decades. To the extent that extensive areas can be found to have been burned by the same fire or at least in the same year, high-resolution dating of fire events would allow stronger characterization of the climate conditions contributing to widespread fire at a temporal scale that may better match the timescale of climate variation that affects fire occurrence. For example, years with a large area burned in the Pacific Northwest in the second half of the 20th century were associated with multi-season drought, usually initiating the previous fall, but they were not necessarily dependent upon longer-term drought (Gedalof et al. 2005).

More careful selection of sample sites and trees for tree-ring analysis of historical climate is needed to strengthen the climate signal relative to disturbance signals, and to provide chronologies that more strongly represent either summer moisture or winter temperature, rather than a mixture of the two signals. For example, sampling of mountain hemlock or Alaska yellow-cedar at high elevations may give a stronger record of winter temperatures and growing season length. Old individuals of these species may be found at high elevations near the crest of the Cascades, where disturbances by fire and insects

are likely to have less of an effect on tree growth. Also, a low elevation chronology that gives a stronger record of summer moisture would be useful, but it might not be possible to find trees of sufficient age at low elevations to document long-term climate patterns. For example, a preliminary chronology developed from incense-cedar trees collected during reconnaissance for this study (mostly at a site at an elevation of 870 m) was more strongly related to summer precipitation and PDSI than the Douglas-fir chronology, but it was difficult to find trees > 300 years old that lacked heartrot.

Several factors other than climatic variation may have contributed to the long-term variation in the fire regime suggested by the ages of shade-intolerant trees across the study area. Native Americans are known to have used fire extensively in the Willamette Valley, and at least locally in the western Cascades to maintain meadows and berry patches, but their effect on the fire regime over the broader landscape is largely unknown (Boyd 1999, Whitlock and Knox 2002). Prior to European settlement, the Molala occupied much of the central western Cascades, spending winters along low-elevation rivers, and then moving into upland areas during the summer (Minor and Pecor 1977), but their population and their effects on the forest are poorly documented. The change from a period of widespread burning from 1470 to 1610 followed by a period with more limited fire to ca. 1780 occurred long before Euro-American settlers influenced the fire regime in the region. In Washington, a large fire (ca. 500,000 ha) is suggested to have occurred around 1800 in an area bounded by Mount Rainier, Mount St. Helens, and Centralia, and has been proposed to have been set either by the Cowlitz tribe against the Nisqually tribe, or by the Nisquallies as a means of generating rain during a drought (Clevinger 1951, as cited by Agee 1993, p. 57). Otherwise, the evidence available to date does not provide a convincing argument that Native American burning had a widespread influence on the fire regime in the rugged terrain of the western Cascades. Also, the period of increased establishment of shade-intolerant trees starting in the late 1700s was initiated at a time when Native American populations probably had been greatly reduced by epidemics of smallpox and malaria (Mackey 1974).

The peak of establishment in the mid-1800s probably was influenced in part by burning activities of Euro-American settlers. This period of establishment has a peak in the mid- to late-1800s (Figures D-1 and D-2b), at a time when lower elevations of the region were heavily used by ranchers and farmers, upper elevations were used by herders, miners, and loggers, and there were numerous travelers throughout the region (Burke 1979). Many fires of the mid to late 19th century and early 20th century are known to have been ignited by Euro-American settlers (Morris 1934). However, there also may have been an over-emphasis on the role of human ignitions during this period, as some accounts suggest the role of lightning in igniting forest fires was not widely recognized at that time (Coville 1898, p. 32–33; Burke 1979; Vale 2002).

Long-term patterns of fuel accumulation also are a possible contributor to the temporal pattern of variation found in the study area. A study of fuel succession along a chronosequnce of stands initiated following stand-replacing fire on the Olympic Peninsula of Washington suggests that fuel loadings and potential fire behavior are lowest in stands ca. 110–180 years old, when most of the dead wood carried over from the previous stand has decayed, but mortality in the new stand has yet to contribute large amounts of new dead woody fuel (Agee and Huff 1987). Thus, to the extent that fuel loading as a function of time since fire affects fire occurrence across the landscape, a period of widespread burning may be followed by a period of limited fire ca. 100–200 years later. However, given the staggering of cohort initiations dates and variable fire severity found within the study area, it is likely that fuel conditions were highly heterogeneous across the study area over the time period analyzed in this study.

It is not possible to exclude the possibility that the synchronous pattern of fire occurrence found between the two study areas is a result of stochastic variation without being driven by an external factor (Lertzman et al. 1998). However, the correspondence of the two major peaks of establishment found in this study to the periods of region-wide extensive fire found in a synthesis of previous fire-history studies (Weisberg and Swanson 2003) makes it less likely that the pattern is due only to stochastic variation. Additional sampling throughout the region is needed to better characterize the temporal

patterns of fire. For example, a large portion of the northeastern Olympic Peninsula is reported to have burned in a single fire or a series of fires around 1700 (Henderson et al. 1989), at a time when little evidence of fire was found in the present study area (Figure D-1) or in the synthesis of Weisberg and Swanson (2003). An estimated magnitude 9 earthquake affected the coastline of Oregon and Washington in the winter of 1700, at a time when low-elevation soils would have been wet, which might have led to substantial treefall. Agee and Krusemark (2001) suggested the drying of the dead wood caused by such an earthquake may have contributed to the conditions conducive to widespread fire at that time.

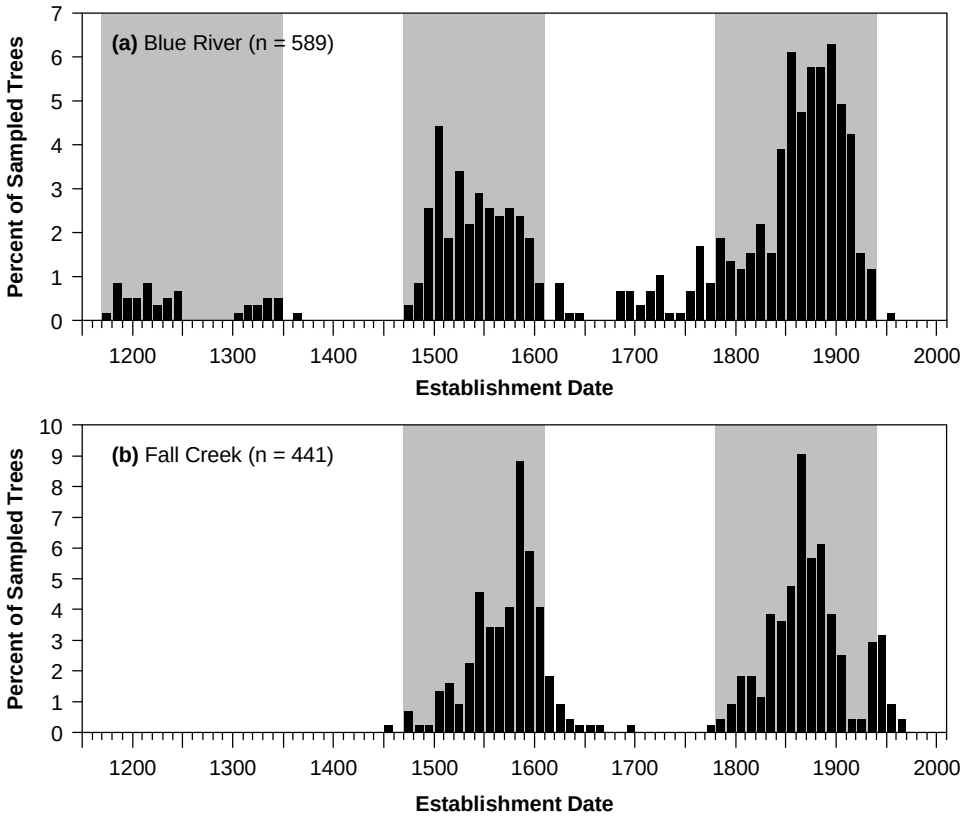

Figure D-1. Comparison of establishment dates for shade-intolerant trees (96% of which were Douglas-fir) aggregated across all sample sites in the (a) Blue River, and (b) Fall Creek study areas. Gray shading represents periods of widespread establishment, from 1470 to 1610 and from 1780 to 1940 that correspond to periods of region-wide extensive fire suggested in a previous synthesis of ten fire-history studies west of the crest of the Cascades in Oregon and Washington (Weisberg and Swanson 2003). An earlier period of widespread establishment, from 1170 to 1350, was found at the Blue River study area.

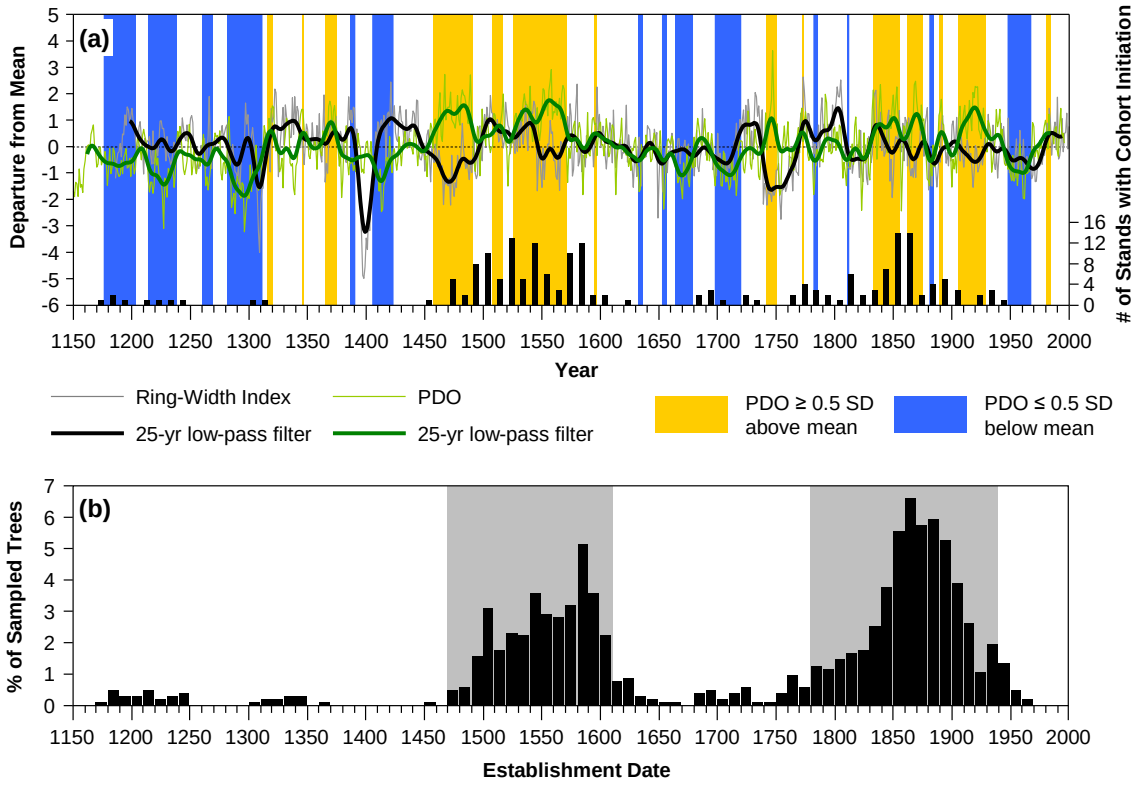

Figure D-2. The relationship of the establishment of shade-intolerant trees in the central western Cascades of Oregon to the Pacific Decadal Oscillation, as reconstructed by MacDonald and Case (2005), and ring-width index for the oldest Douglas-fir trees (n = 58 trees > 650 years old) sampled in the study area. In (a), the number of stands that recorded cohort initiation in each decade is shown in relation to ring-width index and the PDO. Multiple cohorts per stand had to meet the criteria of an interval of at least 80 years with no recorded establishment of any species prior to cohort initiation or a healed-over fire scar identified within an increment core (chapter 2). In (b), the composite histogram of establishment dates for all 1,030 shade-intolerant trees sampled in the Blue River and Fall Creek study areas is shown. Gray shading represents periods of widespread establishment (1470–1610 and 1780–1940) that correspond with periods of region-wide extensive fire identified in a previous synthesis of ten fire-history studies west of the crest of the Cascades in Oregon and Washington (Weisberg and Swanson 2003).

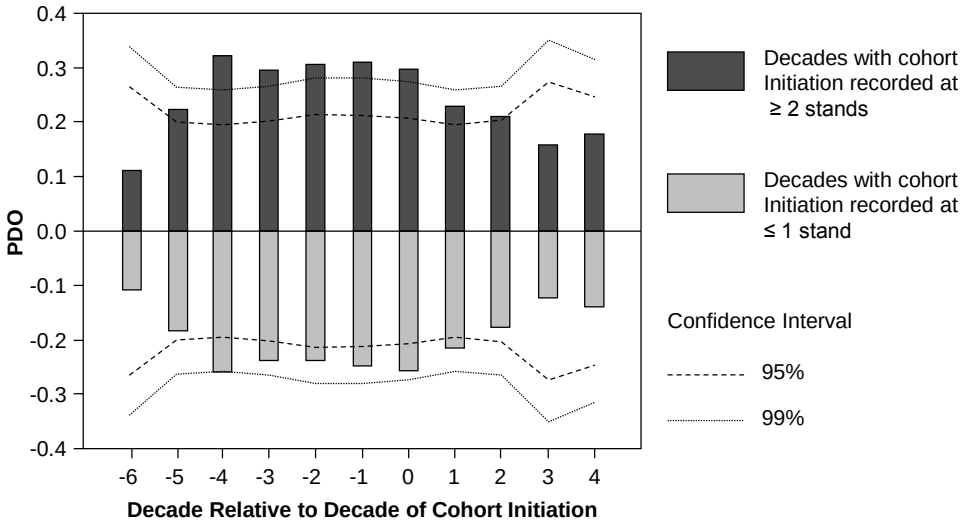

Figure D-3. The relationship of the timing of initiation of cohorts of shade-intolerant trees in the central western Cascades of Oregon to the Pacific Decadal Oscillation (PDO), as determined by Superposed Epoch Analysis (SEA). SEA was used to compare the relationship of decades when cohort initiation was recorded at two or more stands and those when cohort initiation was absent or recorded only at one stand to the PDO at lags from six decades prior to the decade of cohort initiation to four decades after the decade of cohort initiation. Confidence intervals were determined by bootstrap sampling with 1,000 replications.

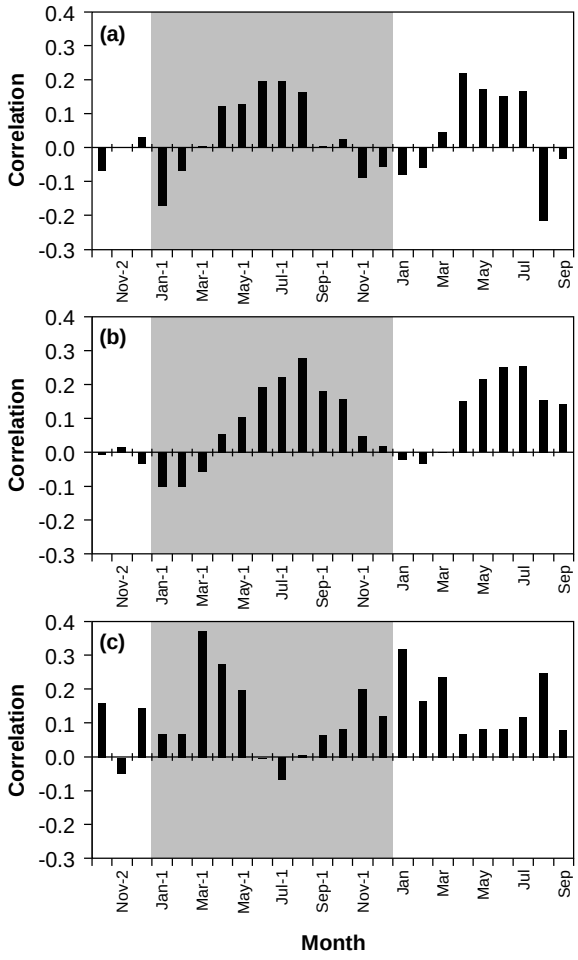

Figure D-4. Comparison of the correlation of ring width in a chronology of 58 of the oldest (> 650 years old) Douglas-fir trees sampled in the study area with monthly (a) precipitation, (b) Palmer Drought Severity Index (PDSI), and (c) temperature, during the year of ring formation and the preceding year (shaded). Climate data are for Oregon Division 2, over the period from 1895 to 2006, obtained from the National Climatic Data Center (http://www7.ncdc.noaa.gov/CDO/CDODivisionalSelect.jsp). The tree-ring chronology was developed by detrending with an exponential curve followed by a 250-year spline.